Impact of Environmental Factors on Pavement Performance in the Absence of Heavy Loads

PUBLICATION NO. FHWA-HRT-16-084

MARCH 2019

U.S. Department of Transportation
Federal Highway Administration

Research, Development, and Technology
Turner-Fairbank Highway Research Center
6300 Georgetown Pike
McLean, VA 22101-2296

LTPP™

FOREWORD

This report documents the analysis of data collected through the Long-Term Pavement Performance program to characterize the impact of environmental factors on pavement performance. The objectives of this analysis were to identify and quantify the effects of environmental factors and pavement design on pavement performance in the absence of heavy loads; develop recommendations for mitigating these effects through effective design, materials selection, and construction; estimate the portion of pavement damage caused by environmental factors; and establish a database of pavement design features, materials properties, and performance to be used in the future for similar analyses.

The study showed that, for flexible pavements that have been in service for 15 yr with normal traffic loading, 36 percent of total damage is related to environmental factors (e.g., subgrade and climate variables). For rigid pavements that have been in service for 15 yr with normal traffic loading, 24 percent of total damage is related to environmental factors.

Results related to the impact of specific subgrade, climate, traffic, and design factors on pavement performance will be of interest to pavement, materials, and pavement-management engineers concerned with the design, materials properties, and performance of flexible and rigid pavements.

Cheryl Allen Richter, Ph.D., P.E.
Director, Office of Infrastructure
Research and Development

Notice

This document is disseminated under the sponsorship of the U.S. Department of Transportation (USDOT) in the interest of information exchange. The U.S. Government assumes no liability for the use of the information contained in this document.

The U.S. Government does not endorse products or manufacturers. Trademarks or manufacturers' names appear in this report only because they are considered essential to the objective of the document.

Quality Assurance Statement

The Federal Highway Administration (FHWA) provides high-quality information to serve Government, industry, and the public in a manner that promotes public understanding. Standards and policies are used to ensure and maximize the quality, objectivity, utility, and integrity of its information. FHWA periodically reviews quality issues and adjusts its programs and processes to ensure continuous quality improvement.

TECHNICAL REPORT DOCUMENTATION PAGE

1. Report No. FHWA-HRT-16-084	2. Government Accession No.	3. Recipient's Catalog No.
4. Title and Subtitle Impact of Environmental Factors on Pavement Performance in the Absence of Heavy Loads		5. Report Date March 2019 6. Performing Organization Code
7. Author(s) Leslie Titus-Glover, Michael I. Darter, and Harold Von Quintus		8. Performing Organization Report No.
9. Performing Organization Name and Address Applied Research Associates, Inc. 100 Trade Centre Drive, Suite 200 Champaign, IL 61820		10. Work Unit No. (TRAIS) 11. Contract or Grant No.
12. Sponsoring Agency Name and Address Office of Infrastructure Research and Development Federal Highway Administration 6300 Georgetown Pike McLean, VA 22101-2296		13. Type of Report and Period Covered Final Report; January 2011–December 2015 14. Sponsoring Agency Code HRDI-30
15. Supplementary Notes The Contracting Officer's Technical Representative was Jack Springer (HRDI-30).		

16. Abstract

The objectives of this study were to identify and quantify the effects of environmental factors and pavement design on pavement performance in the absence of heavy loads; establish what the environmental effects are and develop recommendations for mitigating these effects through effective designs, materials selection, and construction; estimate the portion of total pavement damage caused by environmental factors; and establish a database of pavement design features, materials properties, and performance to be used in the future for similar analyses. Site-by-site analyses of the Long-Term Pavement Performance program's Specific Pavement Study (SPS)-8 sections were conducted. Next, researchers determined the effect of environmental factors in SPS-8 and companion sections from other SPSs and General Pavement Studies (GPSs) on the performance of flexible and rigid pavements. Finally, an estimate of the portion of pavement damage caused by environmental factors was made through a comparison of the pavement damage of low-traffic SPS-8 sections with higher-traffic companion SPS and GPS sections. Results showed an average of 36 and 24 percent of total damage was related to environmental factors for flexible and rigid pavements, respectively, at an age of 15 yr.

In addition, many results were obtained through an analysis of the performances of SPS-8 and companion SPS and GPS sections. One such finding was that the occurrence of transverse cracking of asphalt-concrete pavement was significantly higher for companion pavements subjected to higher traffic loadings (SPS-1 and GPS-1) than under low-traffic loadings (SPS-8). Transverse cracking also occurred in nonfreeze climates. Based on the results from this study, suggestions for improvements to pavement designs and materials to minimize distress and to maximize performance in various climatic regions are presented.

17. Key Words	18. Distribution Statement
LTPP, Pavement performance, Damage, Environmental factors, JPCP, ACP, Subgrade, SPS-8, Truck loadings, Cost allocation	No restrictions. This document is available to the public through the National Technical Information Service, Springfield, VA 22161. http://www.ntis.gov

19. Security Classif. (of this report)	20. Security Classif. (of this page)	21. No. of Pages	22. Price
Unclassified	Unclassified	260	

Form DOT F 1700.7 (8-72) Reproduction of completed page authorized.

SI* (MODERN METRIC) CONVERSION FACTORS

APPROXIMATE CONVERSIONS TO SI UNITS

Symbol	When You Know	Multiply By	To Find	Symbol
		LENGTH		
in	inches	25.4	millimeters	mm
ft	feet	0.305	meters	m
yd	yards	0.914	meters	m
mi	miles	1.61	kilometers	km
		AREA		
in^2	square inches	645.2	square millimeters	mm^2
ft^2	square feet	0.093	square meters	m^2
yd^2	square yard	0.836	square meters	m^2
ac	acres	0.405	hectares	ha
mi^2	square miles	2.59	square kilometers	km^2
		VOLUME		
fl oz	fluid ounces	29.57	milliliters	mL
gal	gallons	3.785	liters	L
ft^3	cubic feet	0.028	cubic meters	m^3
yd^3	cubic yards	0.765	cubic meters	m^3
		NOTE: volumes greater than 1000 L shall be shown in m^3		
		MASS		
oz	ounces	28.35	grams	g
lb	pounds	0.454	kilograms	kg
T	short tons (2000 lb)	0.907	megagrams (or "metric ton")	Mg (or "t")
		TEMPERATURE (exact degrees)		
^oF	Fahrenheit	5 (F-32)/9 or (F-32)/1.8	Celsius	^oC
		ILLUMINATION		
fc	foot-candles	10.76	lux	lx
fl	foot-Lamberts	3.426	$candela/m^2$	cd/m^2
		FORCE and PRESSURE or STRESS		
lbf	poundforce	4.45	newtons	N
lbf/in^2	poundforce per square inch	6.89	kilopascals	kPa

APPROXIMATE CONVERSIONS FROM SI UNITS

Symbol	When You Know	Multiply By	To Find	Symbol
		LENGTH		
mm	millimeters	0.039	inches	in
m	meters	3.28	feet	ft
m	meters	1.09	yards	yd
km	kilometers	0.621	miles	mi
		AREA		
mm^2	square millimeters	0.0016	square inches	in^2
m^2	square meters	10.764	square feet	ft^2
m^2	square meters	1.195	square yards	yd^2
ha	hectares	2.47	acres	ac
km^2	square kilometers	0.386	square miles	mi^2
		VOLUME		
mL	milliliters	0.034	fluid ounces	fl oz
L	liters	0.264	gallons	gal
m^3	cubic meters	35.314	cubic feet	ft^3
m^3	cubic meters	1.307	cubic yards	yd^3
		MASS		
g	grams	0.035	ounces	oz
kg	kilograms	2.202	pounds	lb
Mg (or "t")	megagrams (or "metric ton")	1.103	short tons (2000 lb)	T
		TEMPERATURE (exact degrees)		
^oC	Celsius	1.8C+32	Fahrenheit	^oF
		ILLUMINATION		
lx	lux	0.0929	foot-candles	fc
cd/m^2	$candela/m^2$	0.2919	foot-Lamberts	fl
		FORCE and PRESSURE or STRESS		
N	newtons	0.225	poundforce	lbf
kPa	kilopascals	0.145	poundforce per square inch	lbf/in^2

*SI is the symbol for the International System of Units. Appropriate rounding should be made to comply with Section 4 of ASTM E380.
(Revised March 2003)

TABLE OF CONTENTS

LIST OF FIGURES

LIST OF TABLES

LIST OF ABBREVIATIONS

AADTT	average annual daily truck traffic
AASHO	American Association of State Highway Officials
AASHTO	American Association of State Highway and Transportation Officials
AC	asphalt concrete (hot-mix asphalt)
ANOVA	analysis of variance
CTE	coefficient of thermal expansion
DGAB	dense-graded aggregate base
ESAL	equivalent single-axle load
FHWA	Federal Highway Administration
FWD	falling-weight deflectometer
GPS	General Pavement Study
GWT	groundwater table
ICM	Integrated Climatic Model
IRI	International Roughness Index
JPCP	jointed plain concrete pavement
LTE	load-transfer efficiency
LTPP	Long-Term Pavement Performance
M&R	maintenance and rehabilitation
ME	mechanistic-empirical
MEPDG	*Mechanistic-Empirical Pavement Design Guide*
NCDC	National Climatic Data Center
NWIS	National Water Information System
PCC	portland cement concrete
PCI	Pavement Condition Index
PI	Plasticity Index
PMATLS	percent surface area with asphalt-concrete materials durability-related distress
PRESS	predicted residual sum of squares
SHRP	Strategic Highway Research Program
SLE	significance level of entry
SPS	Specific Pavement Study
SSURGO	Soil Survey Geographic
Superpave	Super Performing Asphalt Pavement
VIF	variance inflation factor

CHAPTER 1. INTRODUCTION

BACKGROUND

Traditionally, pavement design procedures have only considered truck-traffic loadings as demonstrated by earlier versions of the American Association of State Highway and Transportation Officials's (AASHTO's) pavement design methodology.[1–3] Historically, thicknesses of asphalt concrete (AC) or portland cement concrete (PCC) have been determined through the use of equations correlating AC- and PCC-layer thickness to cumulative traffic applications without regard to environmental conditions. Flexible-pavement design may include a regional factor that is more of a calibration factor than a factor directly related to climate because its sole purpose is to multiply the number of design axle loadings by a factor to provide a thicker or thinner pavement. No environmental considerations have been available for rigid pavements at all.

Research studies that have been conducted since the American Association of State Highway Officials (AASHO) Road Test was performed (1958–1960) showed that agencies can optimize design and materials to maintain desired minimum levels of service using fewer resources if the impact of environmental factors (i.e., climate and subgrade factors) is fully considered during the design process.[4–11] Although traffic loads contribute significantly to pavement deterioration and eventual failure, the environment in which a pavement is situated often accelerates traffic-related deterioration and, in many cases, can initiate deterioration that leads to early maintenance and rehabilitation (M&R) needs.

The AASHTO pavement design procedure has been modified several times over the years. Modifications have been based on improved awareness of the contribution of environmental factors to pavement deterioration.[1–3] Examples of such improvements include the following:

- The 1972, 1986, and 1993 versions of the *AASHTO Guide for Design of Pavement Structures* use regional factors to create local adjustments to the flexible pavement performance prediction model.[1–3]

- The 1972, 1986, and 1993 versions of the *AASHTO Guide for Design of Pavement Structures* also use seasonal subgrade resilient modulus and modulus of subgrade reaction values to characterize pavement foundation subgrade support and the effect of freeze–thaw cycles and moisture on foundation support.[1–3]

Federal and State highway agencies also expended considerable effort and resources over the years to further understand the impact of environmental factors on pavement damage/deterioration, distress manifestation, and smoothness with the goal of improving pavement performance. These efforts culminated in the 2008 version of AASHTO's *Mechanistic-Empirical Pavement Design Guide [MEPDG] Interim Edition: A Manual of Practice* models for asphalt and concrete pavements.[5,12] This guide provides indepth consideration of climate and subgrade aspects in relation to pavement design. Empirical climate and subgrade factors have since been replaced with more objective mechanistic-based algorithms and relationships that have the capability to characterize and quantify the following:

- In situ pavement temperature and moisture conditions.

- Relationship between pavement temperature, moisture conditions, and material properties (e.g., effect of temperature on AC dynamic modulus).

- Effect of temperature and moisture gradients on PCC slab curling and joint opening and closing affecting joint load transfer.

- Interactions between climate factors and pavement design features, paving material properties, and traffic characteristics (e.g., long-term durability and performance).

- Complex mathematical models for relating ambient conditions to in situ conditions.

- Models that are able to capture the influence of temperature and moisture cycles on pavement material durability as these significantly influence long-term pavement performance.

Thus, these and other advancements over the past few decades have resulted in significant improvements in the knowledge of the impact of environmental factors on pavement performance, tools for simulating pavement-temperature and -moisture conditions, and methodologies for mitigating the impact of environmental factors on pavement performance. Examples of environmental considerations include the following:

- Incorporation of environmental factors, such as temperature, freeze–thaw cycles, freezing index, rainfall, subgrade type, gradation, plasticity, etc., into pavement-performance prediction models for pavement design checks and management (e.g., MEPDG models for asphalt and concrete pavements).[5,12]

- Development of a new and improved AC–mix design methodology, Super Performing Asphalt Pavement (Superpave), under the Strategic Highway Research Program (SHRP). Superpave provides pavement designers with the guidance needed to select asphalt binders and accompanying AC-mix properties based on environmental factors (e.g., location-specific highest and lowest ambient temperature) and cumulative truck traffic over the design period. It significantly improves an AC mix's ability to resist rutting and low-temperature transverse cracking. Few of the AC pavements from the Long-Term Pavement Performance (LTPP) program used in the analyses included Superpave binders.

- Adoption of more effective PCC curing methods (i.e., curing compounds) to improve PCC strength and minimize the development of built-in thermal gradients in freshly placed PCC slabs that create upward curling and early cracking.

- Development of new, high-quality PCC mixes to produce more durable PCC slabs.

- Improvements in coarse aggregate material testing and characterization to help identify aggregates that are susceptible to freeze–thaw damage and have high coefficients of thermal expansion (CTEs) or contraction (key property related to PCC transverse cracking and AC low-temperature cracking).

- Development of comprehensive databases with detailed climate data for use in simulating ambient climate conditions over the pavement design life. For example, the National Oceanic and Atmospheric Administration's National Climatic Data Center (NCDC) database contains archives of historical hourly, daily, monthly, seasonal, and yearly measurements of temperature, precipitation, wind speed, and percent sunshine exposure.[13]

- Development of one-dimensional finite element models for simulating the flow of moisture and heat within a pavement structure. These models can be used to simulate in situ pavement temperature and moisture profiles on an hourly basis. For example, the Integrated Climatic Model (ICM) uses a finite element heat transfer and moisture transmission model to simulate transient flow of heat and moisture through a pavement structure.[14,15] ICM has been incorporated into the AASHTOWare pavement mechanistic-empirical (ME) design software.[5,12,16]

- Development of improved models and algorithms that relate in situ pavement temperature and moisture conditions to pavement material properties (e.g., impact of temperature on AC dynamic modulus).

Under SHRP and, later, the Federal Highway Administration's (FHWA's) LTPP program, significant progress has been made in deepening the pavement-engineering community's understanding of the factors that most impact long-term pavement performance. To achieve this goal, the LTPP program set up more than 2,500 experimental pavement test sections in the United States and Canada.[17] Within those sections, Specific Pavement Studies (SPSs) experiments were set up to monitor environmental effects on pavements in the absence of heavy loads (i.e., SPS-8). SPS-8 was specifically designed to provide information on the effect of climatic factors and subgrade type (e.g., frost susceptible, expansive, fine, and coarse) on flexible- and rigid-pavement projects incorporating different designs and located in different environments as the SPS-8 projects were subjected to very limited traffic loading.[18–22] Most of the SPS-8 projects have now been in service for 10 to nearly 20 yr. This time period, over which the environmental effects that have been acting on these SPS-8 sections, is considerable and can be evaluated.

Evaluating the performance of the SPS-8 test sections requires comparisons with projects that are similar but have been subjected to high traffic loading. SPS-1 and SPS-2 experiments were used for this comparison as they included pavements with similar designs and environments, but they were subjected to normal heavy traffic loading.[17] Additional projects can be obtained from the LTPP General Pavement Study (GPS) experiments for comparison.[17] This study was based on the SPS-8 sections and selected companion sections from other SPS and GPS experiments.[17] The sites generally had good drainage and controlled maintenance.

PROJECT OBJECTIVES

FHWA initiated this study to further characterize the impact of environmental factors on pavement performance. Key objectives of this study were as follows:

- Identify and quantify the effects of environmental factors and design on the performance of AC pavement and jointed plain concrete pavement (JPCP) in the absence of heavy loads.
- Establish what the environmental effects are, and develop recommendations for mitigating these effects through effective designs, materials selection, and construction.
- Estimate the portion of total pavement damage caused by environmental factors.
- Establish a database of pavement design features, materials properties, and performance to be used in the future for similar analysis and evaluation by State transportation departments.

In the context of this study, environment is defined as including climatic factors (moisture, rainfall, temperature, and freeze–thaw cycles) and foundation/subgrade type (frost-susceptible, expansive, fine-grained, and coarse-grained as well as soil properties such as percent clay and silt). The absence of heavy loads, in the context of this study, is defined as traffic applied to an SPS-8 experimental section that is typically less than 10,000 equivalent single-axle loads (ESALs) per year.

PROJECT SCOPE

This project consists of two phases. The scope of phase I was to perform site-by-site analyses of each SPS-8 project to gain an understanding of the performance of each individual test section. The scope of phase II was as follows:

- Determine the effect of the SPS-8 environmental experimental factors on the performance of AC pavements in the absence of heavy loads.
- Determine the effect of the SPS-8 environmental experimental factors on the performance of JPCP in the absence of heavy loads.
- Estimate the proportion of pavement damage caused by environmental factors.

ORGANIZATION OF THIS REPORT

This report summarizes the environmental factors that affect pavement performance in the absence of heavy loads, as seen in the SPS-8 experiments, over a 15-yr period. This report is organized as follows:

- Chapter 2 describes factors that initiate and aggravate pavement deterioration.
- Chapter 3 provides an overview of the analysis plan for determining the impact of environmental factors on pavement performance.
- Chapter 4 shows the development of a project sampling template.
- Chapter 5 describes the development of the project database.
- Chapter 6 describes the analysis of SPS-8 and companion AC pavement projects' fatigue-cracking distress.
- Chapter 7 provides the analysis of SPS-8 and companion AC pavement projects' rutting distress.
- Chapter 8 describes the analysis of SPS-8 and companion AC pavement projects' transverse-cracking distress.
- Chapter 9 describes the analysis of SPS-8 and companion AC pavement projects' materials-durability distress.
- Chapter 10 provides the analysis of SPS-8 and companion AC pavement projects' smoothness.
- Chapter 11 provides the analysis of SPS-8 and companion JPCP projects' fatigue-cracking distress.
- Chapter 12 describes the analysis of SPS-8 and companion JPCP projects' transverse joint-faulting distress.
- Chapter 13 describes the analysis of SPS-8 and companion JPCP projects' transverse joint spalling.
- Chapter 14 provides the analysis of SPS-8 and companion JPCP projects' smoothness.
- Chapter 15 summarizes the proportion of overall pavement damage due to environmental factors.
- Chapter 16 suggests improvements to AC pavement and JPCP design and materials selection to mitigate the impact of environmental factors.

CHAPTER 2. FACTORS THAT INITIATE AND CAUSE THE PROGRESSION OF PAVEMENT DETERIORATION

The concept of pavement design was formalized with the completion of the AASHO Road Test in the early 1960s, and this led to the development of the first-generation AASHO pavement design guide.[23] This guide includes a system of regression equations based on field data that relates pavement materials and design properties to performance and traffic loading. With the adoption of the AASHO pavement design guide in the early 1960's came the realization that, although the new pavement technology works adequately for the climate in some locations, it does not always perform well in other regions of the country, leading to early pavement distresses. The early failures were usually caused by inadequate designs that did not fully consider environmental impacts. The weaknesses of the AASHO Road Test models were improved somewhat in subsequent versions of the empirical pavement design guide, as summarized in table 1.[1–4,23.]

Table 1. Significant revisions to the original AASHO pavement models to consider environmental impacts on pavement materials' durability and performance.

Environmental Factors	Revision
Impact of subgrade	A very soft silty-clay (A-6) subgrade existed at the AASHO Road Test site.[24] The effect of this single subgrade was built into the model. The ability to consider other subgrades through the resilient modulus was added to the 1986 version.[3]
Paving material strength and durability	• A dense, crushed, unbound limestone aggregate base was used at the AASHO Road Test. The subbase layer was uncrushed and unbound dense gravel/sand. The ability to consider other bases, at least empirically, was incorporated using the empirical structural coefficient method. • The effect of different AC mixes was added through the structural coefficient approach. Thickness was a variable contained in the original data. New and improved asphalt mixtures developed since the AASHTO Road Test, such as Superpave, have led to modification of the AC structural coefficients.
Pavement subdrainage and moisture condition	Original flexible and rigid pavements were built as a bathtub, resulting in very poor subdrainage conditions. A conceptual drainage coefficient was added to adjust for the improved drainage conditions of unbound aggregate base and subbase layers, but the proper magnitude was difficult to determine.
Characterization of climate effect	The design performance models were developed over a 2-yr period at the Northern Illinois AASHO Road Test site; thus, they have been calibrated for just one short-term 2-yr climatic cycle. The ability to adjust for other climates and many more yearly cycles was originally included by adding a regional factor for flexible pavement (which simply multiplied the number of design traffic loads), but there was no such factor developed for rigid pavement. Thus, there was little or no way to consider different climates for either type of pavement.

Experience has shown that the environment has a significant effect on pavement performance, and failure to consider environmental effects in pavement design and construction can lead to

early failures and increased lifecycle costs. State transportation departments have invested significant resources in investigating the impact of environmental factors on pavement performance. The outcomes have been published and used to enhance pavement design and performance-simulation technology. A summary of significant findings and advancements in pavement design and performance-simulation technology is presented in this chapter.

ENVIRONMENTAL FACTORS AND THEIR EFFECTS ON PAVEMENT PERFORMANCE

This section describes the effects of both climatic- and subgrade-related factors on pavement performance.

Effect of Climatic Factors on Pavement Performance

Roberts et al. described the moisture susceptibility of AC mixes related to stripping (i.e., the loss of bond between the asphalt binder and aggregate).[25] AC-mix moisture susceptibility is governed by the mix design and compaction. Moisture damage usually begins at the bottom of the AC layer and results in a gradual loss of AC strength over a period of years. Yilmaz and Sargin reported that typical AC moisture damage/distress manifestations include the following:[26]

- **Stripping**: Debonding of aggregates and binder at the bottom of the AC layer.
- **Rutting**: Surface depressions along the wheel path.
- **Corrugation and shoving**: Plastic movement typified by ripples or an abrupt wave across the pavement surface.
- **Raveling**: Progressive disintegration of the AC layer.
- **Localized failures (potholes)**: Progressive loss of adhesion or cohesion between the binder and aggregates.

Early alligator (fatigue) cracking can also occur when stripping exists. Moisture damage typically begins when water infiltrates the AC pavement and there is inadequate surface or subsurface drainage. Hicks et al identified the following factors that contribute to adverse effects of water in AC pavement:[27]

- **AC-mix design**: Binder and aggregate chemistry, binder content, air voids, additives, etc.
- **AC-mix production**: Percent aggregate coating and quality of aggregates passing the No. 200 sieve, temperature at production plant, excess aggregate moisture content, and presence of clay.
- **AC placement and construction**: Insufficient compaction resulting in high in-place air voids, high permeability, mix segregation, and significant change between mix design and field production, increasing materials variability.

- **Climate**: High rainfall areas, freeze–thaw cycles, etc.

- **Other factors**: Surface drainage, subsurface drainage, and rehabilitation strategies such as chip seals over marginal AC materials.

Herrington, Reilly, and Cook reported that environmental factors cause the oxidation of asphalt binders, making them brittle.[28] Oxidation occurs faster in AC mixes with high porosity compared to conventional dense mix and leads to AC particle loss and disintegration (e.g., raveling). Resistance to AC particle loss depends not only on selecting more oxidation resistance asphalt binders, but also on asphalt binder film thickness, aggregate gradation, and AC-mix percentage of air voids. Transverse cracking in AC pavements has long been observed in both the northern and southern Unites States and Canada (i.e., in both cold (arctic and subarctic) and warm climates). Many studies have been conducted to ascertain the causes of transverse cracking and mitigating factors.[6,9,11]

For cold climates, the primary causes of transverse cracking are environmental factors that trigger the following mechanisms:[11]

- The combination of pavement base and subgrade material types and properties and extremely low temperature cycles causes the contraction of the entire pavement structure, including the subgrade. Specifically, transverse cracking extends across the entire pavement, including the subgrade, and can be up to 1 inch wide. This type of cracking is more associated with the base and subgrade than the AC surface mix and can occur on both paved and unpaved pavements. Crack spacing is typically 40–300 ft.[11]

- Low temperature also leads to volumetric contraction of the AC material, causing it to shorten if unrestrained. If the AC material is restrained (as is the case of pavements), the tendency for contraction leads to the development of thermal tensile stresses that, if greater than the material strength, can cause fracture. Note that although AC materials in warm climates are viscoelastic by nature and can dissipate thermal stresses through stress relaxation, for colder climates, AC materials behave like elastic materials and thus thermal stresses lead to cracking.[11]

- Repeated lower temperatures over time (along with oxidation hardening over time) can result in fatigue fracture of the AC across the pavement. These conditions result in progressively shorter crack spacing over time. The MEPDG AC transverse-cracking model assumes transverse cracks are caused by low-temperature events, either a one-time event or repeated cycles of lower-temperature events, and thus, accounts for only this mechanism for transverse cracking distress prediction.[5,12,11]

For warmer (nonfreeze) climates, studies have shown that transverse cracks are a result of actual AC shrinkage over time as the mix goes through daily and seasonally hot and cold cycles.[9,29] Transverse cracks caused by shrinkage exhibit a typical spacing of 20 to over 100 ft, and the width of these cracks continually increases over time as actual shrinkage of the AC mix occurs with temperatures cycling.[9,30] The progressive shrinkage results in higher tension of the AC until fracture occurs.[29] Although permanent progressive shrinkage may be the primary cause of transverse cracking in the warmer climates, shrinkage-induced transverse cracking is not

confined to the southern climates. The Utah Department of Transportation has reported significant shrinkage and widening of transverse cracks over time, particularly with highly absorptive aggregates.[9,29] As part of the local calibration of the MEPDG in Arizona, transverse cracks were found in warm desert valleys almost as often as at higher elevations and colder temperatures.[5,31] Many of these cracks in the warm desert had reached considerable width (e.g., 1 inch or more).

Ovik et al. reported that pumping excess water from under PCC slabs causes faulting and/or corner breaks.[10] The mechanics of pumping begin with the creation of a void under a PCC slab that water can infiltrate. (Voids are typically caused by curling and warping of a PCC slab.) Yasarer and Najjar reported that PCC permeability is an important factor for long-term PCC durability.[32] Ovik et al. also reported that differential temperatures between the surface and bottom of a slab can cause temperature gradients (as a result of the cooler side of the slab contracting while the warmer side expands, as shown in figure 1).[10] The results of the temperature gradients are curling stresses of a PCC slab. When combined with truck axle loading due to truck traffic passing over the curled-up slab, distresses, such as corner breaks, transverse midpanel and longitudinal cracking could occur. Armaghani et al. confirmed these results, observing that temperature and moisture gradients in the PCC layer contribute to critical curling stresses at the top and bottom of the PCC slab.[33] Negative temperature gradients within the slab cause an upward curling at the slab corner, leading to loss of support, corner cracks, other cracking, pumping (due to upward curling), and faulting. This phenomenon, which is usually indicative of hot, sunny, and dry paving weather and/or large temperature drops in the days following construction, is typical in pavements that exhibit large built-in gradients.

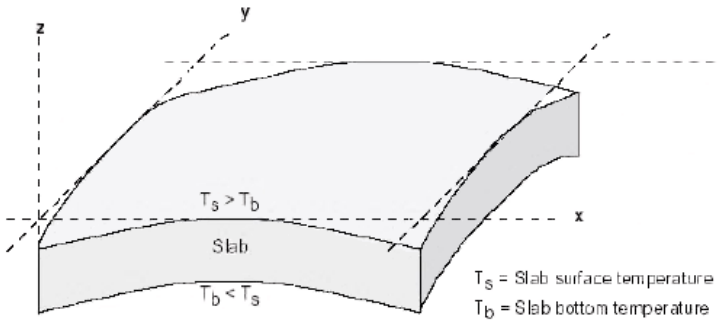

© 2008 Pavement Interactive.[24]

A. Day (surface temperature is greater than bottom temperature).

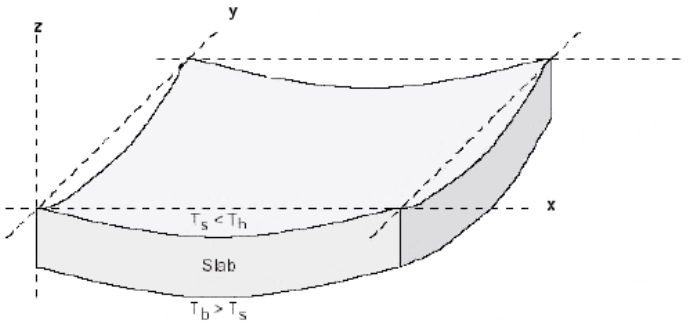

© 2008 Pavement Interactive.[24]

B. Night (bottom temperature is greater than surface temperature).

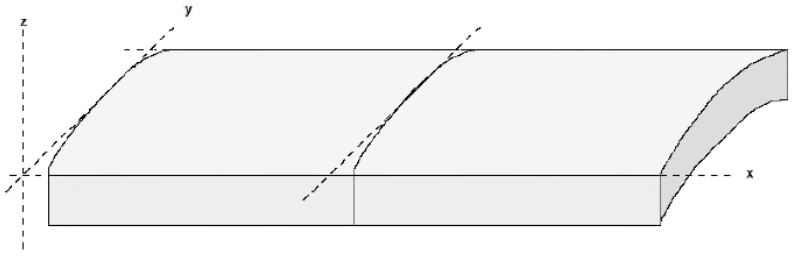

© 2008 Pavement Interactive.[24]

C. Constrained transverse joints (high mean temperature and surface temperature is greater than the bottom temperature).

Figure 1. Illustrations. Curling stresses in a typical PCC slab.[24]

Joshi et al. also observed that transverse joint load-transfer efficiency (LTE) varies cyclically because of variations in PCC slab temperature.[34] As the slab temperature decreases, the transverse joint opening tends to widen, decreasing the contact between two adjacent slabs. As aggregate interlock and friction across the PCC interface at the joint contribute to joint LTE, the increased joint opening could lead to a decrease in LTE at the joint.

Jackson and Puccinelli reviewed the performance of flexible and rigid pavements that had been in service for approximately 20–25 yr and observed the following:[8]

- Pavements in wet, nonfreeze regions exhibited less roughness than those located in wet and dry, deep-freeze regions.

- Rutting accumulations in wet and dry, moderate-freeze regions were significantly higher than in wet, nonfreeze regions.

- Wet and dry, deep-freeze regions and wet, nonfreeze regions accumulated significantly larger quantities of fatigue/wheel-path cracking than wet and dry, moderate-freeze regions.

- Wet and dry, deep-freeze regions exhibited significantly larger quantities of AC transverse cracking than wet and dry, moderate-freeze regions. The wet and dry, moderate-freeze regions also had significantly larger quantities of AC transverse cracking than the wet, nonfreeze regions.

- The magnitude of joint faulting was found to be significantly higher in dry, deep-freeze regions than in dry, moderate-freeze regions.

Doré et al. analyzed the performance of a limited number of flexible pavements in Canadian regions subjected to substantial frost penetration.[7] They observed that frost depth contributed most to the development of transverse thermal cracking in AC pavements.

Ovik et al. suggested that the environmental factor that has the most effect on PCC materials' durability is exposure to freeze–thaw cycles.[10] The most common damage from frost penetration in PCC is cracking and spalling, which are caused by the progressive expansion of the cement-paste matrix when subjected to repeated freeze–thaw cycles. The researchers also reported that scaling may occur when PCC surfaces are exposed to repeated freeze–thaw cycles with moisture and deicing chemicals present. Finally, exposure to harsh climates also can cause D-cracking (cracks that form around PCC slab corners or parallel to cracks or joints due to aggregate expansion and degradation). Ovik et al. also reported that PCC's resistance to frost damage is defined by its porosity/permeability, pore structure, degree of saturation, and rate of cooling.[10] Resistance can be enhanced by increasing PCC's tensile strength, which helps to prevent cracking or rupture and by providing the right amount of air entrainment to allow avenues of escape for moisture in the cement-paste matrix. Proper aggregate–cement mix proportions and adequate PCC curing also can enhance PCC pore structure and increase resistance to damage.

Figure 2 shows the impact of freeze–thaw cycles on the strength of PCC and cement-treated materials. PCC subjected to more frequent freeze–thaw cycles exhibited significant loss of strength when compared to the control PCC samples exposed to minimal freeze–thaw cycles.[35] Thompson et al. reported that disintegration of the lower portions of transverse joints of JPCP and jointed reinforced concrete pavement (where bases are nonpermeable) in areas like Minnesota and Michigan could be attributed to freeze–thaw cycles and the presence of deicing salts.[35] Additionally, in JPCP, joint spalling is typical in climates with large numbers of freeze–thaw cycles, particularly in PCC mixes with poor air entrainment.

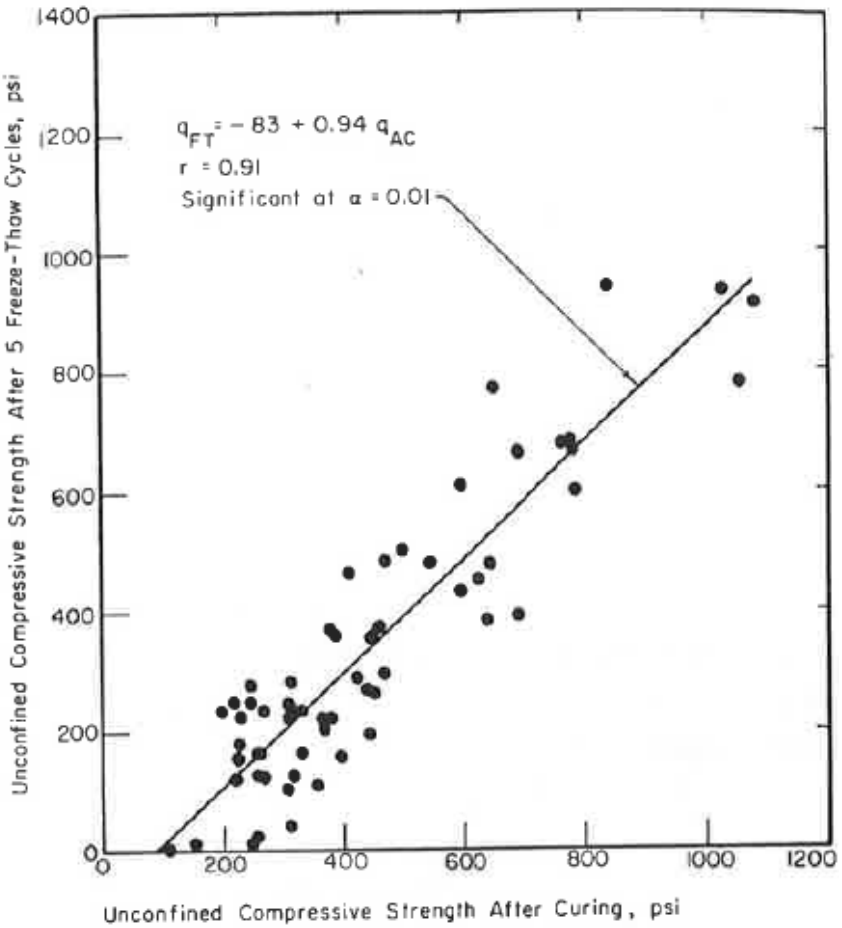

© 1987 Thompson et al.

q_{FT} = Unconfined compressive strength after 5 freeze–thaw cycles, psi;
q_{AC} = Unconfined compressive strength after curing, psi; r = Correlation coefficient;
α = Level of significance.

Figure 2. Graph. Relationship between strength of cured cement-stabilized materials and cement-stabilized materials subjected to freeze–thaw cycles.[(35)]

Thompson et al. also observed that higher-strength PCC or cement-stabilized materials generally exhibited enhanced durability and were better able to withstand imposed traffic and environmental stresses.[(35)] For example, strength development in PCC, cement-treated, or pozzolanic-stabilized materials depends on degree days of curing (defined as maturity), with materials subjected to higher levels of degree days of curing exhibiting higher strength levels (figure 3). McLeod and Kirkvold reviewed the outcomes of multiple studies investigating the causes and prevention of D-cracking in Kansas, and their study suggests that D-cracking was due to freezing and thawing of water-saturated, nondurable coarse aggregates.[(36)]

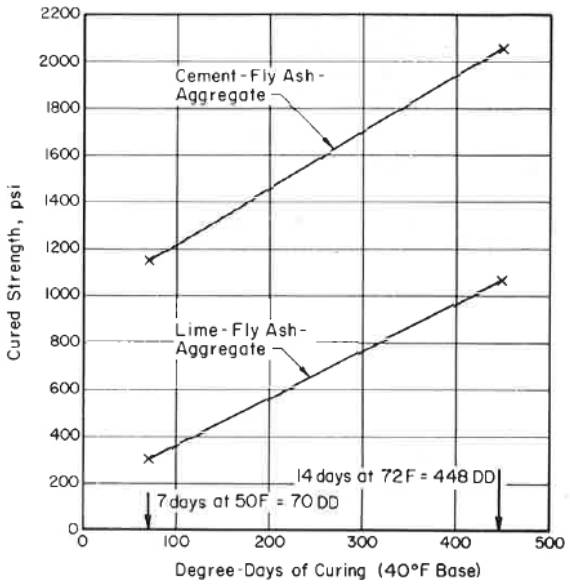

© 1987 Thompson et al.

Figure 3. Graph. Cured Strength versus degree days of curing for cement-stabilized base.[35]

Effect of Foundation/Subgrade Type on Pavement Performance

Thompson et al. reported that subgrade gradation, mineralogy, and plasticity index (PI) influence water retention characteristics.[35] The mechanical behaviors of subgrades are affected by the presence of excessive moisture with increasing or decreasing moisture content, resulting in significant loss of strength and modulus. Wet unbound materials and subgrades are more likely to experience shear failure when subjected to traffic loads, and materials that contain significant amounts of fines are more likely to pump water when subjected to the combined effects of excessive moisture and traffic loading (figure 4).

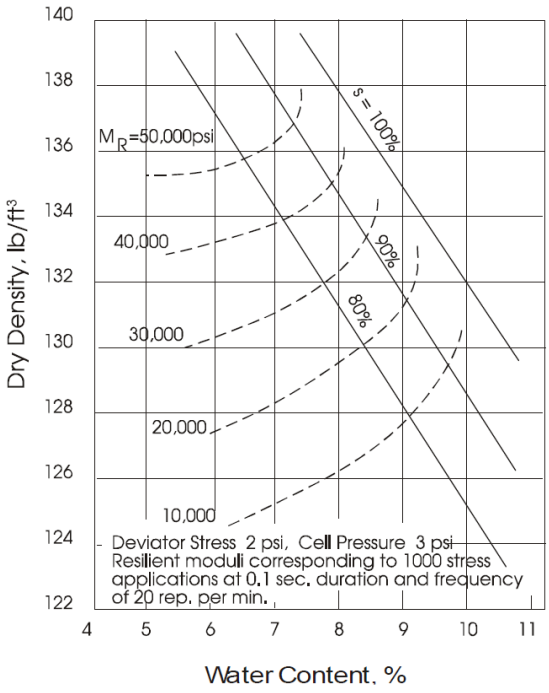

© 1989 Carl L. Monismith.
M_R = resilient modulus, psi; S = percent saturation.

Figure 4. Graph. Relationship between resilient modulus of unbound base material and water content.[37]

Ovik et al. reported that free water infiltrating into the voids beneath the PCC (that does not easily drain out) may cause a loss of cohesion in the soil and create a mud-like mixture of water and soil.[10] The application of traffic loads on the PCC slab overlying a weak saturated mud-like base or subgrade material would cause significantly higher levels of PCC slab corner/edge deflections, resulting in the ejection of underlying base or subgrade material and water through the joints, cracks, or edge of the slab. There also would be movement of material from under the approach to leave the slab if joint or crack LTE is low. This loss or movement of supporting material under the PCC slab will eventually lead to faulting and corner cracking.

Several research studies have reported various mechanisms initiated when moisture infiltrates a swell-susceptible soil.[38–40] Collectively, these studies reported that moisture loss or drying causes shrinkage of subgrades, resulting in a decrease in volume. Internal stresses generated within the soil as it dries up cause shrinkage or desiccation cracks to appear. The cracks are created in preexisting planes of weakness within soil clods. Shrinkage of the soil also causes a decrease in its height and subsidence at the surface of the soil. An increase in the soil's moisture content, however, can result in an increase in soil volume and swelling. The process of swelling is due mainly to chemical actions resulting from an interaction between water molecules and the soil's (clay) active ingredients.

Zhang and Macdonald also observed that changes in subgrade material properties may not be attributable to moisture changes alone.[41] For pavements subjected to deep frost and freeze–thaw cycles, plastic strain in the subgrade can increase up to 60 to 75 percent during the thaw period.

The researchers attributed this increase in strain to movement, reorientation, and resettlement of the subgrade particles displaced by previous frost heave.

Based on the analysis of limited laboratory resilient modulus test data, Zhang and Macdonald observed that subgrade moisture content has a major influence on resilient modulus.[41] The authors also reported that the percentage of fines in a subgrade was not the best indicator of a material's sensitivity to moisture (characterized in terms of the effect of moisture content on subgrade resilient modulus). Rather, the coefficient of uniformity and coefficient of curvature are better indicators for identifying soils with a good correlation between moisture content and resilient modulus.

Janoo et al. reported that three conditions must be present for frost heaving to occur: frost-susceptible soils, freezing temperatures, and water.[42] Frost susceptibility of a soil generally depends on the amount of fines passing the No. 200 sieve. These findings agree with Casagrande, who observed that a soil can be considered non-frost-susceptible if less than 3 percent of its particle sizes are less than 0.787 mil.[43] A uniform soil with a nonuniformity index of less than 5 only shows frost-susceptible properties if it includes more than 10 percent particle sizes of less than 0.787 mil.

Ducker further investigated the issue of what makes a soil frost-susceptible.[44] The author reported that there was no natural dividing line between non-frost-susceptible and frost-susceptible soils. The frost properties of a subgrade are influenced not only by the percentage of grain sizes below 0.787 mil but also by the mineralogy and chemical composition of its fine materials, as these properties determine the amount of water available that can be subjected to freezing and thawing, the amount of water at the frost line, and the extent of frost heave, which is based on the amount of free water available.

It is generally agreed that, for unbound base and subgrades to perform adequately in environments experiencing repeated seasonal freeze–thaw cycles, they must exhibit an exceptionally low heave during freezing and retain a significant amount of strength during thawing. Figure 5 shows the mechanism of frost damage in pavements. State transportation departments routinely base the adequacy of unbound materials and subgrades on properties such as the amount and plasticity of fines within the materials. An example is the Federal Housing Administration report relating swelling potential to the Unified Classification System (table 2).[45] Regardless of which swell potential classification system is applied, it generally is agreed that unbound materials and soils having clay content of 30 percent or greater and a PI of greater than 35 percent will have high swelling potential.

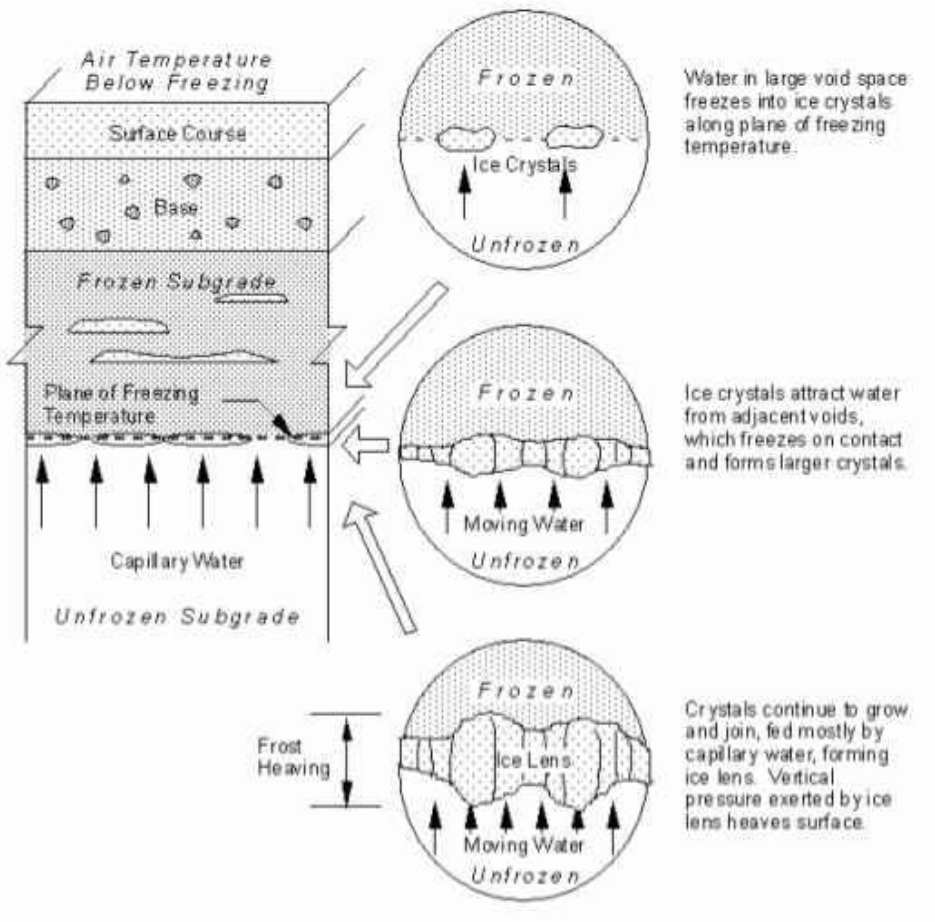

© 2008 Pavement Interactive.

Figure 5. Illustration. Mechanism of frost damage in pavements.[46]

Table 2. Swell potential for unbound materials and subgrades (data from Federal Housing Administration 1960).[45]

Swell Potential	Unified Classification System Soil Class
Little or no expansion	GW, GP, GM, SW, SP, SM
Moderate expansion	GC, SC, ML, MH
High volume change	CL, OL, CH, OH
No rating	Peat

The classification system shown in the table 2 is as follows:

- **First letter**: G = gravel, S = sand, M = silt, C = clay, and O = organic.
- **Second letter**: P = poorly graded (uniform particle sizes), W = well graded (diversified particle sizes), H = high plasticity, and L = low plasticity.

The major effect that expansive subgrades have on pavement performance is loss of smoothness. Johnson reported that, in general, pavements constructed over expansive clay subgrades

experience significant increase in International Roughness Index (IRI), whether heavily trafficked or not.[47] The cause of IRI increase on such pavements is attributed to the differential volume change in the subgrade. Swell- and heave-susceptible subgrade materials for all pavement types are more likely to deform with increased wet/dry seasonal cycles and deep frost penetration.

A significant portion of the United States includes soils and climate conditions that are conducive to heaving or settlement from moisture change or from deep frost penetration.[8,48] To mitigate the effect of frost-susceptible soils on pavement performance, States that routinely experience deep frost (e.g., Alaska, Idaho, Illinois, Indiana, Michigan, New York, North Carolina, Ohio, and Pennsylvania) have utilized construction specifications requiring additional surfacing or replacement of frost-susceptible soils with frost-free surfacing for a depth of 3–6 ft.[8]

MITIGATING THE EFFECTS OF THE ENVIRONMENT ON PAVEMENT DETERIORATION

Pavement engineers have routinely considered the effects of environment on LTPP in pavement design, construction, materials selection, and M&R treatment design by performing the following:

- Employing regional factors to create local adjustments to general pavement design equations or requiring special material properties to control environmental distresses.
- Incorporating environment-related variables, such as subgrade type and annual rainfall, in models to predict pavement performance.
- Modeling ambient and in situ pavement moisture and temperature regimes, including full-scale simulation of the interaction between in situ pavement moisture and temperature regimes and short- and long-term paving material properties (e.g., strength and modulus).
- Developing paving materials that resist environmental effects (e.g., Superpave mixes).
- Improving construction practices (e.g., curing) to mitigate the effect of environmental factors, such as built-in temperature gradients in PCC.

Cumulatively, these advances in research have helped the pavement community gain more indepth understanding of the interaction between pavement performance and environmental factors and develop actions to mitigate the impact of environmental factors on performance.

SUMMARY

This review of past studies shows that damage and distresses in pavements cannot be attributed to a single factor but rather are caused by the combination of traffic loading, materials, subgrade, environment, and construction. For example, pumping and erosion of a JPCP could not occur without a pumping-susceptible base material containing excessive moisture from either seepage of rainfall into the pavement structure or high water table causing capillary suction from the

underlying water table. Likewise, without repeated heavy truck-traffic loading, there could be no pumping. Properly sized dowels and tied PCC shoulders would reduce deflections so much that less pumping and erosion would occur. Therefore, the primary causes of pumping include heavy truck traffic, lack of load-transfer devices, and excess free water in pavement sublayers. Contributing factors include materials and climate (particularly temperature gradients causing upward curling of slabs). Other distress types have similar causes. An asphalt example would include low-temperature transverse cracking of which low temperature is a major cause; however, the characteristics of the AC mix would contribute greatly to the extent of cracking. Load would also contribute to the severity of the transverse cracks after they form and deteriorate from low to medium to high severity. Table 3 and table 4 are based on the authors experience and supplemented by information from the literature. (See references 8, 17, 31, and 33.) Table 3 and table 4 summarize the predominant causes of pavement damage/distress for flexible and rigid pavements, respectively.

For pavement distress to occur, two sets of factors need to be present simultaneously on a given project: initiators and aggravators. Initiators induce mechanisms, such as critical strain, stress, deflection, and differential deflection across joints and cracks, that initiate damage that eventually manifests as major distress and IRI increase. Distress cannot occur without an initiator. Aggravators magnify the impact of initiators and are responsible for distress progression in terms of extent and severity.

Table 3. Common AC pavement distresses and their predominant causes. (See references 8, 17, 31, and 33.)

Distress Type	Description and Failure Mechanism	Load	Environment			Material	Construction
			Moisture	Temp.	Subgrade		
Alligator cracking	Alligator cracking is caused by horizontal tensile strain at the bottom of the AC layer due to repeated application of heavy truck axles. The horizontal strains initiate the development of microcracks that eventually propagate to the top of the AC layer. The extent of cracking is aggravated by the presence of a weak AC surface, base, or subgrade layer; thin AC surface or base layer; and poor drainage.	P	C	C	C	C	C
Bleeding	Bleeding is due to excessive asphalt in the surface AC mix relative to the available air-void space. This situation leads to the excess asphalt that cannot be accommodated by the available air-void space being forced out through the AC surface, resulting in bleeding in hot temperatures. Bleeding can also be caused by placement of too heavy a prime or bond/tack coat under the AC layer or the use of excessive AC sealant in the cracks or joints under an overlay. Application of truck traffic can cause densification/compaction of the AC layer, forcing excess asphalt in the AC mix to the surface during hot temperatures.	C	C	C	N	P	C
Block cracking, contraction, and shrinkage fracture	Block cracking, contraction, and shrinkage fracture are caused by the permanent shrinking and hardening of the asphalt due to age and/or environment (temperature) or placement of dry AC mix or fine-aggregate AC mix with low penetration asphalt and absorptive aggregates. Block cracking is typically aggravated by low-traffic volume.	N	C	C	N	P	C
Corrugation	Corrugation is caused by horizontal plastic movement in the AC surface layer when subjected to traffic and typically occurs when the surface AC mix has excessive amounts of asphalt cement or fine aggregates, smooth coarse aggregates, low air voids, excessive moisture or contamination of excess fines in the granular base, and softness of the AC grade.	P	C	C	N	C	C
Depression	Depression is localized consolidation or movement of the pavement's lower base or subbase supporting layers. Localized consolidation is mostly due to variability and weakness or instability of the base or subbase layer materials or application of improper construction techniques.	P	C	N	C	C	C

Distress Type	Description and Failure Mechanism	Load	Environment			Material	Construction
			Moisture	Temp.	Subgrade		
Edge cracking	Edge cracking is caused by a combination of axle loading at the pavement edge (usually related to the use of narrow lanes that allows wheel loads at the edge), lack of lateral support at the pavement edge (again due to the use of narrow lanes), settlement of underlying material, shrinkage or drying out of soil, weak base or subgrade layer, poor drainage, and frost heave and settlement.	C	C	N	P	N	C
Transverse cracking	Transverse cracking is caused by several mechanisms and/or a combination of mechanisms, including shrinkage of asphalt surface due to low temperatures and/or repeated low temperatures, excessive hardening of asphalt cement, permanent shrinkage of the AC mix due to absorption of asphalt into aggregates or reduction of air voids, or reflective cracks projected from cracks below the AC layer. Transverse cracks caused by low temperature are referred to as thermal cracks.	N	N	P	N	C	C
Longitudinal cracking in the wheel path	Longitudinal cracking in the wheel path could be the initial stage of bottom–up fatigue (alligator) cracking or from top–down fatigue cracking, which may occur in thick AC layers. Top–down fatigue cracking is associated with the state of tensile bending stress near a wheel load.	P	N	C	C	C	C
Longitudinal cracking outside the wheel path	Longitudinal cracking outside the wheel path is caused by poorly constructed paving joints, reflection from underlying pavement joints, shrinkage of surface layers due to temperature cycling, or hardening of asphalt.	N	N	C	C	C	P
Potholes	Potholes are localized pavement disintegration because of traffic loads and inadequate strength in one or more layers of the pavement, usually accompanied by the presence of water.	C	C	C	N	P	C
Pumping	Pumping is the seeping or ejection of water and fines from beneath the AC surface layer through cracks or joints under the applications of heavy vehicle loadings, causing loss of support.	P	C	N	C	C	N
Raveling (weathering)	Raveling (also known as weathering) is the result of a loss of adhesion between the asphalt binder and the aggregate causing the loss of material from the pavement surface.	C	C	C	N	P	C
Rutting	Rutting is caused by excessive vertical compressive stresses, resulting in permanent vertical strain and nonrecoverable permanent deformation in the AC, unbound base, and subgrade.	P	C	C	C	C	C

Distress Type	Description and Failure Mechanism	Load	Environment			Material	Construction
			Moisture	Temp.	Subgrade		
Shoving	Shoving is due to plastic movement in the AC surface layer caused by traffic action on unstable AC mixes with excessive amounts of asphalt, fine aggregates, or smooth coarse aggregates. The distress usually appears in localized areas, and the deformation can be longitudinal as well as vertical.	P	C	C	N	C	C
Swelling and bumps	Caused by excessive uneven stress concentration at the crack and attributable to unstable crack filler, unstable AC with low shear strength, and excessive moisture in the crack.	N	C	C	P	C	N

Temp. = temperature; P = primary factor; C = contributing factor; N = negligible factor.

Table 4. Description of common PCC pavement distresses and their predominant causes. (See references 8, 17, 31, and 33.)

Distress Type	Description and Failure Mechanism	Load	Environment			Material	Construction
			Moisture	Temp.	Subgrade		
Alkali-aggregate reactivity	Alkali-aggregate reactivity is caused by a chemical reaction that occurs when free alkalis in the PCC combine with siliceous aggregates to form an alkali-silica gel. As the gel forms, it absorbs water and expands, which cracks the surrounding concrete.	N	P	C	N	P	N
Blow-up	A blow-up occurs mostly on long JRCPs with far fewer on shorter JPCP and continuously reinforced concrete pavement. It is caused by excessive compressive pressure at PCC joints or cracks. Infiltration of incompressible materials into the joint or crack during cold periods results in high compressive stresses during hotter periods when the slabs expand. When this compressive pressure becomes too great, a localized upward movement of the slab and a complete shattering occurs near the joint. Blow-ups are accelerated due to the spalling away of the slab at the bottom, thus creating an area of reduced joint contact.	N	C	P	N	C	N
Corner breaking	Corner breaking results from heavy repeated loads combined with pumping, poor load transfer across joints, and thermal curling and moisture warping stresses. Corner breaks can also result from a weak or a thin concrete section constructed on a weak base.	P	C	C	N	N	N
Depression	Depression is due to differential settlement, consolidation, or movement of the underlying layer foundation soil. Settlement and consolidation commonly occur due to poor compaction or varying moisture contents of underlying pavement layers, densification of backfill, or at grade points between cut and fill sections.	N	C	N	P	N	C

Distress Type	Description and Failure Mechanism	Load	Environment			Material	Construction
			Moisture	Temp.	Subgrade		
D-cracking	D-cracking is caused by freeze–thaw expansive pressures of certain types of saturated coarse aggregates and typically begins at the bottom of the slab but also at the top of the slab.	N	P	P	N	P	N
Transverse joint faulting	The buildup of eroded or infiltrated material under the approach slab is caused by pumping materials backwards from traffic direction from under the curled-up leave slab and shoulder (free moisture under pressure) due to deflections from heavy loads. Four conditions must exist to cause pavement faulting: (1) slab curling due to thermal and moisture gradients within the PCC slab, (2) fines in the underlying base or subbase that can be moved around by water infiltration into the underlying pavement layers to pump/carry the fines from the underlying materials, (3) significant difference in deflection when adjacent slabs are subjected to wheel loads at the joint (i.e., poor load transfer), and (4) many repeated heavy axle loads.	P	P	C	C	C	N
Joint-seal failure	Typical types of joint-seal damage are stripping of joint sealant, extrusion of joint sealant, weed growth, hardening of the filler (oxidation), loss of bond to slab edges, and the lack of sealant in the joint. Poor construction of the joint seal can be a factor in the extent of joint seal damage.	N	C	C	N	P	C
Lane/shoulder drop-off	Lane/shoulder drop-off occurs when the outside shoulder settles due to underlying granular or subgrade materials or to pumping of the underlying materials.	C	P	P	C	C	N
Longitudinal slab cracking	Longitudinal slab cracking is caused by a combination of heavy load repetitions, loss of foundation support, and thermal and moisture gradient stresses caused by excessive upward slab curling. Early longitudinal cracks can be caused by improper construction of longitudinal joints, inadequate saw-cut depth, late sawing of longitudinal joints, wide slabs (greater than 12 ft), and/or opening the pavement to traffic before the concrete has achieved adequate strength.	P	C	P	C	C	P
Spalling (longitudinal and transverse joints)	Spalling is caused by slab expansion and contraction, which opens joints and allows incompressible debris to be trapped in the joint. As the joints close, trapped incompressible debris causes excessive stresses, resulting in fractures of the slab and enlarging of the joints. The enlarged joints permit larger debris to be trapped and consequently cause greater fractures. Spalling is aggravated by weak concrete at the joint, joint sawing time or insertion method	C	C	P	N	P	C

Distress Type	Description and Failure Mechanism	Load	Environment			Material	Construction
			Moisture	Temp.	Subgrade		
	during construction, poorly designed or constructed load transfer device (misalignment or corrosion), heavy repeated traffic loads, and disintegration of the concrete from freeze–thaw action.						
Aggregate polishing	Aggregate polishing occurs when the surface mortar and texturing have been worn away. The exposed coarse aggregates (unless they exhibit excessive hardness) are then polished through the continuous attrition or abrasion caused by repeated traffic application.	C	N	N	N	P	N
Popouts	Popouts are caused by the use of unsound weak coarse aggregates or D-cracking that expands when saturated.	N	C	C	N	P	C
Pumping	Pumping is the movement of base or subbase material underlying the PCC slab caused by the buildup of high-differential water pressure beneath adjacent PCC slabs when one slab is deflected under a heavy moving wheel load. The buildup of differential water pressure occurs when load transfer across the PCC joint or crack causing high differential deflections is inadequate.	P	P	N	C	C	N
Random (map) cracking, scaling, and crazing	Random cracking, sealing, and crazing are usually caused by over-finishing of the slab, resulting in excess water and mortar at the surface, premature finishing, or early freezing of PCC that may lead to scaling of the surface. Scaling can also be caused by reinforcing steel, such as dowels and tie bars, placed too close to the PCC surface.	N	N	C	N	C	P
Shattered slab	Shattered slab is caused by a combination of heavy load repetitions on pavement with weak foundation support, upward slab curling, and loss of support of base or subgrade moisture-induced stresses.	P	C	N	C	C	N
Swelling	Swelling is caused by the presence of expansive soils (which swell in the presence of increased moisture) and frost heave (in which ice lenses grow beneath the pavement, causing the pavement to crack).	N	P	P	C	C	N
Transverse slab fatigue cracking	Fatigue cracking occurs when tensile stresses at the top or bottom of slabs result in significant bending fatigue damage. This is typically a result of a combination of stresses due to temperature gradients within the PCC, PCC drying shrinkage, thermal curling, PCC–base interface constraint, and moisture warping combined with heavy-traffic axle loads.	P	N	C	C	C	P

Temp. = temperature; P = primary factor; C = contributing factor; N = negligible factor; JRCP = jointed reinforced concrete pavement.

Figure 6 illustrates factors (i.e., traffic loadings, pavement structure, and climate) that lead to pavement deterioration and distress. The figure also shows factors that initiate distress and factors that aggravate the amount and severity of distress. Of course, there are many interactions between all of these factors, initiators, and aggravators.

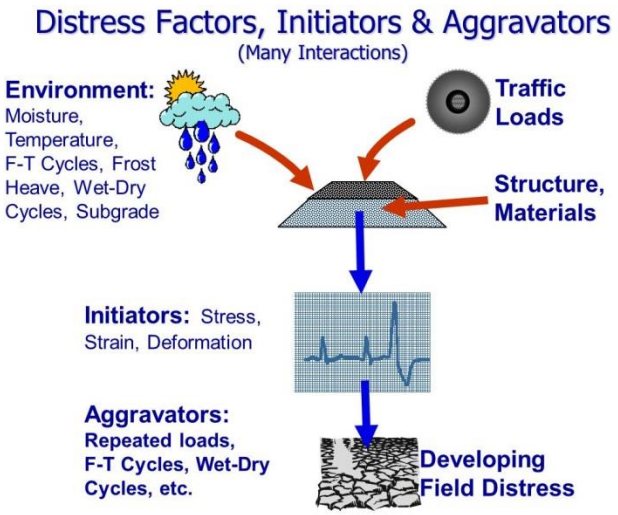

Source: FHWA.
F-T = freeze–thaw.

Figure 6. Illustration. Factors, initiators, and aggravators affecting pavement performance.

Recently, pavement design techniques have been improved to include mechanistic-based distress prediction models (e.g., initiators of distress directly considered) that have been empirically calibrated to explain and mitigate some environmentally induced distress. These techniques have been used with some success to predict when such distresses will become too high and design or material changes are needed to prevent this from occurring. However, most of these prediction models are related to traffic loadings and only a few (e.g., transverse cracking of AC pavement) to specific environmentally induced distresses. What the highway community lacks is a larger set of field performance data that allows the calibration, validation, and incorporation of additional environmental distress prediction models in pavement design procedures over a wide range of climatic conditions. (LTPP can provide a lot of these data.)

CHAPTER 3. OVERVIEW OF ANALYSIS PLAN FOR DETERMINING THE IMPACT OF ENVIRONMENTAL FACTORS ON FLEXIBLE AND RIGID PAVEMENT PERFORMANCE

A key objective of this study was to determine the impact of environmental factors on AC and PCC pavement performance. To achieve this objective, a pavement-evaluation and -analysis plan was developed. Key aspects of this plan include the following:

- Identifying AC and PCC pavement with similar designs, materials, and construction practices subjected to similar environmental conditions across the United States.
- Separating the identified pavement projects into those that are heavily trafficked and those that are low trafficked (SPS-8).
- Comparing the performance of the heavily trafficked and low-trafficked pavement projects after 15 yr in service.

By comparing the condition of pavements that experience different amounts of traffic in various environmental regions after 15 yr in service, the impact of environmental factors and traffic loadings on pavement performance was characterized. The analysis and evaluation plan was also designed to quantify the effectiveness of increasing AC and PCC thicknesses to mitigate the onset and progression of distress. Key components of the pavement-analysis and -evaluation plan were as follows:

1. Develop a project-sampling template.
2. Identify heavily trafficked and low-trafficked LTPP projects for populating the sampling template.
3. Determine key data variables (e.g., design, construction, climate, subgrade, and performance) required for conducting pavement performance and condition evaluation and comparison.
4. Assemble a project database with relevant data variables for use in analysis.
5. Review and clean the assembled database. Perform a preliminary review of the assembled data to determine reasonableness of data, identify outliers and erroneous data, and clean the assembled data as needed.
6. Perform a data analysis by evaluating and quantifying pavement performance and the impact of environmental (i.e., climate and subgrade), traffic (i.e., truck applications), and design (e.g., AC and PCC thickness) factors on performance. Determine the extent of pavement damage due to environmental factors, traffic, and a combination of the two.

Detailed descriptions of the steps are presented in the following subsections.

STEP 1—DEVELOP PROJECT-SAMPLING TEMPLATE

A detailed, statistically sound experimental plan was developed as part of the LTPP program to evaluate the performance of in-service AC and PCC pavement in the absence of heavy loads and compare that to the performance of similar designs subjected to typical numbers of heavy loads. This experimental plan formed the basis for analysis and pavement evaluation for this project. The approach was as follows:

1. Identify in-service typical AC and PCC pavement projects constructed with typical pavement materials and designs within the United States that have similar environmental conditions loaded by typical volumes and weights of trucks as well as very low volumes of trucks.

2. Divide the identified pavement projects into those heavily trafficked (meaning normal axle weight distributions and numbers of trucks) and those subjected to only a small number of heavy trucks but having the same design thicknesses and materials.

By comparing the performance of the two pavement groupings, the impact of environmental factors on performance could be estimated. Since the objective of this study was to identify and quantify the impact of environmental factors on pavement performance in the absence of heavy traffic, baseline projects for performance analysis and evaluation were the in-service AC and PCC LTPP projects exposed to very low levels of heavy truck loads, while companion projects were those of similar designs, construction practices, and material types subjected to typical volumes of heavy truck traffic.

A project sampling template was developed to help identify potential LTPP projects for evaluation and analysis methods to meet project objectives (figure 7).

Structure			Traffic Loading																									
			Low Truck Traffic—Absence of Heavy Loads												Typical Truck Traffic—Presence of Heavy Loads													
			Wet						Dry						Wet						Dry							
			Freeze			Nonfreeze			Freeze			Nonfreeze			Freeze			Nonfreeze			Freeze			Nonfreeze				
Type	Surface Thickness, in	Base Thickness, in	Active	Fine	Coarse	Active	Fine	Coarse	Active	Fine	Coarse	Active	Fine	Coarse	Active	Fine	Coarse	Active	Fine	Coarse	Active	Fine	Coarse	Active	Fine	Coarse		
AC	4	8																										
	7	12																										
PCC	8	6																										
	11	6																										

Source: FHWA.

Figure 7. Screenshot. Sampling template for heavily and low-trafficked pavement projects.

STEP 2—IDENTIFY PROJECTS FOR POPULATING THE SAMPLING TEMPLATE

Populating the sampling template required SPS-8 projects exposed to low and heavy truck-traffic volumes and companion projects exposed to heavy truck-traffic volumes. The LTPP experiments from which heavily trafficked projects were identified are the following:[17]

- **GPS-1—AC on granular base:** Projects used from this experiment include a dense-graded AC surface layer placed over an untreated granular base. One or more subbase layers may also be present but are not required. Sampling design factors for this study are moisture, temperature, subgrade type, heavy truck traffic, aggregate base thickness, and AC thickness. All factors have two levels except AC thickness, which has three.

- **GPS-2—AC on bound base:** Pavements used from GPS-2 include a dense-graded AC surface layer with or without other AC layers placed over an unbound base layer. Sampling design factors for this study are moisture, temperature, subgrade type, traffic rate, surface thickness, base thickness, and binder type. All factors have two levels.

- **GPS-3— JPCP:** Pavements used from GPS-3 include a jointed unreinforced PCC slab placed over untreated aggregate base course only. One or more subbase layers may also be present but are not required. The transverse joints include smooth dowels. Jointed slabs with load transfer devices other than dowels are not included. A seal coat is also permissible above a granular base layer. Sampling design factors for this study are moisture, temperature, subgrade type, traffic rate, dowels, PCC thickness, and base type. All factors have two levels.

- **SPS-1—strategic study of structural factors for flexible pavements:** SPS-1 examines the effects of climatic region, subgrade (fine- and coarse-grained), and traffic rate (as a covariate) on pavement sections incorporating different levels of structural factors. Sections used from SPS-1 include AC surface thickness (4 and 7 inches), untreated aggregate base type (untreated dense-graded aggregate base (DGAB)), and base thickness (8 and 12 inches for undrained sections). The study design stipulates a traffic loading level in the study lane in excess of 100,000 ESALs per yr.

- **SPS-2—strategic study of structural factors for rigid pavements:** SPS-2 examines the effects of climatic region, subgrade (fine- and coarse-grained), and traffic rate (as a covariate) on doweled JPCP sections incorporating different levels of structural factors. Sections utilized from SPS-2 include concrete thickness (8 and 11 inches), base type (only DGAB), concrete flexural strength (550 and 900 psi at 14 d), and lane width (12 ft only). The study requires that all test sections be constructed with perpendicular joints at 15-ft spacing with dowels and stipulate a traffic load level in the lane in excess of 200,000 ESALs per yr.

Only projects similar in design and environmental exposure to the original SPS-8 projects were of interest and relevance to this study. Original projects are defined as those that conform to pavement types, designs, etc., described and specified in the SPS-8 experimental plan. The non-SPS-8 projects that met the same design standards and environmental exposure with significant truck-traffic applications were selected. LTPP projects that no longer conformed to the original

designs were included in the project database up to the point where they were no longer in conformance due to being subjected to M&R activities or reconstruction. For example, the placement of an AC overlay over an existing SPS-1 project implied the project was no longer in conformance.

STEPS 3 AND 4—DETERMINE KEY DATA VARIABLES AND ASSEMBLE PROJECT DATABASE

The LTPP program collects a vast number of data elements and variables to characterize design features, construction practices, material properties, site conditions, climate, traffic, and performance.[18–22] Of relevance to this study were data required for defining and characterizing pavement structure and properties, characterizing and forecasting future pavement performance, and performing forensic evaluation to explain possible causes of good performance or premature failures. Specifically, data variables are required for defining the following aspects of pavement for analysis:

- Pavement structure.
- Design features.
- Construction practices.
- Truck-traffic applications since construction.
- Environmental exposure (foundation and climate) since construction.
- Performance history since construction.
- M&R history since construction.

Table 5 presents the data variables and elements required from various LTPP data tables and other national databases, such as the NCDC, the U.S. Department of Agriculture's Soil Survey Geographic (SSURGO) database, and the U.S. Geological Survey's National Water Information System (NWIS) database, for use in developing the project database.[13,49,50]

Table 5. Data elements and variables collected for SPS-8 and companion projects.

Data Category	Data Elements and Variables	Data Source			
		LTPP [17]	NCDC [13]	SSURGO [49]	NWIS [50]
Inventory	State, SHRP ID, route, route signing, etc.	X	—	—	—
Construction and design	Construction reports (history, construction practices, and anomalies encountered)	X	—	—	—
Construction and design	Construction issues (layer placement, traffic opening dates, and quality-assurance testing)	X	—	—	—
Construction and design	Structure definition (materials types and thicknesses)	X	—	—	—
Construction and design	Shoulder type, width, lane width, slab width, and edge support	X	—	—	—
Construction and design	PCC transverse joint load transfer mechanism details (type, dowel diameter, length, and spacing)	X	—	—	—
Materials	AC (bulk/maximum specific gravity, asphalt content, modulus, viscosity/ penetration, gradation, etc.)	X	—	—	—
Materials	PCC (compressive/flexural/ tensile strength), elastic modulus, mix proportions, aggregate gradation and durability, CTE, curing method, and texturing method	X	—	—	—
Materials	Unbound base or subbase and subgrade (gradation, Atterberg limits, resilient modulus, etc.)	X	—	X	—
Performance	Deflections (FWD), backcalculated layer moduli, visual distress (cracking, raveling, pumping, etc.), longitudinal profile (for smoothness, faulting, etc.), transverse profile (for rut depth, etc.), and skid resistance	X	—	—	—
Traffic	Historical and monitored truck volumes and ESALs, vehicle class distribution, hourly distribution, monthly adjustment factors, and axle load spectrum	X	—	—	—
Climate	Ambient temperature, rainfall, humidity, sunshine/radiation exposure, wind speed, and depth to GWT	—	X	—	X
M&R	Significant M&R events description, timing, and materials and structural properties (material type, thickness, etc.)	X	—	—	—

—Data item not included in data source.
X = Data item included in data source; ID = identification; FWD = falling-weight deflectometer; GWT = groundwater table.

STEP 5—REVIEW ASSEMBLED DATA AND IDENTIFY/CLEAN OUTLIERS AND ERRONEOUS INPUTS

Step 5 involved the following activities:

1. Extracting and assemble all data variables identified in table 5.

2. Reviewing data for accuracy, reasonableness, and consistency; identifying outliers and erroneous data; and cleaning data as needed. Data review involved developing bivariate plots of distress and IRI versus pavement age and reviewing the plots to determine if observed trends in distress/IRI progression are reasonable, identify potential anomalies (e.g., significant decrease in distress/IRI magnitude indicating an occurrence of significant rehabilitation or maintenance event), and identifying potential outliers. For other elements, their magnitude was compared to typical values or LTPP specifications for reasonableness. Individual data and observations identified as outliers or erroneous were removed. Examples include 0 measurements that could represent nonentry values and significantly high or low values deemed unreasonable.

STEP 6—PERFORM DATA ANALYSIS

Researchers evaluated and quantified pavement performance and the impact of environmental and design factors on performance. This evaluation was achieved as described in the following subsections.

Perform Preliminary Data Analysis

A preliminary data analysis was performed as follows:

1. Group performance indicators according to mechanism of initiation and progression when possible to decrease variability and anomalies in trends and observations of a given failure type (e.g., alligator and longitudinal cracking in the wheel path for AC pavements were grouped as AC fatigue cracking).

2. Develop plots of distress and IRI versus pavement age since construction.

3. Forecast pavement distress to 15 yr. This time was chosen because most of the SPS-1, -2, and -8 projects were in service for close to 15 yr.

4. Develop histograms of mean 15-yr distress for various combinations of traffic, design, and environmental factors that impact pavement damage/distress and compare mean 15-yr distress/IRI values of the various groupings to determine significant differences. For the preliminary evaluation, significance in mean 15-yr distress values was established if the actual difference in values was greater than 1 standard deviation of the typical distress/IRI measurement error.

Perform a Detailed Statistical Analysis

Statistical analysis for this report was conducted using SAS/STAT® software Version 9.3.[51] The SAS® software generalized model selection procedure, GLMSELECT, which implements statistical model selection in the framework of general linear models, was used to determine the subset of environmental and other (traffic and AC thickness) variables most correlated to distress/IRI. The goal was to determine the environmental factors that initiated distress/IRI development (analysis of low-trafficked SPS-8 projects) and the environmental and other variables that initiates, aggravates, and/or causes the progression distress/IRI (analysis of both low- and high-trafficked projects). Once the initiator and aggravator variables were identified, an analysis of variance (ANOVA) was performed to determine the significance of the identified variables on distress/IRI. Detailed statistical analysis (model variable selection and ANOVA) was performed as follows:

1. Analyze the assembled distress/IRI dependent variable and design, traffic, and environmental independent variables using the statistical model selection procedure through GLMSELECT to determine the best subset of independent variables that impact predicted distress/IRI after 15 yr. This step is key as, when faced with several independent variables that could possibly impact distress/IRI, a natural question is what subset of the variables most impacts the distress. Selection of independent variables that influence distress/IRI was based on two criteria: a 15 percent significance level of entry (SLE) and the selection process terminated when adding additional variables to the model increased the predicted residual sum of squares (PRESS). Determination of variables that most impact distress/IRI was done separately for low-trafficked SPS-8 projects and for the low- and high-trafficked companion projects together.

2. Perform ANOVA using the variables identified to determine significance of initiators and aggravators. The steps for conducting ANOVA were as follows:

    a. Assemble data items of relevance (distress/smoothness after 15 yr in service, thickness, subgrade type, climate, etc.) from SPS-8 and companion projects into a format required for performing ANOVA.

    b. Develop generalized linear models for use in ANOVA, as shown in figure 8. For the generalized linear models, traffic, surface AC or PCC thickness, climate, and subgrade were classified into categories (e.g., thin and thick) rather than continuous variables to facilitate development of design and construction recommendations. The interactions of these factors were also investigated (e.g., is thickness more significant in cold or wet climates?).

$$PERF\_IND = \alpha + \alpha_1 THK + \alpha_2 TRAF + \alpha_3 FREEZE + \alpha_4 ACTIVE + \alpha_5 FINE + \alpha_6 COARSE + \alpha_7 WET + \alpha_8 INTERACTIONS$$

Figure 8. Equation. Generalized linear model relating performance indicators to pavement environmental, design, and traffic variables.

Where:

PERF_IND = performance indicator (distress, IRI).
α, α_1, α_2, α_3... α_8 = regression coefficients.
THK = thickness of AC or PCC.
TRAF = traffic level.
FREEZE = freeze-temperature zone.
ACTIVE = active subgrade (potential for swelling or frost heave).
FINE = fine-grained subgrade.
COARSE = coarse-grained subgrade.
WET = wet/dry climate.
INTERACTIONS = interactions between any of these variables.

c. Run the SAS® ANOVA procedure for each distress/IRI performance indicator type and determine which of the independent variables identified through the statistical model selection procedure were significant for SPS-8 projects only (absence of heavy loads) or SPS-8 and other SPS/GPS companion projects (low and heavy loads).

d. Summarize ANOVA output results for SPS-8 (alone) and SPS-8 and companion projects (combined) separately.

e. Compare output summaries and determine independent variables that are initiators and aggravators of each distress/IRI of interest separately. A key objective of this study was to determine the impact of environmental variables on distress/IRI initiation and progression. Steps 1 and 2 were designed to answer this key study objective and will help determine the levels of environmental factors that are highly detrimental to pavement performance and will require special design considerations to minimize their effects (temperature, moisture, subgrade type, etc.).

Determine the Proportion of Overall Pavement Damage Due to Environmental Factors

The procedure for estimating pavement damage was based on a methodology developed and successfully implemented in several past pavement research studies, including the AASHO Road Test and the FHWA-sponsored highway cost allocation studies.[4,52] Pavement damage was determined as follows:

1. Estimate pavement damage. Pavement damage was estimated separately for each distress type and IRI for each project. Distress/IRI pavement damage was defined based on a modified version of the AASHO Road Test mathematical definition of pavement damage as shown in figure 9.[4] This pavement damage model was used to estimate damage for each project for each distress type and IRI separately.

$$g = \left(\frac{P_i - P}{P_i - P_t}\right)$$

Figure 9. Equation. Determination of pavement damage from performance indicators.

Where:

g = damage ranging from 0 to 1.
P_i = initial pavement distress/IRI condition (defined based on distress/IRI of interest).
P = distress/IRI value after 15 yr in service.
P_t = terminal distress/IRI value.

The research team adopted a consensus acceptable terminal distress/IRI values based on current highway agency practices.

2. Estimate pavement damage by traffic (i.e., low and high traffic) and other environmental and design factors as needed for each distress type and IRI. Estimate mean damage for each group. Total damage for a group was defined as the mean damage computed for the high-trafficked pavement projects within the group, while damage due to environmental factors alone was that computed for SPS-8 projects alone within the group. The proportion of total damage due to environmental factors alone for a given group was computed using the equation shown in figure 10. Note that the methodology described was used to estimate damage for individual distress types (e.g., alligator cracking, transverse cracking) for various combinations of traffic and environmental factors.

$$\text{PCT\_DAM}_{\text{ENV-P}} = 100 * \frac{g_{ENV-P}}{g_{TOTAL-P}}$$

Figure 10. Equation. Determination of percentage of pavement damage for a given performance indicator.

Where:

PCT_DAM_{ENV-P} = percentage of overall pavement damage attributed to environmental factors only.
g_{ENV-P} = overall pavement damage due to environmental factors computed for SPS-8 projects only.
$g_{TOTAL-P}$ = overall total pavement damage computed for non SPS-8 projects only.

3. Determine the portion of overall (i.e., all distress types and IRI combined) pavement damage due to environmental factors using the following steps:

   a. Determine weighting factors for each distress type and IRI. Weights were determined using the deduct-value (*DV*) approach and weighting factors developed for the Pavement Condition Index (PCI) (i.e., ASTM D6433).[51] Thus, overall pavement damage was defined mathematically as a weighted average of the individual distress type/group damage as shown in figure 11. By adopting this overall-damage approach, the impact of all causes of overall pavement damage was considered in computing overall pavement damage. The approach also allowed for the adoption of various weighting scenarios (PCI *DV*s weighting versus equal weighting) and assessment of weights on damage-proportioning analysis.

$$g_{TOTAL} = \frac{\sum_{i=1}^{k}(W_i * g_i)}{\sum_{i=1}^{k}(W_i)}$$

Figure 11. Equation. Determination of overall pavement damage for all selected performance indicators of interest.

Where:

W_i = weight assigned to a given distress/IRI damage (i) based on the PCI *DV*s.
g_i = given distress/i (specific distress/IRI).

b. Estimate mean damage for each group. *Total damage* is defined as the damage computed for the high-trafficked pavement projects (GPS-1 and -3 and SPS-1 and -2), while damage due to environmental factors alone was computed for only SPS-8 projects.

The proportion of total damage due to environmental factors alone was computed using the equation in figure 12. By comparing the overall damage estimated from lightly loaded SPS-8 projects and from heavily loaded non-SPS-8 projects, the portion of overall damage that can be attributed to environmental factors was determined. The outcomes are described in subsequent chapters of this report.

$$\text{PCT\_DAM}_{\text{ENV\_TOTAL}} = 100 * \frac{g_{ENV\_TOTAL}}{g_{TOTAL\_DAMAGE}}$$

Figure 12. Equation. Determination of percentage of overall pavement damage for all selected performance indicators.

Where:

$PCT\_DAM_{ENV\_TOTAL}$ = percentage of overall pavement damage attributed to environmental factors only.
$g_{ENV\text{-}TOTAL}$ = overall pavement damage computed for SPS-8 projects only.
$g_{TOTAL\text{-}DAMAGE}$ = overall pavement damage computed for non SPS-8 projects only (high-trafficked projects).

CHAPTER 4. DEVELOPMENT OF PROJECT SAMPLING TEMPLATE AND POPULATE WITH LTPP PROJECTS

DEVELOPMENT OF SAMPLING TEMPLATE

A project-sampling template was developed for identifying heavily trafficked and low-trafficked projects for performance evaluation. Key issues considered in developing the template were design features, environmental factors, and traffic. The key factors for defining the sampling template were adapted after LTPP SPS experimental plans and are described in further detail in this chapter.

Key climate factors include the following:

- **Wet regions:** Average annual rainfall less than 20 inches.
- **Dry regions:** Average annual rainfall greater than 20 inches.
- **Freeze regions:** Average annual freezing index less than 150 °F per d.
- **Nonfreeze regions:** Average annual freezing index greater than 150 °F per d.

Large variations in climatic conditions exist within all of these broad climatic regions.

Key subgrade factors include the following:

- **Active:** Active soils (which can be fine or coarse) are either swelling (expansive) or frost-susceptible type. Some coarse soils, like silty sands, can be frost susceptible and, therefore, qualify for the active soil category. Active soils were identified using the following criteria:[53]

    - **Expansive soils:** Colloidal content greater than 15 percent and PI greater than 18 percent.

    - **Frost-susceptible soils:** Silt, coarse clay (i.e., AASHTO A-4 and A-5 soils) having greater than 15 percent material finer than 0.78 mil.[23]

    Some of the active soils were treated prior to the construction of pavements, which could have reduced their potential to swell or heave.

- **Fine-grained:** Greater than 35 percent of a fine-grained soil will pass through a No. 200 sieve.

- **Coarse-grained:** Less than 35 percent of a coarse-grained soil will pass through a No. 200 sieve.

Key traffic factors include the following:

- Mean annual ESAL for the measured lane of the high-trafficked AC pavements was 280,124.

- Mean annual ESAL for the measured lane of the high-trafficked JPCP was 693,123.
- Mean annual ESAL for the SPS-8 measured lane was 7,586.

IDENTIFICATION OF LTPP PROJECTS FOR POPULATING EXPERIMENTAL SAMPLING TEMPLATE

As shown in figure 7, the sampling template is basically a combination of the original LTPP SPS-8 experimental design and companion heavily trafficked AC and PCC pavement projects. This design required 24 flexible and 24 rigid pavement test sections constructed at 12–24 sites to satisfy the combinations of all the key SPS-8 study factors. The template includes portions of the SPS-1 and -8 projects that have similar structural designs and materials types located in similar environments but are subjected to heavy truck-traffic loads. By combining the original SPS-8 experiment, as originally planned, and aspects of the SPS-1 (flexible) and -2 (rigid) experimental plans, a full array of pavement projects can be obtained for determining the main study factors along with the interaction of the main effects on pavement performance. The SPS-8 and portions of the SPS-1 and -2 experiments were designed to contain sufficient numbers of projects to provide a full experimental factorial of 48 projects each. Additional projects were also available from the GPS experiments. The following subsections describe the projects selected and used for populating the sampling template.

SPS-8 Experiment Projects

Construction of the SPS-8 sites began in June 1993 and continued through June 2000. To date, 53 individual test sections have been successfully completed. Figure 13 shows the locations of the SPS-8 projects. (Not all of the original projects are still in service.) Two flexible SPS-8 sections in Ohio experienced early failure and were reconstructed with subgrade stabilization (lime stabilized). Only the reconstructed projects are available for analysis. Table 6 summarizes the inventory information for the constructed SPS-8 projects, and table 7 summarizes the project locations, pavement types, and maintenance history as of 2010. Table 8 presents the final status of the SPS-8 experiment.

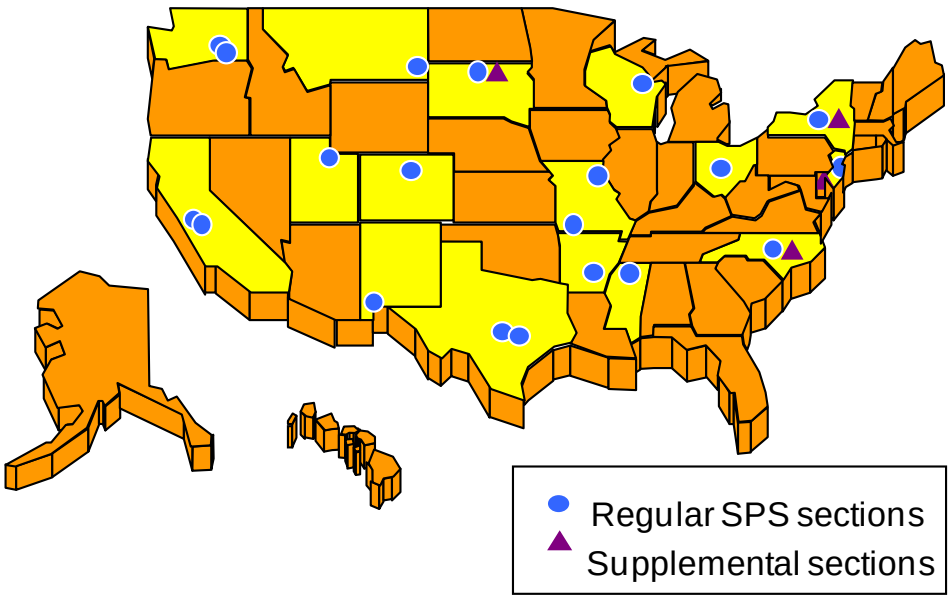

Source: FHWA
Note: States without a circle do not have an SPS-8 experimental site. These States are AK, AL, AZ, FL, GA, HI, IA, ID, IL, IN, KS, KY, LA, MD, ME, MI, MN, ND, NE, NH, NV, OK, OR, RI, SC, TN, VA, VT, WV, and WY. All States with a circle include one or more SPS-8 experimental sites. These States are AR, CA, CO, DE, MO, MS, MT, NC, NM, NY, OH, SD, TX, UT, WA, and WI. States with a triangle have one or more supplemental JPCP sections. These States are NC, NY, and SD.

Figure 13. Map. Locations of SPS-8 projects across the United States.

Table 6. Constructed SPS-8 core and supplemental sections.

State	County	SHRP ID	Construction Date	Pavement Type	Functional Class	Route Signing	Route No.	Direction of Travel
Arkansas	Jefferson	0803	12/1/1997	AC with granular base	Urban collector	U.S.	65	South
Arkansas	Jefferson	0804	12/1/1997	AC with granular base	Urban collector	U.S.	65	South
Arkansas	Jefferson	0809	12/1/1997	JPCP over unbound base	Urban collector	U.S.	65	South
Arkansas	Jefferson	0810	12/1/1997	JPCP over unbound base	Urban collector	U.S.	65	South
California	Merced	0811	7/1/1999	JPCP over unbound base	Rural local collector	Local/other	N/A	North
California	Merced	0812	7/1/1999	JPCP over unbound base	Rural local collector	Local/other	N/A	North
California	Merced	A805	9/1/1999	AC with granular base	Rural local collector	Local/other	N/A	North
California	Merced	A806	9/1/1999	AC with granular base	Rural local collector	Local/other	N/A	North
Colorado	Adams	0811	10/1/1993	JPCP over unbound base	Rural local collector	Local/other	N/A	East
Colorado	Adams	0812	10/1/1993	JPCP over unbound base	Rural local collector	Local/other	N/A	East
Mississippi	Panola	0805	10/1/1996	AC with granular base	Rural other principal arterial	State	315	North
Mississippi	Panola	0806	10/1/1996	AC with granular base	Rural other principal arterial	State	315	North
Missouri	Christian	0801	7/1/1998	AC with granular base	Rural local collector	Local/other	65WOR	South
Missouri	Christian	0802	7/1/1998	AC with granular base	Rural local collector	Local/other	65WOR	South
Missouri	Christian	0807	7/1/1998	JPCP over unbound base	Rural local collector	Local/other	65WOR	South
Missouri	Christian	0808	7/1/1998	JPCP over unbound base	Rural local collector	Local/other	65WOR	South
Missouri	Harrison	A801	12/1/1998	AC with granular base	Rural local collector	U.S.	61	North
Missouri	Harrison	A802	12/1/1998	AC with granular base	Rural local collector	U.S.	61	North
Missouri	Harrison	A807	12/1/1998	JPCP over unbound base	Rural local collector	U.S.	61	North
Missouri	Harrison	A808	12/1/1998	JPCP over unbound base	Rural local collector	U.S.	61	North
Montana	Deer Lodge	0805	6/1/1994	AC with granular base	Rural local collector	State	273	North
Montana	Deer Lodge	0806	6/1/1994	AC with granular base	Rural local collector	State	273	North
New Jersey	Hudson	0801	6/1/1993	AC with granular base	Rural minor arterial	Local/other	T/W 0	South
New Jersey	Hudson	0802	6/1/1993	AC with granular base	Rural minor arterial	Local/other	T/W 0	South
New Jersey	Hudson	0859	6/1/1993	AC with granular base	Rural minor arterial	Local/other	T/W 0	South
New Jersey	Hudson	0860	6/1/1993	AC with granular base	Rural minor arterial	Local/other	T/W 0	South
New Mexico	Grant	0801	11/1/1996	AC with granular base	Rural local collector	Local/other	1014	East
New Mexico	Grant	0802	11/1/1996	AC with granular base	Rural local collector	Local/other	1014	East
New York	Orleans	0801	8/1/1994	AC with granular base	Rural minor arterial	State	947A	East
New York	Orleans	0802	8/1/1994	AC with granular base	Rural minor arterial	State	947A	East
New York	Orleans	0859	8/1/1994	AC with granular base	Rural minor arterial	State	947A	East
North Carolina	Onslow	0801	12/1/1997	AC with granular base	Rural local collector	Local/other	1245	North
North Carolina	Onslow	0802	12/1/1997	AC with granular base	Rural local collector	Local/other	1245	North
North Carolina	Onslow	0859	12/1/1997	AC with granular base	Rural local collector	Local/other	1245	North

State	County	SHRP ID	Construction Date	Pavement Type	Functional Class	Route Signing	Route No.	Direction of Travel
Ohio	Delaware	0809	11/1/1994	JPCP over unbound base	Rural local collector	U.S.	23	South
Ohio	Delaware	0810	11/1/1994	JPCP over unbound base	Rural local collector	U.S.	23	South
Ohio	Delaware	A803	10/31/1997	AC with granular base	Rural local collector	Local/other	23	South
Ohio	Delaware	A804	10/31/1997	AC with granular base	Rural local collector	Local/other	23	South
South Dakota	Campbell	0803	6/1/1993	AC with granular base	Rural major collector	State	1804	South
South Dakota	Campbell	0804	6/1/1993	AC with granular base	Rural major collector	State	1804	South
South Dakota	Campbell	0859	6/1/1993	AC with granular base	Rural major collector	State	1804	South
Texas	Brazos	0801	7/1/1996	AC with granular base	Rural local collector	Local/other	2223	East
Texas	Bell	0802	7/1/1996	AC with granular base	Rural local collector	Local/other	2223	East
Texas	Bell	A807	1/1/2000	JPCP over unbound base	Rural local collector	Local/other	2670	East
Texas	Bell	A808	1/1/2000	JPCP over unbound base	Rural local collector	Local/other	2670	East
Utah	Wasatch	0803	10/1/1997	AC with granular base	Rural minor arterial	State	SH-35	East
Utah	Wasatch	0804	10/1/1997	AC with granular base	Rural minor arterial	State	SH-35	East
Washington	Columbia	0801	10/1/1995	AC with granular base	Rural local collector	Local/other	91150	North
Washington	Columbia	0802	10/1/1995	AC with granular base	Rural local collector	Local/other	91150	North
Washington	Walla	A809	6/1/2000	JPCP over unbound base	Rural local collector	Local/other	Smith Springs	East
Washington	Walla	A810	6/1/2000	JPCP over unbound base	Rural local collector	Local/other	Smith Springs	East
Wisconsin	Marathon	0805	11/30/1997	AC with granular base	Urban other principal arterial	State	29	East
Wisconsin	Marathon	0806	11/30/1997	AC with granular base	Urban other principal arterial	State	29	East

N/A = not available.

Table 7. Summary of SPS-8 sections by State, pavement type, and maintenance history.

State Code	State	SHRP ID	Project Type	Construction Assign Date	Recorded Maintenance Activity	Project Status
5	Arkansas	5_0803	AC	1/1/1996	None	In service
5	Arkansas	5_0804	AC	1/1/1996	None	In service
5	Arkansas	5_0809	JPCP	1/1/1996	Lane shoulder joint sealing in 7/2001	In service
5	Arkansas	5_0810	JPCP	1/1/1996	Lane shoulder joint sealing in 7/2001	In service
6	California	6_0811	AC	5/1/1999	Partial depth patching in 8/2001 and 8/2009	In service
6	California	6_0812	AC	5/1/1999	None	In service
6	California	6_A805	AC	5/1/1999	None	In service
6	California	6_A806	AC	5/1/1999	None	In service
8	Colorado	8_0811	JPCP	1/1/1993	None	In service
8	Colorado	8_0812	JPCP	1/1/1993	None	In service
28	Mississippi	28_0805	AC	1/1/1996	None	In service
28	Mississippi	28_0806	AC	1/1/1996	None	In service
29	Missouri	29_0801	AC	1/1/1998	None	In service
29	Missouri	29_0802	AC	1/1/1998	None	In service
29	Missouri	29_0807	JPCP	1/1/1998	None	In service
29	Missouri	29_0808	JPCP	1/1/1998	None	In service
29	Missouri	29_A801	AC	1/1/1998	None	Deassigned 12/31/2005
29	Missouri	29_A802	AC	1/1/1998	None	Deassigned 12/31/2005
29	Missouri	29_A807	JPCP	1/1/1998	None	Deassigned 12/31/2005
29	Missouri	29_A808	JPCP	1/1/1998	None	Deassigned: 12/31/2005
30	Montana	30_0805	AC	1/1/1993	Aggregate seal coat in 9/2003	In service
30	Montana	30_0806	AC	1/1/1993	Aggregate seal coat in 9/2003	In service
34	New Jersey	34_0801	AC	1/1/1993	Patch pot holes in 8/1993	Deassigned 12/1/1999
34	New Jersey	34_0802	AC	1/1/1993	None	Deassigned 12/1/1999
34	New Jersey	34_0859*	AC	1/1/1993	None	Deassigned 12/1/1999
34	New Jersey	34_0860*	AC	1/1/1993	Patch pot holes in 8/1993	Deassigned 12/1/1999
35	New Mexico	35_0801	AC	9/11/1995	None	In service
35	New Mexico	35_0802	AC	9/11/1995	None	In service
36	New York	36_0801	AC	6/1/1994	None	Deassigned 10/15/2008
36	New York	36_0802	AC	6/1/1994	None	Deassigned 10/15/2008
36	New York	36_0859*	AC	6/1/1994	None	Deassigned 10/15/2008
37	North Carolina	37_0801	AC	8/1/1997	None	In service
37	North Carolina	37_0802	AC	8/1/1997	None	In service
37	North Carolina	37_0859*	AC	8/1/1997	None	In service

State Code	State	SHRP ID	Project Type	Construction Assign Date	Recorded Maintenance Activity	Project Status
39	Ohio	39_0809	JPCP	1/1/1994	None	In service
39	Ohio	39_0810	JPCP	1/1/1994	None	In service
39	Ohio	39_A803**	AC	8/4/1997	None	Deassigned 9/1/2012
39	Ohio	39_A804**	AC	8/4/1997	None	In service
46	South Dakota	46_0803	AC	1/1/1992	None	In service
46	South Dakota	46_0804	AC	1/1/1992	None	In service
46	South Dakota	46_0859*	AC	1/1/1992	Crack sealing in 6/1995 and skin patching in 9/2005	In service
48	Texas	48_0801	AC	1/1/1995	None	In service
48	Texas	48_0802	AC	1/1/1995	None	In service
48	Texas	48_A807	JPCP	11/8/1999	None	In service
48	Texas	48_A808	JPCP	11/8/1999	Full depth patching of PCC pavements in 6/2005	In service
49	Utah	49_0803	AC	1/1/1996	Fog seal coat in 8/1998	In service
49	Utah	49_0804	AC	1/1/1996	Fog seal coat in 8/1998	In service
53	Washington	53_0801	AC	1/1/1993	Crack sealing in 6/2000 and 7/2003; aggregate seal coat in 6/2005	In service
53	Washington	53_0802	AC	1/1/1993	Crack sealing in 6/2000 and 7/2003; aggregate seal coat in 6/2005	In service
53	Washington	53_A809	JPCP	5/1/1999	None	In service
53	Washington	53_A810	JPCP	5/1/1999	None	In service
55	Wisconsin	55_0805	AC	1/1/1997	None	In service
55	Wisconsin	55_0806	AC	1/1/1997	None	In service

*Supplemental sections.
**Reconstructed sections.

Table 8. Final status of SPS-8 experiment.

Pavement Type	Structural Factors		LTPP Section Numbers (SHRP IDs) Organized by Climate and Subgrade Type[1]							
			Wet				Dry			
			Freeze		Nonfreeze		Freeze		Nonfreeze	
	Surface[2] Thickness (Inches)	DGAB Thickness (Inches)	Fine and Active	Coarse	Fine and Active	Coarse	Fine and Active	Coarse	Fine and Active	Coarse
Flexible	4	8	29-0801, 29-A801, and 39-A803	34-0801, 36-0801, and 55-0805	5-0803, 48-0801, and 28-0805	37-0801 and 37-0859[3]	46-0859[3], 53-0801, and 49-0803	30-0805 and 46-0803	35-0801	6-A805
Flexible	7	12	29-0802, 29-A802, and 39-A804	34-0802, 34-0859, 34-0860, 36-0802, 36-0859, and 55-0806	48-0802 and 28-0806	05-0804 and 37-0802	53-0802, 46-0804, and 49-0804	30-0806	35-0802	06-A806
Rigid	8	6	29-A807, 29-0807, and 39-0809	Missing	5-0809 and 48-A807	Missing	53-A809 and 8-0811	Missing	Missing	6-0811
Rigid	11	6	29-0808, 29-A808, and 39-0810	Missing	5-0810 and 48-A808[4]	Missing	53-A810 and 8-0812[4]	Missing	Missing	6-0812

Note: Cells labeled "Missing" represent either missing sections or filled cells that were not originally planned to be filled.
[1]Active soil can be either frost-susceptible or swelling (expansive) type.
[2]Dense-graded AC and JPCP, respectively.
[3]Thin AC layer (1.4–2.6 inches).
[4]Thick PCC layer (greater than 12 inches).

Companion Projects

The SPS-1 and -2 experiments were designed to provide projects similar to SPS-8 but subjected to high traffic loads. There are also some existing flexible (GPS-1 and -2) and rigid (GPS-3) projects with designs roughly similar to SPS-8 test sections that could be used for comparative analysis of pavements subjected to heavy loads. A thorough review of all LTPP AC and JPCP projects was performed to identify pavement sections that had similar designs and environmental exposure to the SPS-8 projects. Similarity in terms of design and environmental exposure was defined based on the SPS-8 study factors. Criteria for selection of companion heavily trafficked projects are as follows:

- Comparable pavement design criteria are as follows:
  - Total pavement thickness (AC or PCC) must be similar to that of typical SPS-8 projects.
  - Base or subbase type must be untreated granular materials.
  - For JPCP, the slab width must range from 10–12 ft.
- Environmental exposure criteria are as follows:
  - Projects must be located in the same climate.
  - Projects must have similar subgrade types (i.e., fine- or coarse-grained or active) or at least support levels.
  - Truck-traffic volume levels for the complementary projects must be significantly higher than the SPS-8 projects.
  - The PCC strength properties and AC binder type and mix volumetric properties must be reasonably similar.

Based on these criteria, companion AC pavement and JPCP projects were selected (table 9). A summary of the features of the companion projects include the following:

- Companion test sections were identified for most of the flexible and rigid pavement cells. For flexible pavement, suitable projects could not be identified for two cells, while suitable projects could not be identified for eight rigid pavement cells.
- The distance from SPS-8 test sections and companion project varied. While some of the SPS-1 and -2 companion projects were co-located with the SPS-8 projects (e.g., Ohio), most of the GPS companion projects were located several miles away.
- Soil conditions varied between most of the SPS-8 test sections and companion projects (e.g., fine-grained A-6 versus fine-grained A-7-6 soils) but stayed within the AASHTO definition of fine- and coarse-grained soils.[23]
- Although companion and SPS-8 test sections may reside in a single climate, actual exposure to temperature, precipitation, and freezing index varied.

- The extent of variations was considered minimal and was not expected to significantly impact analysis outcomes.

- Mean annual number of ESAL for the LTPP measured lane of the heavily trafficked AC pavements was 280,124.

- Mean annual number of ESAL for the LTPP measured lane of the heavily trafficked JPCP was 693,123.

- Mean annual number of ESAL for the LTPP measured lane for SPS-8 AC pavements and JPCP was 7,586.

The difference in ESAL applications for the low-trafficked SPS-8 and the high-trafficked non-SPS-8 projects was significant (37 times higher for flexible and 91 times higher for rigid). This should make it possible to draw meaningful direct performance comparisons on the effect of traffic and environmental factors on pavement damage and performance.

Table 9. Identified companion flexible and rigid pavement projects.

Pavement Type	Structural Factors		LTPP Section Numbers (SHRP IDs) Organized by Climate and Subgrade Type[1]							
			Wet				Dry			
			Freeze		Nonfreeze		Freeze		Nonfreeze	
	Surface[2] Thickness (Inches)	DGAB Thickness (Inches)	Fine and Active	Coarse	Fine and Active	Coarse	Fine and Active	Coarse	Fine and Active	Coarse
Flexible	4	8	19-0102, 87-1620, 26-0113, 39-0102, and 39-0159	10-0102, 26-1004, 27-1019, and 87-0961	37-1802, 37-1817, 22-0113, 51-0113, 6-8153, and 48-1174	5-0113, 6-1253, 37-0859, and 48-1123	8-1029, 53-1501, 8-1053, 8-1057, 53-1002, and 8-1047	30-0901, 30-0902, 30-0903, 49-1017, 53-1008, 30-7088, and 56-7775	Missing	6-8156 and 6-7454
Flexible	7	12	9-1803, 19-0107, 21-1010, 51-2021, 26-0114, 26-0120, and 39-0101	10-0101, 25-1003, 26-1013, 29-1002, 34-1003, 34-1031, 34-1033, 47-9025, and 27-1003	48-0902, 1-1021, 48-0903, 48-1096, 48-1181, 51-0114, and 48-1039	1-1019, 5-0114, 5-0120, 5-0121, 28-1016, 48-1060, and 48-1087	Missing	30-0114	35-0101	32-1020 and 35-1003
Rigid	8	6	19-0214, 26-0214, 39-0201, 46-3053, 55-3009, and 38-0214	Missing	5-0809 37-3044	Missing	38-3006, 53-0201, 53-3013, and 38-3005	Missing	Missing	Missing

Pavement Type	Structural Factors		LTPP Section Numbers (SHRP IDs) Organized by Climate and Subgrade Type[1]							
			Wet				Dry			
			Freeze		Nonfreeze		Freeze		Nonfreeze	
	Surface[2] Thickness (Inches)	DGAB Thickness (Inches)	Fine and Active	Coarse	Fine and Active	Coarse	Fine and Active	Coarse	Fine and Active	Coarse
Rigid	11	6	20-0204, 21-3016, 46-3012, 46-3052, 19-0215, 19-0216, 19-3055, 26-0215, 39-0204, 39-0259, 55-3008, 55-3010, 38-0215, 38-0260, and 38-0261	Missing	1-3028, 37-0204, and 48-3589	Missing	8-7776, 53-0204, 53-3019, and 56-3027	6-0204 and 6-0812	Missing	6-0201 and 6-0811

Note: Cells labeled "Missing" represent either missing sections or filled cells that were not originally planned to be filled.
[1]Active soil can be either frost-susceptible or swelling (expansive) type.
[2]Dense-graded AC and JPCP, respectively.

SUMMARY DESCRIPTION OF THE IDENTIFIED SPS-8 AND COMPANION PROJECTS

A total of 37 flexible and 16 rigid SPS-8 projects along with 68 flexible and 38 rigid companion SPS-1 and -2 and GPS-1, -2, and -3 projects were identified, selected, and used to populate the sampling template. No suitable projects were identified for 2 of the 16 flexible-pavement cells, and no suitable projects were identified for 8 of the 16 rigid pavement cells. Thus, in general, an approximate full flexible-pavement factorial was obtained while a half factorial was obtained for rigid pavement. This was deemed adequate for analysis to meet the study objectives. Figure 14 and figure 15 show the locations of the selected SPS-8 and companion projects across the United States. Table 10 and table 11 show how the selected projects fill the sampling template.

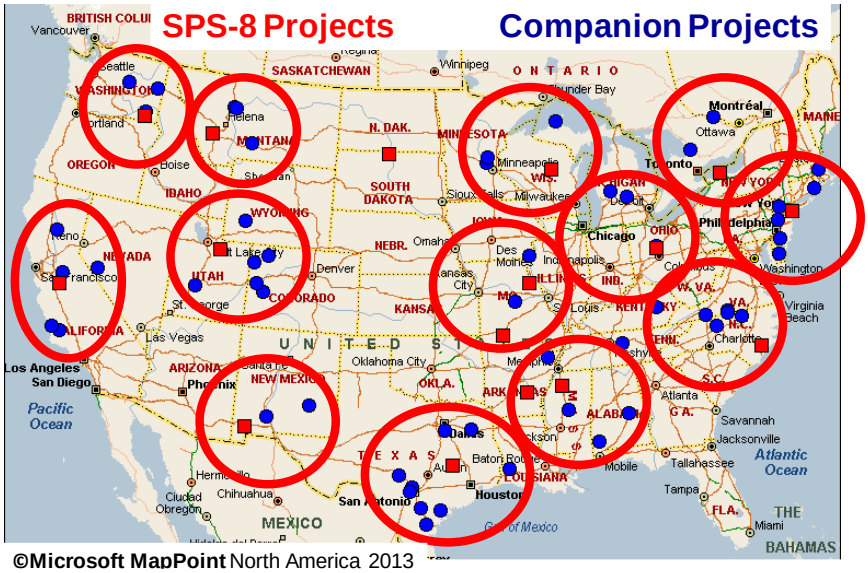

©Microsoft MapPoint North America 2013
Modified by FHWA.
Large circles: Groups of LTPP sections in a relatively similar climate.
Square points: SPS-8 low-traffic projects.
Circular points: Companion LTPP sections (SPS-1, GPS-1,2 high-traffic projects).

Figure 14. Map. Selected projects identified for detailed analysis for AC pavements.

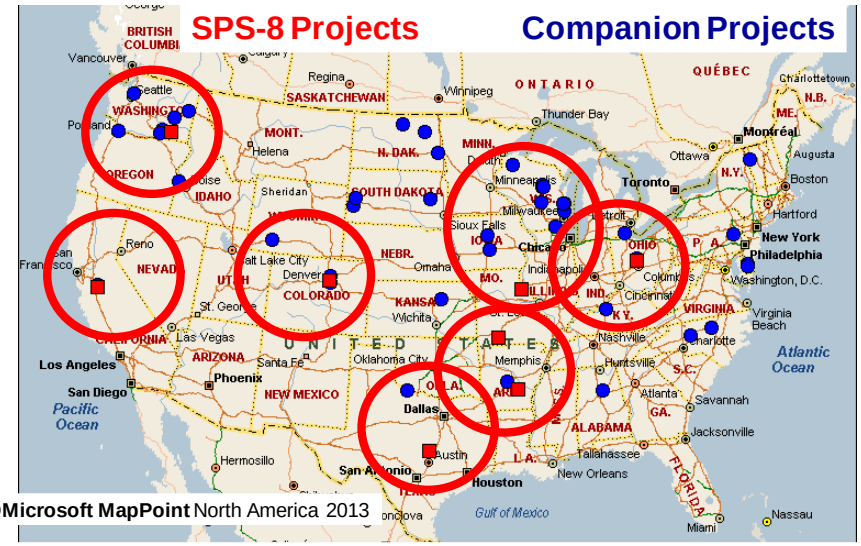

Modified by FHWA.
Large circles: Groups of LTPP sections in a relatively similar climate.
Square points: SPS-8 low-traffic projects.
Circular points: Companion LTPP sections (SPS-2, GPS-3 high-traffic projects)

Figure 15. Map. Selected projects identified for detailed analysis for JPCP.

Table 10. SPS-8 and companion flexible pavement projects.

Subgrade Type[1]	SPS-8 Pavement Structural Factors		Moisture and Temperature			
			Wet		Dry	
	Surface[2] Thickness (Inches)	DGAB Thickness (Inches)	Freeze	Nonfreeze	Freeze	Nonfreeze
Fine and active	4	8	**39-A803, 29-A801,** and **29-0801**	**28-0805, 5-0803,** and **48-0801**	**53-0801, 49-0803,** and **46-0803**	—
Fine and active	4	8	19-0102, 87-1620, 26-0113, 39-0102, and 39-0159	37-1802, 37-1817, 22-0113, 51-0113, 6-8153, and 48-1174	8-1029, 53-1501, 8-1053, 8-1057, 53-1002, 8-1047, and 46-0859	—
Fine and active	7	12	9-1803, 19-0107, 21-1010, 51-2021, 39-A804, 26-0114, 26-0120, 39-0101, **29-A802,** and **29-0802**	48-0902, 1-1021, **5-0804, 28-0806, 48-0802,** 48-0903, 48-1096, 48-1181, 51-0114, and 48-1039	**53-0802, 49-0804,** and **46-0804**	**35-0802** and 35-0101
Coarse	4	8	10-0102, 26-1004, 27-1019, 34-0801, 87-0961, 36-0801, and **55-0805**	5-0113, 6-1253, 37-0801, 37-0859, and 48-1123	**30-0805,** 30-0901, 30-0902, 30-0903, 49-1017, 53-1008, 30-7088, and 56-7775	6-8156, **6-A805,** and 6-7454
Coarse	7	12	10-0101, 25-1003, 26-1013, 29-1002, **34-0802, 34-0859, 34-0860,** 34-1003, 34-1031, 34-1033, 47-9025, 27-1003, **36-0802, 36-0859,** and **55-0806**	1-1019, 5-0114, 5-0120, 5-0121, 28-1016, **37-0802,** 48-1060, and 48-1087	**30-0806** and 30-0114	**6-A806,** 32-1020, and 35-1003

—Cells with no LTPP sections.

Note: Bolded text indicates low-traffic SPS-8 projects. Nonbold text indicates high-traffic companion sections.

[1]Active soil can be either frost-susceptible or swelling (expansive) type.

[2]Dense-graded AC.

Table 11. SPS-8 JPCP and companion JPCP projects.

Subgrade Type[1]	Pavement Structural Factors		Moisture and Temperature			
			Wet		Dry	
	JPCP Thickness (Inches)	DGAB Thickness (Inches)	Freeze	Nonfreeze	Freeze	Nonfreeze
Fine and active	8	6	19-0214, 26-0214, 39-0201, 39-0809, 46-3053, 55-3009, **29-A807, 29-0807**, and 38-0214	**5-0809,** 37-3044, and **48-A807**	38-3006, 53-0201, 53-3013, **53-A809, 8-0811**, and 38-3005	—
Fine and active	11	6	20-0204, 21-3016, 46-3012, 46-3052, 19-0215, 19-0216, 19-3055, 26-0215, 39-0204, 39-0259, 39-0810, 55-3008, 55-3010, **29-A808, 29-0808,** 38-0215, 38-0260, and 38-0261	1-3028, 5-0810, 37-0204, 48-3589, and **48-A808**	8-7776, 53-0204, 53-3019, **53-A810, 8-0812**, and 56-3027	—
Coarse	8	6	—	—	—	6-0201 and **6-0811**
Coarse	11	6	—	—	—	6-0204 and **6-0812**

—Cells with no LTPP sections.

Note: Bolded text indicates SPS-8 JPCP projects. Nonbold text indicates high-traffic companion sections.

[1]Active soil can be either frost-susceptible or swelling (expansive) type.

CHAPTER 5. DEVELOPMENT OF PROJECT DATABASE

This chapter discusses the development of a project database containing key data required for achieving the objectives of this study.[54] In order to develop the project database, the following tasks were performed:

1. Identified all key data elements and variables required.
2. Determined the availability of the identified data variables.
3. Assembled the identified data variables and reviewing for completeness and accuracy.
4. Estimated computed parameters as needed using the data assembled as inputs.
5. Developed the project database for use in analysis.

Detailed descriptions of data variables assembled in the project database is presented in the following subsections. The project database created for this study was the 2013 LTPP database Standard Data Release 27.[54]

PAVEMENT DESIGN/MATERIALS DATA

This section describes data elements and pavement-structure definitions used in the analysis.

Inventory-Type Information

Pavement inventory information includes data elements, such as SHRP identification, State, pavement type, construction dates, county, functional class, route signing and number, and direction of travel.

Pavement Structure Definition

The main repository of pavement structure definitions (layer type and location within structure, layer material type, and thickness) can be found in LTPP tables TST_L05A and TST_L05B.[17] Table TST_L05A generally contains measured layer-thickness data, while table TST_L05B contains representative layer-thickness data. As the data in table TST_L05B are sufficient for most analyses, the researchers focused on the data available in it. As described in chapter 3, the main criteria for defining pavement structures were layer-material types (e.g., AC over granular base) and layer thicknesses, while the criteria for selecting companion projects included ensuring that the pavement structures were similar to those of the SPS-8 projects.

For the thin AC projects in SPS 8 and GPS-1/SPS-1 (the companion studies), the mean AC thicknesses were 4.16 and 4.15 inches, respectively, while for the thick AC projects in those studies, the AC thicknesses were 7.14 and 6.99 inches, respectively. The difference in mean thickness per grouping was not found to be significant. Differences in granular-base thicknesses were also measured. For the thin AC projects in SPS 8 and GPS-3/SPS-2, mean base thicknesses were 7.83 and 9.74 inches, respectively, while for the thick AC projects in those studies, base thickness was 11.33 and 9.68 inches, respectively.

The SPS-8 experimental plan called for two target PCC surface thicknesses—8 and 11 inches. For the thin PCC pavements, the mean thickness was 8.4 inches. For the thicker, rigid

pavements, mean thickness was 11.3 inches. The mean thicknesses were close to the target of 8 and 11 inches. Figure 16 presents the distribution of AC thicknesses for the SPS-8 and companion GPS-1/SPS-1 projects, respectively, while figure 17 presents the distribution of JPCP thicknesses for the SPS-8 and companion GPS-3/SPS-2 projects, respectively.

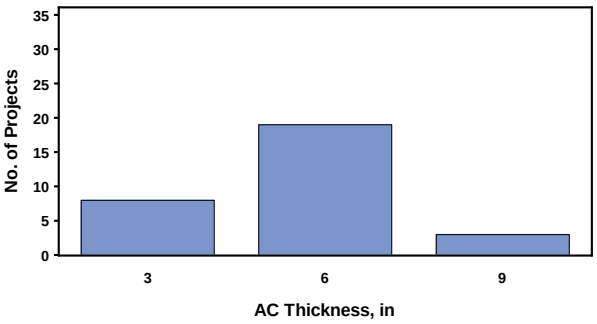

Source: FHWA.

A. SPS-8 AC pavements.

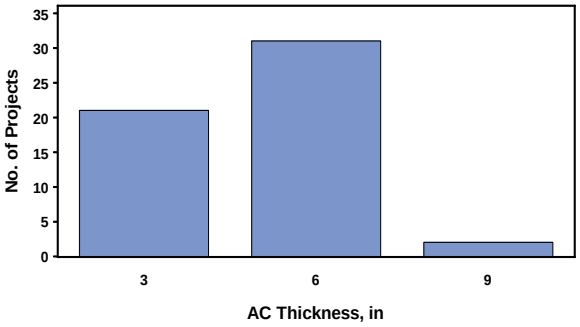

Source: FHWA.

B. Companion GPS-1 and SPS-1 AC pavements.

Figure 16. Graphs. Distribution of AC thicknesses for AC pavements.

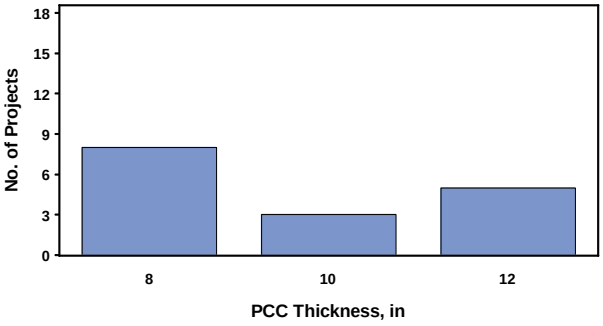

Source: FHWA.

A. SPS-8 JPCPs.

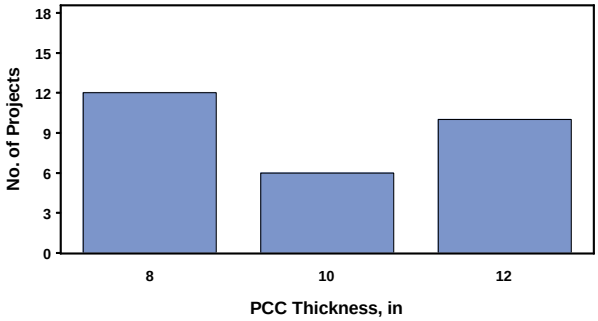

Source: FHWA.

B. GPS-3 and SPS-2 JPCPs.

Figure 17. Graphs. Distribution of slab thickness for JPCP projects.

CLIMATE FACTORS

Climate conditions for the SPS-8 and companion GPS-1 and SPS-1 projects were characterized based on the measured climate variables (i.e., temperature, rainfall, snowfall, exposure to sun radiation, etc.) collected by weather stations throughout the United States. Raw climate variables from the weather stations closest to each LTPP project were used to estimate site-specific values for the climate variables of interest. The climate data, which were reported on an hourly, daily, and annual basis, were stored in several LTPP data tables, including those listed in table 12. Figure 18 shows the distribution of climates in which SPS-8 and companion projects were located for AC pavements and JPCPs, respectively. The distributions represented in figure 19 show that all the LTPP climates were well represented for both AC pavements and JPCPs.

Table 12. Information assembled from LTPP climate data tables.[17]

Table Name	Data Type	Data Variables Description
CLM_VWS_HUMIDITY_DAILY	Humidity	Minimum, maximum, and average humidity by month
CLM_VWS_PRECIP_DAILY	Precipitation and snowfall	Total precipitation, number of wet days, number of days with intense precipitation, total snowfall, and total snow-covered days
CLM_VWS_TEMP_DAILY	Temperature	Minimum, maximum, and average temperatures; number of days above 90 °F; number of days below 32 °F; freezing index; and number of freeze–thaw cycles
CLM_VWS_WIND_DAILY	Wind speed	Mean wind speed and maximum gust of wind speed for year/month

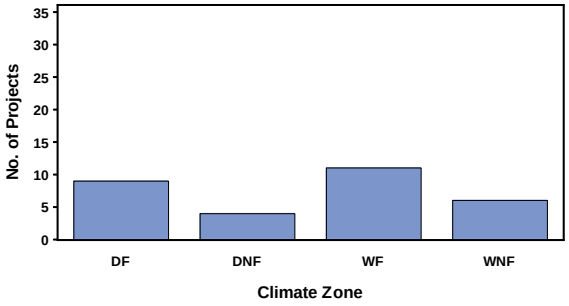

Source: FHWA.
Note: DF = dry freeze; DNF = dry nonfreeze; WF = wet freeze; WNF = wet nonfreeze.

A. SPS-8 AC pavements.

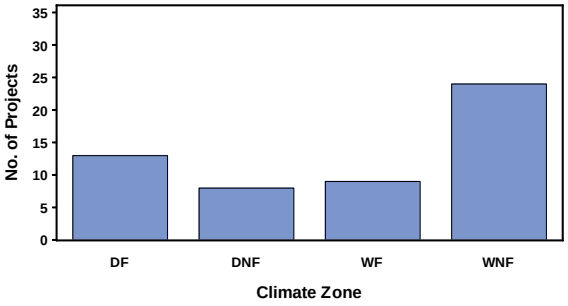

Source: FHWA.
Note: DF = dry freeze; DNF = dry nonfreeze; WF = wet freeze; WNF = wet nonfreeze.

B. Companion GPS-1 and SPS-1 AC pavements.

Figure 18. Graphs. Distribution of climates for AC pavement projects.

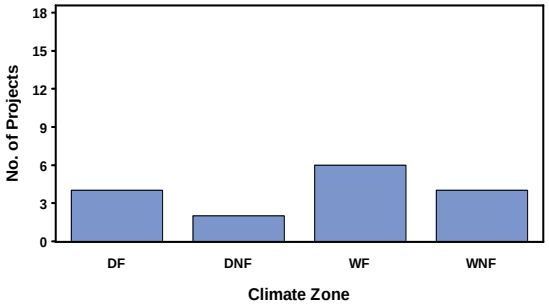

Source: FHWA.
Note: DF = dry freeze; DNF = dry nonfreeze; WF = wet freeze; WNF = wet nonfreeze.

A. SPS-8 JPCPs.

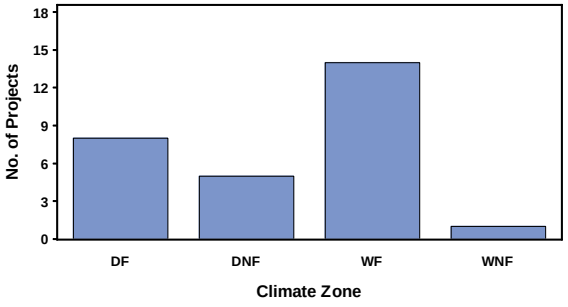

Source: FHWA.
Note: DF = dry freeze; DNF = dry nonfreeze; WF = wet freeze; WNF = wet nonfreeze.

B. Companion GPS-3 and SPS-2 JPCPs.

Figure 19. Graphs. Distribution of climates for JPCP projects.

Figure 20 through figure 33 show the distributions of climate variables for the SPS-8 and companion projects. The distributions show that, on average, all ambient climate conditions used to define environmental factors as part of the SPS-8 experiment were well represented.

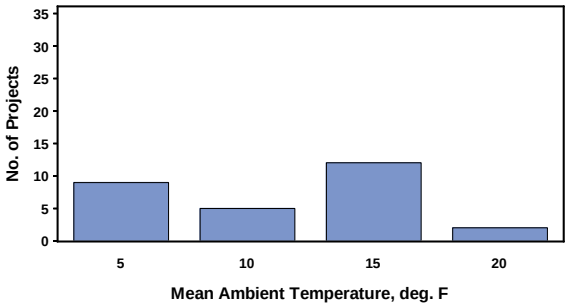

Source: FHWA.

A. SPS-8 AC pavements.

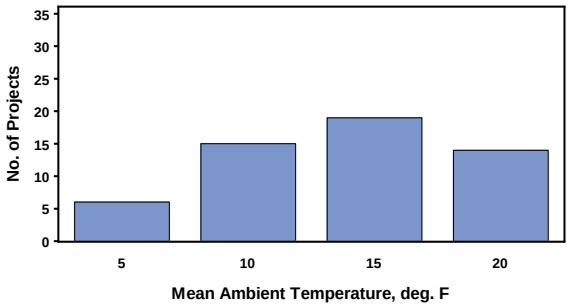

Source: FHWA.

B. Companion GPS-1 and SPS-1 AC pavements.

Figure 20. Graphs. Distribution of mean ambient temperature for AC pavement projects.

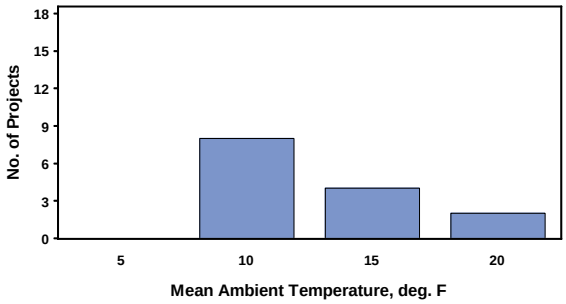

Source: FHWA.

A. SPS-8 PCC pavements.

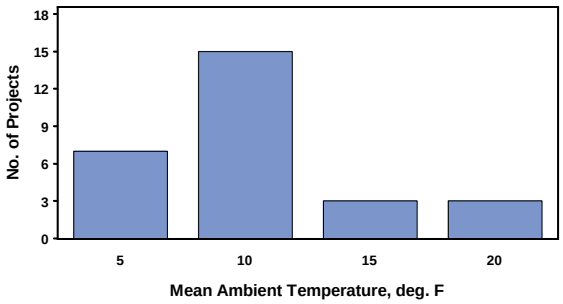

Source: FHWA.

B. Companion GPS-3 and SPS-2 PCC pavements.

Figure 21. Graphs. Distribution of mean ambient temperature for JPCP projects.

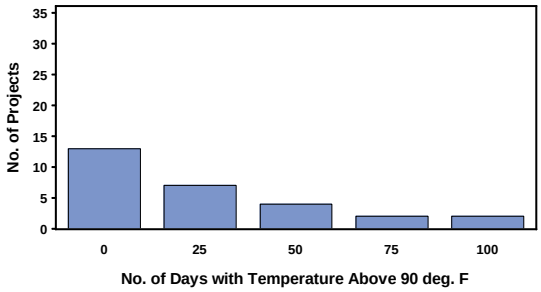

Source: FHWA.

A. SPS-8 AC pavements.

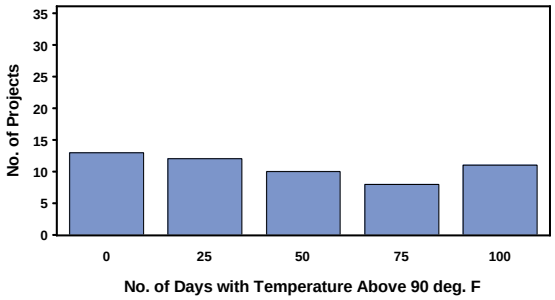

Source: FHWA.

B. Companion GPS-1 and SPS-1 AC pavements

Figure 22. Graphs. Distribution of annual number of days with temperature above 90 °F for AC pavement projects.

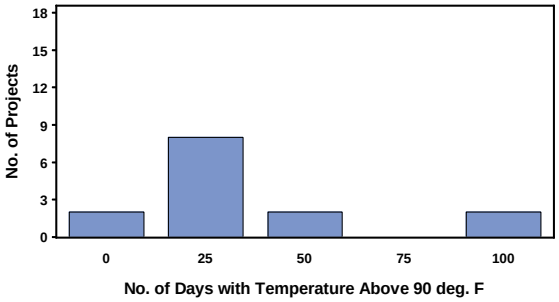

Source: FHWA.

A. SPS-8 PCC pavements.

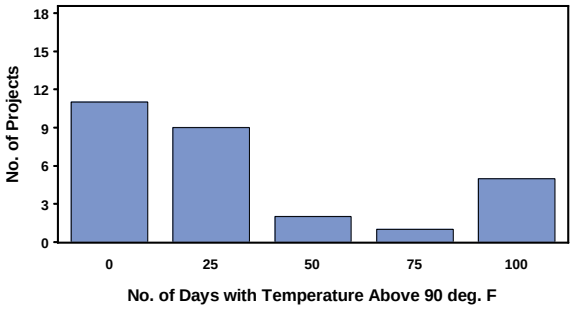

Source: FHWA.

B. Companion GPS-3 and SPS-2 PCC pavements.

Figure 23. Graphs. Distribution of annual number of days with temperature above 90 °F for PCC pavement projects.

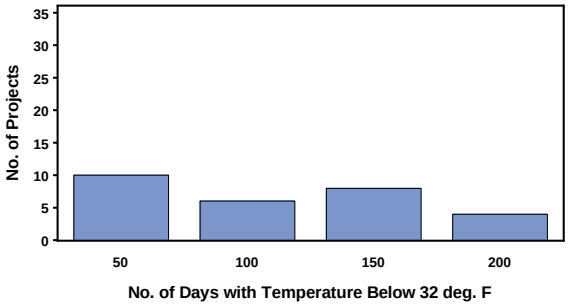

Source: FHWA.

A. SPS-8 AC pavements.

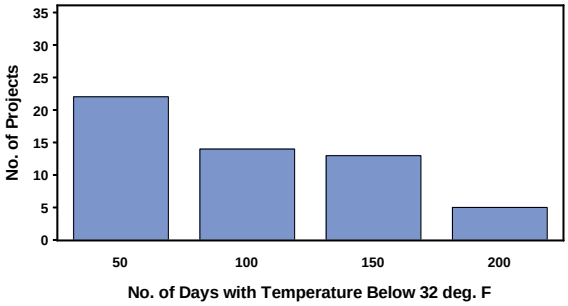

Source: FHWA.

B. Companion GPS-1 and SPS-1 AC pavements.

Figure 24. Graphs. Distribution of annual number of days with temperature below 32 °F for AC pavement projects.

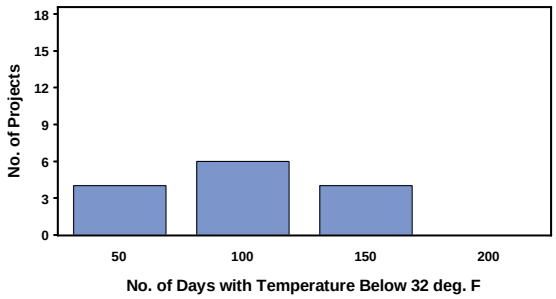

Source: FHWA.

A. SPS-8 PCC pavements.

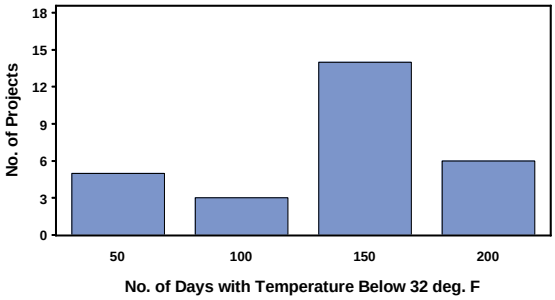

Source: FHWA.

B. Companion GPS-3 and SPS-2 PCC pavements.

Figure 25. Graphs. Distribution of annual number of days with temperature below 32 °F for PCC pavement projects.

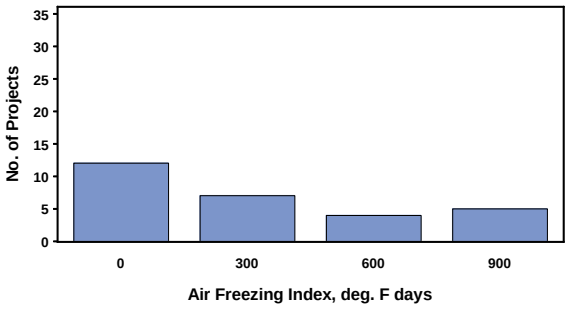

Source: FHWA.

A. SPS-8 AC pavements.

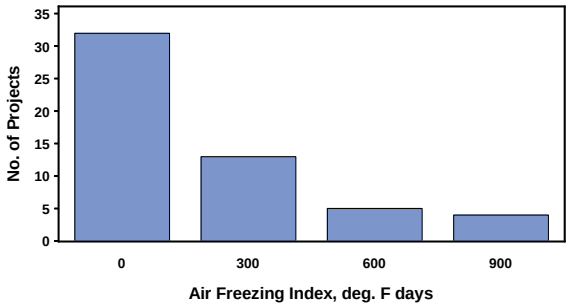

Source: FHWA.

B. Companion GPS-1 and SPS-1 AC pavements.

Figure 26. Graphs. Distribution of air freezing index for AC pavement projects.

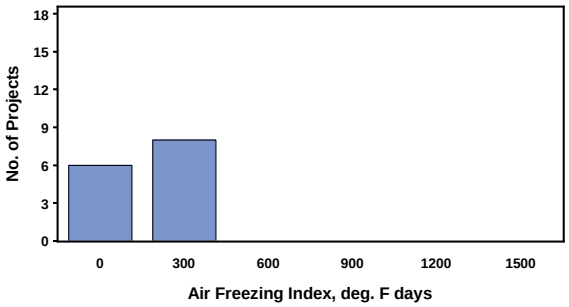

Source: FHWA.

A. SPS-8 PCC pavements.

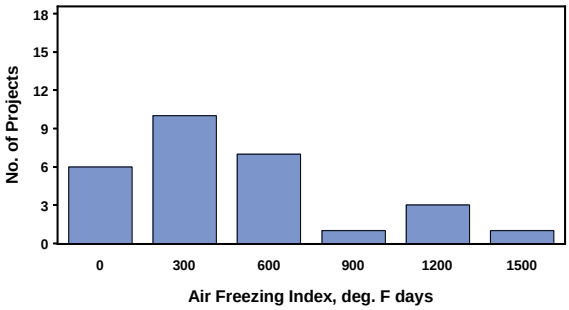

Source: FHWA.

B. Companion GPS-3 and SPS-2 PCC pavements.

Figure 27. Graphs. Distribution of air freezing index for PCC pavement projects.

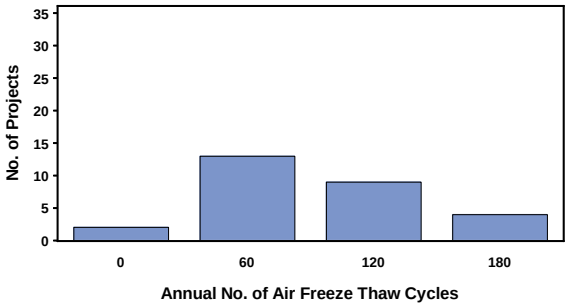

Source: FHWA.

A. SPS-8 AC pavements.

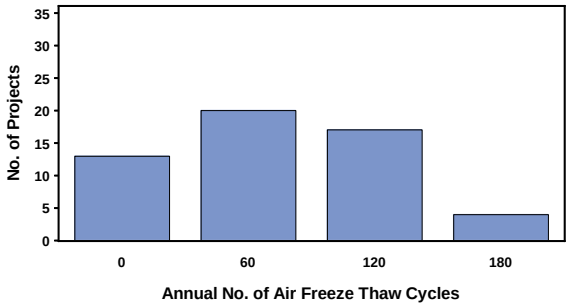

Source: FHWA.

B. Companion GPS-1 and SPS-1 AC pavements.

Figure 28. Graphs. Distribution of annual number of air freeze–thaw cycles for AC pavement projects.

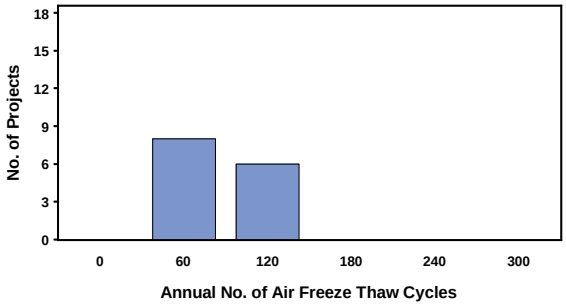

Source: FHWA.

A. SPS-8 PCC pavements.

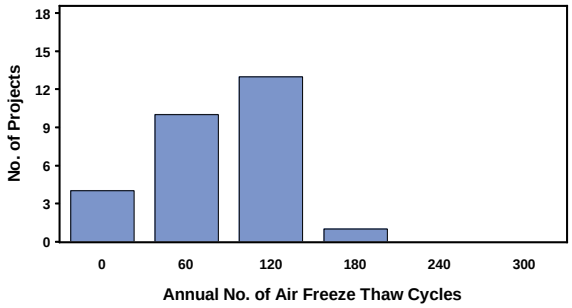

Source: FHWA.

B. Companion GPS-3 and SPS-2 PCC pavements.

Figure 29. Graphs. Distribution of annual number of air freeze–thaw cycles for PCC pavement projects.

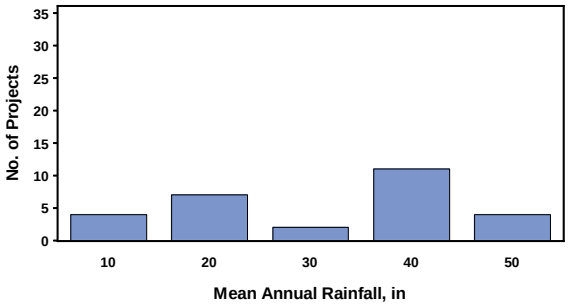

Source: FHWA.

A. SPS-8 AC pavements.

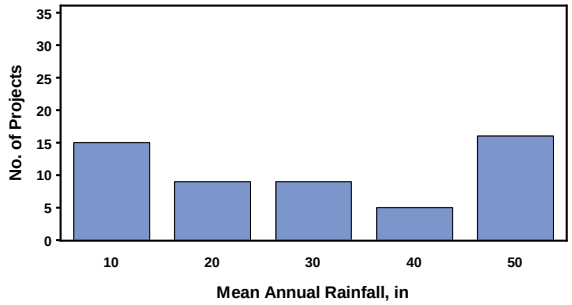

Source: FHWA.

B. Companion GPS-1 and SPS-1 AC pavements.

Figure 30. Graphs. Distribution of mean annual rainfall for AC pavement projects.

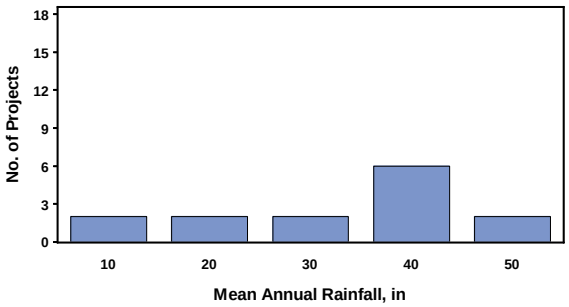

Source: FHWA.

A. SPS-8 PCC pavements.

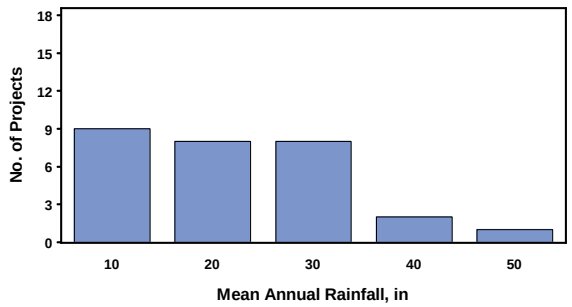

Source: FHWA.

B. Companion GPS-3 and SPS-2 PCC pavements.

Figure 31. Graphs. Distribution of mean annual rainfall for PCC pavement projects.

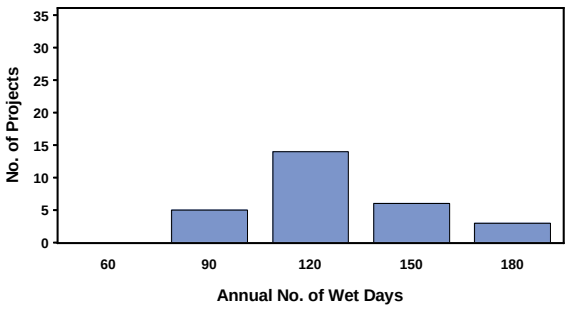

Source: FHWA.

A. SPS-8 AC pavements.

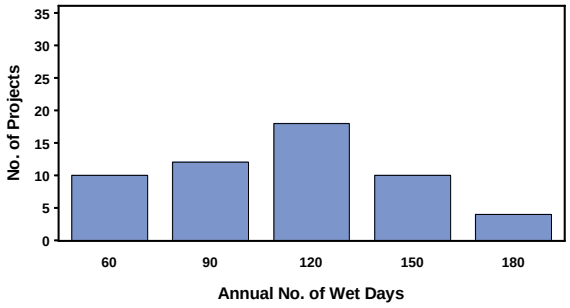

Source: FHWA.

B. Companion GPS-1 and SPS-1 AC pavements.

Figure 32. Graphs. Distribution of annual number of wet days for AC pavement projects.

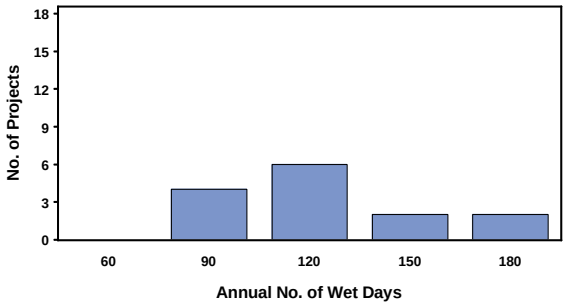

Source: FHWA.

A. SPS-8 PCC pavements.

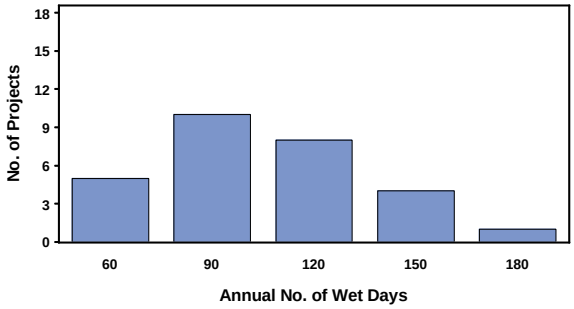

Source: FHWA.

B. Companion GPS-3 and SPS-2 PCC pavements.

Figure 33. Graphs. Distribution of annual number of wet days for JPCP projects.

SUBGRADE FOUNDATION FACTORS

Figure 34 through figure 45 present the distribution of key variables used to characterize pavement subgrade materials for the low- and high-trafficked projects. A comparison of distributions shows that both the low- and high-trafficked projects are well represented in the various subgrade types and characteristics.

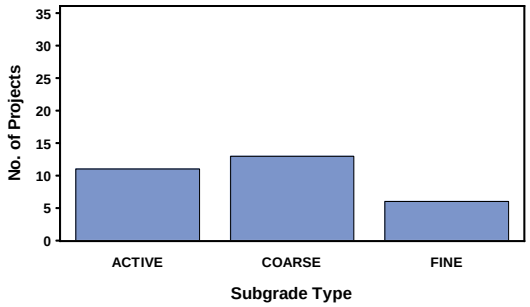

Source: FHWA.

A. SPS-8 AC pavements.

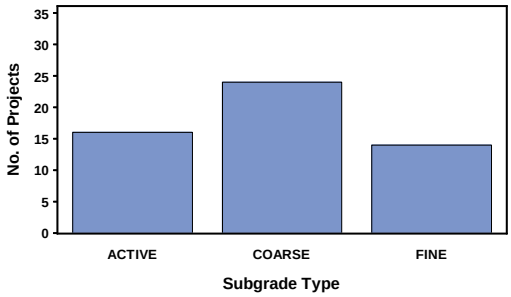

Source: FHWA.

B. Companion GPS-1 and SPS-1 AC pavements.

Figure 34. Graphs. Distribution of subgrade type for AC pavement projects.

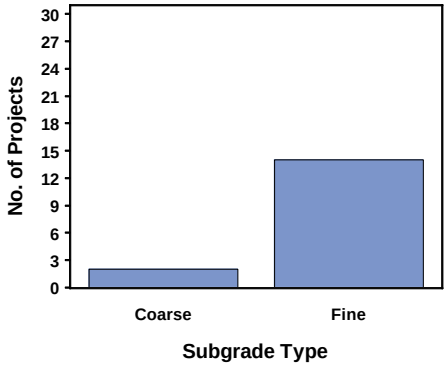

Source: FHWA.

A. SPS-8 JPCPs.

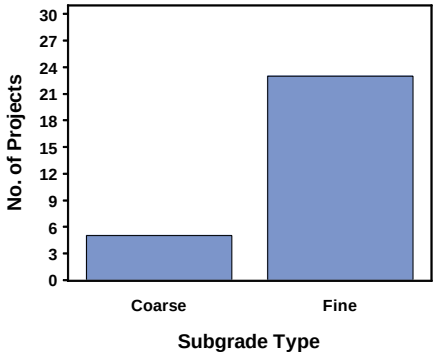

Source: FHWA.

B. Companion GPS-3 and SPS-2 JPCPs.

Figure 35. Graphs. Distribution of subgrade type for JPCP projects.

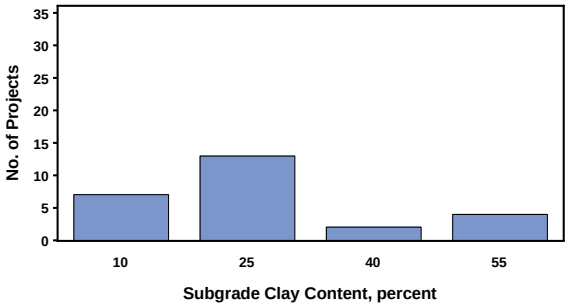

Source: FHWA.

A. SPS-8 AC pavements.

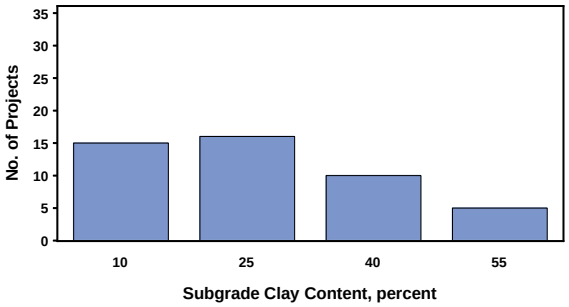

Source: FHWA.

B. Companion GPS-1 and SPS-1 AC pavements.

Figure 36. Graphs. Distribution of subgrade clay content for AC pavement projects.

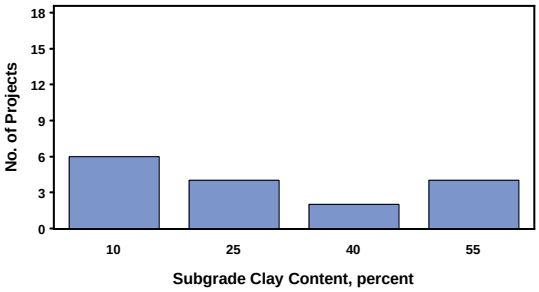

Source: FHWA.

A. SPS-8 JPCPs.

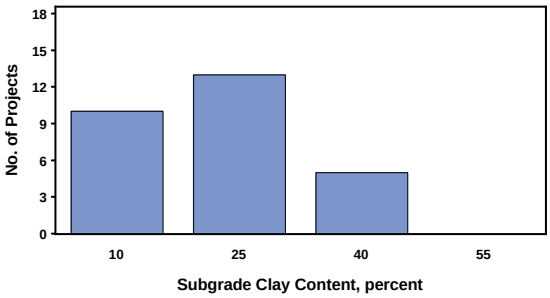

Source: FHWA.

B. Companion GPS-3 and SPS-2 JPCPs.

Figure 37. Graphs. Distribution of subgrade clay content for JPCP projects.

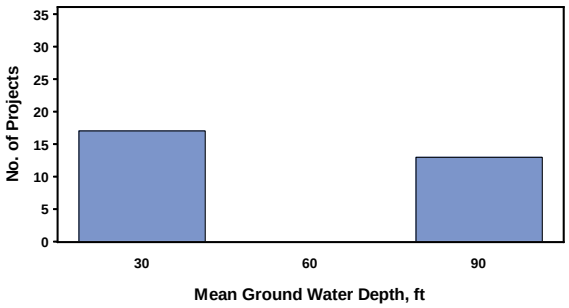

Source: FHWA.

A. SPS-8 AC pavements.

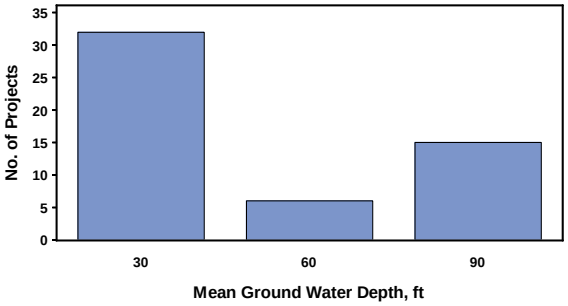

Source: FHWA.

B. Companion GPS-1 and SPS-1 AC pavements.

Figure 38. Graphs. Distribution of mean depth to GWT for AC pavement projects.

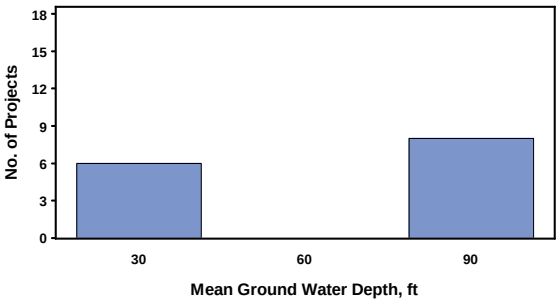

Source: FHWA.

A. SPS-8 JPCPs.

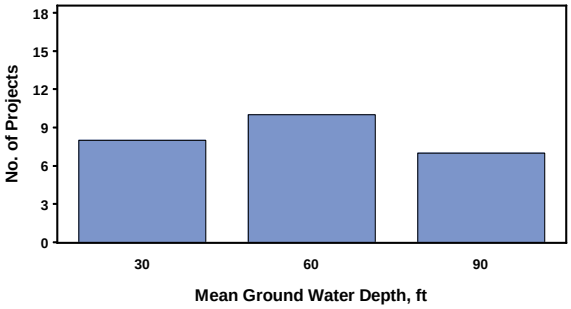

Source: FHWA.

B. Companion GPS-3 and SPS-2 JPCPs.

Figure 39. Graphs. Distribution of mean depth to GWT for JPCP projects.

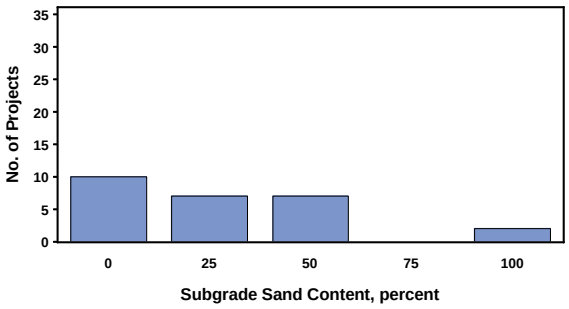

Source: FHWA.

A. SPS-8 AC pavements.

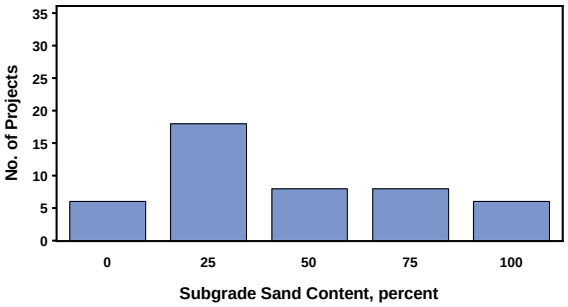

Source: FHWA.

B. Companion GPS-1 and SPS-1 AC pavements.

Figure 40. Graphs. Distribution of subgrade sand content for SPS-8 projects and GPS-1/SPS-1 companion projects.

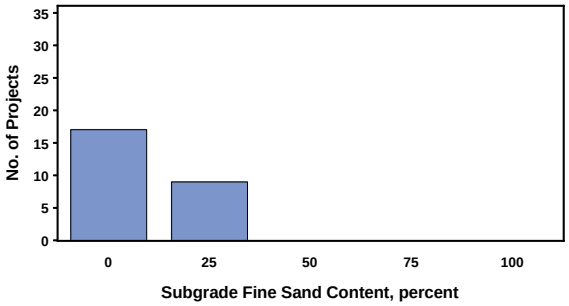

Source: FHWA.

A. SPS-8 JPCPs.

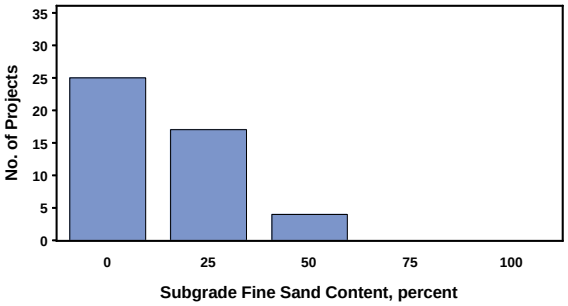

Source: FHWA.

B. Companion GPS-3 and SPS-2 JPCPs.

Figure 41. Graphs. Distribution of subgrade fine-sand content for SPS-8 projects and GPS-3/SPS-2 JPCP projects.

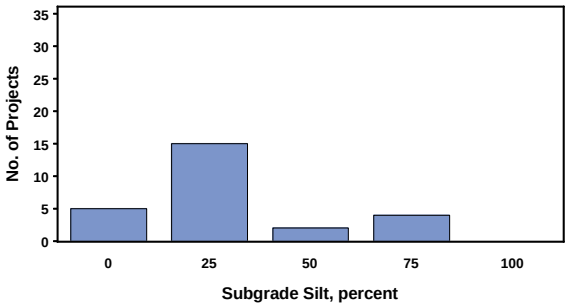

Source: FHWA.

A. SPS-8 AC pavements.

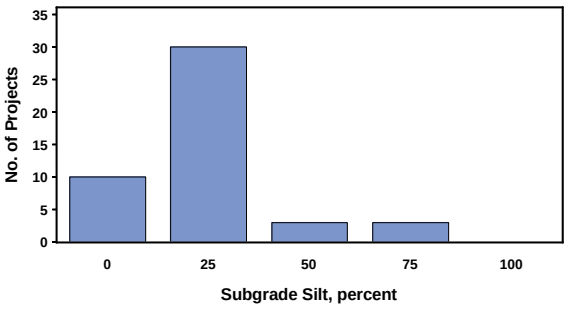

Source: FHWA.

B. Companion GPS-1 and SPS-1 AC pavements.

Figure 42. Graphs. Distribution of subgrade silt content for SPS-8 projects and GPS-1/SPS-1 AC projects.

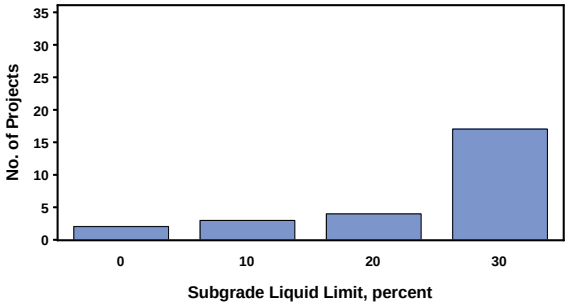

Source: FHWA.

A. SPS-8 AC pavements.

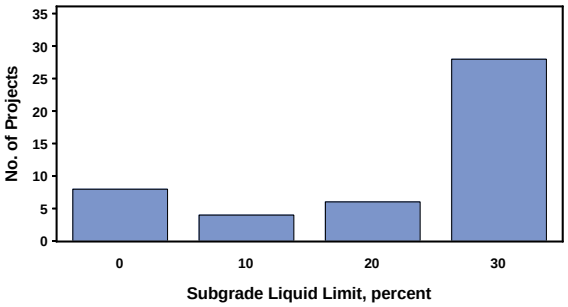

Source: FHWA.

B. Companion GPS-1 and SPS-1 AC pavements.

Figure 43. Graphs. Distribution of subgrade material liquid limit for SPS-8 projects and GPS-1/SPS-1 companion projects.

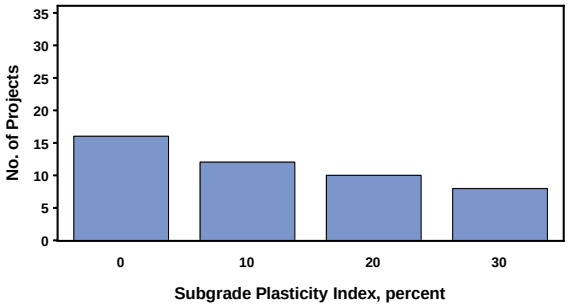

Source: FHWA.

A. SPS-8 AC pavements.

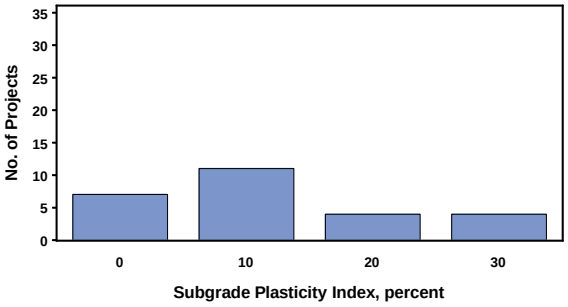

Source: FHWA.

B. Companion GPS-1 and SPS-1 AC pavements.

Figure 44. Graphs. Distribution of subgrade material PI for SPS-8 AC projects and GPS-1/SPS-1 companion projects.

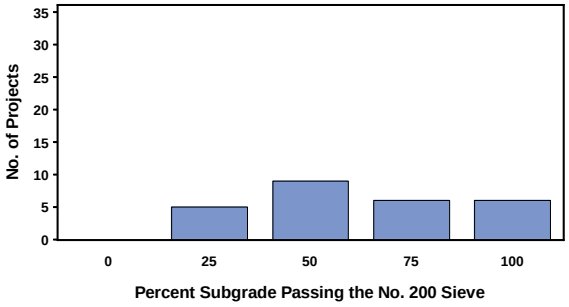

Source: FHWA.

A. SPS-8 AC pavements.

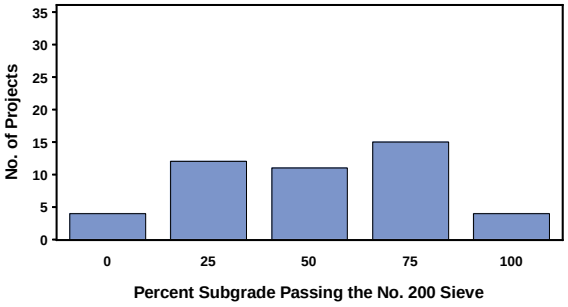

Source: FHWA.

B. Companion GPS-1 and SPS-1 AC pavements.

Figure 45. Graphs. Distribution of subgrade material percent passing the No. 200 sieve size for SPS-8 AC projects and GPS-1/SPS-1 projects.

STATISTICAL COMPARISON OF PAVEMENT THICKNESS FOR LOW- AND HIGH-TRAFFICKED AC PROJECTS

All key variables previously listed in chapter 5 were used to characterize pavement design and environmental exposure to determine whether the high-trafficked GPS-1/SPS-1 companion projects and low-trafficked SPS-8 projects were statistically similar. The statistical analysis conducted was the independent two-sample *t*-test used to test the following hypotheses:

- **Null hypothesis**: $V_{POP\_G/SPS-1\_MEAN} = V_{POP\_SPS8\_MEAN}$.
- **Alternate hypothesis**: $V_{POP\_G/SPS-1\_MEAN} \neq V_{POP\_SPS8\_MEAN.}$

Where:

$V_{POP\_G/SPS-1\_MEAN}$ = mean values of any variable of interest for the GPS-1 and SPS-1 projects.

$V_{POP\_SPS8\_MEAN}$ = mean values of any variable of interest for the SPS-8 projects.

The statistical program SAS® was used to test these hypotheses by computing the following:

- Mean values of the variables of interest for the GPS-1, SPS-1, and SPS-8 projects.
- The 95-percent significance interval of the difference in means.
- The statistical *t*-test along with degrees of freedom.
- The two-tailed probability *p*-value.

For most engineering statistical comparison analyses, when the *p*-value is less than the conventional 0.05, the null hypothesis is rejected, and the alternate hypothesis is accepted. It must be noted, however, that *p*-values should not be strictly interpreted (i.e., a change in *p*-value from 0.04 to 0.06 should not necessarily imply change from significance to insignificance). Engineering judgment should be exercised in such situations to determine engineering significance. The outcomes of computations for statistical *t*-tests and *p*-values are very much dependent on whether the variances from both samples for a given variable are known or unknown or equal or unequal. Thus, the first step in performing the two-sample *t*-test is to test the equality of variance. Once that is determined, the appropriate methodology for determining the *p*-value (based on equal or unequal variance assumption) must be selected.

Table 13 lists the design variables of interest used to determine whether the high- and low-trafficked projects were statistically similar, along with the outcomes from the test of equality of variance from the two populations. Based on the results presented in table 13, a *t*-test was performed for the AC pavement design variables of interest. The results are presented in table 14.

Table 13. Design variables of interest (AC and granular base layer thickness) and outcomes from the test of equality of variance from the SPS-8 and GPS-1/SPS-1 populations.

Pavement Type	Thickness Variable	*p*-Value	Interpretation of Results	Implications for *t*-test
Thin AC	AC layer	0.1309	No significant difference	Assume equal variance
Thin AC	Granular-base layer	0.0006	Significant difference	Assume unequal variance
Thick AC	AC layer	0.0032	Significant difference	Assume unequal variance
Thick AC	Granular-base layer	0.1674	No significant difference	Assume equal variance

Table 14. Summary of results from the *t*-test of key design variables from the SPS-8 and GPS-1/SPS-1 flexible pavement populations.

Pavement Type	Thickness Variable	Test Method and Assumed Variances	*p*-Value	Interpretation of Results at 95-Percent Significance Level
Thin AC	AC layer	Pooled/equal	0.9977	No significant difference
Thin AC	Granular-base layer	Satterthwaite/unequal	0.0317	Significant difference
Thick AC	AC layer	Satterthwaite/unequal	0.5296	No significant difference
Thick AC	Granular-base layer	Pooled/equal	0.0264	Significant difference

Both thin and thick AC layers for the SPS-8 and GPS-1/SPS-1 projects represented the same population and, thus, were good for direct comparison. The base thicknesses, however, were different. The actual mean base thicknesses for the thin AC projects of SPS-8 and GPS-1/SPS-1 were 7.83 and 9.74 inches, respectively; for the thick AC projects, the base thicknesses were 11.33 and 9.68, respectively. From an engineering perspective, however, the differences in base thickness of this magnitude for an unbound base course were not believed to have a significant effect on long-term pavement performance.

STATISTICAL COMPARISON OF RAINFALL-RELATED VARIABLES FOR LOW- AND HIGH-TRAFFICKED AC/PCC PAVEMENT PROJECTS

Table 15 presents the rainfall-related variables of interest used to determine whether the high- and low-trafficked projects were statistically similar, along with the outcomes of the test of equality of variance from the two populations. Based on the results presented in table 15, a *t*-test was performed for the AC/PCC pavement rainfall-related variables. The results are presented in table 16.

Table 15. Rainfall-related variables of interest and outcomes from the test of equality of variance from the SPS-8 and companion populations.

Climate	Climate Variable	*p*-Value	Interpretation of Results at 95-Percent Significance	Implications for *t*-test
Dry	Annual rainfall	0.1508	No significant difference	Assume equal variance
Dry	Annual wet days	0.2531	No significant difference	Assume equal variance
Wet	Annual rainfall	0.0311	Significant difference	Assume unequal variance
Wet	Annual wet days	0.7582	No significant difference	Assume equal variance

Table 16. Summary of results from the *t*-test of key rainfall-related variables from the SPS-8 and companion populations.

Climate	Climate Variable	Test Method and Assumed Variances	*p*-Value	Interpretation of Results
Dry	Annual rainfall	Pooled/equal	0.0027	Significant difference
Dry	Annual wet days	Pooled/equal	0.0050	Significant difference
Wet	Annual rainfall	Satterthwaite/unequal	0.6161	No significant difference
Wet	Annual wet days	Pooled/equal	0.3462	No significant difference

For the wet climates, there was no significant difference in mean annual rainfall and mean annual number of wet days for the SPS-8 and companion projects (i.e., they represented the same population). For the dry climates, the opposite was true at the 95 percent statistical level. Considering that both rainfall and number of wet days for the dry climates is small, the impact of this difference on performance was not considered significant.

STATISTICAL COMPARISON OF TEMPERATURE-RELATED VARIABLES FOR LOW- AND HIGH-TRAFFICKED AC AND PCC PAVEMENT PROJECTS

Table 17 lists the temperature-related variables of interest used to determine whether the high- and low-trafficked projects were statistically similar and outcomes from the test of equality of variance from the two populations. Based on the results presented, the *t*-test was performed for AC pavement and JPCP temperature-related variables. The results are presented in table 18. The temperature-related variables selected for use in characterizing pavement environment were essentially from the same population. Thus, the impact of these variables on similar pavement performance is expected to be about the same.

Table 17. Environmental temperature-related variables of interest and outcomes from the test of equality of variance from the SPS-8 and companion populations.

Climate	Climate Variable	*p*-Value	Interpretation of Results	Assumed Variance for *t*-test
Freeze	Mean ambient temperature	0.8842	No significant difference	Assume equal variance
Freeze	Mean number of days greater than 90 °F	0.0226	Significant difference	Assume unequal variance
Freeze	Mean number of days less than 32 °F	0.0856	No significant difference	Assume equal variance
Freeze	Freezing index	0.4318	No significant difference	Assume equal variance
Freeze	Annual number of freeze–thaw cycles	0.1312	No significant difference	Assume equal variance
Nonfreeze	Mean ambient temperature	0.167	No significant difference	Assume equal variance
Nonfreeze	Mean number of days greater than 90 °F	0.0804	No significant difference	Assume equal variance
Nonfreeze	Mean number of days less than 32 °F	0.801	No significant difference	Assume equal variance
Nonfreeze	Freezing index	0.6859	No significant difference	Assume equal variance
Nonfreeze	Annual number of freeze–thaw cycles	0.9203	No significant difference	Assume equal variance

Table 18. Summary of results from the *t*-test of temperature-related variables from the SPS-8 and companion populations.

Climate	Climate Variable	Test Method and Assumed Variances	*p*-Value	Interpretation of Results
Freeze	Mean ambient temperature	Pooled/equal	0.2919	No significant difference
Freeze	Mean number of days greater than 90 °F	Satterthwaite/ unequal	0.2268	No significant difference
Freeze	Mean number of days less than 32 °F	Pooled/equal	0.2164	No significant difference
Freeze	Freezing index	Pooled/equal	0.7323	No significant difference
Freeze	Annual number of freeze–thaw cycles	Pooled/equal	0.1356	No significant difference
Nonfreeze	Mean ambient temperature	Pooled/equal	0.4125	No significant difference
Nonfreeze	Mean number of days greater than 90 °F	Pooled/equal	0.7825	No significant difference
Nonfreeze	Mean number of days less than 32 °F	Pooled/equal	0.2841	No significant difference
Nonfreeze	Freezing index	Pooled/equal	0.5843	No significant difference
Nonfreeze	Annual number of freeze–thaw cycles	Pooled/equal	0.2957	No significant difference

STATISTICAL COMPARISON OF THE POPULATIONS OF THE LOW- AND HIGH-TRAFFICKED AC/PCC PAVEMENT PROJECTS AND SUBGRADE-RELATED VARIABLES

Table 19 lists the subgrade-related variables of interest used to determine whether the high- and low-trafficked projects were statistically similar and outcomes from the test of equality of variance from the two populations. Based on the results presented, a *t*-test was performed for the AC/PCC pavement environmental subgrade-related variables. The results are presented in table 20.

The percent sand content, percent silt content, and depth to groundwater table (GWT) were the variables used to characterize subgrade material properties that were significantly different at the 95-percent significance level for the two groupings. Further examination of the differences indicates that, from an engineering perspective, the mean differences in percent sand content, percent silt content, and the depth to GWT will not result in significantly different levels of performance.

Table 19. Subgrade-related variables of interest and outcomes from the test of equality of variance from the SPS-8 and companion populations.

Subgrade Type	Subgrade Variable	*p*-Value	Interpretation of Results (Difference in Equality of Variance)	Assumed Variance for *t*-test
Coarse	Percent passing No. 40 sieve	0.6589	No significant difference	Equal variance
Coarse	Percent passing No. 200 sieve	0.8257	No significant difference	Equal variance
Coarse	Percent sand content	0.7996	No significant difference	Equal variance
Coarse	Percent fine-sand content	0.5826	No significant difference	Equal variance
Coarse	Percent silt content	0.0144	Significantly different	Unequal variance
Coarse	Percent clay content	0.1705	No significant difference	Equal variance
Coarse	Liquid limit	0.1891	No significant difference	Equal variance
Coarse	PI	0.0491	No significant difference	Equal variance
Coarse	Mean GWT depth	<0.0001	Significant difference	Unequal variance
Fine	Percent passing No. 40 sieve	0.0707	No significant difference	Equal variance
Fine	Percent passing No. 200 sieve	0.1819	No significant difference	Equal variance
Fine	Percent sand content	0.2328	No significant difference	Equal variance
Fine	Percent fine-sand content	0.0497	No significant difference	Equal variance
Fine	Percent silt content	0.0549	No significant difference	Equal variance
Fine	Percent clay content	0.3551	No significant difference	Equal variance
Fine	Liquid limit	0.1779	No significant difference	Equal variance
Fine	PI	0.7233	No significant difference	Equal variance
Fine	Mean GWT depth	0.0306	Significant difference	Unequal variance

Table 20. Summary of results from the *t*-test of subgrade-related variables of interest from the SPS-8 and companion populations.

Climate	Climate Variable	Test Method and Assumed Variances	*p*-Value	Interpretation of Results
Coarse	Percent passing No. 40 sieve	Pooled/equal	0.5441	Equal variance
Coarse	Percent passing No. 200 sieve	Pooled/equal	0.7798	Equal variance
Coarse	Percent sand content	Pooled/equal	0.4174	Equal variance
Coarse	Percent fine-sand content	Pooled/equal	0.4343	Equal variance
Coarse	Percent silt content	Satterthwaite/unequal	0.0287	Unequal variance
Coarse	Percent clay content	Pooled/equal	0.2285	Equal variance
Coarse	Liquid limit	Pooled/equal	0.3671	Equal variance
Coarse	PI	Pooled/equal	0.2296	Equal variance
Coarse	Mean GWT depth	Satterthwaite/unequal	0.0087	Unequal variance
Fine	Percent passing No. 40 sieve	Pooled/equal	0.0919	Equal variance
Fine	Percent passing No. 200 sieve	Pooled/equal	0.0551	Equal variance
Fine	Percent sand content	Pooled/equal	0.0235	Equal variance
Fine	Percent fine-sand content	Pooled/equal	0.0843	Equal variance
Fine	Percent silt content	Pooled/equal	0.0838	Equal variance
Fine	Percent clay content	Pooled/equal	0.6784	Equal variance
Fine	Liquid limit	Pooled/equal	0.5878	Equal variance
Fine	PI	Pooled/equal	0.7768	Equal variance
Fine	Mean GWT depth	Satterthwaite/unequal	0.003	Unequal variance

NON-LTPP ENVIRONMENTAL DATA

Although the LTPP database contained very detailed information on ambient conditions (e.g., temperature and rainfall) and subgrade type/strength for pavement projects, for the purposes of this present study, the database lacked sufficiently detailed information on the in situ temperature and moisture conditions within the pavement layers and foundation and a definition and characterization of the entire pavement foundation (up to 15 ft of soil material or bedrock, whichever was higher).[17] The researchers investigated non-LTPP data sources to characterize

pavement in situ moisture, temperature conditions, and subgrade foundation. Two sources of additional data were identified: the NWIS and SSURGO databases.[50,49] The following subsections briefly describe these databases and their relevance to the current study.

NWIS Database[50]

The NWIS includes extensive information on both bodies of surface water and groundwater (e.g., depth, quality) across the United States.[50] It contains over 850,000 records of groundwater data gathered from wells, springs, test holes, and excavations. The locations from which data were gathered is referenced by site-descriptive information, including latitude and longitude. Groundwater levels in these wells were monitored continuously (sometimes over 40 yr) and stored as discrete field-water-level measurements or as continuous time-series data from automated recorders. The raw data are used to compute parameters such as daily, monthly, and annual groundwater depth. The GWT depths for each SPS-8 and complementary site were estimated from this database as follows:

1. The closest well in the database was identified.

2. The distance from the SPS-8 project and closest well was computed (using the latitude and longitude coordinates available for both pavement and well/test holes, etc.).

3. Time-based groundwater-depth data were assembled and reviewed for reasonableness and consistency (i.e., seasonal variation).

4. GWT depth for each site was computed. In the calculation of average groundwater depths, seasonal variations were ignored, but a trimmed mean was applied that essentially neglected any single value that varied more than 25 percent from the mean.

Table 21 summarizes the seasonal and average groundwater depths determined for each SPS-8 project.

Table 21. GWT data for all LTPP sites obtained from the NWIS database.[50]

NWIS Well Site Number	SHRP ID	Latitude (Degrees)	Longitude (Degrees)	Elevation (ft)	Well Depth (ft)	Distance from Project to Well (mi)	Depth to GWT by Season (ft)				
							Fall	Spring	Winter	Summer	Mean
323503085160901	1_0101	32.6	–85.3	151	55	1.8	25.5	25.5	25.5	25.5	25.5
323503085160901	1_0102	32.6	–85.3	151	55	1.8	25.5	25.5	25.5	25.5	25.5
311338085334901	1_4155	31.2	–85.6	325	468	1.0	69.4	69.4	69.4	69.4	69.4
352516114133701	4_0113	35.4	–114.3	3,580	—	2.4	49.5	49.5	49.5	49.5	49.5
352516114133701	4_0114	35.4	–114.3	3,580	—	2.4	49.5	49.5	49.5	49.5	49.5
332603112435301	4_0215	33.5	–112.7	1,100	325	1.2	84.2	84.2	84.2	84.2	84.2
332603112435301	4_0262	33.5	–112.7	1,100	325	1.2	84.2	84.2	84.2	84.2	84.2
332603112435301	4_0265	33.5	–112.7	1,100	325	1.2	84.2	84.2	84.2	84.2	84.2
332445112345501	4_1007	33.4	–112.6	1,044	—	1.7	140.8	142.1	143.4	142.1	142.1
340924114153701	4_1034	34.2	–114.3	419	245	0.4	103.7	103.9	102.6	114.8	106.2
354251114284901	4_1036	35.7	–114.5	2,406	460	0.3	390.3	391.8	389.4	400.0	392.9
354309090365301	5_0113	35.7	–90.6	222	—	2.0	12.3	12.3	11.1	13.6	12.3
354309090365301	5_0114	35.7	–90.6	222	—	2.0	12.3	12.3	11.1	13.6	12.3
341238091582101	5_0803	34.2	–92.0	208	88	0.8	16.8	16.4	16.9	16.5	16.6
341238091582101	5_0804	34.2	–92.0	208	88	0.8	16.8	16.4	16.9	16.5	16.6
341238091582101	5_0809	34.2	–92.0	208	88	0.8	16.8	16.4	16.9	16.5	16.6
341238091582101	5_0810	34.2	–92.0	208	88	0.8	16.8	16.4	16.9	16.5	16.6
372457120454001	6_0201	37.4	–120.8	120	139	0.3	25.0	25.0	25.0	25.0	25.0
372523120455601	6_0811	37.4	–120.8	118	100	0.1	27.0	27.0	27.0	27.0	27.0
372523120455601	6_0812	37.4	–120.8	118	100	0.1	27.0	27.0	27.0	27.0	27.0
351258120364501	6_8153	35.2	–120.6	252	—	0.3	23.5	28.0	39.8	30.5	30.5
350547120070401	6_8156	35.1	–120.1	1,084	99	2.0	65.8	60.0	62.9	62.9	62.9
372457120454001	6_A805	37.4	–120.8	118	139	0.1	25.0	25.0	25.0	25.0	25.0
372457120454001	6_A806	37.4	–120.8	118	139	0.1	25.0	25.0	25.0	25.0	25.0
395544104472600	8_0215	39.9	–104.8	5,077	30	0.4	7.0	3.2	3.3	4.5	4.5
395636104470201	8_0811	39.9	–104.8	5,095	366	0.1	31.4	31.4	31.4	31.4	31.4
395636104470201	8_0812	39.9	–104.8	5,095	366	0.1	31.4	31.4	31.4	31.4	31.4
400515108495301	8_1047	40.1	–108.8	5,260	12	1.0	10.2	10.2	10.2	10.2	10.2
384108108024401	8_1053	38.7	–108.0	5,140	23	1.4	19.3	19.3	19.3	19.3	19.3
390419108294601	8_1057	39.1	–108.5	4,586	47	2.0	12.9	12.9	12.9	12.9	12.9
394439104420002	8_7776	39.7	–104.7	5,280	979	0.3	337.5	369.9	305.0	337.5	337.5
412013072030601	9_1803	41.4	–72.0	165	18	4.1	15.5	14.5	14.4	16.1	15.1

NWIS Well Site Number	SHRP ID	Latitude (Degrees)	Longitude (Degrees)	Elevation (ft)	Well Depth (ft)	Distance from Project to Well (mi)	Depth to GWT by Season (ft)				
							Fall	Spring	Winter	Summer	Mean
264022081054101	12_0101	26.5	–80.7	14	11	27.5	2.3	2.7	2.0	2.3	2.3
264022081054101	12_0102	26.5	–80.7	14	11	27.5	2.3	2.7	2.0	2.3	2.3
255222080123001	12_1060	25.7	–80.3	10	96	14.2	7.1	7.1	7.1	7.1	7.1
331304084100901	13_1004	33.2	–84.2	760	185	1.4	46.8	46.8	46.8	46.8	46.8
323522083424501	13_1005	32.6	–83.7	452	95	1.9	55.4	55.4	55.4	55.4	55.4
334259085173401	13_3016	33.7	–85.3	1,218	160	2.4	21.8	21.8	21.8	21.8	21.8
205925156402002	15_1006	21.0	–156.7	70	65	0.2	60.5	60.5	60.5	60.5	60.5
474628116472101	16_1001	47.8	–116.8	2,150	360	0.0	307.0	303.6	309.1	308.2	307.0
443736116263701	16_1005	44.6	–116.4	3,232	176	0.3	121.9	121.4	122.4	121.8	121.9
403425093024601	19_0215	41.6	–93.5	945	85	75.1	61.6	61.6	61.6	61.6	61.6
403425093024601	19_0259	41.6	–93.5	945	85	75.1	61.6	61.6	61.6	61.6	61.6
425246091042101	19_3055	42.4	–93.6	1,186	229	131.6	9.9	8.9	9.6	9.6	9.5
362838100000401	20_0163	37.6	–99.3	2,177	411	88.4	142.4	138.5	134.5	138.5	138.5
400508096555001	20_0201	39.0	–97.0	1,194	123	75.4	47.6	45.7	42.9	45.4	45.4
420100072322901	25_1002	42.2	–72.6	88	250	10.9	20.0	20.0	20.0	20.0	20.0
415755071500001	25_1003	42.2	–71.3	128	100	30.3	20.0	20.0	20.0	20.0	20.0
424832087482001	26_0113	43.0	–84.5	810	1,500	167.3	138.0	129.0	120.0	129.0	129.0
424832087482001	26_0114	43.0	–84.5	810	1,500	167.3	138.0	129.0	120.0	129.0	129.0
440317087410101	26_0215	41.8	–83.7	677	203	257.3	28.0	28.0	28.0	28.0	28.0
444700092472201	27_3003	44.4	–94.4	1,066	295	83.8	130.0	130.0	130.0	130.0	130.0
462956092164501	27_6251	47.5	–94.9	1,364	400	141.1	48.5	58.8	73.9	61.5	60.7
342548089531901	28_0805	34.4	–89.9	276	310	0.6	50.0	50.0	50.0	50.0	50.0
342548089531901	28_0806	34.4	–89.9	276	310	0.6	50.0	50.0	50.0	50.0	50.0
365844093143001	29_0801	37.0	–93.2	1,315	345	0.9	174.1	187.3	187.3	200.5	187.3
365844093143001	29_0802	37.0	–93.2	1,315	345	0.9	174.1	187.3	187.3	200.5	187.3
365844093143001	29_0807	37.0	–93.2	1,315	345	0.9	174.1	187.3	187.3	200.5	187.3
365844093143001	29_0808	37.0	–93.2	1,315	345	0.9	174.1	187.3	187.3	200.5	187.3
383255092114501	29_1002	38.5	–92.4	785	610	9.1	150.0	150.0	150.0	150.0	150.0
392040091202001	29_A801	39.5	–91.4	660	425	13.3	209.0	209.0	209.0	209.0	209.0
392040091202001	29_A802	39.5	–91.4	660	425	13.3	209.0	209.0	209.0	209.0	209.0
392040091202001	29_A807	39.5	–91.4	660	425	13.3	209.0	209.0	209.0	209.0	209.0
392040091202001	29_A808	39.5	–91.4	660	425	13.3	209.0	209.0	209.0	209.0	209.0
472325111342801	30_0114	47.4	–111.6	3,343	123	0.6	7.5	7.5	7.5	7.5	7.5

NWIS Well Site Number	SHRP ID	Latitude (Degrees)	Longitude (Degrees)	Elevation (ft)	Well Depth (ft)	Distance from Project to Well (mi)	Depth to GWT by Season (ft)				
							Fall	Spring	Winter	Summer	Mean
460802112533201	30_0805	46.1	–112.9	4,200	77	0.4	68.8	66.0	67.1	61.5	65.8
460802112533201	30_0806	46.1	–112.9	4,200	77	0.4	68.8	66.0	67.1	61.5	65.8
461710109100001	30_8129	46.3	–109.1	4,440	785	2.6	110.0	110.0	110.0	110.0	110.0
404042117005401	32_0101	40.7	–117.0	4,550	811	1.1	57.0	57.0	57.0	57.0	57.0
404042117005401	32_0102	40.7	–117.0	4,550	811	1.1	57.0	57.0	57.0	57.0	57.0
404344117030601	32_0204	40.7	–117.0	4,550	645	0.9	50.0	50.0	50.0	50.0	50.0
410443073414101	34_0801	40.7	–73.8	410	250	29.9	5.5	4.9	4.6	6.8	5.5
410443073414101	34_0802	40.7	–73.8	410	250	29.9	5.5	4.9	4.6	6.8	5.5
410443073414101	34_0859	40.7	–73.8	410	250	29.9	5.5	4.9	4.6	6.8	5.5
410443073414101	34_0860	40.7	–73.8	410	250	29.9	5.5	4.9	4.6	6.8	5.5
323930107041401	35_0101	32.7	–107.1	4,117	23	1.4	15.5	15.2	17.2	16.5	16.1
323930107041401	35_0102	32.7	–107.1	4,117	23	1.4	15.5	15.2	17.2	16.5	16.1
321750108192501	35_0801	32.2	–108.3	4,554	142	7.3	33.3	33.3	33.3	33.3	33.3
321750108192501	35_0802	32.2	–108.3	4,554	142	7.3	33.3	33.3	33.3	33.3	33.3
332651104311801	35_1003	33.4	–104.7	3,800	223	13.0	43.2	43.2	43.2	43.2	43.2
360313107473401	35_1022	36.4	–107.8	6,727	5,687	22.2	13.5	13.5	13.7	13.2	13.5
323536103301101	35_1112	32.6	–103.5	3,760	70	2.6	56.5	56.9	58.4	54.2	56.5
323536103301101	35_3010	32.6	–103.5	3,760	70	2.7	56.5	56.9	58.4	54.2	56.5
394905075401101	36_0801	43.4	–77.9	250	185	270.7	37.4	37.4	37.4	37.4	37.4
394905075401101	36_0802	43.4	–77.9	250	185	270.7	37.4	37.4	37.4	37.4	37.4
394905075401101	36_0859	43.4	–77.9	250	185	270.7	37.4	37.4	37.4	37.4	37.4
325816081320401	37_0801	34.8	–77.7	44	119	256.0	21.1	21.1	21.1	21.1	21.1
325816081320401	37_0802	34.8	–77.7	44	119	256.0	21.1	21.1	21.1	21.1	21.1
325816081320401	37_0859	34.8	–77.7	44	119	256.0	21.1	21.1	21.1	21.1	21.1
345455083143101	37_1801	35.6	–82.4	2,270	33	65.7	20.2	20.2	20.2	20.2	20.2
385128077001601	37_1802	36.3	–78.6	500	398	196.4	22.6	11.6	33.6	22.6	22.6
345455083143101	37_1817	36.1	–80.2	850	33	191.2	20.2	20.2	20.2	20.2	20.2
425625098342901	38_0215	46.9	–97.2	932	—	280.0	251.1	252.5	253.6	252.4	252.4
425625098342901	38_0260	46.9	–97.2	932	—	280.0	251.1	252.5	253.6	252.4	252.4
425625098342901	38_0261	46.9	–97.2	932	—	280.0	251.1	252.5	253.6	252.4	252.4
394905075401101	42_1597	42.0	–77.2	1,093	185	169.9	37.4	37.4	37.4	37.4	37.4
345454083143201	45_1008	34.8	–83.1	936	385	14.2	106.4	106.4	106.4	106.4	106.4
320124080510101	45_1011	32.8	–80.0	12	575	73.0	34.0	31.0	34.2	37.7	34.2

NWIS Well Site Number	SHRP ID	Latitude (Degrees)	Longitude (Degrees)	Elevation (ft)	Well Depth (ft)	Distance from Project to Well (mi)	Depth to GWT by Season (ft)				
							Fall	Spring	Winter	Summer	Mean
455745104053201	46_0803	45.9	–100.4	1,680	200	177.4	102.0	102.0	102.0	102.0	102.0
455745104053201	46_0804	45.9	–100.4	1,680	200	177.4	102.0	102.0	102.0	102.0	102.0
455745104053201	46_0859	45.9	–100.4	1,680	200	177.4	102.0	102.0	102.0	102.0	102.0
425231103235801	46_3053	43.9	–103.5	4,849	39	73.3	10.0	10.0	10.0	10.0	10.0
275228099115201	48_0114	26.7	–98.1	84	—	103.2	161.3	161.3	161.3	161.3	161.3
310345096264601	48_0801	30.8	–96.4	331	1,100	20.2	87.8	79.0	87.8	96.7	87.8
310345096264601	48_0802	30.8	–96.4	331	1,100	20.2	87.8	79.0	87.8	96.7	87.8
343251100271201	48_1077	34.5	–100.4	1,835	70	1.2	30.5	31.8	31.0	34.0	31.8
322624095554601	48_1087	32.4	–95.3	545	45	35.3	12.0	12.0	12.0	12.0	12.0
292110099054501	48_1092	29.4	–99.1	828	1,654	1.1	142.1	149.6	142.2	153.2	146.8
292046098494601	48_1096	29.4	–98.8	774	1,366	0.7	60.0	60.0	60.0	60.0	60.0
282108097394701	48_1174	27.8	–97.9	109	31	41.0	10.5	10.5	10.5	10.5	10.5
282958098125401	48_1181	28.6	–98.2	195	120	6.2	62.5	62.5	62.5	62.5	62.5
334213100511202	48_3609	33.6	–100.8	2,289	110	7.6	35.5	35.0	34.4	35.2	35.0
305457097353601	48_A807	31.0	–97.8	804	95	11.8	72.2	72.2	72.6	72.4	72.3
305457097353601	48_A808	31.0	–97.8	804	95	11.8	72.2	72.2	72.6	72.4	72.3
420205111152501	49_0803	40.6	–111.1	6,485	69	102.1	22.0	22.0	22.0	22.0	22.0
420205111152501	49_0804	40.6	–111.1	6,485	69	102.1	22.0	22.0	22.0	22.0	22.0
385128077001601	51_0113	36.7	–79.4	643	398	199.3	22.6	11.6	33.6	22.6	22.6
385128077001601	51_0114	36.7	–79.4	643	398	199.3	22.6	11.6	33.6	22.6	22.6
471316117000101	53_0201	47.1	–118.4	1,631	227	67.7	36.3	36.3	36.3	36.3	36.3
471316117000101	53_0204	47.1	–118.4	1,631	227	67.7	36.3	36.3	36.3	36.3	36.3
462125117022001	53_0801	46.3	–117.9	1,985	304	40.8	247.1	241.7	243.8	249.2	245.5
462125117022001	53_0802	46.3	–117.9	1,985	304	40.8	247.1	241.7	243.8	249.2	245.5
462233117024201	53_1002	46.4	–117.9	1,557	115	42.9	50.2	51.4	49.1	50.2	50.2
480548117013801	53_1006	48.0	–119.9	820	163	132.7	105.7	106.2	107.3	106.2	106.3
473143117003301	53_1008	47.6	–117.4	2,356	140	18.1	106.7	106.7	106.7	106.7	106.7
474132117022701	53_1501	47.6	–119.6	2,622	150	119.9	98.1	98.1	97.9	98.4	98.1
474038117021101	53_3013	47.6	–117.4	2,356	170	18.1	98.0	98.0	98.0	98.0	98.0
462233117024201	53_A809	46.4	–118.4	1,256	115	66.3	50.2	51.4	49.1	50.2	50.2
462233117024201	53_A810	46.4	–118.4	1,256	115	66.3	50.2	51.4	49.1	50.2	50.2
444958089184601	55_0805	44.9	–89.3	1,267	92	3.4	18.0	18.0	18.0	18.0	18.0
444958089184601	55_0806	44.9	–89.3	1,267	92	3.4	18.0	18.0	18.0	18.0	18.0

NWIS Well Site Number	SHRP ID	Latitude (Degrees)	Longitude (Degrees)	Elevation (ft)	Well Depth (ft)	Distance from Project to Well (mi)	Depth to GWT by Season (ft)				
							Fall	Spring	Winter	Summer	Mean
434239087502701	55_3009	43.8	–87.9	750	150	3.2	33.0	33.0	33.0	33.0	33.0
434720087473801	55_3010	43.8	–87.8	690	740	2.6	11.0	11.0	11.0	11.0	11.0
405126108435801	56_3027	41.6	–109.2	6,359	86	57.2	76.0	75.5	75.5	75.1	75.5
421252111034701	56_7775	42.0	–109.7	6,433	166	74.1	2.0	2.0	2.0	2.0	2.0
485640113022201	81_1805	50.9	–113.9	3,379	35	141.3	27.0	27.0	27.0	27.0	27.0
460040092214401	83_6450	49.7	–96.3	958	76	311.8	46.4	46.4	46.4	46.4	46.4
460040092214401	83_6451	49.7	–96.3	958	76	312.0	46.4	46.4	46.4	46.4	46.4
485927106283401	90_6410	52.1	–106.6	1,680	180	212.2	97.1	97.1	97.1	97.1	97.1
485927106283401	90_6412	52.1	–106.6	1,678	180	212.3	97.1	97.1	97.1	97.1	97.1

—Data are missing.

SSURGO Database[49]

Pavement foundation strata definition information (i.e., strata/horizon, soil type, thickness, depth to bedrock, etc.) is available in the SSURGO database.[49] Along with the information described, this database contains extensive data on soil features, engineering properties, chemical properties, water features, and more. A summary of the data assembled is presented in table 22. The Distance to Project is from a given known point. The Horizon Surface Depth is the distance from the Earth's surface to the top of the deposit. The Horizon Bottom Depth is the distance from the Earth's surface to the bottom of the deposit.

Table 22. Example subgrade foundation material type and properties table data obtained from the SSURGO database.[49]

SHRP ID	Distance to Project (mi)	Soil Horizon Name	Horizon Surface Depth (ft)	Horizon Bottom Depth (ft)	Horizon Thickness (Inches)	Passing No. 200 Sieve (%)	Sand (%)	Fine Sand (%)	Silt (%)	Clay (%)	Hydraulic Conductivity (ft/d)	Liquid Limit (%)	PI (%)	Soil Class
1_0101	3.8	H1	0	8	8	29	66.8	19.8	19.2	14	28.2	21.5	3.5	A-2-4
1_0101	3.8	H2	8	74	66	63	47.7	15.1	2.3	50	9.2	51.5	22	A-7-6
1_0101	3.8	H3	74	132	58	45	37.1	11.6	40.4	22.5	9.2	27.5	10	A-4
1_0101	3.8	H4	132	178	46	37.5	67.2	20	15.3	17.5	9.2	21.5	3	A-4
4_0265	0.7	H1	0	8	8	30	68.8	33	16.2	15	28.0	20	5	A-2-4
4_0265	0.7	H2	8	102	94	60	63.8	24.6	23.7	12.5	9.0	20	5	A-4
4_0265	0.7	H3	102	137	35	22.5	66.3	12.5	18.7	15	28.0	20	5	A-2-4
4_0265	0.7	H4	137	152	15	65	44.3	13.7	40.7	15	9.0	20	5	A-4
5_0804	0.2	H1	0	15	15	97.5	12.1	3.7	27.9	60	0.2	60	33.5	A-7-6
5_0804	0.2	H2	15	76	61	97.5	8.9	2.7	21.1	70	0.2	70	41.5	A-7-6
5_0804	0.2	H3	76	152	76	85	8.9	2.7	21.1	70	0.2	62.5	36	A-7-6
6_A806	1.2	H1	0	25	25	15	96	37.8	1.5	2.5	91.7	—	0	A-2-4
6_A806	1.2	H2	25	76	51	10	96	37.8	1.5	2.5	91.7	—	0	A-2-4
6_A806	1.2	H3	76	127	51	25	80.5	27.4	17	2.5	91.7	—	0	A-2-4
6_A806	1.2	H4	127	178	51	20	96	37.8	1.5	2.5	91.7	—	0	A-2-4
29_0808	0.7	Ap	0	13	13	45	11	2.8	72.5	16.5	28.0	26	8	A-4
29_0808	0.7	E	13	41	28	50	13.5	3	69.3	17.2	28.0	27	8	A-4
29_0808	0.7	Bt1	41	56	15	55	13.5	2.6	57.2	29.3	28.0	37	16	A-6
29_0808	0.7	2Bt2	56	76	20	45	15.2	2.9	41.5	43.3	9.0	46	27	A-7-6
29_0808	0.7	2Bt3	76	152	76	70	1.5	0.4	17.6	80.9	9.0	66	39	A-7-6
32_0102	0.1	H1	0	28	28	60	63.8	20.5	26.2	10	9.2	22.5	2.5	A-4
32_0102	0.1	H2	28	41	13	—	—	—	—	—	0.0	—	—	ROCK
32_0102	0.1	H3	41	107	66	55	45.3	13.9	43.2	11.5	9.2	20	2.5	A-4
32_0102	0.1	H4	107	152	45	15	68.5	29.8	21.5	10	91.7	20	2.5	A-2-4
35_0802	3.8	H1	0	8	8	82.5	18.1	5.2	50.9	31	2.8	35	15	A-6
35_0802	3.8	H2	8	58	50	67.5	28.1	9.8	29.4	42.5	0.9	50	22.5	A-7-6
35_0802	3.8	H3	58	152	94	57.5	33.5	10.5	36.5	30	2.8	40	15	A-6
46_0803	0.4	H1	0	13	13	67.5	43	13.4	38.5	18.5	9.2	30	8	A-4
46_0803	0.4	H2	13	56	43	67.5	39.1	12.3	36.9	24	9.2	32.5	10.5	A-6
46_0803	0.4	H3	56	152	96	67.5	—	—	—	24	9.2	32.5	10.5	A-6
48_1092	2.6	H1	0	13	13	25	41.1	12.8	36.9	22	9.2	30	11.5	A-2-6
48_1092	2.6	H2	13	30	17	24	34.7	10.8	37.8	27.5	9.2	35	15.5	A-2-6
48_1092	2.6	H3	30	36	6	—	—	—	—	—	2.2	—	—	ROCK

SHRP ID	Distance to Project (mi)	Soil Horizon Name	Horizon Surface Depth (ft)	Horizon Bottom Depth (ft)	Horizon Thickness (Inches)	Passing No. 200 Sieve (%)	Sand (%)	Fine Sand (%)	Silt (%)	Clay (%)	Hydraulic Conductivity (ft/d)	Liquid Limit (%)	PI (%)	Soil Class
48_1092	2.6	H4	36	152	116	—	—	—	—	—	7.8	—	—	ROCK
48_A807	0.5	H1	0	51	51	70.5	35.4	11.2	33.6	31	9.2	34	16	A-6
48_A807	0.5	H2	51	127	76	67.5	37.2	11.7	35.3	27.5	9.2	34	16	A-6
48_A807	0.5	H3	127	152	25	79.5	34.7	10.9	32.8	32.5	9.2	36	18	A-6

—Data not available.

IN SITU PAVEMENT COMPUTED ENVIRONMENT-RELATED DATA VARIABLES

Characterizing in situ pavement temperature/moisture profiles allows for greater insights into the interaction of ambient climate condition and pavement properties, response to traffic and climate loading, and long-term pavement performance. Such detailed characterization can be obtained either directly from temperature and moisture measuring sensors embedded in the pavement or by simulating the temperature and moisture conditions within the pavement structure using one-dimensional finite element models or other simulation techniques.

Only 17 of the selected SPS-8 and companion projects were wired to collect detailed in situ pavement-temperature and moisture-condition data as part of the LTPP Seasonal Monitoring Program. Embedded sensors in these pavements were used to collect temperature, moisture, and freeze–thaw changes in each project's pavement structures on a routine basis. Since this level of in situ pavement-temperature and moisture-condition data was not available for most of the selected projects, the best approach for obtaining such data was through simulation of climatic effects on in situ pavement condition using the ICM. The ICM is a one-dimensional coupled heat and moisture flow program originally developed for FHWA and now used regularly by pavement engineers to simulate in situ pavement temperature and moisture condition as part of design and forensic analysis (incorporated into the AASHTO Pavement ME Design software).[16]

The ICM consists of the following three major components:

- Infiltration and drainage model.
- Climatic materials structural model.
- Frost-heave and thaw-settlement model.

Together, these models compute and forecast the following information among others throughout the entire pavement structure and foundation: temperature, pore-water pressure, water content, and frost and thaw depths.[14] The original version of the ICM has been enhanced and improved over many years.[15]

Several inputs are required to run the ICM. Table 23 lists the required inputs and where they were obtained for this analysis. With these data assembled for each selected project, the ICM was run, and simulation results used to compute key parameters were used to characterize in situ pavement temperature and moisture condition. The ICM runs consisted of the following steps:

1. Assemble all key ICM inputs and create ICM input files.

2. Create project-specific virtual weather stations.

3. Select the closest NCDC weather stations for use in creating virtual weather stations.

4. Use ICM to retrieve from these weather stations all needed information, including hourly air temperature, precipitation, wind speed, percentage of sunshine, and relative humidity.

5. Use the assembled climate data to create virtual weather stations (weighted averages) based on distance from the project site to weather stations and difference in elevation.

6. Run the ICM and obtain results. Store results in several files depending on pavement, layer, and material type.

7. Extract computed in situ pavement temperature and moisture variables (hourly estimates) of interest, including the following:

    a. **AC**: Temperature profile (i.e., temperature from 10 uniformly spaced nodes throughout the AC thickness, including the top and bottom surfaces in degrees Fahrenheit).

    b. **PCC**: Temperature profile (i.e., temperature from 10 uniformly spaced nodes throughout the PCC thickness, including the top and bottom surfaces in degrees Fahrenheit).

    c. **All layers**: Freeze–thaw and a summary of freeze and nonfreeze conditions throughout the pavement profile.

    d. **Unbound base, subgrade, and foundation**: Volumetric moisture content.

Table 23. Summary of key inputs required by the ICM.

Data Category	Data Variables	Source
Model initialization	Base and subgrade construction dates	LTPP[54]
Climatic/boundary conditions	Latitude	LTPP[54]*
Climatic/boundary conditions	Longitude	LTPP[54]*
Climatic/boundary conditions	Elevation	LTPP[54]*
Climatic/boundary conditions	Depth to GWT	NWIS[50]
Pavement structure	Layer thickness	LTPP[54]
Pavement structure	Material type	LTPP[54]
AC and PCC materials	Thermal conductivity	ICM default value[15]
AC and PCC materials	Heat capacity	ICM default value[15]
Unbound materials (compacted or natural)	Atterberg limits	LTPP[54]
Unbound materials (compacted or natural)	Sieve analysis	LTPP[54]
Unbound materials (compacted or natural)	Soil classification	LTPP[54]
Unbound materials (compacted or natural)	Specific gravity of solids	ICM default value[15]
Unbound materials (compacted or natural)	Saturated hydraulic conductivity	Computed using ICM models[15]
Unbound materials (compacted or natural)	Maximum dry unit weight	Computed using ICM models[15]
Unbound materials (compacted or natural)	Optimum moisture content	Computed using ICM models[15]
Unbound materials (compacted or natural)	Dry thermal conductivity	ICM default value[15]
Unbound materials (compacted or natural)	Heat capacity	ICM default value[15]
Unbound materials (compacted or natural)	Soil-water characteristic curve parameters	ICM default value[15]

*Latitude and longitude information was used to identify the closest NCDC weather stations with climate-related data available for obtaining raw climate data required for running the ICM.

The ICM output estimates of temperature, frost, and moisture were used to compute the indices/parameters presented in figure 46 through figure 48.

$$TI_{AC} = \sum_{i=1}^{365}\left(\frac{\sum_{j=1}^{10} TEMP_j * THK_j}{\sum_{j=1}^{10} THK_j}\right)$$

Figure 46. Equation. Determination of AC layer temperature index.

Where:

TI_{AC} = AC layer temperature index.
$TEMP_j$ = mean AC temperature (middle of the AC layer) for a given day j.
THK_j = AC layer thickness for thickness increment j (note the ICM divides total AC thickness into 10 increments and estimates temperature at the midpoint of each thickness increment).
i = day of the year, with January 1 being day 1 and December 31 being day 365.
j = ICM AC/PCC thickness increment (i.e., total thickness divided by 10).

$$\text{FROST}_{\text{AREA}} = \sum_{i=1}^{365}\left[\text{F}THK_{\text{i}}\right]$$

Figure 47. Equation. Determination of frost area.

Where:

$FROST_{AREA}$ = total frost area.
$FTHK_i$ = frost thickness for given day i.

$$\text{MOIST} = \sum_{i=1}^{365}\left[\text{VMC}_{\text{i}}\right]$$

Figure 48. Equation. Determination of moist index.

Where:

$MOIST$ = average weighted base or subgrade volumetric moisture content.
VMC_i = average base or subgrade volumetric moisture content for day i.

Figure 49 shows examples of freeze areas with calculated frost depths using the ICM.

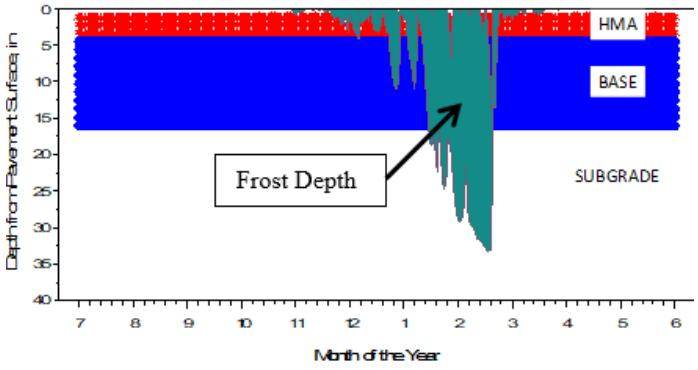

Source: FHWA.

A. Nevada SPS-1 project 0102 pavement structure.

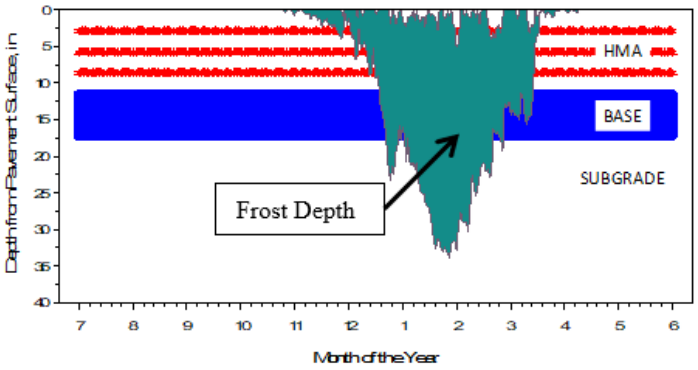

Source: FHWA.

B. Kansas SPS-1 project 0163 pavement structure.

Figure 49. Graphics. Example plots showing deep frost penetration in freeze areas over time estimated using the ICM.

SUMMARY OF DATA AVAILABILITY FOR ANALYSIS AND IDENTIFICATION OF ANOMALIES

Key issues characterized as part of this analysis include the following:

- What important data, if any, are not available from the LTPP database for the SPS-8 flexible and rigid projects constructed as of 2012?[17]
- If data gaps exist, how will they affect analyses?

A summary of findings is presented in the following sections.

Materials Data

Most of the key materials data required for analysis and pavement evaluation were available in the LTPP test tables (e.g., subgrade resilient modulus, unbound base and subgrade classification,

PCC strength, PCC CTE, AC gradation, and binder type).[17] Additional data from the SSURGO and NWIS databases were identified for use in supporting and enhancing the LTPP data.[49,50]

Traffic Data

Truck volume data were available for all non-SPS-8 projects and approximately 90 percent of all SPS-8 projects. Vehicle classification and axle load distribution data were available for all non-SPS-8 projects and approximately 50 percent of all SPS-8 projects. Vehicle classification and axle load distribution data were needed to characterize anomalies in pavement loading and explain the presence of fatigue-related distress, as traffic volumes alone may not be enough to explain discrepancies in measured distress and pavement deterioration.

Climate Data

The data obtained from the LTPP automatic weather stations contained all key climate information (e.g., temperature, precipitation). Seventeen of the test sections for which climate data were obtained from the LTPP virtual weather stations had no humidity and/or wind speed data. Additional data were obtained from the NCDC database.[13]

Construction Data

Data related to construction inputs were obtained from the LTPP database in sufficient detail for the purposes of this study for all the SPS-8 projects.[54] Significant construction deviations and anomalies were reviewed. The information available along with construction-related data in LTPP data tables were used to characterize extent and frequency of construction deviations and determine the impact of construction and materials deviations on pavement performance. Results include the following:

- Few significant construction deviations and material noncompliance issues that could impact future performance existed.
- A possible impact on future performance was noted for phase II analysis (e.g., Missouri A800 flexible test sections from LTPP database exhibited significant fatigue cracking due to application of many unexpected heavy haulage trucks).[17]
- Deviations were mostly minor relative to SPS-8 criteria, and they could be resolved through proper analysis.

Performance Data

Bivariate plots were developed of all SPS-8 manual distress data along with first sensor falling-weight deflectometer (FWD) deflection data, IRI, and PCI (computed using only the LTPP distress and smoothness data available) versus pavement age. A thorough review of the bivariate plots indicated the following:

- In general, the performance indicators were reasonable and followed expected trends.

- Some projects exhibited considerable variation in measured distress values over time. However, this was not considered out of the ordinary but within typical measurement variation.

- Occurrences of significant change in distress/smoothness over time were investigated to determine the cause. Such changes were mostly due to application of M&R treatments.

- There were two SPS-8 projects with significant structural deterioration (characterized by alligator cracking and slab transverse cracking). Examples of structural distress for such projects are presented in figure 50 and figure 51.

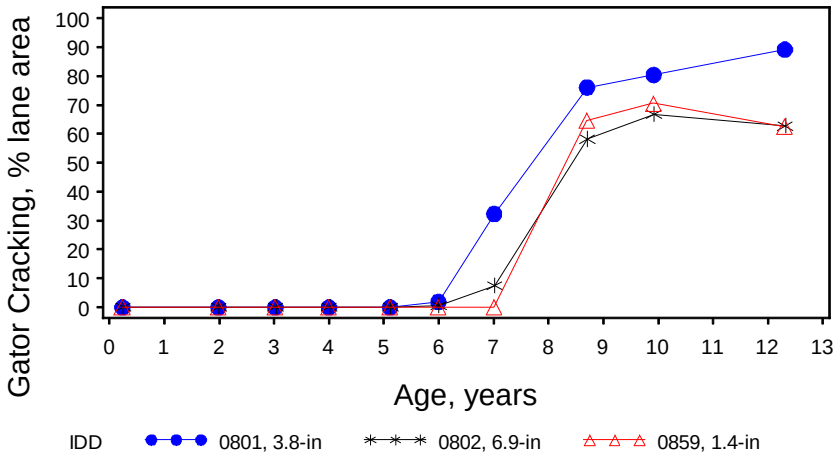

Source: FHWA.

Figure 50. Graph. Measured alligator cracking distress for SPS-8 flexible pavement projects in North Carolina.

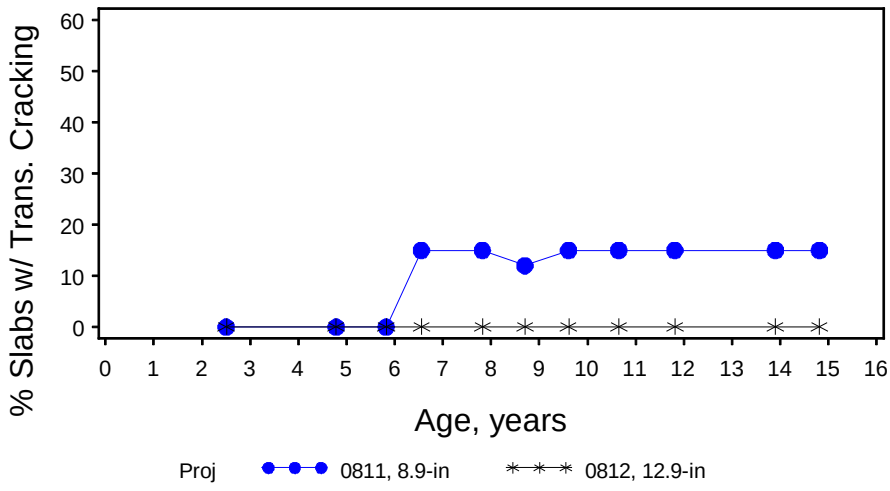

Source: FHWA.

Figure 51. Graph. Measured transverse (actually diagonal) cracking distress for SPS-8 rigid pavement projects in Colorado.

Figure 52 presents a photo of alligator cracking in an SPS-8 project in North Carolina in 2003. The project team reviewed the photo and decided that a very low amount of truck traffic had been applied to this pavement. They concluded that, although it appears as alligator cracking, the cracking present was not traditional bottom–up, AC fatigue, or load initiated.

Source: FHWA

Figure 52. Photo. Alleged alligator cracking or surficial shrinkage cracks for SPS-8 project 0802 in North Carolina.

Figure 53 shows a photo of transverse cracking for SPS-8 project 0811 in Colorado in 2009. The photo shows that the transverse cracking exhibited by this pavement was actually a diagonal crack and clearly not the traditional midpanel truck-load- or fatigue-initiated crack. This crack was probably caused by foundation movement. Note that this cracking did not continue to increase as fatigue transverse cracking typically does. This type of crack was clearly environmental or construction related. This is another example of cracking being classified according to the LTPP distress data-collection protocols but misleading as to actual cause of the distress (load, environmental, construction, etc.).

Source: FHWA.

Figure 53. Photo. Transverse (actually diagonal) cracking for trafficked lane for SPS-8 project 0811 in Colorado.

Figure 54 shows different stages of longitudinal cracking distress and how this distress can be confused with alligator cracking. Note the similarity of this distress to bottom–up fatigue alligator cracking.

Source: FHWA.

A. View of first stage—occurrence of short longitudinal cracks in and/or adjacent to the wheel path.

Source: FHWA.

C. Second view of first stage—occurrence of short longitudinal cracks in and/or adjacent to the wheel path.

Source: FHWA.

B. Second stage—occurrence of parallel longitudinal cracks.

Source: FHWA.

D. Third stage—occurrence of diagonal and/or transverse cracks between longitudinal cracks to form alligator pattern.

Figure 54. Photos. Different stages of top–down cracking (confirmed with cores).

Anomaly Resolution Strategies

Anomalies were resolved using several strategies in combination as needed and as appropriate. Strategies included the following:

- Reviewing distress maps and photos to better characterize distress/condition information.
- Filling gaps/missing data by using non-LTPP data, obtaining estimates from models and mathematical correlations/relationships, or conducting field examinations/testing and/or

interviews with local engineers. (This could include reviewing local records and databases.) This strategy may be applicable in situations such as the following:

  - Estimating GWT depth from NWIS database.[50]
  - Estimating key climate data items from the NCDC climate data tables.[13]
  - Estimating PCC CTE, modulus of rupture, etc., from correlations developed and implemented as part of the AASHTO ME pavement design analysis procedure.[49]
  - Estimating AC dynamic modulus, tensile strength, creep compliance, etc., from correlations developed and implemented as part of the AASHTOWare Pavement ME Design analysis procedure.(See references 20, 49, 12, and 16.)

- Conducting field coring and testing, including traffic data collection to obtain distress/traffic information such as the following:
  - Truck volumes, automatic vehicle classification, and weigh-in-motion from field measurements of local databases.
  - Photos, distress maps, input from local engineers, and site visits to evaluate performance.
  - Layer moduli, subgrade resilient moduli, and *k*-values from FWD deflection data. FWD data are available for all sections.[54]

Possible Impact of Data Anomalies on Analyses

The procedures for data-anomaly resolutions used in this project have been used in the past and are tried and tested. The procedures are able to resolve most, if not all, significant anomalies.

SELECTION OF ENVIRONMENTAL VARIABLES FOR DETAILED ANALYSIS OF IMPACT ON AC/PCC PAVEMENT PERFORMANCE

A wide range of AC/PCC pavement design and environmental variables was assembled for use in performing preliminary and detailed statistical analysis for AC/PCC performance data to determine environmental effects on AC/PCC pavements. The variables generally fell into three categories: temperature, moisture, and subgrade type and properties. Due to the nature and definitions of the assembled variables (they are generally describing the same situation among the three broad categories), there is an increased likelihood of an undesirable situation in which the correlations among the independent variables (within the three categories) are strong. Multicollinearity increases the standard errors of the statistical models' independent variables coefficients. Increasing standard error means that the coefficients may be significantly different from 0 (i.e., the variable does not have a significant impact on performance), whereas without multicollinearity and with lower standard errors, these same coefficients might have been significant. For example, a model may fit the data well even though none of the independent variables have a statistically significant impact on explaining the dependent variable. How is this possible? When two independent variables are highly correlated, they both convey essentially the

same information; when this situation happens, the independent variables are collinear, and the results show multicollinearity.

Assessment of the presence of multicollinearity is done using the variance inflation factor (VIF), which is a measure of multicollinearity in a model. VIFs measure how much the variance of the estimated coefficients is increased over the case of no correlation among the independent variables. If no two independent variables are correlated, then all of the VIFs will be 1. If the VIF for one of the variables is around or greater than 5, there is collinearity associated with that variable.

Possible solutions to the problem of multicollinearity include the following:

- Increasing the sample size. This is a common first step since standard error decreases when sample size increases (factors being equal). This partially offsets the problem that high multicollinearity leads to high standard errors.

- Removing the most intercorrelated variables from analysis. This method is misguided if the variables were necessarily there due to the theory of the model.

- Combining variables into a composite variable through building indexes with theoretical and empirical justification and meaning.

- Centering/transforming the correlated variables by subtracting the mean from the actual values. The resulting centered data may well display considerably lower multicollinearity.

- Dropping the intercorrelated variables from analysis but substituting their cross product as an interaction term or in some other way combine the intercorrelated variables.

For this analysis, the most practical approach was to remove the most intercorrelated variables from analysis. The outcomes of the multicollinearity analysis performed are presented in the following subsections.

Multicollinearity of Temperature-Related Variables

Table 24 shows the outcome of analysis to determine the VIF for all of the temperature-related variables assembled and developed by regressing fatigue cracking, rutting, materials distress, PCC transverse cracking, faulting, etc., (dependent variables) against the temperature-related variables (independent variables). The results showed VIFs greater than 10 for most of the temperature-related variables assembled (variables are highly correlated). Thus, it was necessary to remove the most intercorrelated variables from the list presented in table 25. This was done using engineering judgment, where the least important variables from an engineering viewpoint were removed. The results are presented in table 25.

Table 24. Outcome of multicollinearity analysis for temperature-related variables.

Temperature-Related Variable	VIF
Mean annual temperature (ambient)	71,893.0
Mean annual maximum temperature (ambient)	16,838.0
Mean annual minimum temperature (ambient)	21,423.0
Maximum temperature (ambient)	5.5
Minimum temperature (ambient)	21.8
Mean number of days with temperature below 32 °F	379.0
Mean annual freezing index	72.1
Mean number of days with temperature above 90 °F	13.2
Mean annual freeze–thaw cycles	204.6
Mean annual in situ AC temperature	49.8
Mean annual frost depth	11.7

Table 25. Summary of selected temperature variables (not highly correlated) for analysis.

Temperature-Related Variable	VIF
Mean number of days with temperature above 90 °F	2.39
Mean annual freeze–thaw cycles	2.51
Mean annual in situ AC temperature	6.76
Mean annual frost depth	2.32

Multicollinearity of Moisture-Related Variables

Table 26 shows the outcome of an analysis to determine VIFs for all of the moisture-related variables assembled and developed by regressing fatigue cracking, rutting, materials distress, PCC transverse cracking, faulting, etc., (dependent variables) against the moisture-related variables (independent variables). The results showed that the percent passing the annual number of days with intense rainfall was highly correlated with the other variables. All other variables appeared not to be highly correlated. Thus, there was a need to remove them from the data assembled for detailed statistical analysis. Exclusion of variables was, in general, done based on engineering judgment (i.e., if two variables are highly correlated, the least important from an engineering viewpoint was removed). The moisture-related variables selected for inclusion in detailed analysis are presented in table 27.

Table 26. Outcome of multicollinearity analysis for moisture-related variables.

Moisture-Related Variable	VIF
Annual total rainfall	321.5
Annual number of days with intense rainfall	251.8
Annual number of wet days	13.0
Annual total snowfall	5.6
Annual number of snow-covered days	5.2
Mean in situ base or subgrade moisture	1.1
Mean depth to GWT	1.1

Table 27. Summary of selected moisture variables (not highly correlated) for analysis.

Moisture-Related Variable	VIF
Annual total rainfall	4.3
Annual number of wet days	3.9
Annual total snowfall	5.6
Annual number of snow-covered days	5.0
Mean in situ base or subgrade moisture	1.1
Mean depth to GWT	1.1

Multicollinearity of Subgrade-Related Variables

Table 28 shows the outcome of the analysis to determine VIFs for all of the subgrade-related variables assembled and developed by regressing fatigue cracking, rutting, materials distress, PCC transverse cracking, faulting, etc., (dependent variables) against the subgrade-related variables (independent variables). The results show that the variables' liquid limit and percent passing the No. 200 sieve size were highly correlated. All other variables appeared not to be highly correlated. Thus, it was necessary to remove both variables from the list presented in table 28 using engineering judgment. The results are presented in table 29.

Table 28. Outcome of multicollinearity analysis for subgrade-related variables.

Subgrade-Related Variable	VIF
Percent passing the No. 40 sieve size	5.1
Percent passing the No. 200 sieve size	17.7
Percent sand content	9.7
Percent fine-sand content	8.7
Percent silt content	2.7
Percent clay content	10.5
Liquid limit	20.8
PI	10.8

Table 29. Summary of selected subgrade-related variables (not highly correlated) for analysis.

Subgrade-Related Variable	VIF
Percent passing the No. 40 sieve size	1.7
Percent sand content	8.5
Percent fine-sand content	7.5
Percent silt content	1.6
Percent clay content	7.6
PI	6.6

CATEGORIZATION OF ENVIRONMENTAL VARIABLES FOR PRELIMINARY ANALYSIS OF IMPACT ON AC/PCC PAVEMENT PERFORMANCE

Several environmental variables are routinely used to characterize pavement climate conditions and subgrade properties. The variables are mostly continuous in nature (e.g., temperature, rainfall, and percent passing No. 200 sieve size). For the preliminary statistical analysis and evaluation, the commonly reported climate and subgrade variables were transformed into categorical variables as needed in order to facilitate simple but robust comparisons (e.g., impact of low/high temperature on AC pavement rutting). This was done by dichotomizing the continuous variable into a categorical variable with two levels. The definitions of low/high categories (e.g., wet/dry, freeze/nonfreeze) was done based on industry standard definitions when available (e.g., LTPP definition of wet/dry regions) or through statistical methods (e.g., determine median annual number of air freeze-thaw cycles and use that as the break point for low/high levels). Table 64 in the appendix presents the definitions of low/high and other categories for the environmental variables used in preliminary statistical analysis. It must be noted that for the detailed statistical analysis (GLMSelect, ANOVA, etc.), both the categorical and continuous environmental variables were used as needed.

CHAPTER 6. ANALYSIS OF SPS-8 AND COMPANION AC PAVEMENT FATIGUE CRACKING DISTRESS PROJECTS

This chapter presents the results from the preliminary and detailed analysis of fatigue cracking for the SPS-8 and companion projects. The analysis of load-related cracking uses the definition included in the AASHTO ME pavement design guidance, where wheelpath alligator cracks are assumed to initiate at the bottom of the AC layer, while wheelpath longitudinal cracks are assumed to initiate at the surface.(5) Fatigue cracking for this analysis is the combination of alligator bottom–up wheel-path cracking and longitudinal top–down cracking in the wheel path because there was no way to distinguish between them (e.g., no cores through the cracks were available). The combined distress was expressed as a percentage of total lane area (e.g., a 1.2-ft-wide strip of fatigue cracking in one wheel path would be 10 percent).

Results are presented in terms of higher and lower truck-traffic applications. The high-traffic (i.e., SPS-1/GPS-1 AC pavements) annual ESAL averaged 280,124 for the LTPP measured lane. The low-traffic (i.e., SPS-8) annual ESAL averaged 7,586 for the LTPP measured lane.

PRELIMINARY STATISTICAL ANALYSIS TO CHARACTERIZE IMPACT OF ENVIRONMENTAL FACTORS ON ALLIGATOR CRACKING

The following sections describe a statistical analysis to determine the significance of various environmental factors on AC fatigue cracking.

Impact of Freeze and Nonfreeze Climates

Figure 55 shows the impact of variable freeze and nonfreeze climates on AC pavement fatigue cracking at 15 yr for low- and high-trafficked projects.

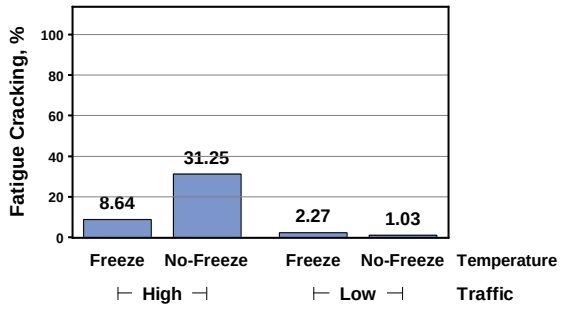

Source: FHWA.

A. Thin AC pavements.

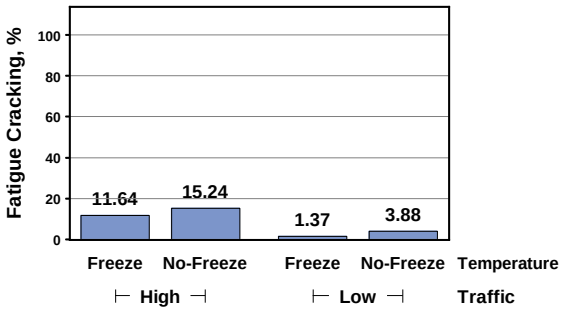

Source: FHWA.

B. Thick AC pavements.

Figure 55. Graphs. Impact of freeze and nonfreeze climates on AC fatigue cracking for low- and high-trafficked projects.

Figure 55 shows the following:

- In the absence of heavy traffic loads (i.e., thin and thick SPS-8 projects AC projects), fatigue cracking was very low (1 to 4 percent) in both freeze and nonfreeze climates.

- For the companion projects subjected to heavy traffic loads (i.e., SPS-1 and GPS-1), the amount of cracking exhibited after 15 yr in service was more than 8 percent regardless of climate.

- The projects located in nonfreeze climates exhibited considerably more fatigue cracking than those in freeze climates. This observation agrees with the results from the AASHTO ME pavement design, where softer AC mixes (nonfreeze warmer climates) exhibit more fatigue cracking than higher modulus AC mixes (in freeze climates).[5] Thin AC sections exhibited approximately two times more fatigue cracking than the thicker AC sections.

Impact of Freeze–Thaw Cycles

Figure 56 shows the impact of the high and low numbers of air freeze–thaw cycles on AC pavement fatigue cracking for low- and high-trafficked projects.

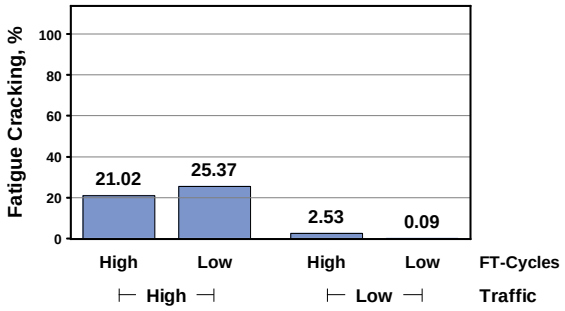

Source: FHWA.

A. Thin AC pavements.

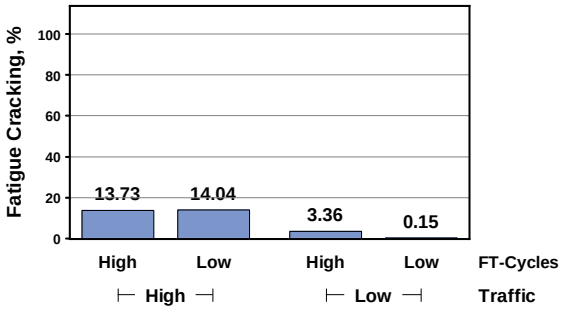

Source: FHWA.

B. Thick AC pavements.

Figure 56. Graphs. Impact of annual number of air freeze–thaw cycles on AC fatigue cracking for low- and high-trafficked projects.

Figure 56 shows the following:

- In the absence of heavy traffic loads, fatigue cracking was very low (0–3 percent) in both freeze and nonfreeze climates.

- For the companion projects subjected to heavy traffic loads, the amount of cracking exhibited after 15 yr in service was 13 percent or higher regardless of extent and amount of freeze–thaw cycles. The difference in fatigue cracking was not much different for projects located in climates with low and high numbers of air freeze–thaw cycles. Thus, air freeze–thaw cycles appeared to have little impact on fatigue cracking for pavements that experience heavy traffic.

Impact of Frost Depth

Figure 57 shows the impact of low and high frost depth on AC pavement fatigue cracking for low- and high-trafficked projects.

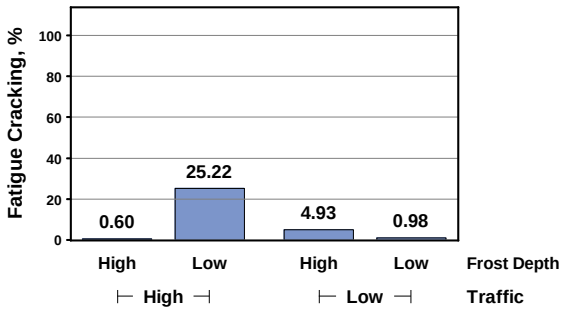

Source: FHWA.

A. Thin AC pavements.

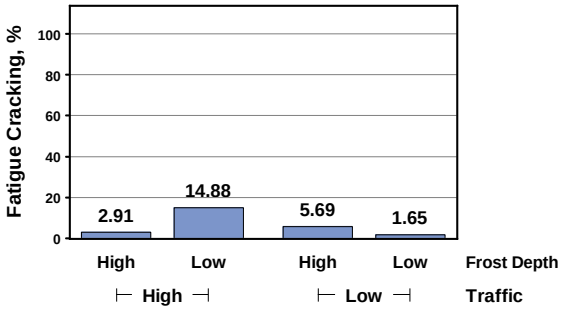

Source: FHWA.

B. Thick AC pavements.

Figure 57. Graphs. Impact of low and high frost depth on AC fatigue cracking for low- and high-trafficked projects.

Figure 57 shows the following:

- For the low-trafficked SPS-8 projects (thin and thick AC sections), fatigue cracking was low (1–6 percent). The extent and duration of frost depth had some impact on increasing fatigue cracking in the absence of heavy traffic loading.

- For the thin and thick AC companion SPS-1 and GPS-1 projects, the amount of fatigue cracking exhibited after 15 yr in service was high (up to 25 percent). On average, the thin AC projects with low frost penetration had 25 percent fatigue cracking versus 0.6 percent for sections with deep frost penetration. The thick AC projects had a similar large difference, with 15 percent for low frost penetration and 3 percent for deep frost penetration. When pavements had deep and long frost penetration, the AC was at a very high modulus, and the base and subgrade were frozen and very stiff, which may explain the reason for far less AC fatigue damage.

Impact of AC Temperature

Figure 58 shows the impact of low and high in situ AC temperature on AC pavement fatigue cracking for low- and high-trafficked projects.

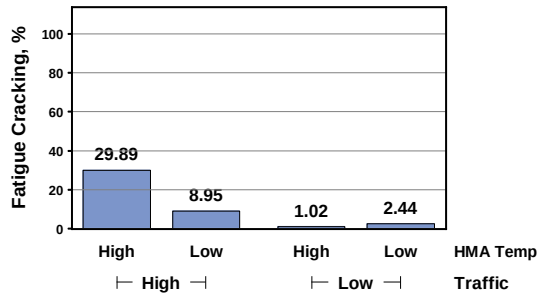

Source: FHWA.

A. Thin AC pavements.

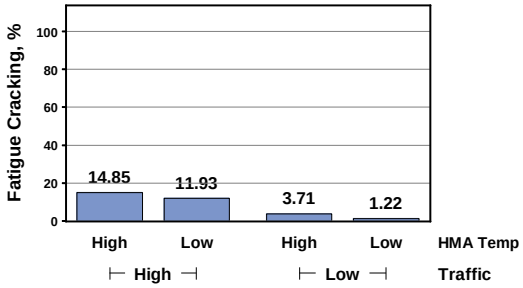

Source: FHWA.

B. Thick AC pavements.

Figure 58. Graphs. Impact of low and high in situ AC temperature on AC fatigue cracking for low- and high-trafficked projects.

Figure 58 shows the following:

- For the low-trafficked projects, fatigue cracking was less than 4 percent at 15 yr. In situ AC temperature had little impact on fatigue cracking in the absence of heavy traffic loading.

- The amount of cracking exhibited after 15 yr in service was high (9 to 30 percent) for all heavily trafficked AC pavements. The higher the annual AC in situ temperature, the higher AC fatigue cracking. For the thin AC sections, exposure to high AC temperatures resulted in higher fatigue cracking levels (70-percent increase in fatigue cracking), while for the thicker AC projects, the increase due to higher temperatures was less at 19 percent.

Impact of Annual Precipitation

Figure 59 shows the impact of rainfall in dry and wet environments on AC pavement fatigue cracking for low- and high-trafficked projects.

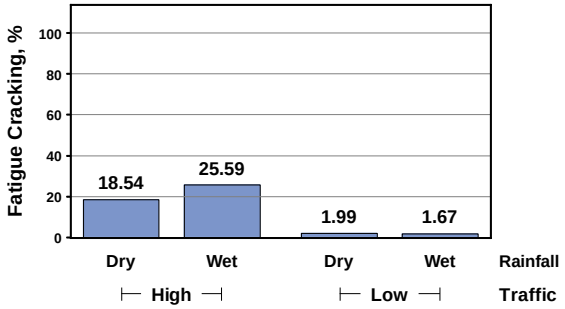

Source: FHWA.

A. Thin AC pavements.

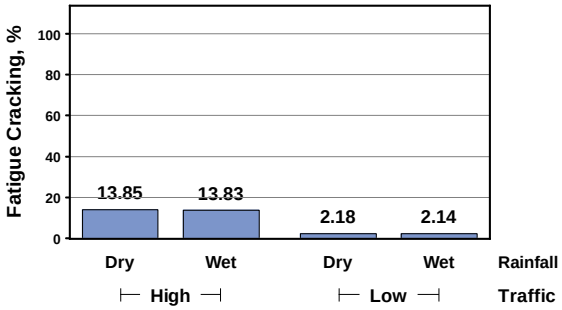

Source: FHWA.

B. Thick AC pavements.

Figure 59. Graphs. Impact of rainfall in dry and wet environments on AC fatigue cracking for low- and high-trafficked projects.

Figure 59 shows the following:

- For the low-trafficked SPS-8 projects, rainfall had no impact on the development and progression of fatigue cracking after 15 yr in service. Measured fatigue cracking was 2 percent or lower.

- The amount of cracking exhibited after 15 yr in service was high for all high-trafficked AC pavements regardless of rainfall, ranging from 14–26 percent. For the thin AC sections, exposure to high rainfall resulted in higher fatigue cracking (27-percent increase in fatigue cracking), while for the thicker AC projects, there was no increase due to higher rainfall.

Impact of Base and Subgrade In Situ Moisture Content

Figure 60 shows the impact of low and high base and subgrade in situ moisture content on AC pavement fatigue cracking for low- and high-trafficked projects.

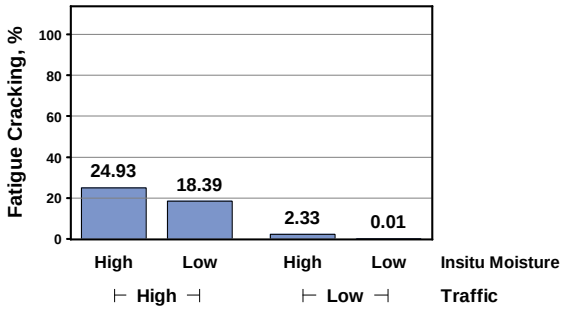

Source: FHWA.

A. Thin AC pavements.

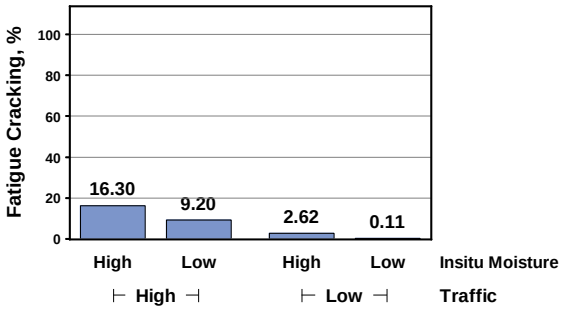

Source: FHWA.

B. Thick AC pavements.

Figure 60. Graphs. Impact of low and high base and subgrade in situ moisture content on AC fatigue cracking for low- and high-trafficked projects.

Figure 60 shows the following:

- For the low-trafficked projects, base and subgrade in situ moisture content was 3 percent or less, but both thin and thick AC did show increased fatigue cracking after 15 yr for the high in situ moisture content base and subgrade.

- For the high-trafficked projects, the amount of cracking exhibited after 15 yr in service was high (less than 5 percent lane area) regardless of climate. Also, pavements exposed to higher base and subgrade in situ moisture contents exhibited considerably higher levels of fatigue cracking for both thin and thick AC sections (i.e., 25 versus 18 percent lane area for thin AC and 16 versus 9 percent for thick AC).

Impact of Subgrade Type

Figure 61 shows the impact of soil material subgrade type (i.e., active, fine, and coarse) on AC pavement fatigue cracking for low- and high-trafficked projects.

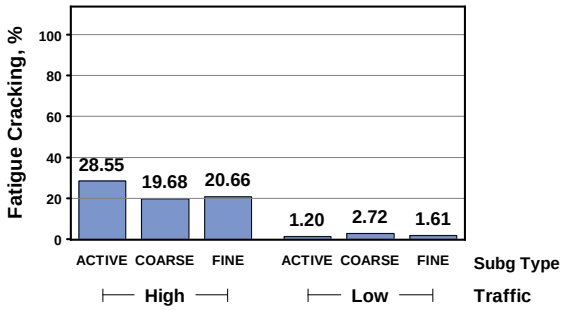

Source: FHWA.

A. Thin AC pavements.

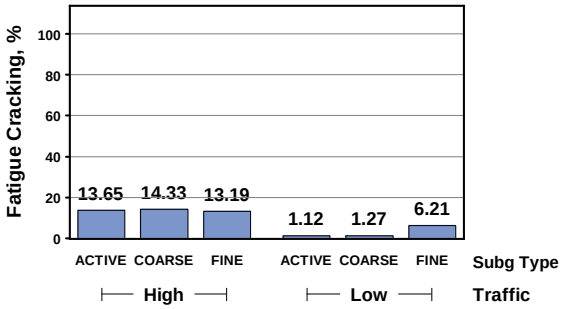

Source: FHWA.

B. Thick AC pavements.

Figure 61. Graphs. Impact of soil material subgrade type on AC fatigue cracking for low- and high-trafficked projects.

Figure 61 shows the following:

- For the low-trafficked projects with thin AC, subgrade type had no apparent impact on the development and progression of fatigue cracking after 15 yr as the values were all less than 3 percent. For the low-trafficked projects with thick AC, a fine-grained subgrade type indicated a much higher fatigue cracking (6 percent).

- For the heavily trafficked projects, the amount of cracking exhibited after 15 yr in service was high, ranging from 13–26 percent, regardless of subgrade type. Pavements constructed over active subgrades exhibited the highest levels of cracking for thin AC sections, while there was no difference in fatigue cracking for pavements constructed over fine and coarse subgrades. For the thick AC sections, subgrade type did not have much of an impact on fatigue cracking after 15 yr in service. Thickness of the AC appears to have overcome any differences in subgrade type support.

Impact of Subgrade Clay Content

Figure 62 shows the impact of low and high subgrade clay content on AC pavement fatigue cracking for low- and high-trafficked projects.

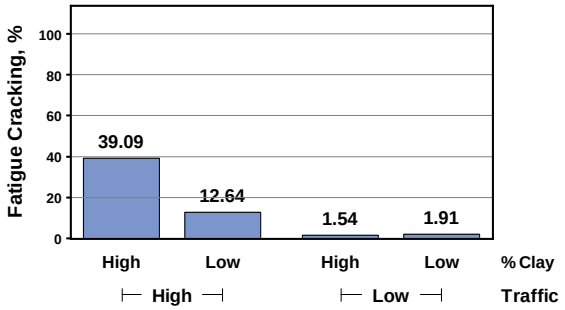

Source: FHWA.

A. Thin AC pavements.

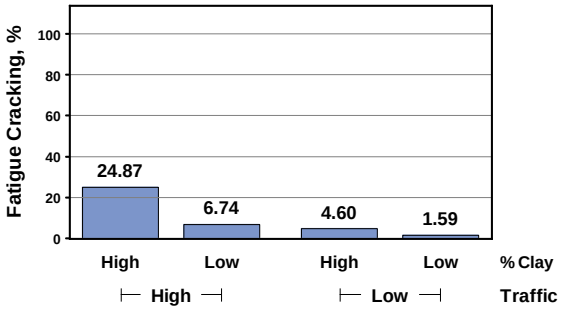

Source: FHWA.

B. Thick AC pavements.

Figure 62. Graphs. Impact of low and high subgrade clay content on AC fatigue cracking for low- and high-trafficked projects.

Figure 62 shows the following:

- For the low-trafficked projects, subgrade clay content had little impact on the development and progression of fatigue cracking. After 15 yr in service, the measured fatigue cracking was only 1.5–5 percent.

- For the heavily trafficked projects, the amount of fatigue cracking exhibited after 15 yr in service was high (7–39 percent lane area) regardless of climate. Also, pavement subgrades containing high clay contents exhibited considerably higher levels of fatigue cracking for both thin and thick AC sections (209 and 269 percent higher, respectively).

Impact of Subgrade Silt Content

Figure 63 shows the impact of low and high subgrade silt content on AC pavement fatigue cracking for low- and high-trafficked projects.

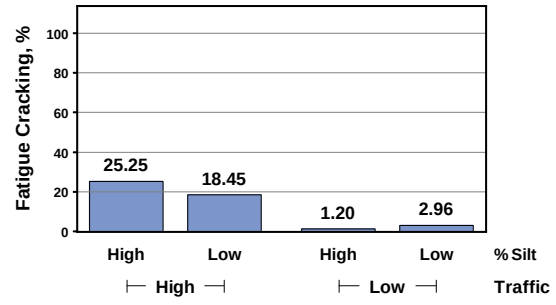

Source: FHWA.

A. Thin AC pavements.

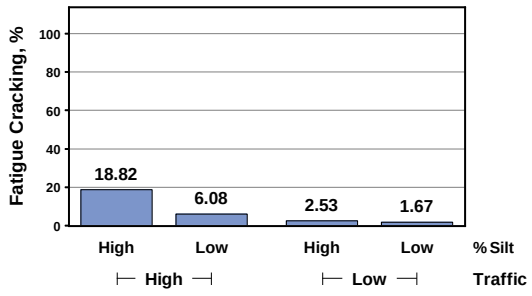

Source: FHWA.

B. Thick AC pavements.

Figure 63. Graphs. Impact of low and high subgrade silt content on AC fatigue cracking for low- and high-trafficked projects.

Figure 63 shows the following:

- For the low-trafficked projects, subgrade silt content had little impact on the development and progression of fatigue cracking. After 15 yr in service, the measured fatigue cracking was less than 3 percent.

- For the heavily trafficked projects, the amount of cracking exhibited after 15 yr in service was high (ranging from 6–25 percent lane area). Pavements with higher subgrade silt content exhibited much higher levels of fatigue cracking for both thin and thick AC sections (37 and 210 percent higher, respectively).

Impact of Subgrade Fine-Sand Content

Figure 64 shows the impact of low and high subgrade fine-sand content on AC pavement fatigue cracking for low- and high-trafficked projects. Presumably, the lower the fine-sand content, the higher the silt and/or clay content.

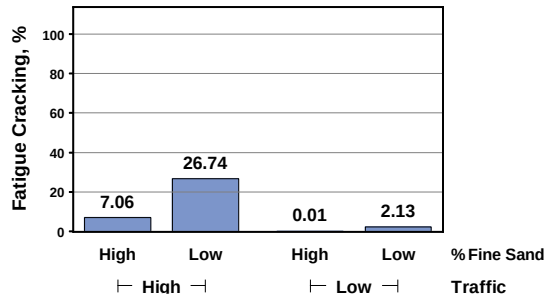

Source: FHWA.

A. Thin AC pavements.

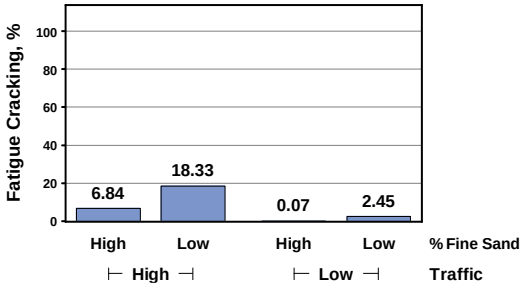

Source: FHWA.

B. Thick AC pavements.

Figure 64. Graphs. Impact of low and high subgrade fine-sand content on AC fatigue cracking for low- and high-trafficked projects.

Figure 64 shows the following:

- For the low-trafficked projects, fine subgrade sand content had little impact on the development of fatigue cracking. After 15 yr in service, the measured fatigue cracking was 2 percent or less.

- For the heavily trafficked projects, the amount of cracking exhibited after 15 yr in service was high (ranging from 7–27 percent lane area) regardless of climate. Pavements with higher subgrade fine-sand contents exhibited considerably lower levels of fatigue cracking for both thin and thick AC sections (279 and 168 percent higher, respectively).

Impact of Subgrade PI

Figure 65 shows the impact of low and high subgrade PI on AC pavement fatigue cracking for low- and high-trafficked projects.

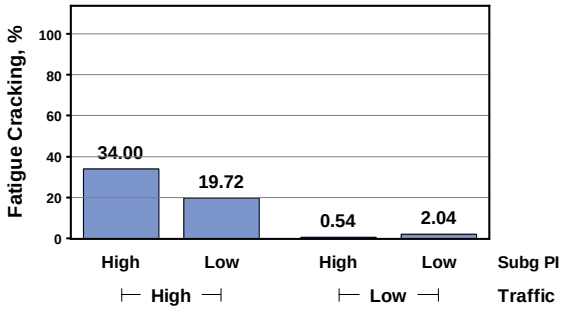

Source: FHWA.

A. Thin AC pavements.

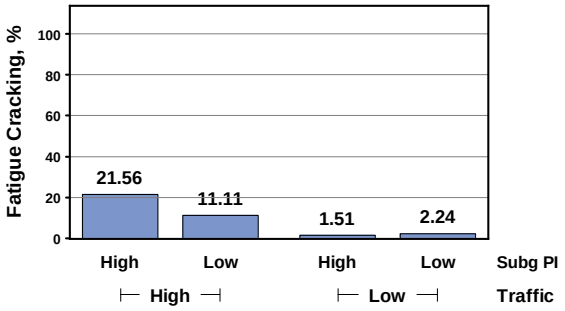

Source: FHWA.

B. Thick AC pavements.

Figure 65. Graphs. Impact of low and high subgrade PI on AC fatigue cracking for low- and high-trafficked projects.

Figure 65 shows the following:

- For the low-trafficked projects, subgrade PI had little impact on the development and progression of fatigue cracking. After 15 yr in service, the measured fatigue cracking was 2 percent or less.

- For the heavily trafficked projects, the amount of cracking exhibited after 15 yr in service was high (ranging from 11–34 percent lane area) regardless of climate. Pavements with higher subgrade PI exhibited considerably higher levels of fatigue cracking for both thin and thick AC sections (72 and 94 percent higher, respectively).

DETAILED STATISTICAL ANALYSIS TO CHARACTERIZE IMPACT OF ENVIRONMENTAL FACTORS ON ALLIGATOR CRACKING

The SAS® statistical model selection procedure, GLMSELECT, which implements statistical model selection in the framework of general linear models, was used to determine the subset of environmental and other (traffic and AC thickness) variables correlated to AC fatigue cracking.[(55)] Once the variables were identified, ANOVA was performed to determine the significance of the identified variables.

AC fatigue cracking was the dependent variable, and design, traffic, and environmental factors were the independent variables. Statistical model selection analysis was performed to determine the best subset of variables that impact and predict AC fatigue cracking after 15 yr in service. This was a key step, as when faced with several independent variables that could possibly impact AC fatigue cracking, a natural question is what subset of the variables most impacts the distress. For this analysis, SAS® procedure GLMSELECT was utilized to determine the subset of variables that significantly impacted AC fatigue cracking. Selection was based on two criteria: a 15-percent SLE and the selection process terminated when adding additional variables to the model increased the PRESS. The variables that most impact AC fatigue cracking were determined separately for low-trafficked projects and then for combined low- and high-trafficked companion projects.

Results from statistical model selection analysis were compared to determine the following:

- Factors that affect the occurrence of AC fatigue cracking obtained from outcome of low-trafficked pavements analysis.
- Factors that affect the occurrence of AC fatigue cracking obtained from outcome of combined low- and high-trafficked pavements analysis.

Outcomes were analyzed, and the AC fatigue cracking initiators (must be theoretically viable), aggravators, and impact on the distress were determined.

Summary of GLMSELECT and ANOVA Results for Low-Trafficked AC Pavements

The analysis using only the SPS-8 sections showed that none of the environmental variables were selected using the GLMSELECT model procedure (figure 66). This circumstance implies that fatigue cracking distress was not initiated by environmental factors. Because the fatigue cracking level exhibited by the SPS-8 projects was very low (typically less than 5 percent), traffic and AC thickness were also found to be insignificant.

GLMSELECT (Stepwise Selection Summary)

The GLMSELECT Procedure

Stepwise Selection Summary

Step	Effect Entered	Effect Removed	Number Effects In	Number Parms In	PRESS	F Value	Pr > F
0	Intercept		1	1	290.1636*	0.00	1.0000

Selection stopped because the candidate for entry has SLE > 0.15 and the candidate for removal has SLS < 0.15.

Source: FHWA.

Figure 66. Screenshot. GLMSELECT results for fatigue cracking for low-trafficked SPS-8 AC pavements indicating that no variable was significant.

Summary of GLMSELECT and ANOVA Results for Low- and High-Trafficked AC Pavements

A statistical ANOVA similar to that described for the low-trafficked SPS-8 AC pavements was performed for all projects (both low- and high-trafficked pavements). All key factors were considered, including traffic, AC thickness, climate (i.e., temperature and moisture factors), and subgrade characteristics (e.g., percent sand, PI). Interactions of variables were also evaluated. The results of the ANOVA for the significant factors and interactions are presented in table 30.

Table 30. ANOVA results for determining factors that significantly influence the development of AC fatigue cracking using all pavement sections (SPS-1 and -8 and GPS-1).

Variable	Categorical Value	DF	Estimate	Standard Error	*t*-Value[1]
Traffic level	High (GPS-1/SPS-1)	1	16.32	4.1600	3.92
Traffic level	Low (SPS-8)	0	0.0000	4.1600	3.92
Temperature level	Freeze	1	–30.94	8.0500	–3.80
Temperature level	Nonfreeze	0	0.0000	8.0500	–3.80
Traffic–AC thickness interaction	—	1	16.3	4.1600	3.92
In situ base and subgrade moisture content	—	1	0.0098	0.0045	2.17
Fine-sand content	—	1	–0.2798	0.1445	–1.94

—No categorical value.
[1]All variables are significant at the 0.15 level of significance.
DF = degrees of freedom.

The results indicate the following:

- Traffic level has a very significant effect on AC fatigue cracking. The SPS-1 and GPS-3 sections have a much higher amount of AC fatigue cracking (16 percent).

- The interaction of traffic and AC thickness has a significant effect on AC fatigue cracking. Higher traffic and thinner AC layer exhibited much higher AC fatigue cracking (16 percent).

- Climate has a significant effect on AC fatigue cracking. Nonfreeze climates have significantly more AC fatigue cracking (31 percent more) than freeze climates. Similarly, nonfreeze climates have higher mean annual in situ AC temperatures. AC mean annual in situ temperature over the year has a significant effect on AC fatigue cracking. The higher the AC in situ temperature, the higher the AC fatigue cracking. This correlates to the previous finding on climate. As noted previously in this chapter, higher AC temperatures produce lower modulus AC mixes that exhibit more fatigue cracking.

- The moisture of the base and subgrade are very significant in affecting AC fatigue cracking. The higher the moisture level, the higher the amount of AC fatigue cracking. Higher water content of unbound layers (aggregate bases or subgrades) results in much lower resilient modulus values, causing higher tensile strain at the bottom of the AC layers and higher amounts of fatigue cracking.

- The fine-sand content in the subgrade has a significant effect on the amount of AC fatigue cracking. The higher the fine-sand content, the lower the AC fatigue cracking. Soils with higher sand content typically exhibit lower PIs and lower percent clay content. Sandy soils generally have higher permeability, so they drain faster, resulting in drier conditions and causing higher resilient modulus values, especially in the drier seasons. The data also show that soils with higher PIs and higher percent clay exhibit higher amounts of fatigue cracking.

The model selection procedure results for low- and high-trafficked projects plus theoretical cause-and-effect relationships show the following:

- Traffic loading is the main initiator of AC fatigue cracking and was very significant in this analysis of low versus high traffic loading similar pavement structures. Repeated axle loading causes repeated bending strains that eventually result in sufficient fatigue damage and fatigue cracking in the wheel paths.

- The interaction of traffic level and AC thickness was significant in affecting fatigue cracking. For the same level of traffic, thicker AC resulted in lower fatigue cracking. A thinner AC layer with heavy traffic resulted in a very large amount of fatigue cracking.

- The environmental factors found to aggravate the progression of the AC fatigue cracking include the following:

    - **Temperature**: The higher the annual in situ temperature of the AC layer, the higher the amount of AC fatigue cracking. The nonfreeze climate experienced much higher AC fatigue cracking.

    - **Base and subgrade moisture content**: Higher moisture content resulted in higher fatigue cracking as the resilient moduli of the base and subgrade were likely reduced.

    - **Subgrade type (as characterized by fine-sand content, clay content, and silt content)**: The lower the fine-sand content, the higher the clay or silt content of the subgrade, and the higher the fatigue cracking. These factors result in lower resilient modulus of the subgrade, which increases bending strain in the AC layer.

AC FATIGUE-CRACKING DAMAGE ANALYSIS

Estimating the proportion of overall AC fatigue-cracking damage due to environmental factors required the following:

- The overall fatigue-cracking damage of a selection of AC pavements subjected to normal heavy traffic loadings (GPS-1 and SPS-1 companion sections) and environmental factors.

- The fatigue-cracking damage of similar thickness and materials AC pavements subjected to low traffic loadings and similar environmental factors (SPS-8 projects). All of these pavements had less than 5 percent fatigue cracking and were considered well within the standard error of measurement. Note that the level of traffic loadings for the SPS-8 projects was so low that theoretically it should not have caused any fatigue cracking, and this was essentially observed in the field by LTPP inspection teams.

The impact of various design and environmental factors on fatigue damage was also assessed. The outcome of the analysis is presented in the following subsections.

Proportion of Overall Fatigue-Cracking Damage Caused by Environmental Factors

Table 31 presents a summary of overall mean fatigue-cracking damage for the companion projects and fatigue-cracking damage due to environmental factors alone for the SPS-8 projects. The proportion of overall fatigue-cracking damage attributable to environmental factors for thin AC pavements was approximately 12 percent. For thick AC pavements, the proportion of damage due to environmental factors was 19 percent. Table 31 shows that the overall fatigue-cracking damage (i.e., measured fatigue cracking after 15 yr in service of the heavily trafficked projects) was 45.2 percent of the lane area. For low-trafficked projects (environmental effects alone), fatigue-cracking damage was 6.7 percent.

Table 31. Impact of AC thickness on AC pavement fatigue-cracking damage.

AC Thickness	Overall Fatigue-Cracking Damage (SPS-1 and GPS-1) (%)	Fatigue-Cracking Damage due to Environmental Factors (SPS-8) (%)	Overall Damage due to Environmental Factors (%)
Thin	51.9	6.1	12
Thick	38.5	7.2	19*
Mean	45.2	6.7	15

*Overall damage of the thicker AC pavements was less than that for the thinner AC pavement. This is because the extra AC thickness reduced fatigue in the AC surface layer. The extra thickness, however, has no significant impact on the amount of environmental damage exhibited by thick and thin AC pavements. Thus, the percentage of environmental induced damage will be greater in the thicker AC pavements.

On average, the amount of AC pavement fatigue-cracking damage exhibited by the heavily trafficked projects was 45.2 percent. Those AC pavements exposed to low traffic exhibited only 6.7 percent cracking. Thus, the proportion of AC fatigue damage ascribed to environmental conditions was 6.7/45.2 = 15 percent.

In general terms, the proportion of fatigue-cracking damage associated with environmental factors (e.g., subgrade characteristics such as fine-sand and moisture content, precipitation, freeze index, freeze–thaw cycles) to that associated with all causes, including loading and the same environmental factors, was approximately 15 percent. This value is not high because fatigue cracking is initiated only by repeated loadings, but its propagation is affected by environmental factors to this extent.

Impact of Design and Environmental Factors on Overall Fatigue-Cracking Damage

Table 32 and table 33 present the impact of environmental factors on AC pavement fatigue-cracking damage.

Table 32. Impact of climate on AC pavement fatigue-cracking damage.

Climate	Overall Fatigue-Cracking Damage (SPS-1 and GPS-1) (%)	Fatigue-Cracking Damage due to Environmental Factors (SPS-8) (%)	Overall Damage due to Environmental Factors (%)
Dry freeze	34.4	5.9	17
Dry nonfreeze	54.2	11.9	22
Wet freeze	23.0	6.7	29
Wet nonfreeze	52.0	5.7	11

Table 33. Impact of subgrade type on AC pavement fatigue-cracking damage.

Subgrade Type	Overall Fatigue-Cracking Damage (SPS-1 and GPS-1) (%)	Fatigue Cracking-Damage due to Environmental Factors (SPS-8) (%)	Overall Damage due to Environmental Factors (%)
Coarse	43.7	6.1	14
Fine/active	48.0	7.1	15

The information presented in table 32 and table 33 shows the following:

- The proportion of environmental damage was highest for wet–freeze climates (29 percent) and lowest for wet–nonfreeze climates (11 percent). For dry–freeze climates, the proportion of environmental damage was 17 percent, while it was 22 percent for dry–nonfreeze climates.

- The proportion of damage due to environmental factors was about the same (14–15 percent) regardless of subgrade type.

CHAPTER 7. ANALYSIS OF RUTTING DISTRESS FOR SPS-8 AND COMPANION AC PAVEMENT PROJECTS

This chapter presents the analysis of rutting for the SPS-8 and companion non-SPS-8 projects. For this analysis, *rutting* (permanent deformation) is defined as the total rutting occurring in the AC, base, and subgrade layers measured at the pavement surface.

For the LTPP projects, rutting was measured at 50-ft intervals over the typically 500-ft AC pavement test section. Rutting was measured in both the left and right wheel paths using the straightedge and wire line methods. For this analysis, the representative rutting for the entire 500-ft sample area was computed as mean rut depth over both the 500-ft section and both wheel paths (average of approximately 20 measurements across the sample area).

PRELIMINARY STATISTICAL ANALYSIS TO CHARACTERIZE IMPACT OF ENVIRONMENTAL FACTORS ON RUTTING

The following sections describe a statistical analysis to determine the significance of various environmental factors on AC pavement wheel path rutting.

Impact of Freeze and Nonfreeze Climates

Figure 67 shows impacts of freeze and nonfreeze climate on AC pavement rutting for low- and high-trafficked projects.

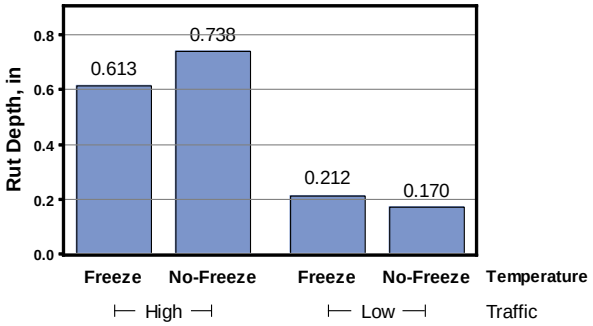

Source: FHWA.

A. Thin AC pavements.

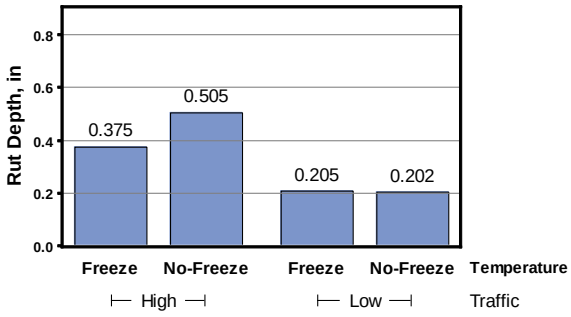

Source: FHWA.

B. Thick AC pavements.

Figure 67. Graphs. Impact of freeze and nonfreeze climates on AC total rutting for low- and high-trafficked projects.

Figure 67 shows the following:

- For the low-trafficked projects, total rutting was low (0.2 inch) after 15 yr in service for both freeze and nonfreeze climates. The climate had little impact on total rutting in the absence of heavy traffic loading.

- For the more heavily trafficked projects, the amount of rutting exhibited after 15 yr in service was higher (mostly greater than 0.5 inch) regardless of climate. It must be noted that some of the pavements exhibiting high rutting levels had experienced significant amounts of AC material defects such as high asphalt content and stripping. The rut depths for these higher traffic companion sites were significantly greater in comparison to many other test sections with higher traffic volumes included in the LTPP program. The projects located in nonfreeze climates exhibited considerably more rutting (20 percent higher for thin AC and 34 percent for thick AC). Thinner AC pavements showed much more rutting than thicker pavements.

Impact of Freeze–Thaw Cycles

Figure 68 presents graphs showing the impact of low and high freeze–thaw cycles on AC pavement total rutting for low- and high-trafficked projects.

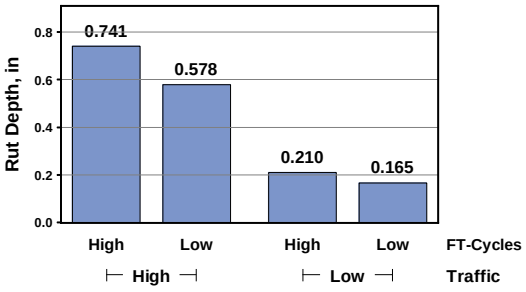

Source: FHWA.

A. Thin AC pavements.

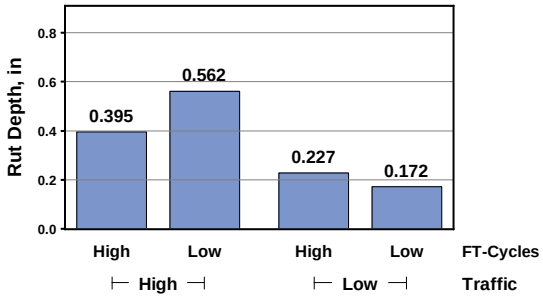

Source: FHWA.

B. Thick AC pavements.

Figure 68. Graphs. Impact of low and high freeze–thaw cycles on AC total rutting for low- and high-trafficked projects.

Figure 68 shows the following:

- For the low-trafficked projects (thin and thick AC sections), total rutting was low (approximately 0.2 inch or less) for both high and low numbers of freeze–thaw cycles after 15 yr in service. The number of freeze–thaw cycles, therefore, had little or no impact on total rutting in the absence of heavy traffic loading.

- For the heavily trafficked projects, the amount of total rutting exhibited after 15 yr in service was higher (mostly greater than 0.5 inch) regardless of number of freeze–thaw cycles. Overall, the average rutting for thin and thick AC pavement for high and low numbers of freeze–thaw cycles showed only a small difference in rutting. Thus, freeze–thaw cycles appeared to have little impact on total rutting.

Impact of Frost Depth

Figure 69 presents graphs showing the impact of low and high frost depth on AC pavement total rutting for low- and high-trafficked projects.

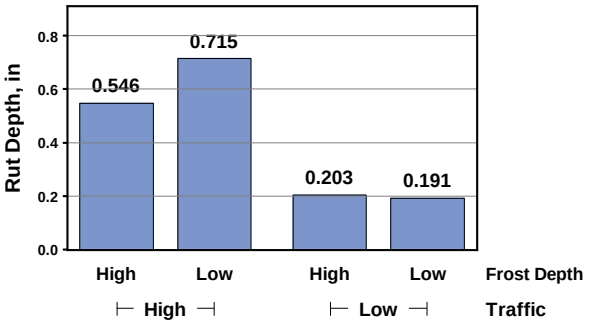

Source: FHWA.

A. Thin AC pavements.

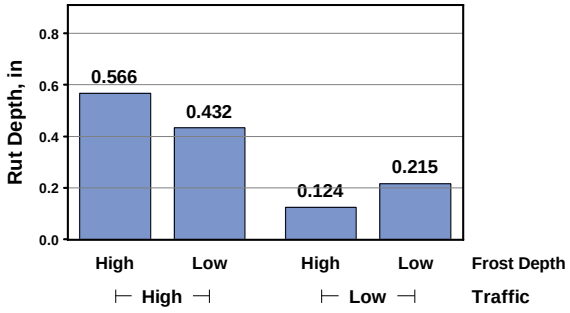

Source: FHWA.

B. Thick AC pavements.

Figure 69. Graphs. Impact of low and high frost depth on AC total rutting for low- and high-trafficked projects.

Figure 69 shows the following:

- For the low-trafficked projects (thin and thick AC sections), total rutting was low at 0.124 to 0.215 inch after 15 yr in service. Thus, frost depth had little or no impact on total rutting in the absence of heavy traffic loading.

- For the more heavily trafficked projects, the amount of total rutting exhibited after 15 yr in service was high (mostly greater than 0.5 inch). For locations exhibiting high frost penetration, AC thickness did not have an impact on total rutting (0.566 inch for thin pavements versus 0.546 inch for thick pavements). For locations with lower levels of frost penetration, thin AC pavements exhibited 0.715 inch of rutting, and the thicker pavements exhibited 0.432 inch of rutting. The information presented indicates the following:

    - Higher traffic load application results in higher rutting levels.

    - With a high level of frost penetration, thin and thick AC pavements exhibited similar levels of rutting. The impact of AC thickness was minimal.

    - Without significant levels of frost penetration, thin AC pavements exhibited higher levels of rutting than thick AC pavements. The impact of AC thickness appears high.

Impact of AC In Situ Temperature

Figure 70 presents graphs showing the impact of low and high in situ AC temperature on AC pavement total rutting for low- and high-trafficked projects.

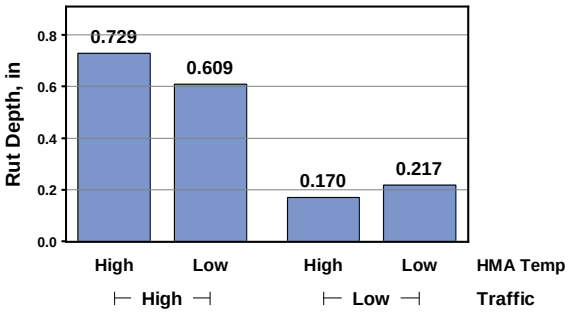

Source: FHWA.

A. Thin AC pavements.

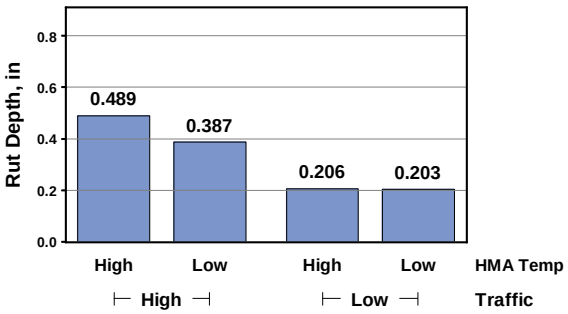

Source: FHWA.

B. Thick AC pavements.

Figure 70. Graphs. Impact of low and high in situ AC temperature on AC total rutting for low- and high-trafficked projects.

Figure 70 shows the following:

- For the low-trafficked projects (thin and thick AC sections), total rutting was low at 0.17 to 0.217 inch after 15 yr in service. Thus, in situ AC temperature had little impact on total rutting in the absence of heavy traffic loading.

- For the heavily trafficked projects, the amount of total rutting exhibited after 15 yr in service was high for the thin AC pavements (0.61 to 0.73 inch) and for the thick AC pavements (0.38 to 0.48 inch). This information shows that for the thin AC sections, exposure to high AC temperatures resulted in higher rutting levels (0.12 inch higher). For the thicker AC projects, the increase in total rutting due to higher temperatures was 0.100 inch. These changes in total rutting are considered to be low. The information presented indicates the following:
  - Higher traffic load application resulted in higher rutting levels.
  - Thicker AC pavements had lower levels of rutting than thin AC pavements.
  - Both thin and thick AC pavements subjected to higher AC in situ temperatures developed greater amounts of total rutting.

Impact of Rainfall

Figure 71 presents graphs showing the impact of rainfall in dry and wet environments on AC pavement total rutting for low- and high-trafficked projects.

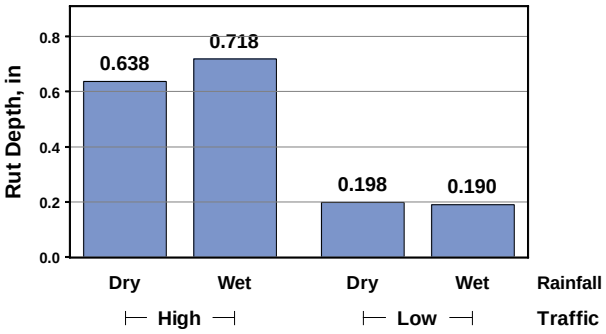

Source: FHWA.

A. Thin AC pavements.

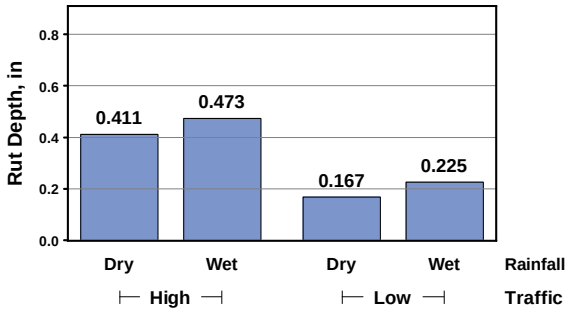

Source: FHWA.

B. Thick AC pavements.

Figure 71. Graphs. Impact of rainfall in dry and wet environments on AC total rutting for low- and high-trafficked projects.

Figure 71 shows the following:

- For the low-trafficked projects (thin and thick AC sections), rainfall had no impact on the development and progression of total rutting after 15 yr in service. Measured total rutting ranged from 0.17 to 0.23 inch. Thus, rainfall had no impact on total rutting in the absence of heavy traffic loading.

- For the heavily trafficked projects, the amount of total rutting exhibited after 15 yr in service was high for the thin AC pavements (greater than 0.2 inch) regardless of rainfall amount. Both thin and thick AC pavements located in wet climates exhibited more rutting than those in dry climates.

Impact of Base and Subgrade In Situ Moisture Content

Figure 72 presents graphs showing the impact of in situ moisture content of base and subgrade on AC pavement total rutting for low- and high-trafficked projects.

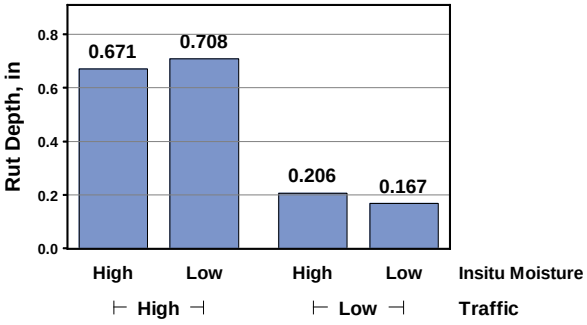

Source: FHWA.

A. Thin AC pavements.

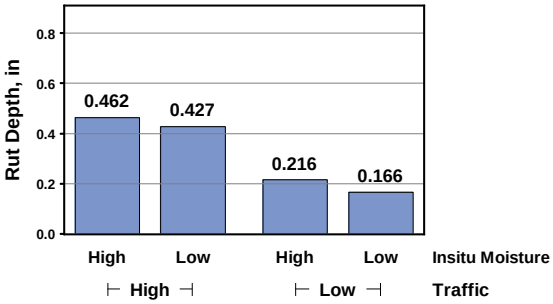

Source: FHWA.

B. Thick AC pavements.

Figure 72. Graphs. Impact of low and high base and subgrade in situ moisture content on AC total rutting for low- and high-trafficked projects.

Figure 72 shows the following:

- For the low-trafficked projects (thin and thick AC sections), base and subgrade in situ moisture content had no impact on the development and progression of total rutting. After 15 yr in service, the measured fatigue cracking was 0.2 inch. Thus, base and subgrade in situ moisture content had no impact on total rutting in the absence of heavy traffic loading.

- For the heavily trafficked projects, the amount of total rutting exhibited after 15 yr in service was higher (greater than 0.2 inch). Thinner AC pavements had higher levels of rutting than thicker AC pavements regardless of moisture content. The impact of base and subgrade moisture on rutting development and progression was minimal, as the difference in rutting between low and high in situ moisture was approximately 0.035 inch.

Impact of Subgrade Type

Figure 73 presents graphs showing the impact of subgrade type (i.e., active, fine, or coarse) on AC pavement total rutting for low- and high-trafficked projects.

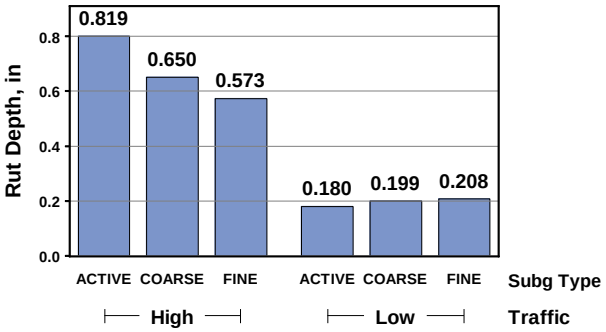

Source: FHWA.

A. Thin AC pavements.

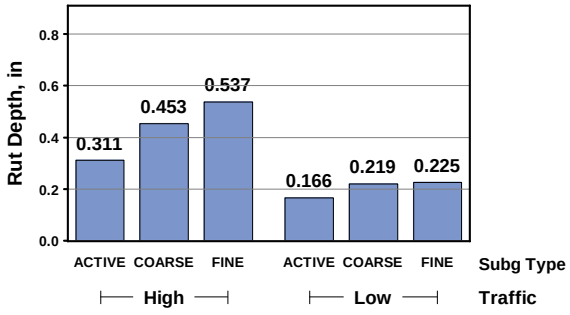

Source: FHWA.

B. Thick AC pavements.

Figure 73. Graphs. Impact of subgrade type on AC total rutting for low- and high-trafficked projects.

Figure 73 shows the following:

- For the low-trafficked projects (thin and thick AC sections), subgrade type had no impact on the development and progression of total rutting. After 15 yr in service, measured total rutting ranged from 0.16 to 0.22 inch. Thus, subgrade type had no impact on total rutting in the absence of heavy traffic loading.

- For the heavily trafficked projects, the total rutting exhibited after 15 yr in service was significant for both the thin and thick AC pavements (greater than 0.2 inch). For the thin AC pavements, projects constructed over active soils exhibited the highest levels of rutting. For thick AC pavements, projects constructed over fine soils exhibited the highest levels of rutting. There were no obvious reasons for this reversal of rutting for soil types between thin and thick AC pavement.

Impact of Subgrade Clay Content

Figure 74 presents graphs showing the impact of low and high subgrade clay content on AC pavement total rutting for low- and high-trafficked projects.

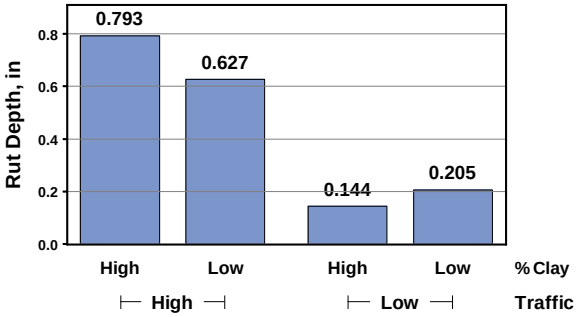

Source: FHWA.

A. Thin AC pavements.

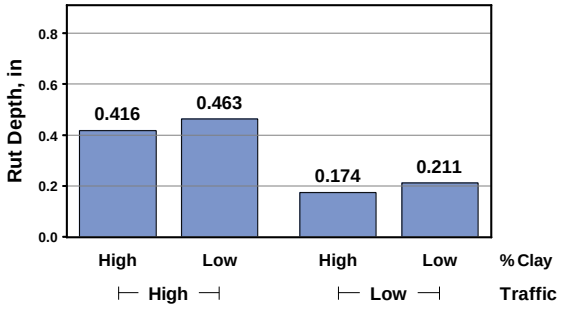

Source: FHWA.

B. Thick AC pavements.

Figure 74. Graphs. Impact of low and high subgrade clay content on AC total rutting for low- and high-trafficked projects.

Figure 74 shows the following:

- For the low-trafficked projects (thin and thick AC sections), subgrade clay content had no impact on the development and progression of total rutting. After 15 yr in service, measured total rutting was low (less than 0.2 inch).

- For the heavily trafficked projects, total rutting exhibited after 15 yr in service was high (greater than 0.2 inch) for both thin and thick AC pavements. Thin AC pavements with high clay content had higher rutting levels than those with low clay content; however, the difference of 0.17 inch was minimal.

Impact of Subgrade Silt Content

Figure 75 presents graphs showing the impact of low and high subgrade silt content on AC pavement total rutting for low- and high-trafficked projects.

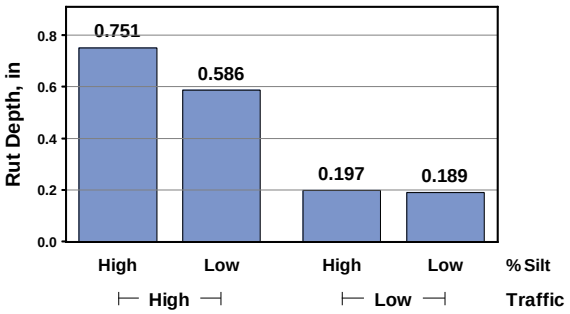

Source: FHWA.

A. Thin AC pavements.

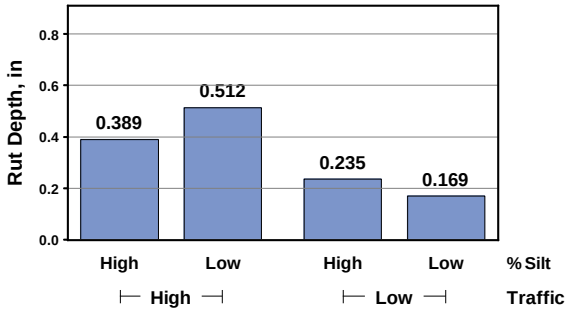

Source: FHWA.

B. Thick AC pavements.

Figure 75. Graphs. Impact of low and high subgrade silt content on AC total rutting for low- and high-trafficked projects.

Figure 75 shows the following:

- For the low-trafficked projects (thin and thick AC sections), subgrade silt content had no impact on the development and progression of total rutting. After 15 yr in service, measured total rutting ranged from 0.17–0.24 inch, which was considered low.

- For the heavily trafficked projects, the amount of total rutting was high for thin AC pavements (0.58–0.75 inch) and considerable for the thick AC pavements (0.39–0.51 inch). The difference in total rutting levels for the thin and thick AC pavements due to subgrade silt content ranged from 0.12–0.165 inch after 15 yr in service. The difference was not great. However, for the thin AC pavements, projects constructed over subgrades with higher levels of silt content exhibited much higher levels of total rutting.

Impact of Subgrade Fine-Sand Content

Figure 76 presents graphs showing the impact of low and high subgrade fine-sand content on AC pavement total rutting for low- and high-trafficked projects.

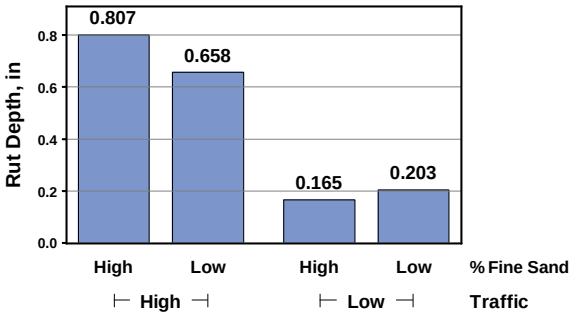

Source: FHWA.

A. Thin AC pavements.

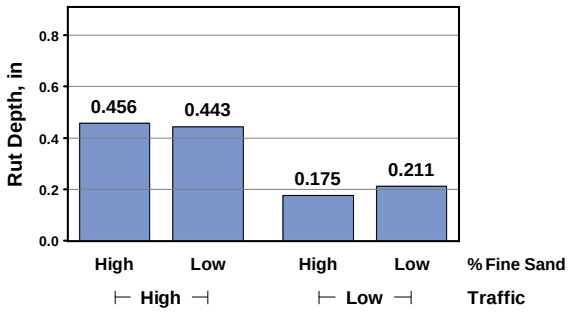

Source: FHWA.

B. Thick AC pavements.

Figure 76. Graphs. Impact of low and high subgrade fine-sand content on AC total rutting for low- and high-trafficked projects.

Figure 76 shows the following:

- For the low-trafficked projects (thin and thick AC sections), fine subgrade sand content had no impact on the development and progression of total rutting. After 15 yr in service, measured total rutting ranged from 0.165–0.211 inch, which is considered low.

- For the heavily trafficked projects, the amount of total rutting exhibited after 15 yr in service was high for the thin AC pavements (0.66–0.81 inch) and considerable for the thick AC pavements (0.44–0.46 inch). For both thin and thick AC pavements, projects constructed over subgrades with higher levels of fine-sand content exhibited higher levels of total rutting, with the difference being more pronounced for the thin AC projects.

Impact of Subgrade PI

Figure 77 presents graphs showing the impact of low and high subgrade PI on AC pavement total rutting for low- and high-trafficked projects.

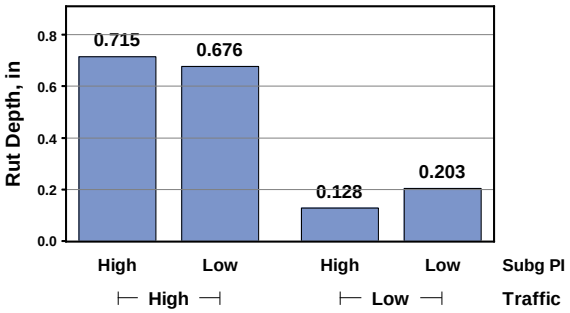

Source: FHWA.

A. Thin AC pavements.

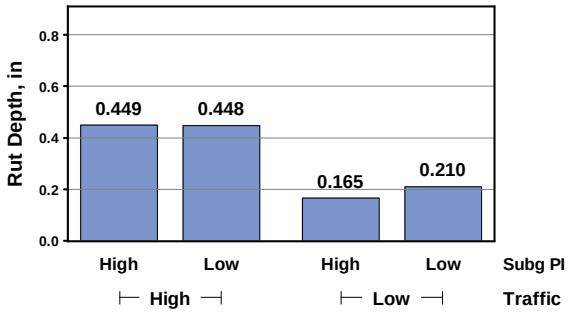

Source: FHWA.

B. Thick AC pavements.

Figure 77. Graphs. Impact of low and high subgrade PI on AC total rutting for low- and high-trafficked projects.

Figure 77 shows the following:

- For the low-trafficked projects (thin and thick AC sections), subgrade PI had no impact on the development and progression of total rutting. After 15 yr in service, measured total rutting ranged from 0.13 to 0.21 inch, which is considered low.

- For the heavily trafficked projects, the amount of total rutting exhibited after 15 yr in service was high for the thin AC pavements (0.67 to 0.71 inch) and considerable for the thick AC pavements (approximately 0.45 inch). For both thin and thick AC pavements, projects constructed over subgrades with higher PI levels did not exhibit higher levels of total rutting.

DETAILED STATISTICAL ANALYSIS TO CHARACTERIZE IMPACT OF ENVIRONMENTAL FACTORS ON RUTTING

Statistical analysis like the one described in chapter 6 was performed with rutting as the dependent variable.

Summary of GLMSELECT and ANOVA Results for Low-Trafficked AC Pavements

The results of the statistical model selection GLMSELECT and ANOVA procedures for low-trafficked AC pavements (SPS-8) are presented in figure 78. An interaction between the annual number of wet days and average annual daily truck traffic (AADTT) was selected as the only variable that had a significant impact on development of total rutting. This implied that, even for low truck-traffic application, the small differences in truck traffic and the number of wet days can significantly impact the extent of rutting present after 15 yr in service. It must be noted that the rutting level exhibited by the SPS-8 projects was low (typically less than 0.25 inch). Design factors such as AC thickness were found to be insignificant for low-trafficked pavements.

AC RUTTING —LOW TRAFFIC SPS-8 ONLY

The GLM Procedure

Dependent Variable: RUT_NL

Source	DF	Sum of Squares	Mean Square	F Value	Pr > F
Model	1	0.03473492	0.03473492	7.78	0.0093
Error	29	0.12954292	0.00446700		
Corrected Total	30	0.16427784			

R-Square	Coeff Var	Root MSE	RUT_NL Mean
0.211440	32.97129	0.066836	0.202708

Source	DF	Type III SS	Mean Square	F Value	Pr > F
AADTT*WETDAYS	1	0.03473492	0.03473492	7.78	0.0093

Parameter	Estimate	Standard Error	t Value	Pr > |t|
Intercept	0.0327566018	0.06211766	0.53	0.6020
AADTT*WETDAYS	0.1305628919	0.04682140	2.79	0.0093

Source: FHWA

Figure 78. Screenshot. Summary of GLMSELECT and ANOVA results for total rutting for low-trafficked AC pavements.

Summary of GLMSELECT and ANOVA Results for Low- and High-Trafficked AC Pavements

Statistical ANOVA similar to that described for low-trafficked AC pavements was performed for all projects (SPS-8 and -1 and GPS-1). All key factors for traffic, AC thickness, climate (i.e., temperature and moisture factors), and subgrade characteristics (e.g., percent sand, PI) were considered. Interactions of variables were also evaluated. However, there are many confounding factors that impacted the level of rutting of flexible pavements that were not considered within this analysis (e.g., asphalt content, asphalt grade, gradation). The results of the ANOVA for the significant factors and interactions are presented in figure 79 and show the following:

- One three-way interaction was significant: traffic, wet days, and AC thickness. The results for these three variables are as follows:
  - **Traffic**—Traffic level has a very significant effect on total rutting. The higher traffic level of SPS-1 and GPS-3 sections results in a much higher amount of rutting (greater than 0.40 inch).

  - **Wet days**—Wet days have a very significant effect on total rutting. This occurred in the SPS-8 analysis and again with combined SPS-8 and -1 and GPS-1 sections. The number of wet days correlates to the moisture in the unbound base and subgrade. Actually, the estimated base and subgrade moisture content did have a similar effect, but wet days were the most significant.

  - **AC thickness**—AC thickness also significantly affects rutting. The thicker the AC layers, the less the total rutting in the pavement. It is expected that significant levels of rutting occurred in the aggregate base and/or subgrade layers of flexible pavements with the thinner AC layers and higher levels of truck traffic.

- The three-way interaction of traffic, wet days, and AC thickness may be due to a situation where an AC pavement is located in a wet climate, has relatively higher truck traffic, and has a thinner AC layer. This situation is expected to result in a large amount of rutting.

AC RUTTING —ALL TRAFFIC SPS-8, SPS-1, GPS-1

The GLM Procedure

Dependent Variable: RUT_NL

Source	DF	Sum of Squares	Mean Square	F Value	Pr > F
Model	1	2.37817270	2.37817270	32.73	<.0001
Error	89	6.46676756	0.07266031		
Corrected Total	90	8.84494026			

R-Square	Coeff Var	Root MSE	RUT_NL Mean
0.268874	63.77476	0.269556	0.422668

Source	DF	Type III SS	Mean Square	F Value	Pr > F
AADTT*WETDAYS/THICK	1	2.37817270	2.37817270	32.73	<.0001

Source: FHWA

Figure 79. Screenshot. Summary of GLMSELECT and ANOVA results for determining factors that significantly influence the development of AC rutting using all pavement sections.

Comparing the model selection procedure results for all projects and low-trafficked projects only showed the following:

- The low-traffic analysis showed that only traffic and number of wet days were significant in a two-way interaction. The higher the traffic (AADTT) and number of wet days, the higher the rutting, although rutting was very low for nearly all sections (e.g., less than 0.25 inch).

- The ANOVA with the combined low- and high-traffic sections showed that the highest variable correlation was a three-way interaction between wet days, traffic level, and AC thickness.

- Traffic loading was the main initiator of rutting and was very significant in this analysis of low versus high traffic. Theoretically, repeated loading and compressive and shear strains were required for permanent deformation.

- The environmental factor that aggravated the progression of rutting was wet days per year. The annual number of wet days correlated with moisture in the unbound base and subgrade layers, resulting in reduced resilient modulus supporting the AC layers. This situation led to increased total rutting in the AC, base, and subgrade.

- AC thickness was also part of the three-way interaction but in the denominator. This means that rutting was higher for thin AC layers than for thick AC layers.

Note that there were no AC-mix properties, such as binder grade, air voids, gradation, unit weight, etc., in the analyses. Some of these may have been significant if included.

TOTAL RUTTING DAMAGE ANALYSIS

Estimating the proportion of overall AC pavement total rutting damage due to environmental factors required the following:

- The overall rutting damage of a selection of AC pavements subjected to normal heavy traffic loadings (GPS-1 and SPS-1 companion sections) and environmental factors.

- The rutting damage of similar thickness and materials of AC pavements subjected to low-traffic loadings and similar environmental factors (SPS-8 projects). All of these pavements had less than 0.20 inch of rutting and were considered well within the standard error of measurement. Note the low level of traffic loadings for the SPS-8 projects was so low that prediction models like the AASHTO ME would not indicate more than approximately 0.20 inch of mean rutting, and this was observed in the field through LTPP surveys.

The impact of various design and environmental factors on total rutting damage was also assessed. A summary of overall total rutting damage (GPS-1 and SPS-1 projects) and total rutting damage due to environmental factors (SPS-8 projects) shows that, on average, overall total rutting damage was 62.2 percent. For low-trafficked SPS-8 (environmental effects alone) projects, the total rutting damage averaged 27.0 percent. Thus, the proportion of overall total rutting damage of the typical heavily trafficked AC pavement due to environmental factors was 43.4 percent.

Table 34 and table 35 present the impact of design and environmental factors on AC pavement total rutting damage.

Table 34. Impact of AC thickness on AC pavement total rutting damage.

AC Thickness	Overall Total Rutting Damage (%)	Total Rutting Damage due to Environmental Factors (%)	Overall Damage due to Environmental Factors (%)
Thin	68.6	26.3	38.3
Thick	55.8	27.7	49.6
Mean	62.2	27.0	43.4

Table 35. Impact of wet days on AC pavement total rutting damage.

Wet Days	Overall Rutting Damage (%)	Rutting Damage due to Environmental Factors (%)	Overall Damage due to Environmental Factors (%)
Low (<100)	66.2	25.4	38.4
High (>100)	61.4	27.3	44.5
Mean	63.8	26.4	41.4

The results indicate the following:

- The proportion of overall rutting damage attributable to environmental factors for thin AC pavements was approximately 38 percent. For thicker AC pavements, the proportion of rutting damage due to environmental factors was 50 percent.

- The proportion of environmental damage was highest for regions with more annual wet days (44 percent) than for regions with fewer wet days (38 percent).

CHAPTER 8. ANALYSIS TRANSVERSE CRACKING DISTRESS FOR SPS-8 AND COMPANION AC PAVEMENT PROJECTS

This chapter presents results of the preliminary and detailed analysis of transverse cracks for the SPS-8 and companion non-SPS and non-GPS projects. For this analysis, transverse cracking is defined as cracks in the AC surface that are predominantly perpendicular to the pavement centerline. More than one mechanism may be acting to cause AC transverse cracking, including stresses associated with very low temperature events and repeated low temperatures, AC-mix shrinkage over time and temperature cycling, and stresses created by traffic loadings.

Transverse cracking for this analysis was measured as feet per mile over the entire 500-ft LTPP sample area. The relative magnitude of transverse cracking can be visualized by the following approximate conversions from feet per mile to crack spacing:

- 2,500 ft/mi = 25-ft crack spacing.
- 1,200 ft/mi = 50-ft crack spacing.
- 600 ft/mi = 100-ft crack spacing.

PRELIMINARY ANALYSIS OF AC PAVEMENT TRANSVERSE CRACKING PERFORMANCE

The following sections describe a statistical analysis to determine the significance of various environmental factors on AC pavement transverse cracking.

Impact of Freeze and Nonfreeze Climates

Figure 80 presents graphs showing the impact of freeze and nonfreeze climates on AC transverse cracking for low- and high-trafficked projects.

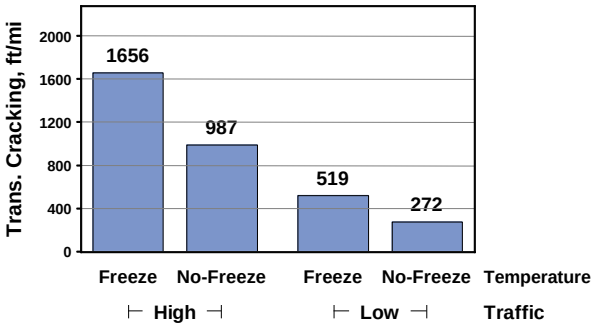

Source: FHWA.

A. Thin AC pavements.

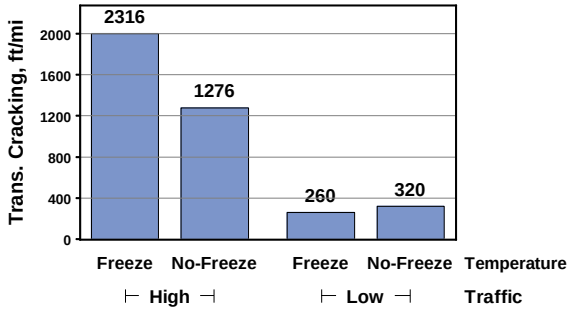

Source: FHWA,

B. Thick AC pavements.

Figure 80. Graphs. Impact of freeze and nonfreeze climates on AC transverse cracking for low- and high-trafficked projects.

Figure 80 shows the following:

- Thin AC sections with low traffic exhibited a 48-percent increase in transverse cracking from nonfreeze to freeze climates. However, the amount of transverse cracking in nonfreeze climates was substantial, indicating that mechanisms other than low temperatures may be contributing to cause this much transverse cracking.

- Thin AC sections with high traffic exhibited a 41-percent increase in transverse cracking from nonfreeze to freeze climates. The extent of transverse cracking present on pavement located in both nonfreeze and freeze climates was very significant (greater than 950 ft/mi).

- Thick AC sections with low traffic exhibited a 23-percent decrease in transverse cracking from nonfreeze to freeze climates.

- Thick AC sections with high traffic exhibited a 45-percent increase in transverse cracking from nonfreeze to freeze climates. The extent of transverse cracking present on pavement located in both nonfreeze and freeze climates was very significant (greater than 1,250 ft/mi).

- The high-trafficked pavements exhibited much more transverse cracking (987 to 2,316 ft/mi) than the low-trafficked pavements (272 to 519 ft/mi), which is a significant finding.

- For both the nonfreeze and freeze climates, AC thickness did not appear to impact the extent of transverse cracking exhibited after 15 yr.

Impact of Freeze–Thaw Cycles

Figure 81 presents graphs showing the impact of low and high freeze–thaw cycles on AC transverse cracking for low- and high-trafficked projects.

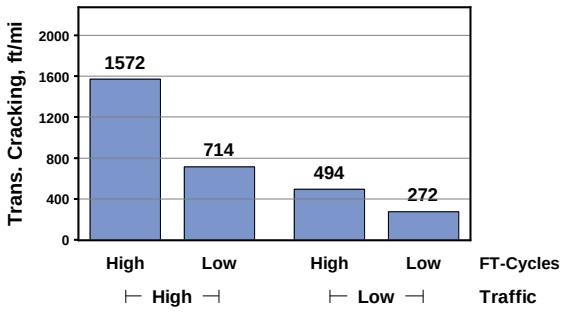

Source: FHWA

A. Thin AC pavements.

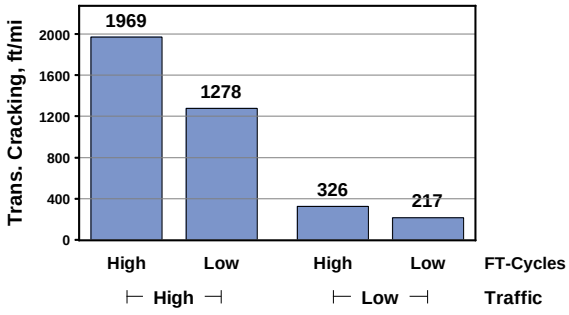

Source: FHWA

B. Thick AC pavements.

Figure 81. Graphs. Impact of low and high freeze–thaw cycles on AC transverse cracking for low- and high-trafficked projects.

The following results shown in figure 81 are similar to those of figure 80:

- **Thin AC sections with low traffic—**Environments subjected to high numbers of freeze–thaw cycles exhibited a 45-percent increase in transverse cracking when compared to environments with low numbers of freeze–thaw cycles.

- **Thin AC sections with high traffic**—Environments subjected to high numbers of freeze–thaw cycles exhibited a 55-percent increase in transverse cracking when compared to environments with low numbers of freeze–thaw cycles.

- **Thick AC sections with low traffic**—Environments subjected to high numbers of freeze–thaw cycles exhibited a 33-percent increase in transverse cracking when compared to environments with low numbers of freeze–thaw cycles.

- **Thick AC sections with high traffic**—Environments subjected to high numbers of freeze–thaw cycles exhibited a 35-percent increase in transverse cracking when compared to environments with low numbers of freeze–thaw cycles.

The high-trafficked pavements exhibited much more transverse cracking (417 to 1,572 ft/mi) than the low-trafficked pavements (272 to 494 ft/mi). Again, this finding is significant and unusual.

Impact of Frost Depth

Figure 82 presents graphs showing the impact of low and high frost depth on AC transverse cracking for low- and high-trafficked projects.

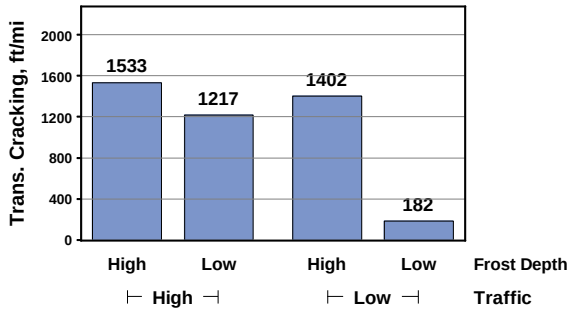

Source: FHWA.

A. Thin AC pavements.

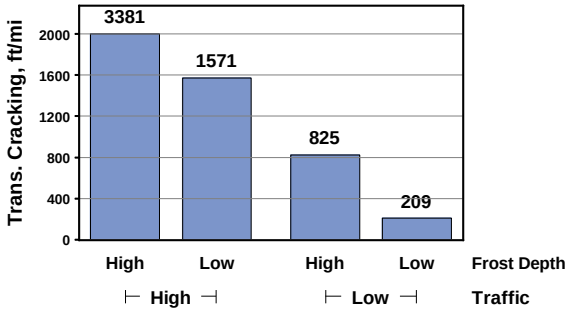

Source: FHWA.

B. Thick AC pavements.

Figure 82. Graphs. Impact of low and high frost depth on AC transverse cracking for low- and high-trafficked projects.

Figure 82 shows the following:

- For thin AC pavements with high traffic, deep frost depth had more transverse cracking than lower frost depth but not much more (1,533 versus 1,217 ft/mi), indicating the possibility of other mechanisms causing this large amount of transverse cracking.

- For thin AC pavements with low traffic, pavements subjected to low frost depth exhibited significantly less transverse cracking (182 ft/mi) than those subjected to high frost depth (1,402 ft/mi).

- Transverse cracking was about the same for pavements with high frost depth regardless of the traffic level applied. For low-trafficked pavements, however, exposure to high frost depth resulted in a significant increase in transverse cracking.

- For thick AC pavements with high traffic, frost depth had a significant impact on the extent of transverse cracking exhibited. Pavements subjected to high frost depths exhibited more than double the amounts of transverse cracking exhibited by pavement subjected to low frost depths (3,381 versus 1,571 ft/mi).

- For thick AC pavements with low traffic, frost depth had significant impact on the extent of transverse cracking exhibited. Pavements subjected to high frost depths exhibited more than double the amounts of transverse cracking exhibited by pavement subjected to low frost depths (825 versus 209 ft/mi).

- Pavements subjected to more traffic applications in general saw much higher levels of transverse cracking. This is a very interesting finding as transverse cracking has not been associated with traffic loadings before.

Impact of AC Temperature

Figure 83 presents graphs showing the impact of low and high in situ AC temperature on AC transverse cracking for low- and high-trafficked projects.

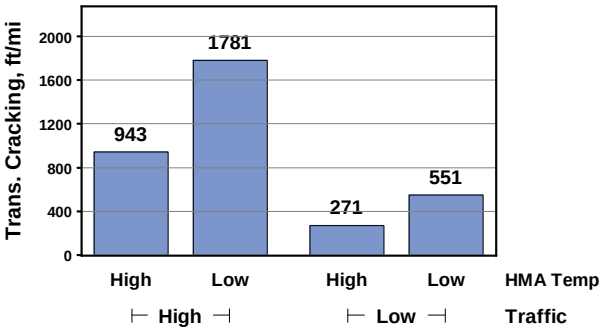

Source: FHWA.

A. Thin AC pavements.

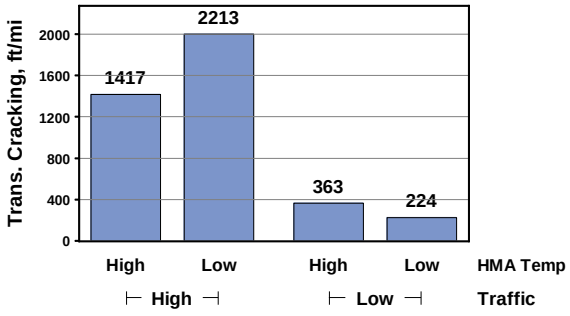

Source: FHWA.

B. Thick AC pavements.

Figure 83. Graphs. Impact of low and high in situ AC temperature on AC transverse cracking for low- and high-trafficked projects.

The information in figure 83 shows the following:

- For thin AC pavements with low-traffic applications, transverse cracking after 15 yr in service was higher for pavements with lower AC temperatures. However, pavements with high AC temperature (warm climates) showed substantial transverse cracking.

- For thin AC pavements with high-traffic applications, transverse cracking after 15 yr in service was significant (greater than 900 ft/mi). The pavements exposed to low temperatures had significantly higher levels of transverse cracking when compared to those in high temperature climates (1,781 versus 943 ft/mi).

- For thick AC pavements with low-traffic applications, transverse cracking exhibited after 15 yr in service was lower for lower temperature AC, which appears to be an anomaly compared to all other temperature results.

- For thick AC pavements with high-traffic applications, transverse cracking exhibited after 15 yr in service was significant (greater than 1,400 ft/mi). The pavements exposed to low temperatures had significantly higher levels of transverse cracking when compared to those in high temperature climates (2,213 versus 1,417 ft/mi).

Impact of Rainfall (Annual Precipitation)

As shown in figure 84, the extent of rainfall had no impact on AC transverse cracking for thick AC pavements. For thin AC pavements, rainfall had a significant impact in lowering cracking. For thin AC pavements with low traffic, AC transverse cracking was approximately 50 percent less for wet environments. For the high-trafficked thin AC pavements, AC transverse cracking was approximately 40 percent less for wet environments.

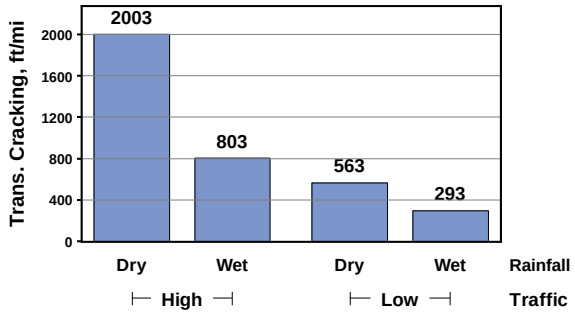

Source: FHWA.

A. Thin AC pavements.

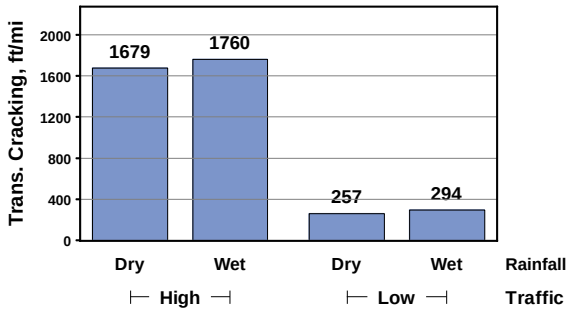

Source: FHWA.

B. Thick AC pavements.

Figure 84. Graphs. Impact of rainfall in wet and dry environments on AC transverse cracking for low- and high-trafficked projects.

Impact of Subgrade Type

As shown in figure 85, subgrade type had little impact on AC transverse cracking for thin and thick AC pavements subjected to high traffic (approximately 15-percent difference in transverse cracking for the different subgrade types). For thin and thick AC pavements subjected to low traffic, however, pavements constructed over fine subgrades exhibited approximately 85 percent more transverse cracking than those built over coarse subgrades. The increase is considered very high and may indicate that ground support and perhaps less restraint could be an initiator of AC transverse cracking.

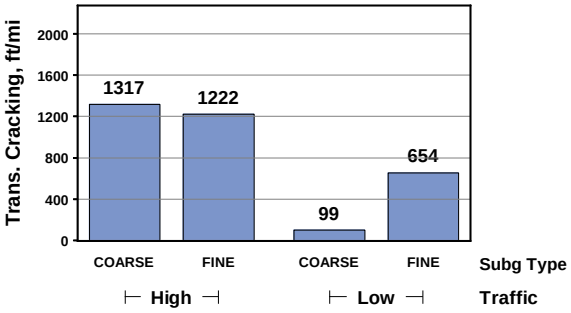

Source: FHWA.

A. Thin AC pavements.

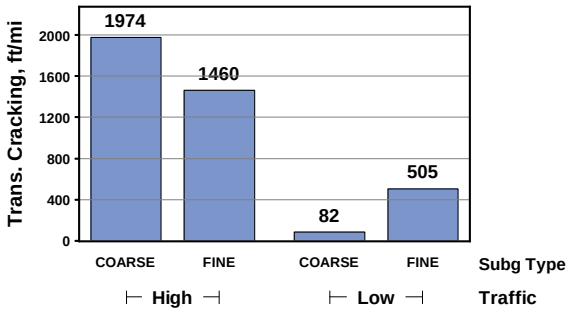

Source: FHWA.

B. Thick AC pavements.

Figure 85. Graphs. Impact of subgrade type on AC transverse cracking for low- and high-trafficked projects.

DETAILED STATISTICAL ANALYSIS TO CHARACTERIZE IMPACT OF ENVIRONMENTAL FACTORS ON TRANSVERSE CRACKING

Statistical analysis like the one described in chapter 6 was performed with transverse cracking as the dependent variable.

Summary of GLMSELECT and ANOVA Results for Low-Trafficked AC Pavements

The results of the statistical analysis for low-trafficked AC pavements (SPS-8) are presented in figure 86.

AC TRANSVERSE CRACKING —LOW TRAFFIC SPS-8 ONLY

The GLM Procedure

Dependent Variable: TEMP_INDEX_NL

Source	DF	Sum of Squares	Mean Square	F Value	Pr > F
Model	8	8638119.474	1079764.934	18.58	<.0001
Error	15	871711.612	58114.107		
Corrected Total	23	9509831.086			

R-Square	Coeff Var	Root MSE	TEMP_INDEX_NL Mean
0.908336	39.00159	241.0687	618.0997

Source	DF	Type III SS	Mean Square	F Value	Pr > F
FOUNDATION	1	3465965.433	1732982.716	29.82	<.0001
SAND	1	2084120.448	2084120.448	35.86	<.0001
SILT	1	4044796.515	4044796.515	69.60	<.0001
CLAY	1	3740938.737	3740938.737	64.37	<.0001
MSUMTEMP*TEMP	2	1336901.134	668450.567	11.50	0.0009
FREEZE THAW	1	259790.561	259790.561	4.47	0.0516

Parameter		Estimate	Standard Error	t Value	Pr > |t|
Intercept		-2622.690015	1188.044330	-2.21	0.0433
FOUNDATION	COARSE	-561.635174	254.954964	-2.20	0.0437
FOUNDATION	FINE	0.000000	. . .		
SAND FINE		-59.309725	9.903878	-5.99	<.0001
SILT		-39.582552	4.744563	-8.34	<.0001
CLAY		-39.770223	4.956881	-8.02	<.0001
ACTEMP*TEMP Freeze		0.264021	0.059430	4.44	0.0005
ACTEMP*TEMP No-Freeze		0.230997	0.049156	4.70	0.0003
FREEZE THAW CYCLES		5.671919	2.682620	2.11	0.0516

Source: FHWA

Figure 86. Screenshot. Summary of GLMSELECT and ANOVA results for AC transverse cracking for low-trafficked AC pavements.

The results show that the main factors significantly affecting AC transverse cracking are subgrade characteristics and temperature related climate variables. Specifically, the results indicate the following:

- Subgrade characteristics appear to affect AC transverse cracking. Pavements on fine-grained subgrades exhibited more transverse cracking than those built over coarse subgrades. Pavements on subgrades with higher amounts of silt and clay materials exhibited higher levels of AC transverse cracking. In the early 1970s, Haas found that subgrades were related to the level of low temperature transverse cracks for some of the provinces in Canada.[30] Subgrades with higher fine-sand content exhibited lower levels of the distress.

- Pavements in freeze climates exhibited more transverse cracking than those in nonfreeze climates. Increasing freeze–thaw cycles also increased the levels of transverse cracking.

- Pavements experiencing lower in situ AC temperatures exhibited higher levels of transverse cracking. However, AC pavement located even in warmer climates with high AC temperatures showed a large amount of transverse cracking. This is a very unusual finding that indicates other mechanisms may be contributing to transverse cracking. Some of the transverse cracking may be load-related or caused by shrinkage of the AC layer itself.

It must be noted that the AC transverse cracking level exhibited by the SPS-8 projects was far lower (typically less than 600 ft/mi) than that exhibited by the high-trafficked SPS and GPS projects. This is a very unusual finding. It is conceivable that traffic could be an initiator variable, but no theory exists to indicate this as a possibility. AC thickness was not found to be significant in predicting AC transverse cracking and thus had little mitigating effect for low traffic loadings.

Summary of GLMSELECT and ANOVA Results for Low- and High-Trafficked AC Pavements

Statistical ANOVA similar to that described for low-trafficked AC pavements was performed for all projects combined. All key factors for traffic, AC thickness, climate, and subgrade characteristics were considered. Interactions of variables were also evaluated, and some were found to be significant. The results of the ANOVA for the significant factors and interactions are presented in figure 87.

AC TRANSVERSE CRACKING —ALL TRAFFIC SPS-8, SPS-1, GPS-1

The GLM Procedure

Dependent Variable: TEMP_INDEX_NL

Source	DF	Sum of Squares	Mean Square	F Value	Pr > F
Model	4	43748254.6	10937063.6	5.82	0.0005
Error	65	122144772.2	1879150.3		
Corrected Total	69	165893026.8			

R-Square	Coeff Var	Root MSE	TEMP_INDEX_NL Mean
0.263714	103.3083	1370.821	1326.922

Source	DF	Type III SS	Mean Square	F Value	Pr > F
TRAFFIC	1	32684146.60	32684146.60	17.39	<.0001
TEMP (Climate Zone)	1	14641931.27	14641931.27	7.79	0.0069
PI*INSITU MOISTURE	2	11338626.21	5669313.10	3.02	0.0559

Parameter		Estimate	Standard Error	t Value	Pr > |t|
Intercept		-406.351811	421.2207058	-0.96	0.3383
TRAFFIC	G/SPS-1	1488.667934	356.9521666	4.17	<.0001
TRAFFIC	SPS8	0.000000	. . .		
TEMP	Freeze	1000.921893	358.5764557	2.79	0.0069
TEMP	No-Freeze	0.000000	. . .		
PI*INSITU MOIST	High	33.145759	14.5271316	2.28	0.0258
PI*INSITU MOIST	Low	4.901681	34.9158700	0.14	0.8888

Source: FHWA

Figure 87. Screenshot. Summary of GLMSELECT and ANOVA results for determining factors that significantly influence the development of transverse cracking using all pavement sections.

The results in figure 87 indicate the following:

- Traffic level has a significant effect on transverse cracking. The higher traffic levels of SPS-1 and GPS-1 sections resulted in a much higher amount of transverse cracking (1,488 ft/mi higher). This result is surprising in that it indicates mechanisms other than low temperature (e.g., traffic loadings) may be contributing to these higher amounts of transverse cracking. Thus, a significant finding from this study is that low-temperature events do not explain the higher amounts of low temperature cracking when loaded with higher traffic.

- Climate showed a significant effect on transverse cracking. Pavements in the freeze climate had 1,000 ft/mi more transverse cracking than those in a nonfreeze climate. This result is not surprising. The fact that there was a significant amount of transverse cracking in nonfreeze climates is surprising, indicating that another mechanism than low temperature was causing this amount of transverse cracking in warm climates.

- An interaction between the PI of the subgrade and in situ moisture was significant in affecting transverse cracking. This means that an AC pavement with a higher subgrade PI and higher in situ moisture content developed a larger number of transverse cracks.

- AC thickness did not significantly affect transverse cracking.

Comparing the model selection procedure results for all projects combined and low-trafficked projects only indicates the following:

- The low-traffic analysis indicated that several subgrade properties were significant, including active and fine subgrades, as well as sand content of the subgrade.

- The low-traffic analysis also showed several climate factors to be significant, including freeze climates, increasing numbers of freeze–thaw cycles, and in situ AC temperatures.

- The combined low- and high-traffic pavement data showed that the highest variable correlation was traffic level, with the higher traffic sections showing much more transverse cracking. In addition, several of the same subgrade and climate variables also were very significant in affecting the amount of transverse cracking. Thickness of AC did not have a significant effect on transverse cracking in the combined analysis.

- One key initiator factor was the annual in situ AC temperature, with colder temperatures resulting in high tensile stress leading to fracture at low temperature. Another one was annual air freeze–thaw cycles that caused a thermal fatigue stress in the AC. However, given that there is a large amount of transverse cracking in warmer climates, another initiator (e.g., AC-mix shrinkage) was likely.

- Another possible initiator was related to the subgrade characteristics, including type of soil, higher PI, and higher percent clay and percent silt or lower sand content. The mechanisms behind these initiators were not clear.

- Traffic appeared to be a major aggravator variable. It is also possible that traffic application initiated AC transverse cracking, as the extent of cracking increased very significantly from low- to high-trafficked projects. Certainly, additional research is needed to explore the mechanisms involved in combining thermal stress and load stress that may result in far more transverse cracking of AC pavement.

ANALYSIS OF AC TRANSVERSE CRACKING DAMAGE

Estimating AC transverse cracking–related damage and the proportion of overall AC pavement damage due to environmental factors was done by defining threshold AC transverse cracking, computing AC transverse cracking damage, and determining overall AC transverse cracking damage (GPS-1 and SPS-1 projects) and AC transverse cracking damage due to environmental factors alone (SPS-8 projects). The impact of various environmental factors on AC transverse cracking damage was also assessed.

A summary of overall AC transverse cracking damage and AC transverse cracking damage due to environmental factors alone shows that, on average, overall AC transverse cracking damage was 54.8 percent. For the low-trafficked SPS-8 sections, AC transverse cracking damage on average was 24.7 percent. Thus, the proportion of overall transverse cracking damage of the typical high-trafficked AC pavement due to environmental factors was 45.1 percent. This low value for AC transverse cracking that has been believed to be exclusively caused by temperature or shrinkage of the AC mix reflects the strong impact of traffic loadings. Table 36 through table 38 present the impact of design and environmental factors on AC pavement transverse cracking damage.

Table 36. Impact of AC thickness on AC transverse cracking damage.

AC Thickness	Overall Transverse Cracking Damage (%)	Transverse Cracking Damage due to Environmental Factors (%)	Overall Damage due to Environmental Factors (%)
Thin	46.8	25.4	54.3
Thick	64.9	24.1	37.1
Mean	55.9	24.8	45.7

Table 37. Impact of climate on AC transverse cracking damage.

Climate	Overall Transverse Cracking Damage (%)	Transverse Cracking Damage due to Environmental Factors (%)	Overall Damage due to Environmental Factors (%)
Freeze	73	28	38.3
Nonfreeze	43.5	12.9	29.6

Table 38. Impact of subgrade type on AC transverse cracking damage.

Subgrade Type	Overall Transverse Cracking Damage (%)	Transverse Cracking Damage due to Environmental Factors (%)	Overall Damage due to Environmental Factors (%)
Coarse	53.8	13.6	25.3
Fine/active	55.7	33.3	59.8

The information presented in table 36 through table 38 indicates the following:

- The proportion of overall transverse cracking damage attributable to environmental factors for thin AC pavements was approximately 54.3 percent. For thicker AC pavements, the proportion of damage due to environmental factors was 37.1 percent.

- The proportion of environmental damage was highest for deep-freeze regions (38.3 percent) as compared to nonfreeze regions (29.6 percent).

- The proportion of environmental damage was highest for AC pavements constructed over fine/active subgrades—59.8 versus 25.3 percent for projects over coarse subgrades.

CHAPTER 9. ANALYSIS OF SPS-8 AND COMPANION AC PAVEMENT PROJECTS MATERIALS DURABILITY DISTRESS

This chapter describes the results of the preliminary and detailed analyses of performance for the SPS-8 and companion SPS and GPS projects in terms of durability-related distresses. Durability-related distresses include bleeding, block cracking, potholes, and raveling. These were combined to compute a percent surface area with AC materials–related distress. The combined measure was needed because the extent and severity of the individual distresses was very low.

For the LTPP projects, bleeding, block cracking, potholes, and raveling were measured over the typical 500-ft AC pavement test section. For this analysis, the representative percent surface area with AC materials–related distress for the entire 500-ft sample area was computed using the formulas presented in figure 88 through figure 92.

$$\text{PCT\_BLEEDING} = 100 * \frac{BLEEDING\ AREA}{(LANE\_WIDTH * 500)}$$

Figure 88. Equation. Percentage of lane area with bleeding.

Where:

PCT_BLEEDING = percent lane area bleeding.
BLEEDING AREA= total area of bleeding distress (ft^2)
LANE_WIDTH = lane width (typically 12 ft).

$$\text{PCT\_BLOCK} = 100 * \frac{BLOCK}{(LANE\_WIDTH * 500)}$$

Figure 89. Equation. Percentage of lane area with block cracking.

Where:

PCT_BLOCK = percent lane area block cracking.
BLOCK = total area of block cracking (all severities) (ft^2).

$$\text{PCT\_PHOLES} = 100 * \frac{PHOLES}{(LANE\_WIDTH * 500)}$$

Figure 90. Equation. Percentage of lane area with potholes.

Where:

PCT_PHOLES = percent lane area potholes.
PHOLES = total area of potholes (all severities) (ft^2).

$$\text{PCT\_RAVELING} = 100 * \frac{RAVELING}{(LANE\_WIDTH * 500)}$$

Figure 91. Equation. Percentage of lane area with raveling.

Where:

PCT_RAVELING = percent lane area raveling.
RAVELING = total area of raveling (all severities) (ft^2).

$$PMATLS = PCT\_BLEEDING + PCT\_BLOCK + PCT\_PHOLES + PCT\_RAVELING$$

Figure 92. Equation. Percentage of lane area with materials-related distress.

Where *PMATLS* is the percent surface area with AC materials durability-related distress.

PRELIMINARY ANALYSIS OF PMATLS

The following sections describe a statistical analysis to determine the significance of various environmental factors on AC pavement materials durability distress.

Impact of Freeze and Nonfreeze Climate

Figure 93 presents graphs showing the impact of freeze and nonfreeze climates on PMATLS for low- and high-trafficked projects.

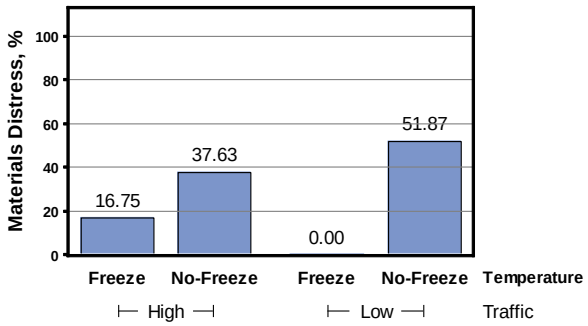

Source: FHWA.

A. Thin AC pavements.

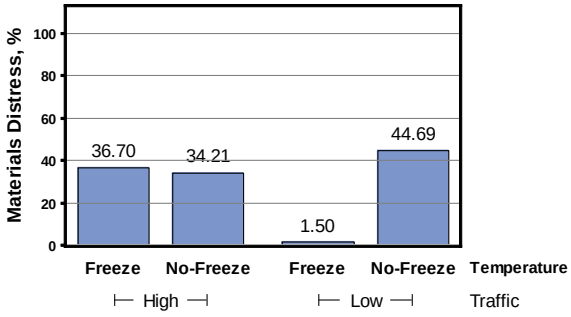

Source: FHWA.

B. Thick AC pavements.

Figure 93. Graphs. Impact of freeze and nonfreeze climates on PMATLS for low- and high-trafficked projects.

Figure 93 shows the following:

- For the low-trafficked projects (thin and thick AC sections), PMATLS was near 0 percent for pavements in freeze climates. Significant amounts of distress (52 and 45 percent for the thin and thick AC, respectively) were observed for pavements located in nonfreeze climates. This indicates that there was substantial AC materials-related distress for low-trafficked pavement observed in warmer climates and very little in colder climates.

- For high-trafficked pavements with thin AC, PMATLS exhibited after 15 yr in service was higher in nonfreeze climates than in freeze climates (38 and 17 percent).

- For high-trafficked pavements with thick AC, PMATLS exhibited after 15 yr in service was considerable, with pavements located in nonfreeze and freeze climates exhibiting about the same amounts of distress (37 and 34 percent).

These results indicate that thickness overall has little or no impact in mitigating materials-related distress (27 percent mean for thin AC and 29 percent mean for thick AC).

Impact of Air Freeze–Thaw Cycles

Figure 94 shows the impact of low and high freeze–thaw cycles on PMATLS for low- and high-trafficked projects.

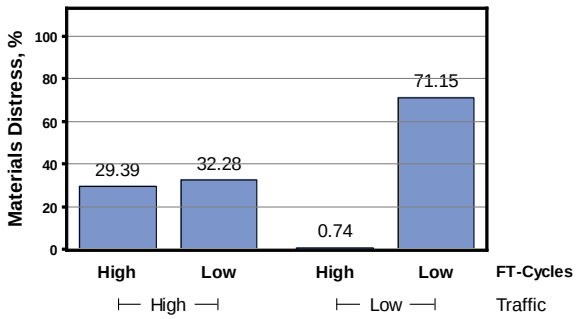

Source: FHWA.

A. Thin AC pavements.

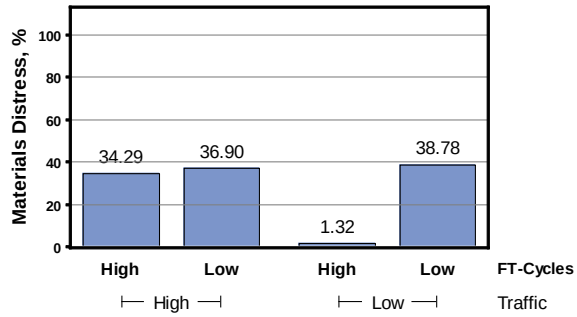

Source: FHWA.

B. Thick AC pavements.

Figure 94. Graphs. Impact of low and high freeze–thaw cycles on PMATLS for low- and high-trafficked projects.

Figure 94 shows the following:

- For the low-trafficked projects (thin and thick AC sections), pavements in climates with fewer freeze–thaw cycles exhibited much more materials distress than those in climates with more freeze–thaw cycles. Also, the thicker AC pavements exhibited significantly less materials distress than the thin pavements (71 versus 39 percent), indicating that in areas with low numbers of freeze–thaw cycles, increasing AC thickness may mitigate the occurrence of materials-related distress.

- For the high-trafficked projects, PMATLS after 15 yr in service was high and about the same for all levels of freeze–thaw cycles.

Impact of Frost Depth

Figure 95 presents graphs showing the impact of low and high frost depth on PMATLS for low- and high-trafficked projects.

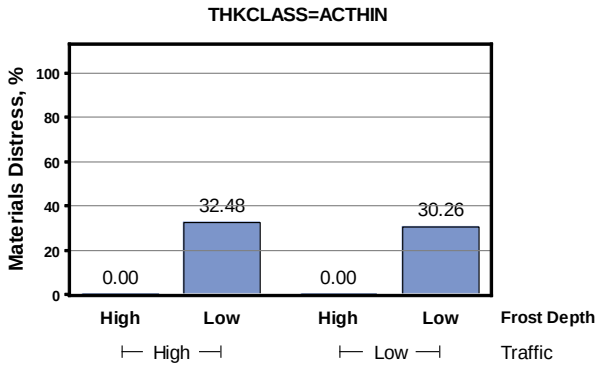

Source: FHWA.

A. Thin AC pavements.

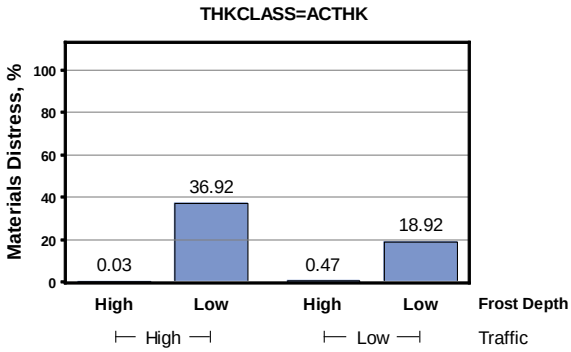

Source: FHWA.

B. Thick AC pavements.

Figure 95. Graphs. Impact of low and high frost depth on PMATLS for low- and high-trafficked projects.

Figure 95 shows the following:

- For the low-trafficked projects (thin and thick AC sections), pavements in climates with low frost depth exhibited much more materials distress than those in climates with high frost depth.
- For the high-trafficked projects, PMATLS exhibited after 15 yr in service was much greater for AC pavements located in low frost depth areas.
- PMATLS was near 0 percent for AC pavements located in climates where high frost penetration was prevalent. This occurred regardless of AC thickness and traffic loading. For climates where high frost penetration was not prevalent, materials-related distress was considerable.
- Traffic did not appear to have much impact on PMATLS.

Impact of AC Temperature

Figure 96 shows the impact of low and high environmental temperature variable in situ AC temperature on PMATLS for low- and high-trafficked projects.

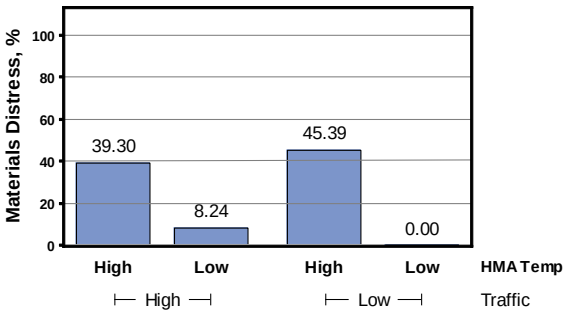

Source: FHWA.

A. Thin AC pavements.

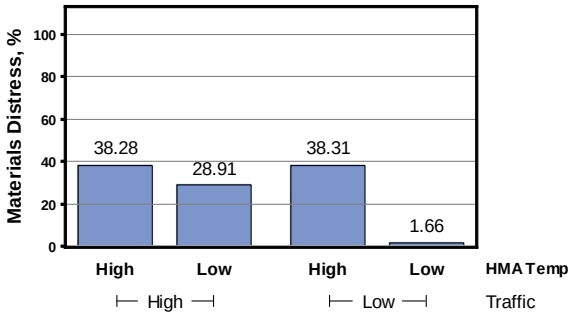

Source: FHWA.

B. Thick AC pavements.

Figure 96. Graphs. Impact of low and high AC temperature on PMATLS for low- and high-trafficked projects.

The results indicate the following:

- For the low-trafficked projects (thin and thick AC sections), pavements in climates with high in situ AC temperature exhibited much more materials-related distress than those in climates with high in situ AC temperature. In fact, PMATLS was nearly 0 percent in colder climates with low AC in situ temperature.
- For the high-trafficked projects, PMATLS exhibited after 15 yr in service was greater for AC pavements located in climates with high AC in situ temperature.
- Traffic and AC thickness did not appear to have an impact on materials-related distress.

Impact of Rainfall

Figure 97 shows the impact of rainfall in dry and wet environments on PMATLS for low- and high-trafficked projects. There were no clear trends regarding the impact of rainfall on materials durability distress. However, for the thin AC pavements, those in wet climates had more materials-related distress than those in dry climates (35 and 25 percent). For the thick AC pavements, the opposite was true.

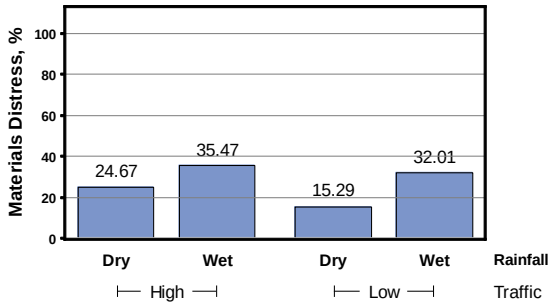

Source: FHWA.

A. Thin AC pavements.

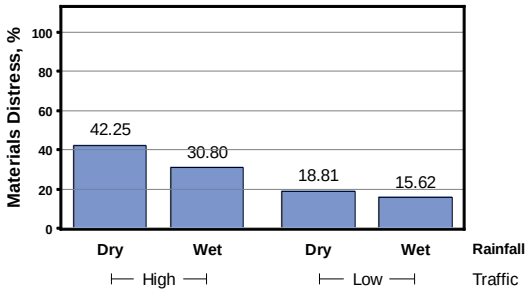

Source: FHWA.

B. Thick AC pavements.

Figure 97. Graphs. Impact of rainfall in dry and web environments on PMATLS for low- and high-trafficked projects.

Impact of Subgrade Type and Foundation Properties

As expected, no clear trends were observed for the effect of pavement subgrade type and foundation materials properties on AC-materials distress. Therefore, their impact on PMATLS was not further investigated.

DETAILED ANALYSIS OF AC MATERIALS-RELATED DISTRESS PERFORMANCE

Statistical analysis like the one described in chapter 6 was performed with percent materials-related distresses as the dependent variable.

Summary of GLMSELECT and ANOVA Results for Low-Trafficked AC Pavements

The results of the statistical model selection GLMSELECT and ANOVA procedures for low-trafficked AC pavements (SPS-8) are presented in figure 98.

AC MATLS—LOW TRAFFIC SPS-8 ONLY

The GLM Procedure

Dependent Variable: MATLS_INDEX_NL

Source	DF	Sum of Squares	Mean Square	F Value	Pr > F
Model	4	15486.46797	3871.61699	6.54	0.0013
Error	22	13014.74997	591.57954		
Corrected Total	26	28501.21794			

R-Square	Coeff Var	Root MSE	MATLS_INDEX_NL Mean
0.543362	151.7270	24.32241	16.03037

Source	DF	Type III SS	Mean Square	F Value	Pr > F
THK6_AC	1	1282.205292	1282.205292	2.17	0.1551
WETDAYS	1	1461.216142	1461.216142	2.47	0.1303
SUMFROSTDEPTH	1	2352.035866	2352.035866	3.98	0.0587
MSUMTEMP	1	8971.285578	8971.285578	15.16	0.0008

Parameter	Estimate	Standard Error	t Value	Pr > |t|
Intercept	-259.0266521	82.79283533	-3.13	0.0049
THK6_AC	-4.2066825	2.85737688	-1.47	0.1551
WETDAYS	0.2879947	0.18324572	1.57	0.1303
SUMFROSTDEPTH	0.0080978	0.00406115	1.99	0.0587
MSUMTEMP	0.0110916	0.00284823	3.89	0.0008

Source: FHWA

Figure 98. Screenshot. Summary of GLMSELECT and ANOVA results for AC materials-related distress for low-trafficked AC pavements.

The low-trafficked results show that the following variables had a significant impact on AC materials distress:

- **AC in situ temperature**—The higher the in situ AC temperature, the higher the AC pavement materials distress. This was the most significant variable.

- **Frost depth**—The higher the frost depth, the lower the AC-materials distress.

- **Wet days**—The higher the number of wet days, the higher the AC-materials distress.

- **AC pavement thickness**—The higher the AC thickness, the lower the AC-materials distress.

The most significant finding is that pavements in hotter climates exhibited significantly more AC-materials distress than those in colder climates. Pavements in wet climates also had significantly more AC-materials distress than those in dry climates, as represented by the number of wet days per year. Thus, annual AC in situ temperature (hot/cold), frost depth, and wet days were all related to AC materials-related distress for SPS-8 sections with low traffic.

Summary of GLMSELECT and ANOVA Results for Low- and High-Trafficked AC Pavements

Statistical analysis similar to that described for low-trafficked AC pavements was performed for all projects combined. Analysis was completed using the following the steps:

1. Perform ANOVA to determine whether there was a significant difference in AC materials-related distress for low- and high-trafficked AC pavements. Determine if AC thickness mitigated the development and progression of the distress.

2. Perform the statistical model selection procedure and determine if any other variables have a significant impact on AC materials–related distress.

The results of the analyses are presented in figure 99 and are summarized as follows:

- Traffic application did not have a significant impact on AC-materials distress. This finding agrees with observations made from previous comparisons as well as theoretical considerations.

- AC thickness did not have a significant impact on AC-materials distress overall. AC thickness did have an impact on low-trafficked SPS-8 sections.

- Freeze–thaw cycles had a significant effect on AC-materials distress. The lower the freeze–thaw cycles over the year (e.g., warmer climate), the higher the AC-materials distress. This effect was very significant in that there was very low AC-materials distress at high levels of frost depth (e.g., cold climates).

- The in situ AC temperature also had a very significant effect; the higher the AC in situ temperature, the higher the AC-materials distress. Again, warmer climates exhibited significantly higher levels of AC-materials distress.

AC MATLS—ALL TRAFFIC SPS-8, SPS-1, GPS-1

The GLM Procedure

Dependent Variable: MATLS_INDEX_NL

Source	DF	Sum of Squares	Mean Square	F Value	Pr > F
Model	2	18981.0377	9490.5188	6.74	0.0023
Error	60	84436.6581	1407.2776		
Corrected Total	62	103417.6958			

R-Square	Coeff Var	Root MSE	MATLS_INDEX_NL Mean
0.183538	130.3862	37.51370	28.77122

Source	DF	Type III SS	Mean Square	F Value	Pr > F
FTCYC	1	3984.264097	3984.264097	2.83	0.0976
HMATEMP	1	4082.897050	4082.897050	2.90	0.0937

Parameter		Estimate	Standard Error	t Value	Pr > |t|
Intercept		28.61353068	14.32316326	2.00	0.0503
FTCYC	High	-20.18904034	11.99862582	-1.68	0.0976
FTCYC	Low	0.00000000	. . .		
HMATEMP	High	20.43740878	11.99862582	1.70	0.0937
HMATEMP	Low	0.00000000	. . .		

Source: FHWA

Figure 99. Screenshot. Summary of GLMSELECT and ANOVA results for AC materials distress using all pavement sections.

In summary, climate had a very significant impact on the development of AC materials distress. In general, the warmer the climate, the greater the AC material distress. In terms of initiator and aggravator factors, the following was postulated:

- AC in situ temperature had the most significant effect on AC materials distress based on the results shown in figure 98 and figure 99. Low AC in situ temperature climate resulted in very low AC materials distress for thin and thick AC at low and high traffic levels. Thus, the AC temperature factor was considered to be an initiator variable. High-temperature climates along with high solar radiation that caused hardening of the asphalt binders appeared to be an initiating variable.

- Freeze–thaw cycles correlated inversely with AC temperature and became more of an aggravation factor over time.

- For the low-trafficked AC pavements only, wet days were a significant factor, indicating that wetter climates had greater AC materials distress.

ANALYSIS OF AC MATERIALS-RELATED DISTRESS DAMAGE

Estimating AC materials–related distress and the proportion of overall AC pavement damage due to environmental factors was done by defining threshold AC materials–related distress, computing AC materials-related distress damage, and determining overall AC materials–related distress damage (GPS-1 and SPS-1 projects) and AC materials-related distress damage due to environmental factors alone (SPS-8 projects). The impact of various environmental factors on AC materials-related distress was also assessed.

Proportion of Overall AC Transverse Cracking Damage due to Environmental Factors

On average, overall AC materials-related distress damage was 43.8 percent. For the less trafficked pavements, AC materials-related distress on average was 25.6 percent. Thus, the proportion of overall AC materials-related distress damage of the typical heavily trafficked AC pavement due to environmental factors was 58.4 percent.

Impact of Design and Environmental Factors on Overall AC Materials-Related Damage

Table 39 and table 40 present the impact of design and environmental factors on AC materials–related distress damage.

Table 39. Impact of AC thickness on materials durability distress damage.

AC Thickness	Overall AC Materials Distress Damage (%)	AC Materials Distress Damage due to Environmental Factors (%)	Overall Damage due to Environmental Factors (%)
Thin	44.7	28.3	63.3
Thick	43.0	23.3	54.2

Table 40. Impact of climate on materials durability distress damage.

Climate	Overall AC Materials Distress Damage (%)	AC Materials Distress Damage due to Environmental Factors (%)	Overall Damage due to Environmental Factors (%)
Freeze	45.5	2.9	6.3
Nonfreeze	42.9	58.9	100

The information presented in table 39 and table 40 shows the following:

- The proportion of overall AC materials-related distress damage attributable to environmental factors for thin AC pavements was approximately 63.3 percent. For thicker AC pavements, the proportion of damage due to environmental factors was 54.2 percent. Although AC thickness did have an impact on AC materials distress, it was deemed not very significant.

- The proportion of environmental damage was highest for nonfreeze regions (i.e., 100 percent) as compared to nonfreeze regions, which was 6.3 percent.

CHAPTER 10. ANALYSIS OF SMOOTHNESS FOR SPS-8 AND COMPANION AC PAVEMENT PROJECTS

This chapter presents the results of the preliminary and detailed analysis of smoothness performance for the SPS-8 and companion projects. For LTPP, longitudinal profile of the entire 500-ft project was measured and converted into IRI. Smoothness was measured in both the left and right wheel paths. For this analysis, the representative IRI for the entire 500-ft sample area was computed as the average of the left and right wheel path IRI measures. As the projects evaluated were constructed with different initial IRI values, comparison of absolute IRI values after 15 yr in service will be misleading. The initial IRI values, if not measured, were backcasted using the IRI trends over time. Thus, the smoothness performance measure used for analysis was Δ*IRI*, which was defined as the change in IRI from initial IRI to IRI at 15 yr.

PRELIMINARY ANALYSIS OF AC PAVEMENT IRI PERFORMANCE

The following sections describe a statistical analysis to determine the significance of various environmental factors on AC pavement smoothness.

Impact of Freeze and Nonfreeze Climates

Figure 100 shows the impact of freeze and nonfreeze climates on ΔIRI for low- and high-trafficked projects.

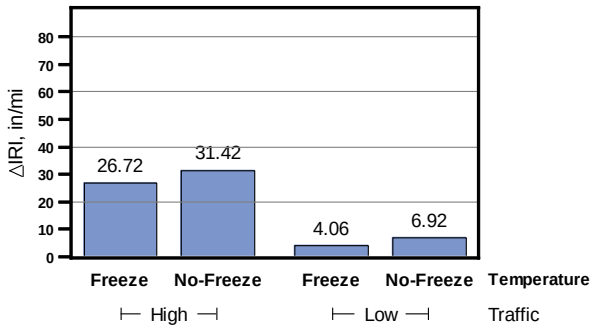

Source: FHWA.

A. Thin AC pavements.

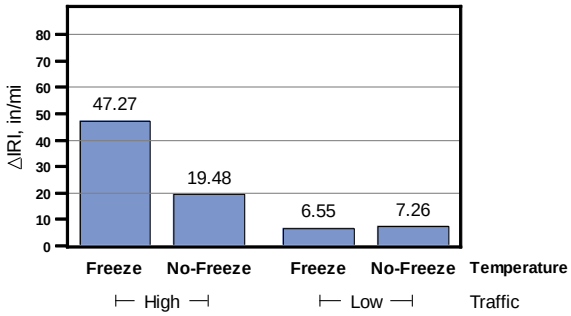

Source: FHWA.

B. Thick AC pavements.

Figure 100. Graphs. Impact of freeze and nonfreeze climates on change in IRI for low- and high-trafficked projects.

Figure 100 shows the following:

- For the low-trafficked projects (both thin and thick AC sections), IRI increased from 4 to 7.3 inches/mi after 15 yr in service, which was very low. There were only small differences in IRI between freeze and nonfreeze climates (less than 3 inches/mi). Thus, in the absence of heavy traffic loading, freeze or nonfreeze climates had little impact on IRI.

- For the high-trafficked projects, the change in IRI after 15 yr in service was high (mostly greater than 25 inches/mi). For thin AC pavements, neither freeze nor nonfreeze climates had much impact. However, for thicker AC pavements, pavements experiencing freeze climates exhibited much higher IRI increase (i.e., from 19 to 47 inches/mi).

- Pavements subjected to higher traffic levels exhibited much higher changes in IRI when compared to low-trafficked pavements regardless of AC thickness.

Impact of Freeze–Thaw Cycles

Figure 101 presents graphs showing the impact of low and high numbers of air freeze–thaw cycles on AC pavement change in IRI for low- and high-trafficked projects.

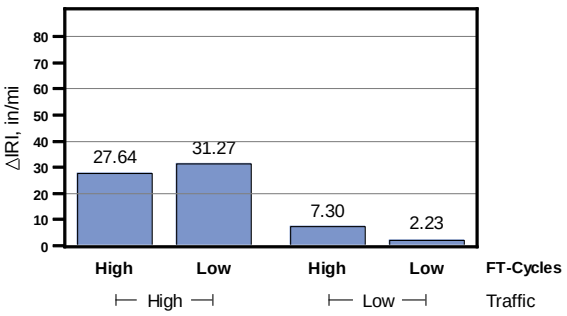

Source: FHWA.

A. Thin AC pavements.

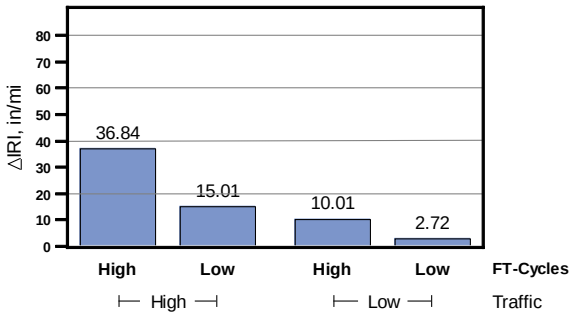

Source: FHWA.

B. Thick AC pavements.

Figure 101. Graphs. Impact of annual number of freeze–thaw cycles on change in IRI for low- and high-trafficked projects.

Figure 101 shows the following:

- For both thin and thick low-trafficked AC pavements, there was increased IRI for high freeze–thaw cycles, although this increase was small.

- Both thin and thick AC pavements subjected to higher traffic levels generally exhibited a higher increase of IRI than low-trafficked pavements (28 inches/mi for high traffic and an average of 6 inches/mi for low traffic).

- Pavements subjected to higher levels of freeze–thaw cycles averaged across AC thicknesses exhibited higher changes in IRI when compared to those subjected to lower levels of freeze–thaw cycles (20 inches/mi for higher freeze–thaw cycles versus 13 inches/mi for lower freeze–thaw cycles).

- AC thickness did not appear to have a significant impact on IRI.

Impact of Frost Depth

Figure 102 presents graphs showing the impact of low and high frost depth on AC pavement change in IRI for low- and high-trafficked projects.

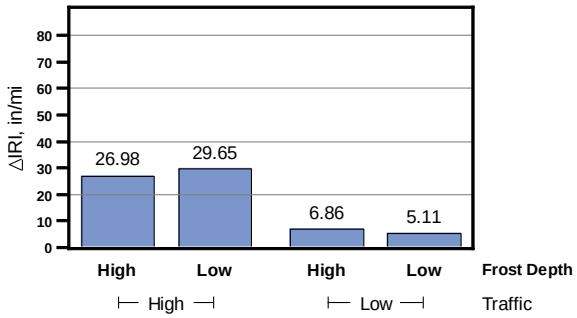

Source: FHWA.

A. Thin AC pavements.

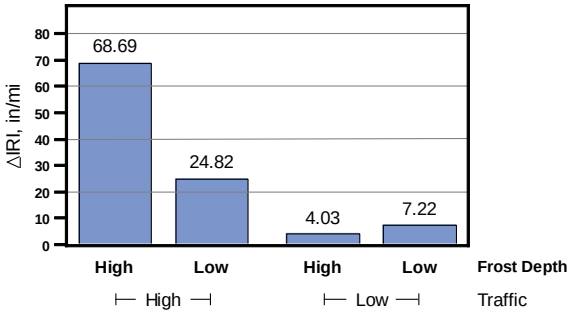

Source: FHWA.

B. Thick AC pavements.

Figure 102. Graphs. Impact of low and high frost depth on change in IRI for low- and high-trafficked projects.

Figure 102 shows the following:

- For the low-trafficked projects (both thin and thick AC sections), IRI increased from 4 to 7 inches/mi after 15 yr in service, which was considered low. There were only small differences in IRI between high and low frost depth. Thus, in the absence of heavy traffic loading, frost depth had no impact on IRI.

- For the high-trafficked projects, the change in IRI after 15 yr in service was deemed significant (mostly greater than 25 inches/mi). For thin AC pavements, frost depth did not appear to have an impact, whereas thicker AC pavements experiencing high levels of frost depth did exhibit more IRI increase.

Impact of AC Temperature

Figure 103 presents graphs showing the impact of low and high in situ AC temperature on AC pavement change in IRI for low- and high-trafficked projects.

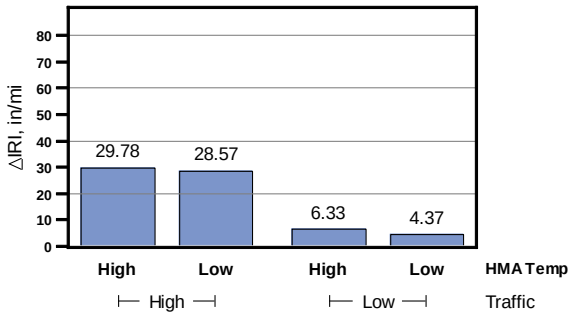

Source: FHWA.

A. Thin AC pavements.

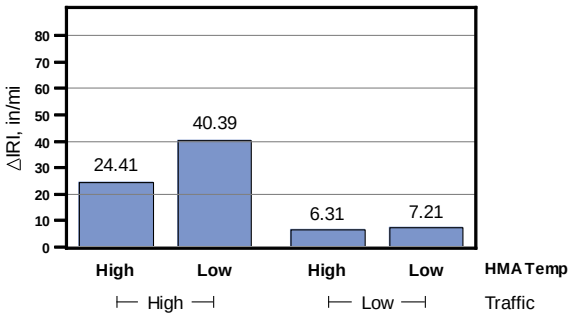

Source: FHWA.

B. Thick AC pavements.

Figure 103. Graphs. Impact of low and high AC temperatures on change in IRI for low- and high-trafficked projects.

Figure 103 shows the following:

- For the low-trafficked projects (thin and thick AC sections), change in IRI was low, ranging from 4 to 7 inches/mi after 15 yr in service. Thus, in situ AC temperature had no impact on IRI increase in the absence of heavy traffic loading.

- For the higher traffic projects, the IRI increase after 15 yr in service was high—30 inches/mi for thin AC pavements and 32 inches/mi for thick AC pavements. The worst performance in terms of IRI increase was thick AC pavements subjected to high-traffic applications and low AC temperatures (change in IRI to 40 inches/mi within 15 yr).

- AC thickness did not appear to have an impact on IRI after 15 yr.

Impact of Rainfall

Figure 104 presents graphs showing the impact of rainfall in dry and wet environments on AC pavement change in IRI for low- and high-trafficked projects.

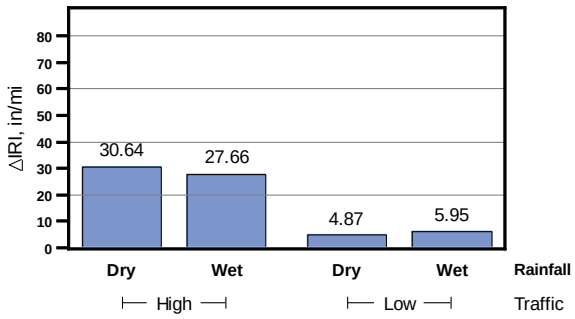

Source: FHWA.

A. Thin AC pavements.

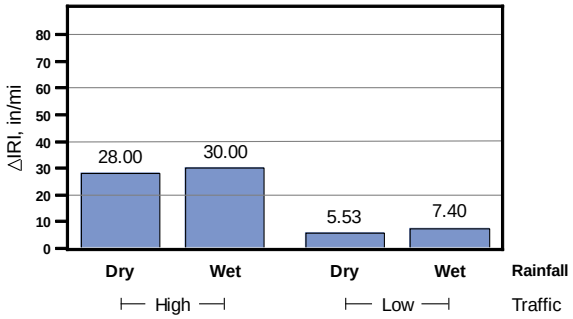

Source: FHWA.

B. Thick AC pavements.

Figure 104. Graphs. Impact of rainfall in dry and wet environments on change in IRI for low- and high-trafficked projects.

Figure 104 shows the following:

- For the low-trafficked projects (thin and thick AC sections), rainfall had little impact on IRI after 15 yr in service. Measured changes in IRI ranged from 5 to 7 inches/mi.

- For the heavily trafficked projects, the change in IRI after 15 yr in service was high (greater than 27 inches/mi) regardless of rainfall amounts. The difference in IRI increase for wet and dry climates was minimal.

- Traffic level had a large effect on IRI increase, with high traffic experiencing an IRI increase of 30 inches/mi and low traffic experiencing an IRI increase of about 6 inches/mi regardless of thickness.

Impact of Base and Subgrade In Situ Moisture Content

Figure 105 presents graphs showing the impact of low and high base and subgrade in situ moisture content on AC pavement on change in IRI for low- and high-trafficked projects.

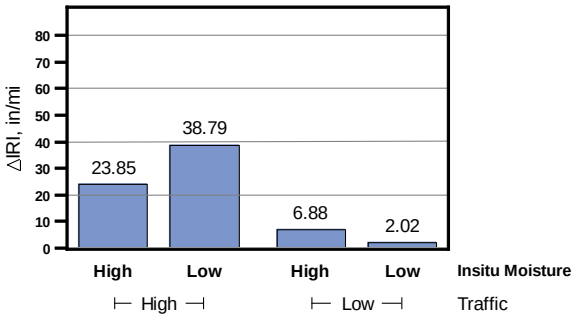

Source: FHWA.

A. Thin AC pavements.

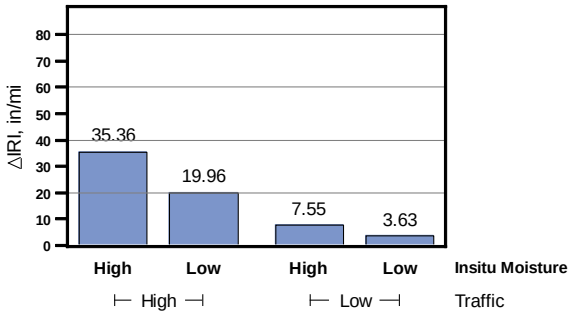

Source: FHWA.

B. Thick AC pavements.

Figure 105. Graphs. Impact of low and high base and subgrade in situ moisture content on change in IRI for low- and high-trafficked projects.

Figure 105 shows the following:

- For the low-trafficked projects (thin and thick AC sections), the change in IRI was higher for high in situ moisture content after 15 yr in service. Thus, base and subgrade in situ moisture content had an impact on changes in IRI in the absence of heavy traffic loading.

- For the heavily trafficked projects, the amount of change in IRI exhibited after 15 yr in service was high (greater than 20 inches/mi). The impact of base and subgrade moisture on IRI increase depended on AC thickness. For thin AC, lower base and subgrade moisture led to an increase in IRI increase from 24 to 39 inches/mi. For thick AC, lower moisture led to a decrease in IRI increase from 35 to 20 inches/mi.

- AC thickness overall appeared to have no impact on IRI increase.

Impact of Subgrade Type

Figure 106 presents a graph showing the impact of subgrade type (i.e., fine or coarse) on AC pavement change in IRI for low- and high-trafficked projects. Note that sufficient sections for thick AC pavements were not available, so only results for thin AC pavements are provided.

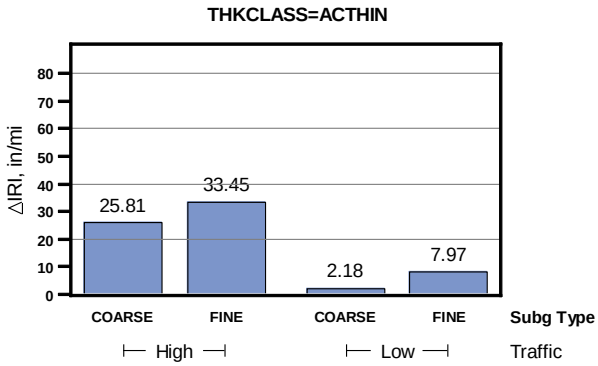

Source: FHWA.

Figure 106. Graph. Impact of subgrade type on change in IRI increase for thin AC pavements for low- and high-trafficked projects.

Figure 106 shows the following:

- For the low-trafficked projects (thin AC sections only), subgrade type had some impact on change in IRI after 15 yr in service. Measured change in IRI ranged from 2.2 inches/mi for coarse-gained soil to 8 inches/mi for fine-grained soil.

- For the heavily trafficked projects, the change in IRI after 15 yr in service was high (greater than 25 inches/mi). However, the change in IRI for fine- and coarse-grained soil was low at less than 10 inches/mi.

Impact of Subgrade Clay Content

Figure 107 presents graphs showing the impact of low and high subgrade clay content on AC pavement change in IRI for low- and high-trafficked projects.

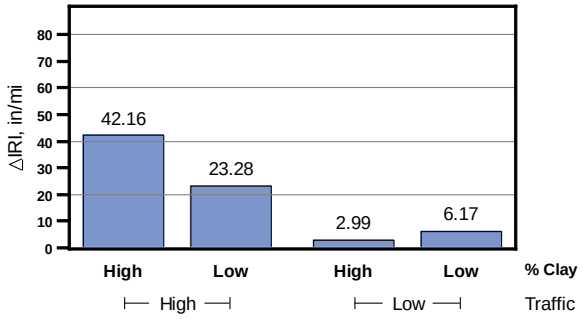

Source: FHWA.

A. Thin AC pavements.

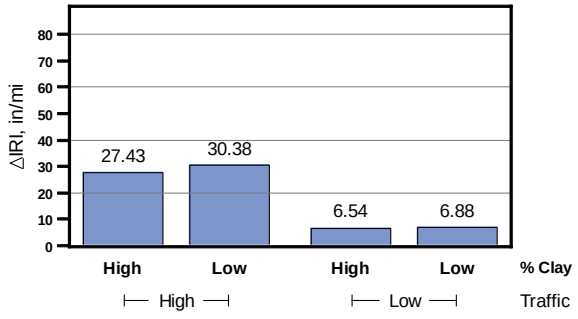

Source: FHWA.

B. Thick AC pavements.

Figure 107. Graphs. Impact of low and high subgrade clay content on change in IRI for low- and high-trafficked projects.

Figure 107 shows the following:

- For the low-trafficked projects (thin and thick AC sections), subgrade clay content had little impact on change in IRI after 15 yr in service, as measured change in IRI was low (less than 7 inches/mi).

- The change in IRI after 15 yr in service was high (greater than 23 inches/mi) for all high-trafficked AC pavements. The difference in IRI increase due to subgrade clay content was low for the thick AC pavements. However, for thin AC pavements, IRI increase was much higher when constructed over subgrades with high clay content.

Impact of Subgrade Silt Content

Figure 108 presents graphs showing the impact of low and high subgrade silt content on AC pavement change in IRI for low- and high-trafficked projects.

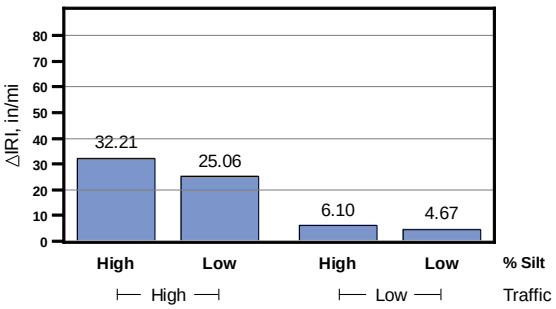

Source: FHWA.

A. Thin AC pavements.

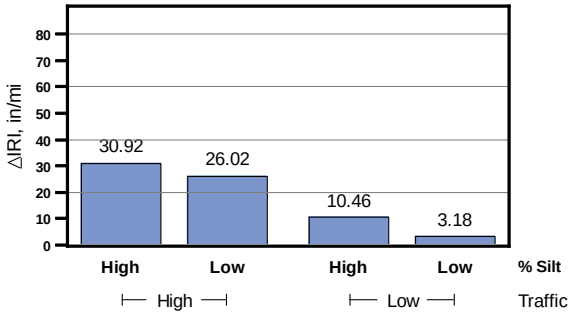

Source: FHWA.

B. Thick AC pavements.

Figure 108. Graphs. Impact of low and high subgrade silt content on change in IRI for low- and high-trafficked projects.

Figure 108 shows the following:

- For the low-trafficked projects (thin and thick AC sections), AC pavements constructed over silty subgrades exhibited higher changes in IRI (difference of 1.5 to 7 inches/mi) after 15 yr in service. Overall, IRI increase for these sections was fairly low at less than 11 inches/mi. Thus, subgrade silt content had little impact on IRI in the absence of heavy traffic loading.

- The change in IRI after 15 yr in service was high (greater than 25 inches/mi) for all heavily trafficked AC pavements regardless of subgrade silt content. The trends also show that AC pavements constructed over silty subgrades exhibited considerably more change in IRI. However, the difference in IRI increase for pavement constructed over subgrades with low/high silt content was relatively low.

- For all cases shown, AC pavement constructed over subgrades with higher silt content exhibited higher levels of changes in IRI, on average. Specifically, AC pavement over subgrade with lower silt content had on average lower IRI increase after 15 yr.

Impact of Subgrade Fine-Sand Content

Figure 109 presents graphs showing the impact of low and high subgrade fine-sand content on AC pavement change in IRI for low- and high-trafficked projects.

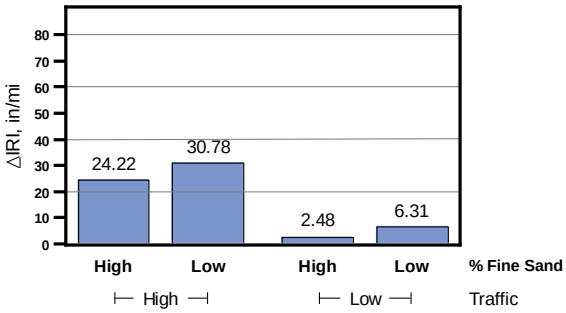

Source: FHWA

A. Thin AC pavements.

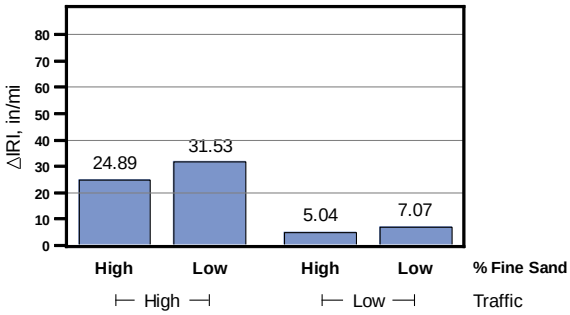

Source: FHWA

B. Thick AC pavements.

Figure 109. Graphs. Impact of low and high subgrade fine-sand content on change in IRI for low- and high-trafficked projects.

Figure 109 shows the following:

- For the low-trafficked projects (thin and thick AC sections), subgrade fine-sand content had no impact on IRI after 15 yr in service (less than 7 inches/mi). Thus, subgrade fine-sand content had no impact on IRI increase in the absence of heavy traffic loading. However, the trends show that AC pavements constructed over subgrades with low fine-sand content do exhibit higher IRI changes.

- The amount of IRI increase exhibited after 15 yr in service was deemed significant (greater than 24 inches/mi) for all heavily trafficked AC pavements regardless of subgrade fine-sand content. However, the difference in changes in IRI for pavement constructed over subgrades with low/high fine-sand content was not considerable (less than 7inches/mi).

- For all cases shown, pavement constructed over subgrades with lower fine-sand content exhibited higher levels of change in IRI. Specifically, AC pavement over subgrades with higher sand content was, on average, smoother after 15 yr.

Impact of Subgrade PI

Figure 110 shows the impact of low and high subgrade PI on AC pavement change in IRI for low- and high-trafficked projects.

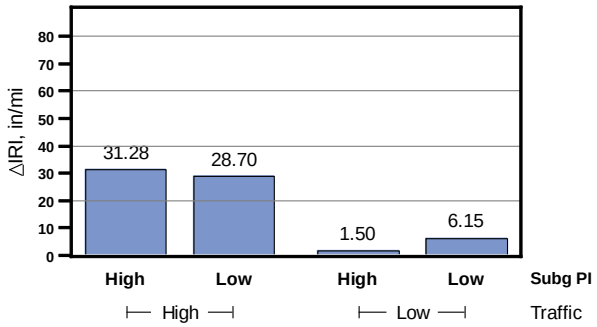

Source: FHWA.

A. Thin AC pavements.

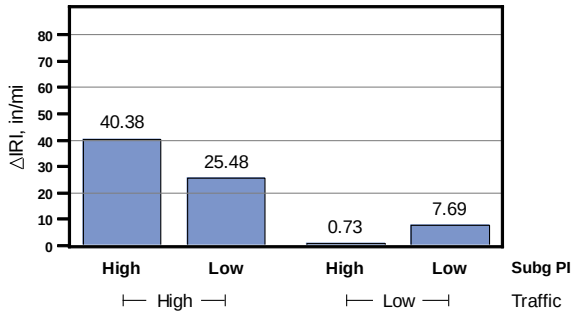

Source: FHWA.

B. Thick AC pavements.

Figure 110. Graphs. Impact of low and high subgrade PI on change in IRI for low- and high-trafficked projects.

Figure 110 shows the following:

- For the low-trafficked projects (thin and thick AC sections), subgrade PI had little impact on changes in IRI after 15 yr in service (IRI increase less than 8 inches/mi). Subgrade PI had little or no impact on changes in IRI in the absence of heavy traffic loading.

- The amount of change in IRI after 15 yr in service was deemed as significant (greater than 25 inches/mi) for all heavily trafficked AC pavements regardless of subgrade PI level. However, the difference in IRI increase for pavement constructed over subgrades with low or high PI was more significant for thicker AC pavements (difference of approximately 15 inches/mi).

DETAILED ANALYSIS OF AC PAVEMENT IRI PERFORMANCE

A statistical analysis like the one described in chapter 6 was performed with IRI as the dependent variable.

Summary of GLMSELECT and ANOVA Results for Low-Trafficked AC Pavements

The results of the statistical model selection GLMSELECT and ANOVA procedures for low-trafficked AC pavements (SPS-8) are presented in figure 111.

AC SMOOTHNESS—LOW TRAFFIC SPS-8 ONLY

The GLM Procedure

Dependent Variable: IRIAVG_L

Source	DF	Sum of Squares	Mean Square	F Value	Pr > F
Model	4	811.125237	202.781309	3.13	0.0376
Error	20	1296.015300	64.800765		
Corrected Total	24	2107.140537			

R-Square	Coeff Var	Root MSE	IRIAVG_L Mean
0.384941	113.5252	8.049892	7.090839

Source	DF	Type III SS	Mean Square	F Value	Pr > F
FTCYC	1	524.6365881	524.6365881	8.10	0.0100
TEMP	1	482.9451448	482.9451448	7.45	0.0129
WETDAYS*SOIL_TYPE	2	284.6385338	142.3192669	2.20	0.1373

Parameter		Estimate	Standard Error	t Value	Pr > |t|
Intercept		-12.30139015	8.59518723	-1.43	0.1678
FTCYC	High	14.93143356	5.24761887	2.85	0.0100
FTCYC	Low	0.00000000	. . .		
TEMP	Freeze	-13.24660813	4.85227999	-2.73	0.0129
TEMP	No-Freeze	0.00000000	. . .		
WETDAYS*SOIL_TYPE	COARSE	0.09729388	0.06239721	1.56	0.1346
WETDAYS*SOIL_TYPE	FINE	0.12770927	0.06321081	2.02	0.0569

Source: FHWA.

Figure 111. Screenshot. Summary of GLMSELECT and ANOVA results for IRI increase for low-trafficked AC pavements.

The results for low-trafficked projects show the following variables to be significant in affecting change in IRI:

- **Number of annual air freeze–thaw cycles**—The higher the number of freeze–thaw cycles, the higher the increase of IRI. The average increase was 15 inches/mi. over 15 yr.

- **Climate**—Moving from a nonfreeze climate to a freeze climate resulted in an average decrease of 13 inches/mi of IRI. Significantly less roughness occurred in freeze climates. This result appears to conflict with the first finding that a higher number of freeze–thaw cycles increases the IRI. It may be that with the broad climates, the number of freeze–thaw cycles varied widely. In areas of high freeze–thaw cycles, the resulting damage resulted in greater IRI increase, but when the broad climates of freeze and nonfreeze are considered, less IRI increase occurred in freeze areas.

- **Interaction of wet days and soil type**—This interaction indicates that a situation with, for example, fine-grained soil type in a wet climate (high wet days) could produce a significantly higher increase in IRI.

Summary of GLMSELECT and ANOVA Results for Low- and High-Trafficked AC Pavements

A statistical analysis similar to that described for low-trafficked AC pavements was performed for all projects combined as follows:

1. Perform an ANOVA to determine whether there was a significant difference in IRI increase for low- and high-trafficked AC pavements.

2. Perform an ANOVA to determine whether AC thickness mitigated the development and progression of IRI increase for the high-trafficked AC pavements.

3. Perform the statistical model selection procedure and determine if any other variables have a significant impact on IRI increase.

The results of the analyses are presented in figure 112.

AC SMOOTHNESS—ALL TRAFFIC SPS-8, SPS-1, GPS-1

The GLM Procedure

Dependent Variable: IRIAVG_L

Source	DF	Sum of Squares	Mean Square	F Value	Pr > F
Model	3	3318.87206	1106.29069	2.34	0.0828
Error	59	27925.49173	473.31342		
Corrected Total	62	31244.36378			

R-Square	Coeff Var	Root MSE	IRIAVG_L Mean
0.106223	106.9286	21.75577	20.34607

Source	DF	Type III SS	Mean Square	F Value	Pr > F
C_AADTT*THKAC	1	1595.294011	1595.294011	3.37	0.0714
FTCYC	1	1296.668543	1296.668543	2.74	0.1032
CLAY	1	1115.139205	1115.139205	2.36	0.1301

Parameter		Estimate	Standard Error	t Value	Pr > |t|
Intercept		9.08355082	5.54358767	1.64	0.1066
C_AADTT/THKAC		14.92700274	8.13067598	1.84	0.0714
FTCYC	High	9.84238980	5.94648711	1.66	0.1032
FTCYC	Low	0.00000000	. . .		
CLAY	High	9.25747077	6.03117897	1.53	0.1301
CLAY	Low	0.00000000	. . .		

Source: FHWA.

Figure 112. Screenshot. Summary of GLMSELECT and ANOVA results for IRI increase using all pavement sections.

In summary, a two-way interaction between AADTT and AC thickness was very significant. Increased traffic levels resulted in a greater loss of smoothness. When matched with thinner AC pavement, there was a very great IRI increase. Two key climatic and subgrade variables included clay content and number of freeze–thaw cycles as follows:

- Increased clay content resulted in increased IRI of 10 inches/mi.
- Increased number of freeze–thaw cycles resulted in increased IRI of 9 inches/mi.

ANALYSIS DAMAGE RELATED TO CHANGE IN IRI

Estimating damage related to changes in IRI and the proportion of overall AC pavement damage due to environmental factors was done by defining threshold IRI increase, computing IRI increase damage, and determining overall IRI increase damage (GPS-1/SPS-1 projects) and IRI increase due to environmental factors alone (SPS-8 projects). The impact of various environmental factors on IRI increase was also assessed.

Proportion of Overall Change in IRI Damage Due to Environmental Factors

A summary of overall increased IRI damage due to environmental factors alone shows that, on average, overall IRI increase damage was 29.2 percent. For the low-trafficked pavements, IRI increase damage on average was 6.2 percent. Thus, the proportion of overall IRI increase damage of the typical heavily trafficked AC pavement due to environmental factors was 21.2 percent.

Table 41 through table 43 present the impact of design and environmental factors on AC pavement IRI increase damage.

Table 41. Impact of AC thickness on IRI increase damage.

AC Thickness	Overall AC IRI Increase Damage (%)	IRI Increase due to Environmental Factors (%)	Overall Damage due to Environmental Factors (%)
Thin	29.3	5.5	18.8
Thick	29.2	6.8	23.3
Mean	29.3	6.2	21.1

Table 42. Impact of subgrade type on IRI increase damage.

Subgrade Type	Overall IRI Increase Damage (%)	IRI Increase due to Environmental Factors (%)	Overall Damage due to Environmental Factors (%)
Coarse	27.1	5.3	19.6
Fine	31.2	7.1	22.8

Table 43. Impact of climate on AC IRI increase damage.

Climate	Overall IRI Increase Damage (%)	IRI Increase due to Environmental Factors (%)	Overall Damage due to Environmental Factors (%)
Freeze	35.2	5.5	15.6
Nonfreeze	25.2	7.1	28.2

The information presented in table 41 through table 43 shows the following:

- The proportion of overall IRI increase damage attributable to environmental factors for thin AC pavements was approximately 18.8 percent. For thicker AC pavements, the proportion of damage due to environmental factors was 23.3 percent. AC thickness did not have a significant impact on IRI increase.

- The proportion of environmental damage was higher for AC pavements constructed over fine subgrades than for those constructed over coarse subgrades. The difference, however, was marginal.

- The proportion of environmental damage was higher for nonfreeze regions (28.2 percent) than for regions with deep freeze (15.6 percent). This implies pavements constructed in the warmer regions were more likely to exhibit significant IRI increase.

CHAPTER 11. ANALYSIS OF FATIGUE CRACKING DISTRESS FOR SPS-8 AND COMPANION JPCP PROJECTS

This chapter presents the results of the preliminary and detailed analysis of fatigue cracking performance for the SPS-8 and companion JPCP projects. Fatigue cracking, in this study, is defined as the combination of transverse top–down and bottom–up midslab panel cracking, longitudinal wheel-path cracking, and corner breaks. The combined distress was expressed as a percentage of all slabs in the traffic lane with any of the listed fatigue-related distresses at all severity levels. Results are presented in terms of high- and low-traffic applications. The higher-traffic (SPS-2/GPS-3 JPCP) AADTT was 693,123 for the design lane. The lower-traffic SPS-8 AADTT was 7,586 for the design lane.

PRELIMINARY ANALYSIS TO CHARACTERIZE IMPACT OF ENVIRONMENTAL FACTORS ON PCC FATIGUE CRACKING

The following sections describe a statistical analysis to determine the significance of various environmental factors on JPCP transverse fatigue cracking.

Impact of Freeze and Nonfreeze Climates

Figure 113 shows the impact of freeze and nonfreeze climates on JPCP fatigue cracking for low- and high-trafficked projects.

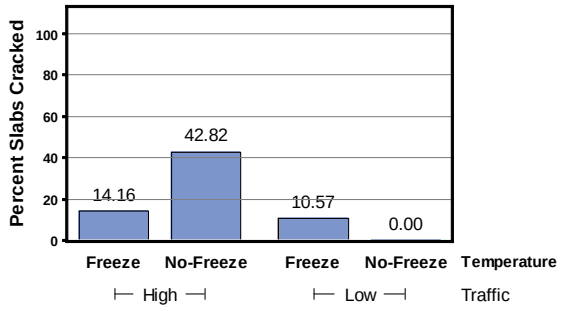

Source: FHWA.

A. Thin JPCPs.

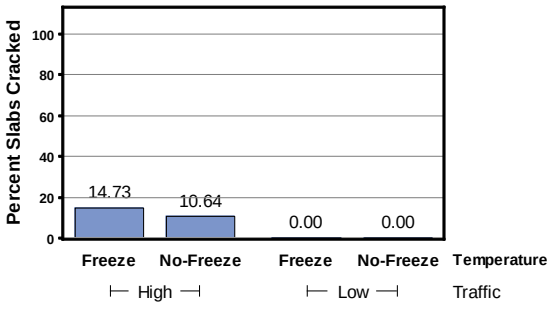

Source: FHWA.

B. Thick JPCPs.

Figure 113. Graphs. Impact of freeze and nonfreeze climates on JPCP fatigue cracking for low- and high-trafficked projects.

Figure 113 shows the following:

- In the absence of heavy traffic loads for both thin and thick SPS-8 JPCP projects, fatigue cracking averaged less than 3 percent of slabs after 15 yr. The amount of cracking exhibited by JPCPs not subjected to heavy traffic loads was 0 percent, with the exception of thin PCC pavement located in freeze climates, which was present in an average of 11 percent of pavement slabs.

- For the companion SPS-2 and GPS-3 JPCP projects subjected to high traffic loads, the amount of cracking exhibited after 15 yr in service was higher regardless of climate. Thin JPCPs located in nonfreeze climates exhibited the highest level of fatigue cracking (42 percent). Similar projects in freeze climates exhibited lower levels of cracking (14 percent). PCC thickness has a major impact on fatigue cracking, as projects with thicker PCC exhibited less cracking (17 percent for thin slabs versus 6 percent for thick slabs).

- In addition, traffic level clearly has an impact on fatigue cracking, with the heavily loaded JPCP averaging 21 percent, and pavements in the absence of heavy loads averaging 3 percent.

Impact of Freeze–Thaw Cycles

Figure 114 shows the impact of low and high numbers of air freeze–thaw cycles on JPCP fatigue cracking for low- and high-trafficked projects. The graphs show nearly identical results to the impact of freeze and nonfreeze climates on JPCP fatigue cracking.

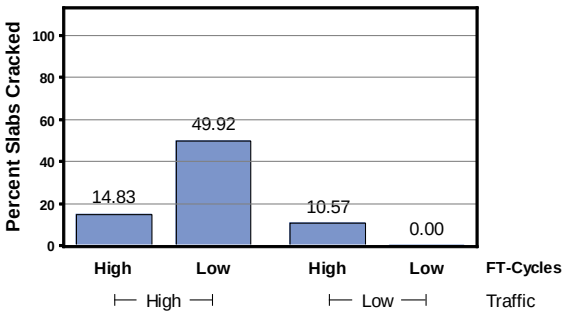

Source: FHWA.

A. Thin JPCPs.

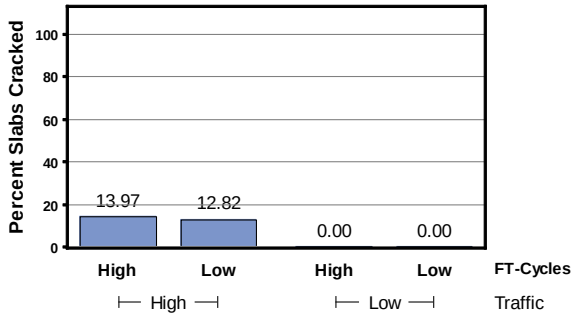

Source: FHWA.

B. Thick JPCPs.

Figure 114. Graphs. Impact of low and high numbers of air freeze–thaw cycles on JPCP fatigue cracking for low- and high-trafficked projects.

Impact of Frost Depth

Figure 115 shows the impact of low and high frost depth on JPCP fatigue cracking for low- and high-trafficked projects.

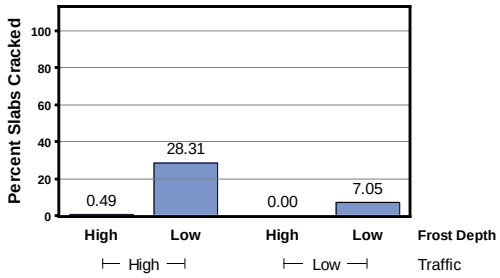

Source: FHWA.

A. Thin JPCPs.

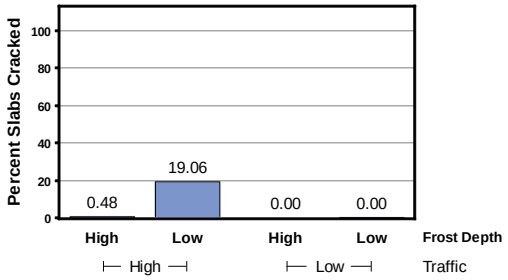

Source: FHWA

B. Thick JPCPs.

Figure 115. Graphs. Impact of low and high frost depth on JPCP fatigue cracking for low- and high-trafficked projects.

Figure 115 shows the following:

- In the absence of heavy traffic loads, fatigue cracking averaged less than 2 percent of slabs after 15 yr. For the low-trafficked projects with thin JPCP sections, high frost penetration resulted in lower levels of fatigue cracking. Projects in warmer climates with higher temperatures and lower frost penetration exhibited higher levels of fatigue cracking. For thicker JPCPs subjected to low traffic and similar foundation and climate conditions, fatigue cracking was 0 percent. This implies that thickness helped mitigate fatigue cracking.

- For the high-trafficked projects, colder regions with higher frost penetration exhibited lower levels of fatigue cracking (less than 1 percent) after 15 yr. For projects in warmer climates, higher levels of fatigue cracking were exhibited (greater than 20 percent), with the thicker JPCP sections exhibiting less cracking than the thinner sections.

- Pavements in cold climates had lower thermal gradients and moisture gradients, which contributed to less slab fatigue damage and cracking. Warmer climates typically developed much higher thermal and moisture gradients and thus accumulated higher fatigue damage at the top of the slabs.

Impact of In Situ JPCP Slab Temperature

Figure 116 shows the impact of low and high in situ JPCP temperature on JPCP fatigue cracking for low- and high-trafficked projects. This parameter was calculated over many years as the mean annual temperature of the JPCP slab.

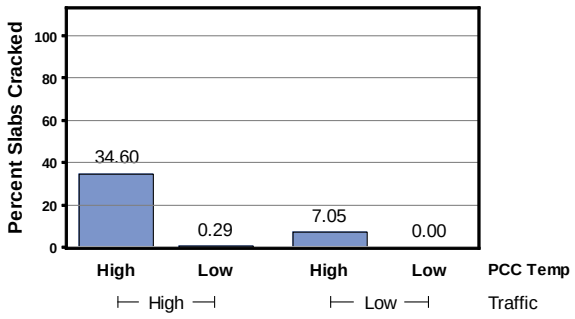

Source: FHWA.

A. Thin JPCPs.

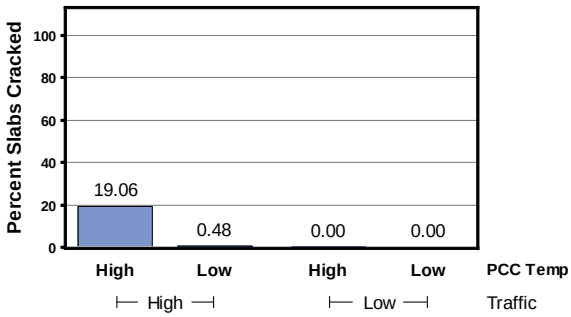

Source: FHWA.

B. Thick JPCPs.

Figure 116. Graphs. Impact of low and high in situ JPCP temperature on JPCP fatigue cracking for low- and high-trafficked projects.

Figure 116 shows the following:

- For low-trafficked projects, thin JPCP sections exhibited 7 percent fatigue cracking when located in regions with higher in situ JPCP slab temperature. Similar projects located in lower in situ PCC temperature climates showed 0 percent fatigue cracking. Thicker slab JPCP sections similarly exhibited 0 percent fatigue cracking.

- High-trafficked JPCP with higher in situ JPCP slab temperatures (warmer climates) exhibited higher fatigue cracking levels. The thinner PCC sections exhibited 35 percent fatigue cracking and the thicker slab JPCP sections experienced 19 percent fatigue cracking. For similar projects with lower in situ slab JPCP temperatures (colder climates), fatigue cracking was 0 percent.

These results again show that thickness had a mitigating effect on fatigue cracking of JPCP.

Impact of Annual Precipitation

Figure 117 shows the impact of rainfall in dry and wet environments on JPCP fatigue cracking for low- and high-trafficked projects.

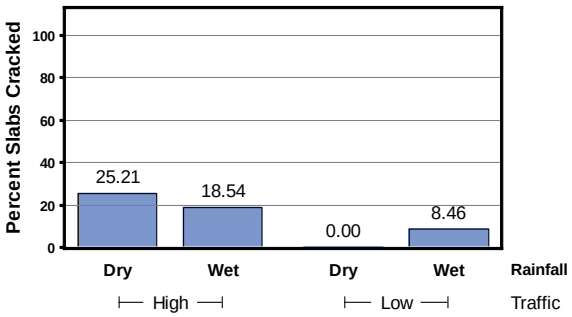

Source: FHWA.

A. Thin JPCPs.

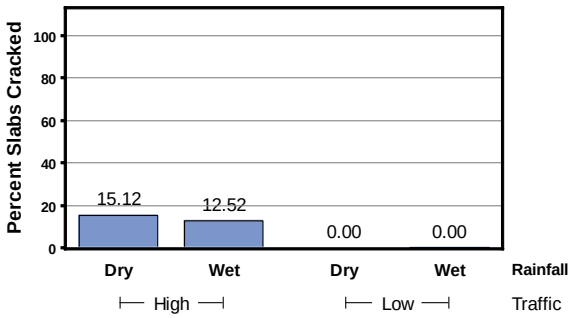

Source: FHWA.

B. Thick JPCPs.

Figure 117. Graphs. Impact of rainfall in dry and wet environments on JPCP fatigue cracking for low- and high-trafficked projects.

Figure 117 shows the following:

- In the absence of heavy traffic loads, fatigue cracking averaged just over 2 percent of slabs after 15 yr. Rainfall had no impact for thick JPCP, as the fatigue cracking in both dry and wet climates was 0 percent. High rainfall climates averaged 8 percent compared to 0 percent for low rainfall climates.

- For the high-trafficked projects, the amount of cracking exhibited after 15 yr in service was much higher (i.e., 12 to 25 percent of slabs were cracked). JPCP cracking in dry climates was consistently higher than in wet climates for both thick and thin slabs. Dry climates had much greater thermal and moisture gradients than wet climates, which in combination with traffic loads, contributed to fatigue cracking.

Impact of Base and Subgrade In Situ Moisture Content

Figure 118 shows the impact of low and high base and subgrade in situ moisture content on JPCP fatigue cracking for low- and high-trafficked projects.

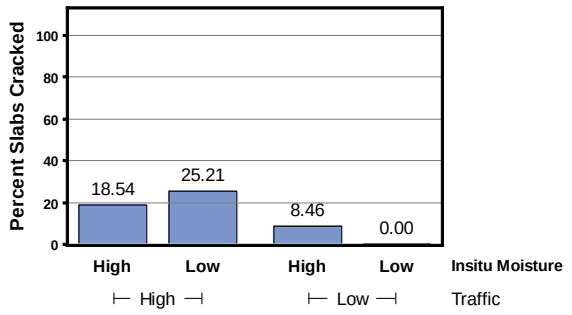

Source: FHWA.

A. Thin JPCPs.

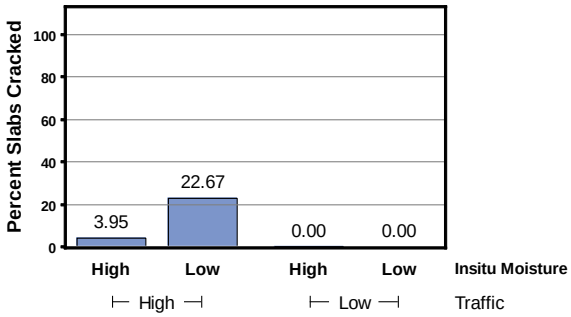

Source: FHWA.

B. Thick JPCPs.

Figure 118. Graphs. Impact of low and high base and subgrade in situ moisture content on JPCP fatigue cracking for low- and high-trafficked projects.

Figure 118 shows the following:

- In the absence of heavy traffic loads, fatigue cracking averaged less than 3 percent of slabs after 15 yr. For the thin JPCP sections, projects with high base and subgrade in situ moisture content exhibited higher levels of fatigue cracking. There was no cracking for thicker JPCP sections.

- For the high-trafficked projects, the amount of cracking exhibited after 15 yr in service ranged from 4 to 25 percent. In general, projects constructed in regions with higher in situ base and subgrade moisture contents exhibited lower levels of fatigue cracking over thin and thick slabs. Reasons for this may be related to differences in moisture gradients through the slab—the drier the climate, the greater the upward curl of the slab much of the time. This saucer shape led to increased potential for top–down fatigue cracking under loading.

Impact of Subgrade Type

Figure 119 shows the impact of subgrade type (i.e., fine or coarse) on JPCP fatigue cracking for low- and high-trafficked projects.

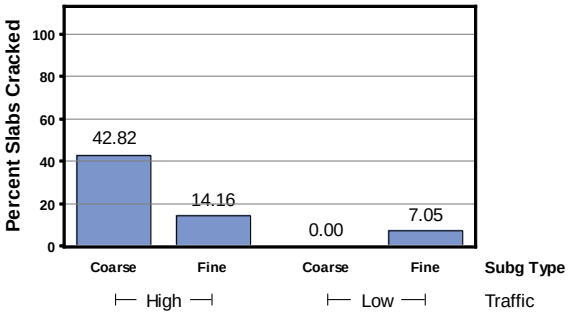

Source: FHWA

A. Thin JPCPs.

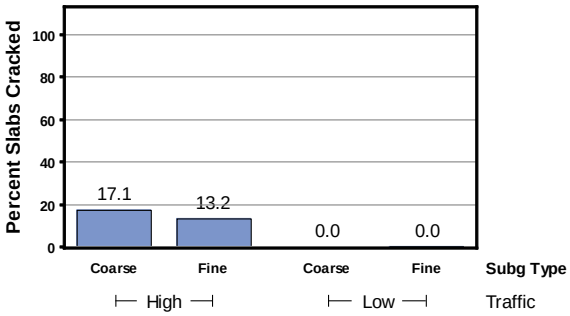

Source: FHWA

B. Thick JPCPs.

Figure 119. Graphs. Impact of subgrade type on JPCP fatigue cracking for low- and high-trafficked projects.

Figure 119 shows show the following:

- In the absence of high traffic loads, fatigue cracking averaged less than 2 percent of slabs after 15 yr. Subgrade type had little impact on fatigue cracking over this period.

- For the high-trafficked projects, the amount of cracking exhibited after 15 yr in service was high (greater than 10 percent slabs cracked) regardless of subgrade type. Pavements constructed over coarse subgrades exhibited higher levels of cracking for both thin and thick JPCP sections. In all cases, thicker JPCP sections exhibited lower cracking levels.

Impact of Subgrade Clay Content

Figure 120 shows the impact of low and high subgrade clay content on JPCP fatigue cracking for low- and high-trafficked projects.

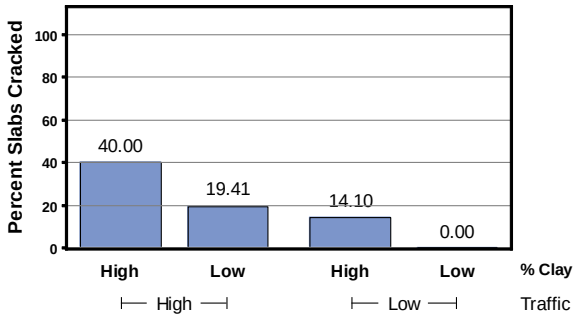

Source: FHWA.

A. Thin JPCPs.

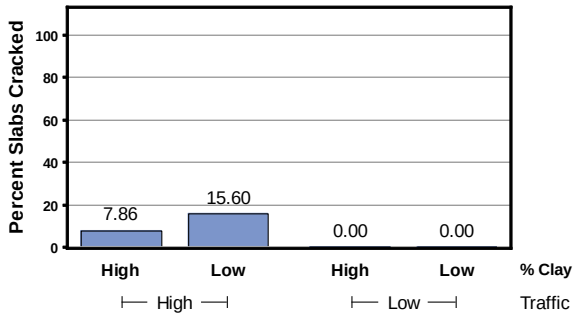

Source: FHWA.

B. Thick JPCPs.

Figure 120. Graphs. Impact of low and high subgrade clay content on JPCP fatigue cracking for low- and high-trafficked projects.

Figure 120 shows the following:

- In the absence of high-traffic loads, fatigue cracking averaged less than 4 percent of slabs after 15 yr. For the thin JPCP sections, projects constructed over foundations with higher subgrade clay content exhibited higher levels of fatigue cracking (14 versus 0 percent). For thicker JPCP sections, fatigue cracking was 0 percent after 15 yr in service.

- For the high-trafficked projects with thin JPCP sections, those constructed over foundations with higher subgrade clay content exhibited significantly higher levels of fatigue cracking after 15 yr in service (40 versus 19 percent). Similar pavements over foundations with lower clay content exhibited half the value observed for high clay content foundations.

- Increasing JPCP thickness significantly reduced observed fatigue cracking.

Impact of Subgrade Silt Content

Figure 121 shows the impact of low and high subgrade silt content on JPCP fatigue cracking for low- and high-trafficked projects.

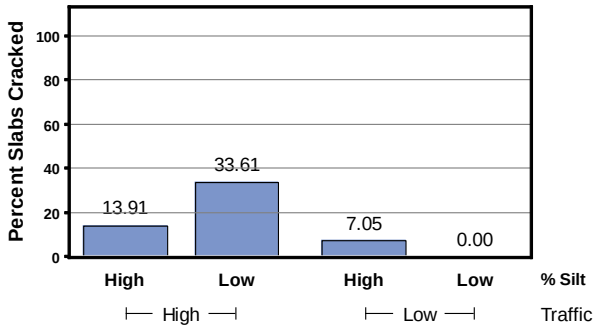

Source: FHWA.

A. Thin JPCPs.

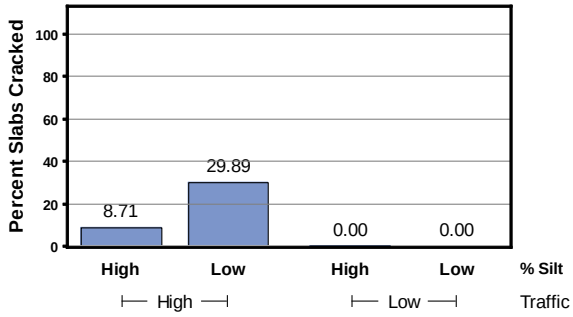

Source: FHWA.

B. Thick JPCPs.

Figure 121. Graphs. Impact of low and high subgrade silt content on JPCP fatigue cracking for low- and high-trafficked projects.

Figure 121 shows the following:

- In the absence of heavy traffic loads, fatigue cracking averaged less than 2 percent of slabs after 15 yr. For low-trafficked projects with thick JPCP sections, observed fatigue cracking was 0 percent.

- Higher amounts of fatigue cracking (greater than 10 percent) generally were observed on high-trafficked GPS-3/SPS-1 projects with thin or thick JPCP sections. For these projects, low foundation soil silt content resulted in higher fatigue cracking levels (perhaps because clay content was high for these sections).

- For high-trafficked non-SPS-8 projects with thick JPCP sections, observed fatigue cracking was lower than that observed for pavements with thin JPCP sections. Again, the projects constructed over foundation soils with low silt content exhibited higher levels of cracking (perhaps because clay content was high for these sections).

Impact of Subgrade Fine-Sand Content

Figure 122 shows the impact of low and high subgrade fine-sand content on JPCP fatigue cracking for low- and high-trafficked projects.

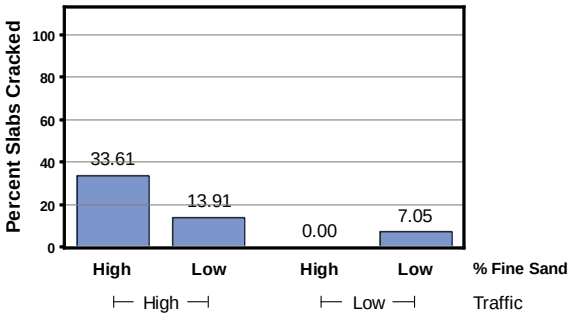

Source: FHWA.

A. Thin JPCPs.

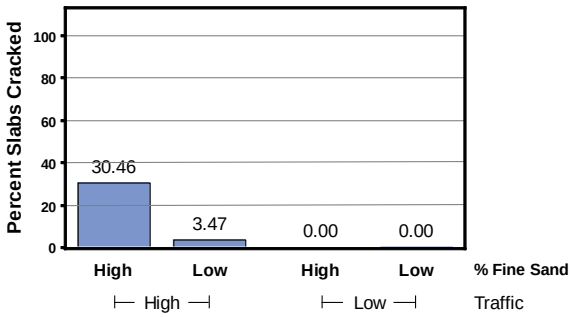

Source: FHWA.

B. Thick JPCPs.

Figure 122. Graphs. Impact of low and high subgrade fine-sand content on JPCP fatigue cracking for low- and high-trafficked projects.

Figure 122 shows the following:

- In the absence of heavy traffic loads, fatigue cracking averaged less than 2 percent of slabs after 15 yr. For low-trafficked projects with thick JPCP sections, observed fatigue cracking was 0 percent.

- For high-trafficked projects with thin JPCP sections, much greater amounts of fatigue cracking were observed (4 to 34 percent). For these projects, high-foundation soil fine-sand content resulted in higher fatigue cracking levels.

- For high-trafficked (i.e., non-SPS-8) projects with thick JPCP sections, observed fatigue cracking was lower than that observed for similar pavements with thin PCC sections. Again, the projects constructed over foundation soils with high foundation soil fine-sand content exhibited higher levels of cracking.

Impact of Subgrade PI

Figure 123 shows the impact of low and high subgrade PI on JPCP fatigue cracking for low- and high-trafficked projects.

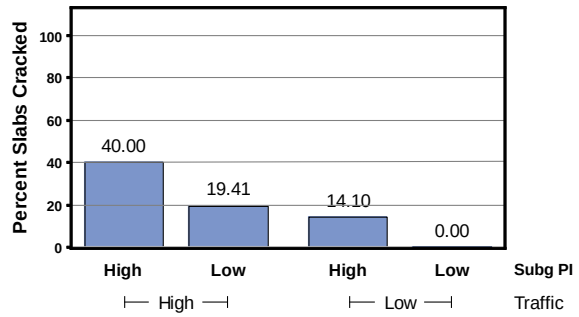

Source: FHWA

A. Thin JPCPs.

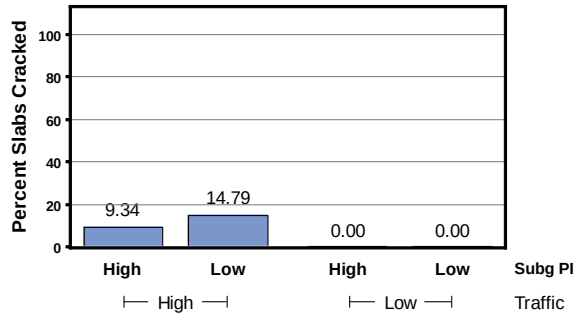

Source: FHWA

B. Thick JPCPs.

Figure 123. Graphs. Impact of low and high subgrade PI on JPCP fatigue cracking for low- and high-trafficked projects.

Figure 123 shows the following:

- In the absence of heavy traffic loads, fatigue cracking averaged less than 4 percent of slabs after 15 yr. For thin JPCP sections, the observed fatigue cracking was significant (14 percent) for pavements constructed over foundation soils with high PI. In the thick JPCP sections, observed fatigue cracking was 0 percent. This shows the impact of JPCP thickness on fatigue cracking and how increasing JPCP thickness helped mitigate the extent of cracking.

- For high-trafficked projects with thin JPCP sections, higher amounts of fatigue cracking were observed (9 to 40 percent). For these projects, high-foundation soil PI resulted in higher fatigue cracking levels.

- For high-trafficked projects with thick JPCP slabs, observed fatigue cracking was lower than that observed for similar pavements with thin JPCP sections. Fatigue cracking was much higher for thin slabs constructed over foundation soils with high foundation soil fine PI (40 percent for high PI versus 19 percent for low PI).

DETAILED STATISTICAL ANALYSIS TO CHARACTERIZE IMPACT OF ENVIRONMENTAL FACTORS ON JPCP FATIGUE CRACKING

GLMSELECT was used to determine the subset of environmental and other (e.g., traffic and slab thickness) variables that were most correlated to JPCP fatigue cracking. Once the variables were identified, ANOVA was performed to determine the significance of the identified variables (on JPCP fatigue cracking).

JPCP fatigue cracking was the dependent variable, while design, traffic, and environmental factors were the independent variables. Statistical model selection analysis was performed to determine the best subset of variables that impact and predict fatigue cracking after 15 yr in service. Determination of variables that most impact JPCP fatigue cracking was done separately for low-trafficked SPS-8 projects and then for combined low and heavily trafficked companion projects.

Results from statistical model selection analysis were compared to determine the following:

- Factors that affect the occurrence of JPCP fatigue cracking obtained from outcome of low-trafficked pavements analysis (SPS-8).

- Factors that affect the occurrence of JPCP fatigue cracking obtained from outcome of combined low- and high-trafficked pavements analysis.

The outcomes of the analysis were compared to determine JPCP fatigue cracking initiators (must be theoretically viable), aggravators, and impact on the distress.

Summary of GLMSELECT Results for Low-Trafficked JPCP

For the low-trafficked SPS-8 projects, no variable showed significance using GLMSELECT for fatigue cracking (figure 124). Fatigue cracking for such a low level of traffic was very low, averaging across all sections as less than 4 percent. No climate or temperature variable or slab thickness was found to be significant. This finding indicates that some other variable initiated fatigue cracking for JPCP.

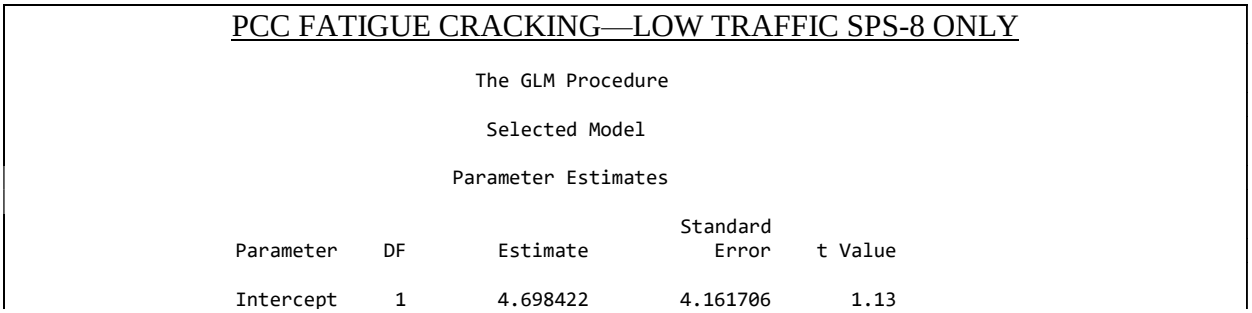

PCC FATIGUE CRACKING—LOW TRAFFIC SPS-8 ONLY

The GLM Procedure

Selected Model

Parameter Estimates

Parameter	DF	Estimate	Standard Error	t Value
Intercept	1	4.698422	4.161706	1.13

Source: FHWA.

Figure 124. Screenshot. Summary of GLMSELECT and ANOVA results for JPCP fatigue cracking for low-trafficked JPCP.

Summary of GLMSELECT and ANOVA Results for Combined Low- and High-Trafficked JPCP

A statistical ANOVA similar to that described for low-trafficked JPCP was done for all projects combined. All key factors for traffic, slab thickness, climate, and subgrade characteristics were considered. Several interactions of variables were also evaluated. The results of the analyses are presented in figure 125.

PCC FATIGUE CRACKING—ALL TRAFFIC SPS-8, SPS-2, GPS-3

The GLM Procedure

Dependent Variable: TC_CRK_NL

Source	DF	Sum of Squares	Mean Square	F Value	Pr > F
Model	5	9920.85080	1984.17016	4.53	0.0025
Error	37	16193.05189	437.65005		
Corrected Total	42	26113.90269			

R-Square	Coeff Var	Root MSE	TC_CRK_NL Mean
0.379907	164.7968	20.92009	12.69447

Source	DF	Type III SS	Mean Square	F Value	Pr > F
AADTT*/(RAIN*THICK)	2	4550.983335	2275.491668	5.20	0.0102
PCCTEMP/THICK	2	1900.890918	950.445459	2.17	0.1283
SOIL_TYPE	1	2139.619524	2139.619524	4.89	0.0333

Parameter		Estimate	Standard Error	t Value	Pr > |t|
Intercept		-26.7008154	20.8115309	-1.28	0.2075
AADTT/(RAIN*THKPC) Dry		6.2712584	2.3929543	2.62	0.0127
AADTT/(RAIN*THKPC) Wet		25.6083507	10.1539977	2.52	0.0161
PCCTEMP/THKPC	High	276.2085976	198.7992150	1.39	0.1730
PCCTEMP/THKPC	Low	152.4020382	200.9283414	0.76	0.4530
SOIL_TYPE	COARSE	17.7469704	8.0263749	2.21	0.0333
SOIL_TYPE	FINE	0.0000000	. . .		

Source: FHWA.

Figure 125. Screenshot. Summary of GLMSELECT and ANOVA results for testing whether there was a significant difference in PCC fatigue cracking for low- and high-trafficked JPCP.

Figure 125 shows the following:

- A three-way interaction between traffic, slab thickness, and annual rainfall was significant. The interaction implies that for certain combinations of these three variables, the amount of fatigue cracking became very high (high traffic, dry climate, and low thickness was 25 percent) or very low (low traffic, wet climate, and high thickness was 0 percent).

- As traffic increased, slab fatigue cracking increased. This is of course logical in that repeated bending stresses are known to create fatigue damage that lead to transverse, longitudinal, and corner cracking. The GPS-3 and SPS-2 projects exposed to significantly higher traffic levels did experience higher levels of the distress after 15 yr.

- As JPCP slab layer thickness increased, slab fatigue cracking decreased. An increase in slab thickness reduced bending stresses in a slab, which led to reduced fatigue cracking.

- The annual precipitation (rainfall) also has a significant effect on slab cracking. The lower the precipitation, the higher the slab cracking. Drier climates had much higher thermal and moisture gradients through the slab, which contributed to severe upward curling and top–down fatigue cracking under loading.

- A two-way interaction between thickness and in situ JPCP slab temperature was significant. As thickness increased, slab fatigue cracking decreased. As JPCP slab temperature increased, slab fatigue cracking increased. Warmer climates had higher thermal gradients and higher moisture gradients, which led to increased upward curling and high tensile stresses in combination with load increase fatigue cracking.

- Soil type, either fine- or coarse-grained, also showed significance. Surprisingly, the results show that coarse-grained soil subgrade resulted in significantly higher fatigue cracking. This result is difficult to explain mechanistically other than the fact that stiffer foundations caused higher thermal curling stresses that contributed to fatigue cracking.

Comparing the model selection procedure results for all projects and low-trafficked projects only indicate the following:

- Traffic was the main initiator of JPCP fatigue cracking. Theoretically, this is obviously true since repeated loading is required for fatigue cracking. The traffic load variable may not be showing its full impact due to the pavements being only 15 yr old and may show much more significant impacts on fatigue cracking over time.

- Significant contributors to fatigue cracking include slab thickness, annual precipitation, in situ JPCP slab temperature, and subgrade class (fine- or coarse-grained). All of these variables aggravated (increased or decreased) the progression of the fatigue cracking in the JPCP slabs.

- The condition surveys and analysis results show that the JPCP projects were in relatively good condition; thus, the trends observed are somewhat tentative. The full impact of design, traffic, and environmental factors will be more fully realized as the pavements are exposed to these site conditions for a longer time period.

ANALYSIS OF PCC FATIGUE-CRACKING DAMAGE

Estimating the proportion of overall JPCP fatigue-cracking damage due to environmental factors required the following:

- The overall fatigue-cracking damage of a selection of JPCPs subjected to normal heavy traffic loadings (GPS-3 and SPS-2 companion sections) and environmental factors.

- The fatigue-cracking damage of similar thickness and materials JPCPs subjected to low traffic loadings and similar environmental factors (SPS-8 projects). All of these pavements had less than 5 percent fatigue cracking and were considered well within the standard error of measurement. The low level of traffic loadings for the SPS-8 projects is so low that, theoretically, it should not cause any fatigue cracking, and this was indeed what was observed in the field by LTPP inspection teams.

The impact of various design and environmental factors on fatigue damage was also assessed.

Proportion of Overall Fatigue-Cracking Damage Caused by Environmental Factors

Table 44 presents a summary of overall mean fatigue-cracking damage (GPS-3/SPS-2 companion projects) and fatigue-cracking damage due to environmental factors alone (SPS-8 projects) for thin and thick JPCP. On average, the overall fatigue-cracking damage was 33.9 percent. For the low-trafficked SPS-8 projects, fatigue-cracking damage on average was 2.8 percent. Thus, on average, the proportion of PCC fatigue damage ascribed to environmental conditions was 2.8/33.9 = 8.3 percent.

Table 44. Impact of JPCP thickness on JPCP fatigue-cracking damage.

JPCP Thickness	Overall Fatigue-Cracking Damage (SPS-2 and GPS-3) (%)	Fatigue Cracking-Damage due to Environmental Factors (SPS-8) (%)	Overall Damage due to Environmental Factors (%)
Thin	52.4	4.5	8.6
Thick	21.5	0	0.0
Mean	33.9	2.8	8.3

The results in this table show that while total damage due to environmental factors was 8.3 percent for all thicknesses, it was nearly all caused in the thinner slabs as there was no fatigue cracking for thick slabs. This makes sense theoretically, since fatigue damage in thick slabs is much lower than in thinner slabs.

The proportion of fatigue-cracking damage associated with environmental factors (e.g., subgrade characteristics such as percent fine-sand and moisture content, precipitation, freeze index, and freeze–thaw cycles) to that associated with all causes, including traffic loading and the same environmental factors, was approximately 8.3 percent. This is not a high value because fatigue crack initiation is caused only by repeated loadings, but then its propagation is affected by environmental factors to this extent.

Impact of Design and Environmental Factors on Overall Fatigue-Cracking Damage

Table 45 and table 46 present the impact of environmental factors on JPCP fatigue-cracking damage.

Table 45. Impact of environmental factors (climate variables) on JPCP fatigue-cracking damage.

Environmental Factor	Overall Fatigue-Cracking Damage (GPS-3 and SPS-2) (%)	Fatigue-Cracking Damage due to Environmental Factors (SPS-8) (%)	Overall Damage due to Environmental Factors (%)
Dry	19.6	0	0.0
Wet	14.6	0.6	4.1
Freeze	14.5	0.9	6.2
Nonfreeze	24.9	0	0.0

Table 46. Impact of environmental factors (subgrade properties) on JPCP fatigue-cracking damage.

Environmental Factor	Overall Fatigue-Cracking Damage (GPS-3 and SPS-2) (%)	Fatigue-Cracking Damage due to Environmental Factors (SPS-8) (%)	Overall Damage due to Environmental Factors (%)
Fine-grained (high PI) soils	19.6	1.5	7.7
Others (low PI soils and coarse-grained materials)	16.7	0	0.0

The results presented in the tables indicate the following for fatigue cracking:

- The proportion of environmental damage for dry and nonfreeze climates was 0 percent.
- The proportion of environmental damage was highest for freeze climates (6.2 percent), followed by wet climates (4.1 percent).
- The proportion of damage due to environmental factors for projects constructed over fine soils with high PI was 7.7 percent. For other soil types, proportion of damage due to environmental factors was approximately 0 percent.

CHAPTER 12. ANALYSIS OF TRANSVERSE JOINT FAULTING DISTRESS FOR SPS-8 AND COMPANION JPCP PROJECTS

This chapter presents the results of the preliminary and detailed analysis of joint faulting performance for the low- and high-trafficked JPCP. Transverse joint faulting was characterized using the mean of joints measured 12 inches from the slab edge (approximate wheel path). It must be noted that all of the projects evaluated were doweled. Dowel diameter ranged from 1 to 1.5 inches. The dowel diameter correlated with JPCP thickness, with the thicker 11-inch JPCP slabs mostly having the 1.5-inch dowels. Some projects had relatively smaller dowels for thicker slabs. Joint spacing for the projects evaluated ranged from 13.5 to 15 ft, with 15 ft being the predominant joint spacing for the regular SPS-2 and SPS-8 JPCP projects.

PRELIMINARY ANALYSIS TO CHARACTERIZE IMPACT OF ENVIRONMENTAL FACTORS ON TRANSVERSE JOINT FAULTING

A visual presentation of the faulting data results in the form of bar charts is presented followed by a statistical ANOVA. Note that all of the joints for these JPCPs were doweled.

Impact of Freeze and Nonfreeze Climates

Figure 126 shows the impact of freeze and nonfreeze climates on JPCP transverse joint faulting for low- and high-trafficked projects.

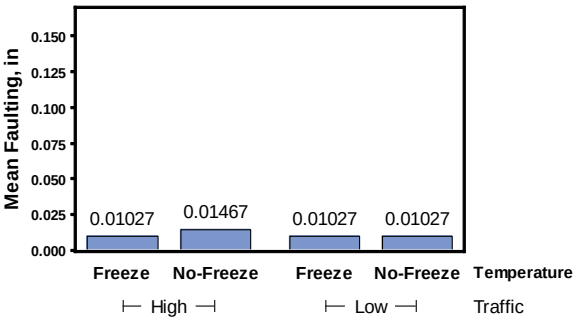

Source: FHWA.

A. Thin JPCPs.

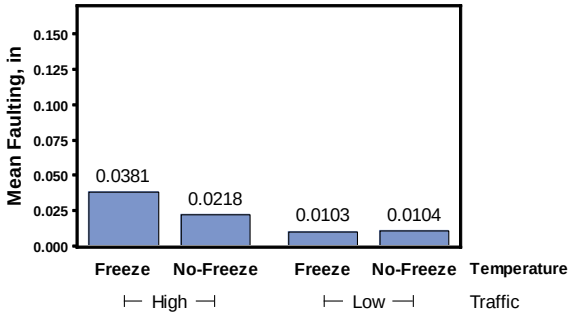

Source: FHWA.

B. Thick JPCPs.

Figure 126. Graphs. Impact of freeze and nonfreeze climates on JPCP transverse joint faulting for low- and high-trafficked projects.

Figure 126 shows the following:

- In the absence of heavy traffic loads, transverse joint faulting was less than 0.011 inch, which was insignificant. This amount of faulting after 15 yr in service was very low and indicates that ambient temperature (freeze and nonfreeze) alone is not an initiator for transverse joint faulting.

- Once heavy traffic was applied to the pavement, transverse joint faulting levels increased slightly, ranging from approximately 0.01 to 0.04 inch. These values are quite insignificant at 15 yr (meaning that this level of faulting did not affect smoothness very much). Thick JPCP sections with high-traffic application showed that projects located in nonfreeze climates exhibited less faulting than those in freeze climates.

Impact of Freeze–Thaw Cycles

Figure 127 shows the impact of low and high numbers of air freeze–thaw cycles on JPCP transverse joint faulting for low- and high-trafficked projects. The results are similar those found for freeze and nonfreeze climates. This was as expected as freeze–thaw cycles are very well correlated with freeze and nonfreeze climate zones.

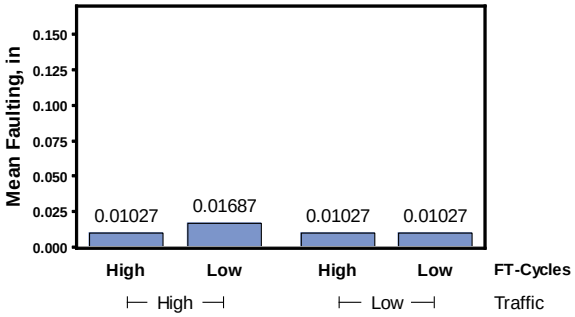

Source: FHWA.

A. Thin JPCPs.

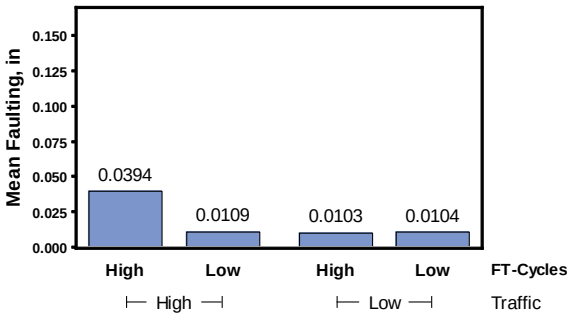

Source: FHWA.

B. Thick JPCPs.

Figure 127. Graphs. Impact of low and high numbers of air freeze–thaw cycles on JPCP transverse joint faulting for low- and high-trafficked projects.

Impact of Frost Depth

Figure 128 shows the impact of low and high frost depth on JPCP transverse joint faulting for low- and high-trafficked projects.

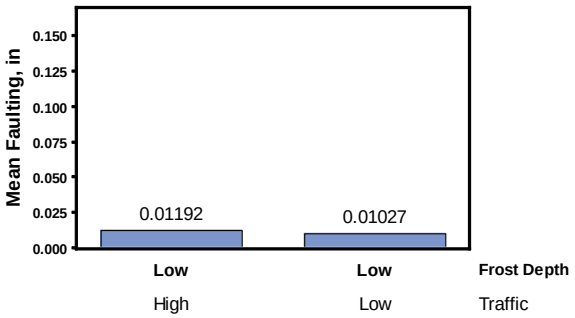

Source: FHWA.

A. Thin JPCPs.

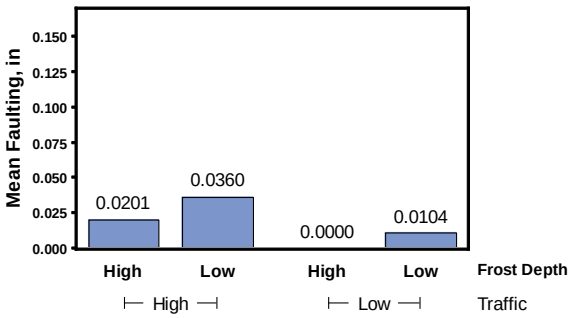

Source: FHWA.

B. Thick JPCPs.

Figure 128. Graphs. Impact of low and high frost depth on JPCP transverse joint faulting for low- and high-trafficked projects.

Figure 128 shows the following:

- For the low-trafficked projects, no comparisons were made for thin JPCP sections, as there were insufficient data (missing project cells). For the thicker JPCP sections, low-trafficked projects showed insignificant faulting.

- High-trafficked projects showed that pavements in climates with higher frost penetration exhibited lower levels of transverse joint faulting. Higher levels of frost penetration may indicate that moisture beneath the slab will be frozen for much of the winter, reducing the amount of pumping and erosion. Slab curling will also be less in low frost (warmer) areas due to reduced thermal and moisture gradients.

Impact of In Situ Slab JPCP Temperature

Figure 129 shows the impact of low and high in situ JPCP temperature on JPCP fatigue cracking for low- and high-trafficked projects. For low-traffic SPS-8 projects, no comparisons were made for thin JPCP sections as there were insufficient data. Higher in situ JPCP temperatures resulted in higher levels of transverse joint faulting for both low- and high-trafficked projects with thicker JPCP sections. This is similar to the results observed for frost depth.

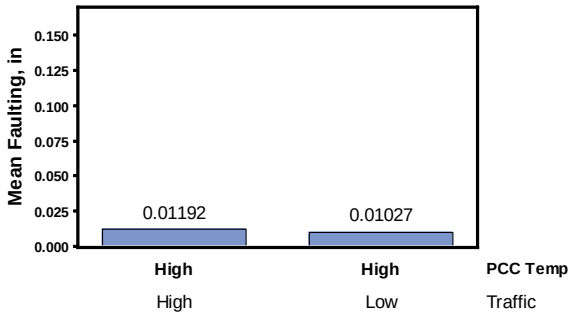

Source: FHWA.

A. Thin JPCPs.

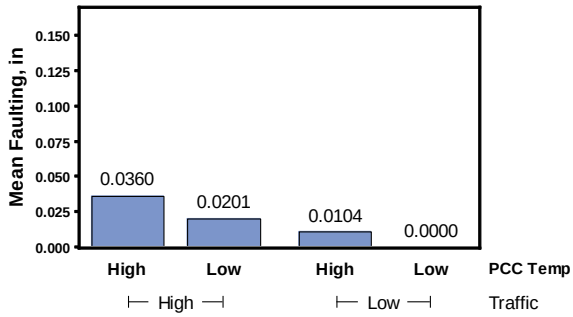

Source: FHWA.

B. Thick JPCPs.

Figure 129. Graphs. Impact of low and high in situ JPCP temperature on JPCP transverse joint faulting for low- and high-trafficked projects.

Impact of Annual Precipitation

Figure 130 shows the impact of rainfall and dry and wet environments on JPCP joint faulting for low- and high-trafficked projects.

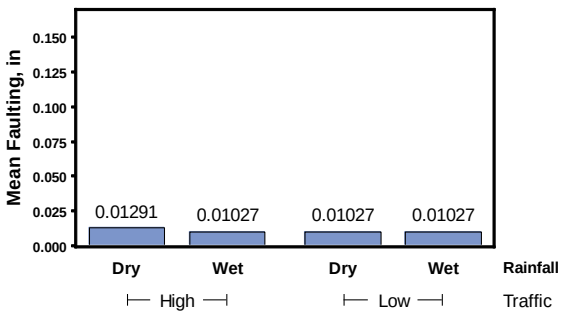

Source: FHWA.

A. Thin JPCPs.

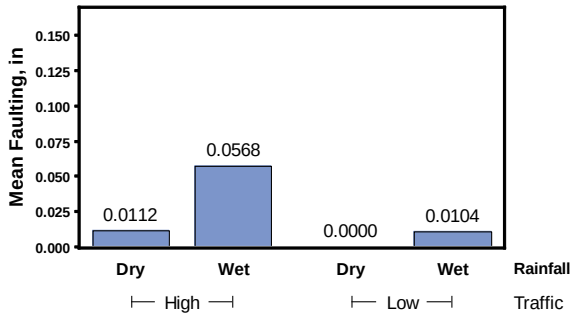

Source: FHWA.

B. Thick JPCPs.

Figure 130. Graphs. Impact of rainfall in dry and wet environments on JPCP transverse joint faulting for low- and high-trafficked projects.

Figure 130 shows the following:

- For the low-trafficked projects, rainfall had no impact on the development and progression of transverse cracking. After 15 yr in service, measured joint faulting was approximately 0.01 inch.

- For the high-trafficked projects, the amount of transverse joint faulting exhibited after 15 yr in service for the thin JPCP sections was very low. For the thicker JPCP sections, however, projects located in wet climates exhibited more transverse joint faulting distress. The presence of free water and moisture in the underlying base and subgrade was a key contributor to transverse joint faulting. Thus, this trend was as expected.

Impact of GWT Depth

Figure 131 shows the impact of GWT depth (deep or shallow) on JPCP transverse joint faulting for low- and high-trafficked projects. A deep GWT depth implies the GWT is more than 40 ft below the pavement surface and, thus, the base and subgrade material moisture content will not be impacted by groundwater.

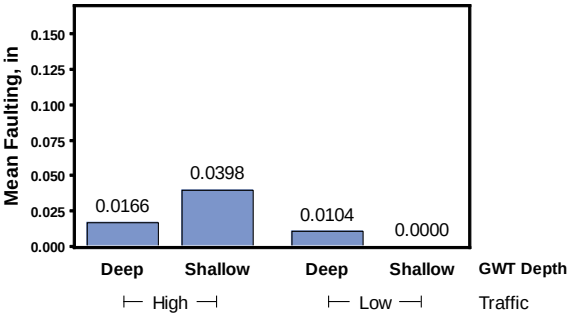

Source: FHWA.

A. Thin JPCPs.

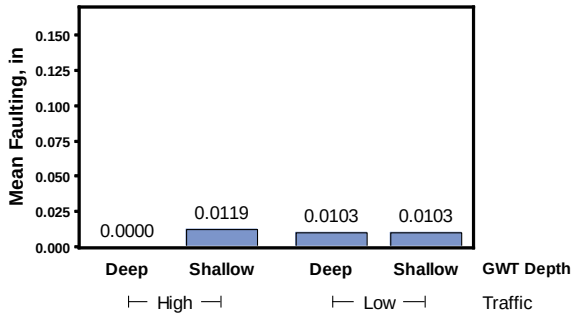

Source: FHWA.

B. Thick JPCPs.

Figure 131. Graphs. Impact of depth to GWT on JPCP transverse joint faulting for low- and high-trafficked projects.

For projects constructed over shallow GWTs, groundwater may periodically permeate the pavement foundation and underlying layers raising base and subgrade moisture contents. The results in the graphs indicate the following:

- For low-traffic projects, transverse joint faulting was insignificant.
- For projects with high traffic, more transverse joint faulting was observed on sections with thicker JPCP, high-traffic applications, and shallow GWT. As noted earlier, the presence of free water in the pavement base or subgrade is a key contributor to transverse joint faulting, so this trend was as expected.

Impact of Subgrade Type

Figure 132 shows the impact of subgrade type (i.e., fine or coarse) on JPCP transverse joint faulting for low- and high-trafficked projects.

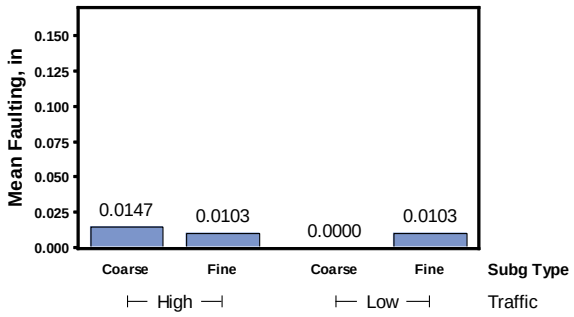

Source: FHWA

A. Thin JPCPs.

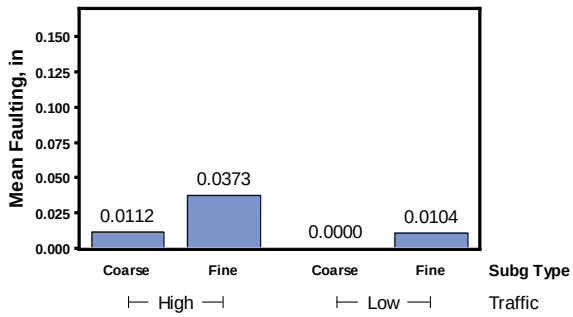

Source: FHWA

B. Thick JPCPs.

Figure 132. Graphs. Impact of subgrade type on JPCP transverse joint faulting for low- and high-trafficked projects.

Figure 132 shows the following:

- For the low-trafficked projects, subgrade type had little impact on the development and progression of transverse joint faulting. After 15 yr in service, measured mean transverse joint faulting was approximately 0.01 inch.
- For the high-trafficked projects, the amount of transverse joint faulting exhibited on thin JPCP sections after 15 yr in service was insignificant. For the thicker JPCP sections, projects constructed over fine subgrades exhibited the highest levels of transverse joint faulting (probably from higher traffic). The presence of fines in the underlying base or subgrade is a key contributor to transverse joint faulting, so this trend is as expected.

Impact of Subgrade Clay, Silt, and Fine-Sand Contents

As shown in figure 132, subgrades with high fine content exhibited higher levels of transverse joint faulting after 15 yr in service for low- and high-trafficked projects. Subgrade material fines can be plastic (clayey) or nonplastic (silty/sandy). Figure 133 through figure 135 were used to

investigate the types of fines that impact JPCP transverse joint faulting for low- and high-trafficked projects.

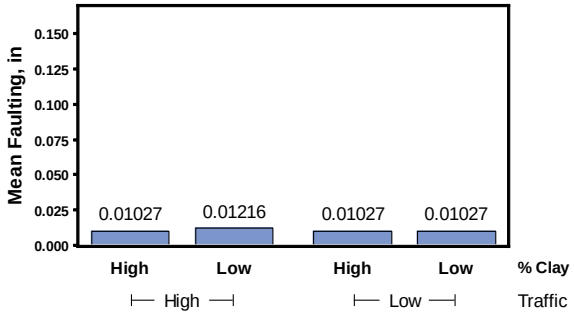

Source: FHWA.

A. Thin JPCPs.

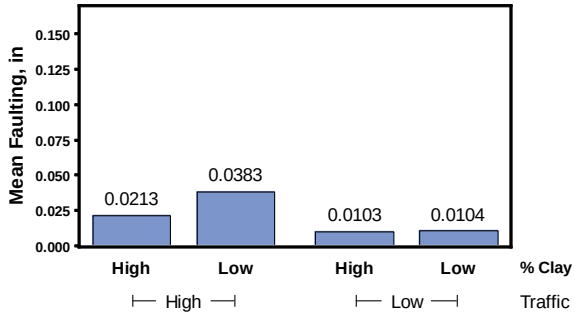

Source: FHWA.

B. Thick JPCPs.

Figure 133. Graphs. Impact of low and high subgrade clay content on JPCP transverse joint faulting for low- and high-trafficked projects.

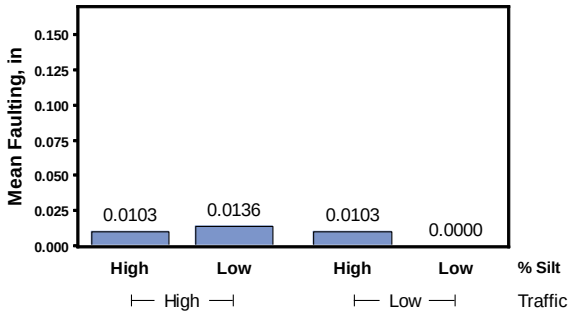

Source: FHWA.

A. Thin JPCPs.

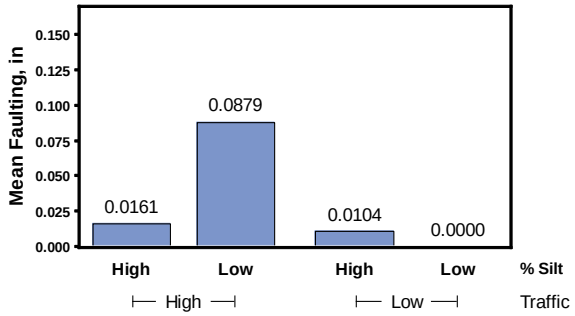

Source: FHWA.

B. Thick JPCPs.

Figure 134. Graphs. Impact of low and high subgrade silt content on JPCP transverse joint faulting for low- and high-trafficked projects.

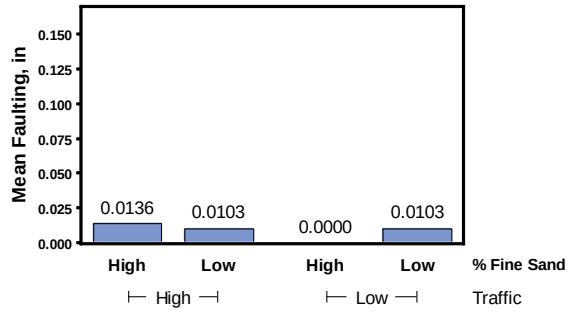

Source: FHWA.

A. Thin JPCPs.

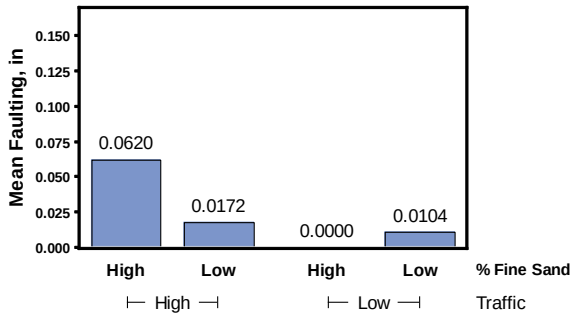

Source: FHWA.

B. Thick JPCPs.

Figure 135. Graphs. Impact of low and high subgrade fine-sand content on JPCP transverse joint faulting for low- and high-trafficked projects.

Figure 133 through figure 135 indicate the following:

- For the low-trafficked projects, subgrade fine-sand content had no impact on the development and progression of transverse joint faulting. After 15 yr in service, measured mean transverse joint faulting was approximately 0.01 inch.

- For the high-trafficked projects, the amount of transverse joint faulting exhibited after 15 yr in service for thin JPCP section was also very low.

- For the thick JPCP sections, projects constructed over fine subgrades with low clay content, low silt content, and high fine-sand content exhibited the highest levels of transverse joint faulting. The differences, however, were insignificant from a practical standpoint.

Impact of Subgrade PI

The trends observed in figure 133 through figure 135 are similar to those presented in figure 136. For the thicker JPCP sections, projects constructed over fine subgrades with low subgrade PI exhibited the highest levels of transverse joint faulting. However, the differences were small.

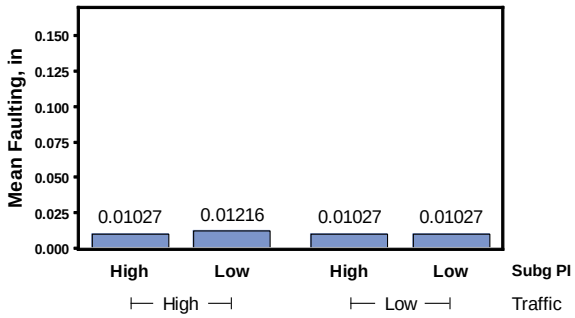

Source: FHWA.

A. Thin JPCPs.

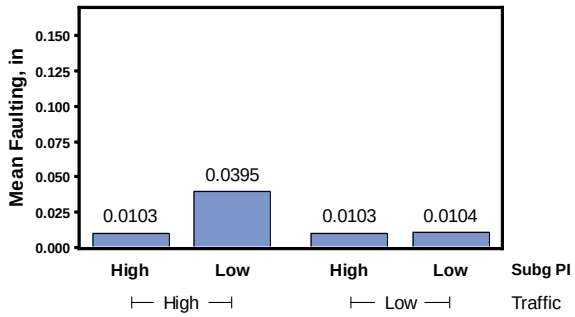

Source: FHWA.

B. Thick JPCPs.

Figure 136. Graphs. Impact of low and high subgrade PI on JPCP joint faulting for low- and high-trafficked projects.

DETAILED STATISTICAL ANALYSIS TO CHARACTERIZE IMPACT OF ENVIRONMENTAL FACTORS ON JPCP TRANSVERSE JOINT FAULTING

Statistical analysis like the one described in chapter 11 was performed with mean transverse joint faulting as the dependent variable.

Summary of GLMSELECT Results for SPS-8 Low-Trafficked JPCP

The only variable selected as significant using GLMSELECT was JPCP thickness for JPCP transverse joint faulting (figure 137).

GLMSELECT (Stepwise Selection Summary)

The GLMSELECT Procedure

Parameter Estimates

Parameter		DF	Estimate	Standard Error	t Value
Intercept		1	0.010352	0.000034728	298.09
THKCLASS	PCCTHIN	1	-0.000077654	0.000041091	-1.89
THKCLASS	PCCTHK	0	0	.	.

Source: FHWA.

Figure 137. Screenshot. Summary of GLMSELECT results for JPCP transverse joint faulting for SPS-8 low-trafficked JPCP.

Increasing PCC thickness (dowel diameter also increased with thickness for these JPCP) resulted in a very small increased JPCP transverse joint faulting (−0.000077-inch difference). Given the low levels of faulting on all sections, even though thickness indicated significance, the relative magnitude was very small. While this result was statistically significant, the magnitude of difference in faulting between thicker and thinner JPCP was essentially 0.

Summary of GLMSELECT and ANOVA Results for Low- and High-Trafficked JPCP

A statistical ANOVA similar to that described for low-trafficked JPCP was done for all projects combined. All key factors for traffic, slab thickness, climate, and subgrade characteristics were considered. Two- and three-way interactions of variables were also evaluated. The results of the analyses are presented in figure 138.

PCC FATIGUE FAULTING—ALL TRAFFIC SPS-8, SPS-2, GPS-3

The GLM Procedure

Dependent Variable: AVGFLT_L

Source	DF	Sum of Squares	Mean Square	F Value	Pr > F
Model	5	0.00198518	0.00039704	54.78	<.0001
Error	24	0.00017395	0.00000725		
Corrected Total	29	0.00215913			

R-Square	Coeff Var	Root MSE	AVGFLT_L Mean
0.919434	20.55623	0.002692	0.013097

Source	DF	Type III SS	Mean Square	F Value	Pr > F
AADTT*JTSP*THICK	2	0.00005500	0.00002750	3.79	0.0370
CLAY	1	0.00178809	0.00178809	246.70	<.0001
PI	1	0.00166826	0.00166826	230.17	<.0001
FROSTDEPTH	1	0.00016152	0.00016152	22.29	<.0001

Parameter		Estimate	Standard Error	t Value	Pr > |t|
Intercept		0.0103380756	0.00080706	12.81	<.0001
AADTT*JTSP*THICK	PCCTHIN	0.0000138397	0.00000503	2.75	0.0112
AADTT*JTSP*THICK	PCCTHICK	0.0000017266	0.00000310	0.56	0.5824
CLAY	High	0.0437800903	0.00278736	15.71	<.0001
CLAY	Low	0.0000000000	. . .		
PI	High	-0.0441785128	0.00291199	-15.17	<.0001
PI	Low	0.0000000000	. . .		
FROSTDEPTH	High	0.0095842010	0.00203025	4.72	<.0001
FROSTDEPTH	Low	0.0000000000	. . .		

Source: FHWA.

Figure 138. Screenshot. Summary of GLMSELECT and ANOVA results for transverse joint faulting for low- and high-trafficked JPCP.

The results in figure 137 and figure 138 indicate the following:

- Truck-traffic level appeared to be the initiator of joint faulting. This is logical since faulting cannot occur without heavy traffic loadings, as demonstrated by the nearly zero faulting for the low-trafficked SPS-8 sections. The GPS-3 and SPS-2 projects exposed to significantly higher traffic levels experienced higher levels of joint faulting. However, the faulting of a vast majority of doweled joints was relatively insignificant because the dowel diameters and spacings were appropriate for the site conditions.

- Increased joint spacing resulted in increased faulting. This is a well-known result due to larger joint openings for longer joint spacings.

- Increased slab thickness showed slightly increased faulting. This result can only be explained by noting that thicker slabs had much higher truck traffic and that some of the dowels were not of sufficient diameter to handle the heavy steel/concrete bearing stress. If dowels are properly sized to the slab thickness, joint faulting should be less for thicker than thinner slabs.

- Projects with higher subgrade clay content showed higher joint faulting.

- Projects with deeper frost penetration exhibited higher faulting. Colder climates have always contributed to higher joint faulting due to greater opening of joints and loss of load transfer.

ANALYSIS OF JPCP TRANSVERSE JOINT FAULTING DAMAGE

Estimating the proportion of overall JPCP transverse joint faulting damage due to environmental factors required the following:

- The overall JPCP transverse joint faulting damage of a selection of JPCP subjected to normal heavy traffic loadings (GPS-3 and SPS-2 companion sections) and environmental factors.

- The JPCP transverse joint faulting damage of similar thickness and materials for JPCP subjected to low traffic loadings and similar environmental factors (SPS-8 projects). All of these pavements had less than 0.1 inch of transverse joint faulting and were considered well within the standard error of measurement.

The impact of various design and environmental factors on JPCP transverse joint faulting damage was also assessed.

Proportion of Overall JPCP Transverse Joint Faulting Damage Caused by Environmental Factors

Table 47 presents a summary of overall mean JPCP transverse joint faulting damage (GPS-3 and SPS-2 companion projects) and JPCP transverse joint faulting damage due to environmental factors alone (SPS-8 projects) for thin and thick JPCPs. The proportion of overall transverse joint faulting damage attributable to environmental factors for thin JPCPs was approximately 85 percent. For thick JPCPs, the proportion of damage due to environmental factors was 39.4 percent. On average, the overall fatigue-cracking damage was 46.8 percent of lane area. For the low-trafficked pavements, fatigue-cracking damage on average was 5.1 percent, while for the high-trafficked projects, damage was 10.9 percent.

Thus, on average, the amount of JPCP transverse joint faulting damage for the heavily trafficked GPS-3 and SPS-2 projects was 10.9 percent. JPCP exposed to low levels of truck traffic (SPS-8) and similar climatic conditions exhibited transverse joint faulting damage of only 5.1 percent. Thus, the proportion of transverse joint faulting damage ascribed to environmental conditions was 5.1/10.9 = 46.8 percent after 15 yr of service.

Table 47. Impact of JPCP thickness on JPCP transverse joint faulting damage.

JPCP Thickness	Overall Faulting Damage (SPS-2 and GPS-3) (%)	Faulting Damage due to Environmental Factors (SPS-8) (%)	Overall Damage due to Environmental Factors (%)
Thin	6	5.1	85.0
Thick	13.2	5.2	39.4
Mean	10.9	5.1	46.8

In general terms, it can be said that the total faulting damage for these projects was 10.9 percent from traffic and environmental factors. The proportion of joint faulting damage associated with only environmental factors to that associated with all causes, including loading and the same environmental factors, was approximately 5.1 percent. Thus, the proportion of damage due to environmental factors was 46.8 percent. This was as expected, as the base and subgrade erodibility and moisture within the JPCP structure contribute significantly to faulting. Also, the low level of overall damage for the high-trafficked pavement was due to the use of a highly effective and efficient load transfer mechanism (typically large-diameter dowels).

Impact of Design and Environmental Factors on Joint Faulting Damage

Table 48 through table 50 present the impact of environmental factors on JPCP transverse joint faulting damage.

Table 48. Impact of climate (wet/dry) on JPCP transverse joint faulting damage.

Climate	Overall Faulting Damage (SPS-2 and GPS-3) (%)	Faulting Damage due to Environmental Factors (SPS-8) (%)	Overall Damage due to Environmental Factors (%)
Dry	5.9	5.1	86.4
Wet	16.7	5.2	31.1

Table 49. Impact of climate (freeze/nonfreeze) on JPCP transverse joint faulting damage.

Climate	Overall Faulting Damage (SPS-2 and GPS-3) (%)	Faulting Damage due to Environmental Factors (SPS-8) (%)	Overall Damage due to Environmental Factors (%)
Freeze	11.5	5.1	44.3
Nonfreeze	9.4	5.2	55.3

Table 50. Impact of subgrade type on JPCP transverse joint faulting damage.

Subgrade Type	Overall Faulting Damage (SPS-2 and GPS-3) (%)	Faulting Damage due to Environmental Factors (SPS-8) (%)	Overall Damage due to Environmental Factors (%)
Fine-grained with high PI	5.1	5.1	100.0
Coarse- and fine-grained with low PI	12	5.2	43.3

The results presented in table 48 through table 50 indicate the following:

- For dry climates, joint faulting damage for the low- and high-trafficked projects was about the same (5.1 to 5.9 percent). Without free moisture in the doweled pavement system, the likelihood of faulting damage was very low. For wet climates, considerable damage (16.7 percent) was reported for the high-trafficked projects. The amount of damage for the low-trafficked projects was similar to that reported for dry climates.

- The proportion of damage due to environmental factors for projects in freeze and nonfreeze climates ranged from 44 to 55 percent.

- The proportion of overall damage due to environmental factors ranged from 43 to 100 percent. The significantly high value of 100 percent for subgrades with high plastic fines content was expected, as soils with high amounts of fines and high PI were highly susceptible to erosion in the presence of free water and repeated slab corner deflections due to truck-traffic loads.

CHAPTER 13. ANALYSIS OF TRANSVERSE JOINT SPALLING FOR SPS-8 AND COMPANION JPCP PROJECTS

This chapter presents the results of the preliminary and detailed analysis of joint performance for the SPS-8 and companion projects for JPCP. Joint performance for this analysis is indicated by transverse joint spalling expressed as a percentage of all transverse joints with spalling at all severity levels.

PRELIMINARY ANALYSIS TO CHARACTERIZE IMPACT OF ENVIRONMENTAL FACTORS ON JPCP TRANSVERSE JOINT SPALLING

The following sections describe a statistical analysis to determine the significance of various environmental factors on JPCP transverse joint spalling.

Impact of Freeze and Nonfreeze Climates

Figure 139 shows the impact of freeze and nonfreeze climates on JPCP transverse joint spalling for low- and high-trafficked projects after 15 yr.

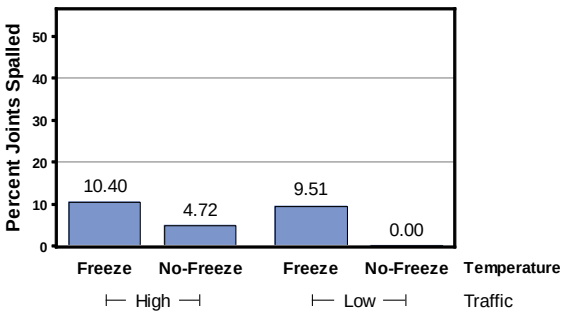

Source: FHWA.

A. Thin JPCPs.

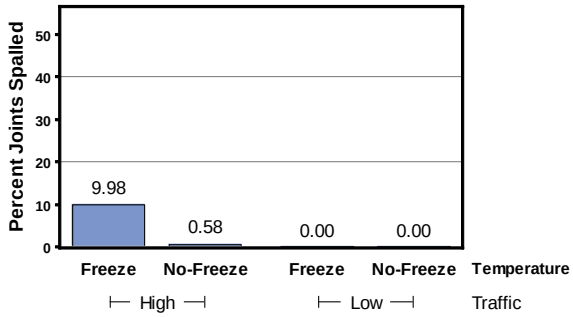

Source: FHWA.

B. Thick JPCPs.

Figure 139. Graphs. Impact of freeze and nonfreeze climates on JPCP transverse joint spalling for low- and high-trafficked projects.

Figure 139 shows the following:

- For projects subjected to low-traffic applications, the only joint spalling occurred on the thin JPCP located in the freeze climate. Thin JPCP in the nonfreeze climate and all thick JPCP in the nonfreeze climate had no joint spalling.

- For projects subjected to high-traffic applications, increased joint spalling occurred for thin and thick JPCP located in freeze climates particularly. Very little joint spalling occurred for thin and thick JPCPs located in the nonfreeze climate.

Impact of Freeze–Thaw Cycles

Figure 140 shows the impact of low and high numbers of air freeze–thaw cycles on JPCP transverse joint spalling for low- and high-trafficked projects.

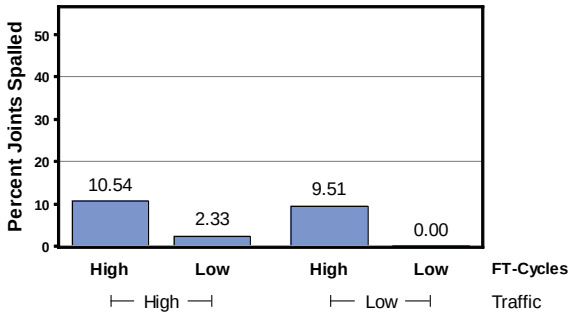

Source: FHWA.

A. Thin JPCPs.

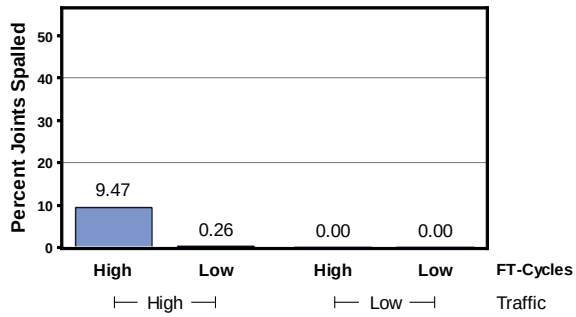

Source: FHWA.

B. Thick JPCPs.

Figure 140. Graphs. Impact of low and high freeze–thaw cycles on JPCP transverse joint spalling for low- and high-trafficked projects.

Figure 140 shows the following:

- For projects subjected to low-traffic applications, the only joint spalling occurred on the thin JPCPs located in a high freeze–thaw cycle climate. Thin JPCPs not subjected to high freeze–thaw cycles and all thick JPCPs had zero joint spalling.

- For projects subjected to high-traffic applications, increased joint spalling occurred for thin and thick JPCPs located in high freeze–thaw cycle climates. Very little joint spalling occurred on thin and thick JPCPs located in climates with low numbers of freeze–thaw cycles.

Impact of Frost Depth

Figure 141 shows the impact of low and high frost depth on JPCP transverse joint spalling for low- and high-trafficked projects.

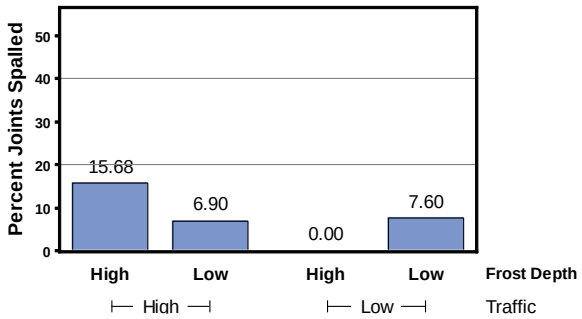

Source: FHWA.

A. Thin JPCPs.

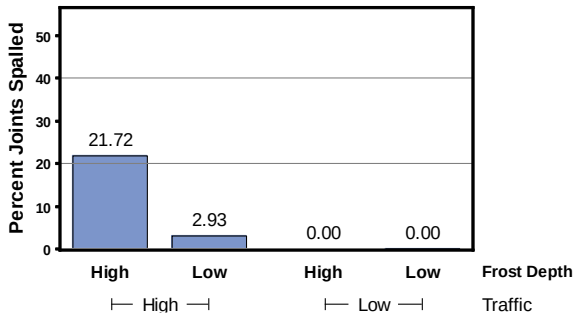

Source: FHWA.

B. Thick JPCPs.

Figure 141. Graphs. Impact of low and high frost depth on JPCP transverse joint spalling for low- and high-trafficked projects.

Figure 141 shows the following:

- For the low-trafficked projects, spalling was 0 percent for all sections except low frost penetration climates after 15 yr in service. The thin JPCP sections with low frost penetration exhibited 8 percent of joints spalled.

- For high-trafficked projects, spalling observed after 15 yr in service for pavements in high frost penetration climates was higher for both thin and thick slabs (15 and 22 percent, respectively) than for lower levels of frost penetration (3 and 7 percent, respectively).

- The observed levels of transverse joint spalling show that frost depth influences the development and progression of transverse joint spalling regardless of slab thickness and increasing traffic load application appears to aggravate joint spalling.

Impact of In Situ PCC Temperature

Figure 142 shows the impact of low and high in situ JPCP slab PCC temperature on JPCP transverse joint spalling for low- and high-trafficked projects.

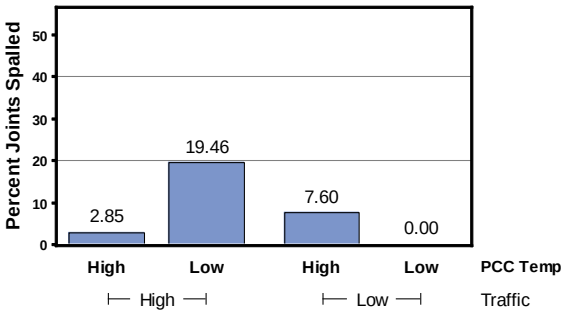

Source: FHWA.

A. Thin JPCPs.

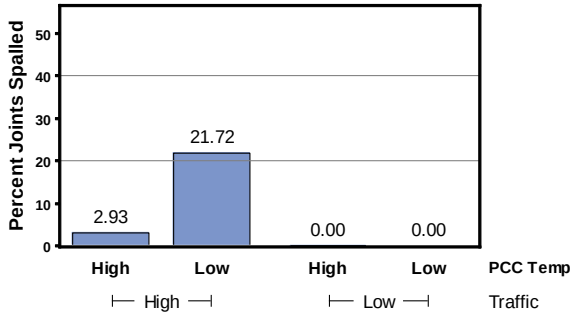

Source: FHWA.

B. Thick JPCPs.

Figure 142. Graphs. Impact of in situ PCC temperature on JPCP transverse joint spalling for low- and high-trafficked projects.

Figure 142 shows the following:

- For the low-trafficked projects, JPCP in situ temperature did not impact spalling development. The observed amount of spalling after 15 yr in service was mostly 0 percent, with the exception of thin JPCP sections with high PCC temperatures that showed 8 percent of joints spalled.

- For high-trafficked projects, spalling observed after 15 yr in service for pavements with low PCC temperatures was very high (19 and 22 percent for thin and thick slabs, respectively). Exposure to higher in situ JPCP temperatures decreased spalling considerably to approximately 3 percent for both thin and thick JPCPs.

- The observed levels of transverse joint spalling show that in situ JPCP temperature influenced the development and progression of transverse joint spalling, with much more spalling occurring in colder climates, and increased traffic load application for this comparison aggravated the spalling.

Impact of Annual Precipitation

Figure 143 shows the impact of rainfall in dry and wet environments on JPCP transverse joint spalling for low- and high-trafficked projects.

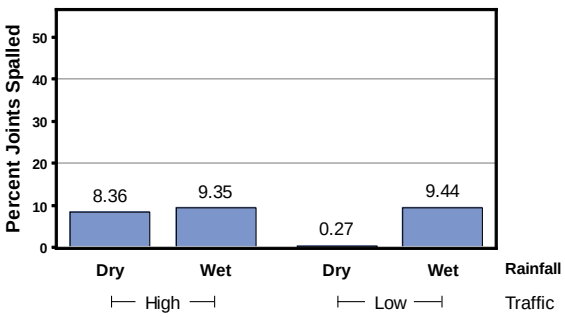

Source: FHWA.

A. Thin JPCPs.

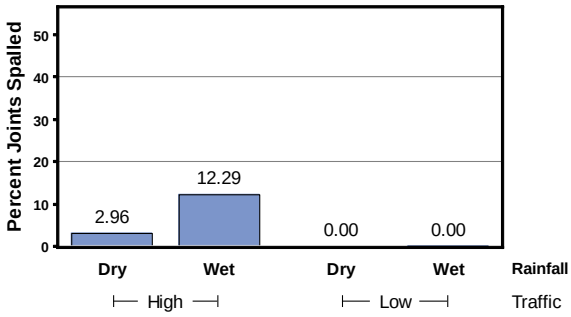

Source: FHWA.

B. Thick JPCPs.

Figure 143. Graphs. Impact of rainfall in dry and wet environments on JPCP transverse joint spalling for low- and high-trafficked projects.

Figure 143 shows the following:

- The low-trafficked projects with thin JPCP sections in wet climates exhibited higher levels of spalling than projects with thin JPCP sections in dry climates (9 versus 0 percent). For the thicker JPCP sections, joint spalling was nonexistent. Thickness appears to have mitigated the distress.

- Spalling was higher on high-trafficked projects located in wet climates. Moisture can contribute to aggravating spalling distress.

DETAILED STATISTICAL ANALYSIS TO CHARACTERIZE IMPACT OF ENVIRONMENTAL FACTORS ON JPCP TRANSVERSE JOINT SPALLING

Statistical analysis like the one described in chapter 11 was performed with mean transverse joint spalling as the dependent variable.

Summary of GLMSELECT Results for Low-Trafficked JPCP

For the low-trafficked projects, none of the design/environmental factors were found to be significant in initiating transverse joint spalling (figure 144). The observed spalling after 15 yr in service was low. Thus, the full impact of environmental factors on the distress over a longer time period may not yet have manifested.

PCC Transverse Spalling—LOW TRAFFIC SPS-8 ONLY

The GLMSELECT Procedure
Selected Model

Parameter Estimates

Parameter	DF	Estimate	Standard Error	t Value
Intercept	1	4.753145	4.714110	1.01

Source: FHWA.

Figure 144. Screenshot. Summary of GLMSELECT results for JPCP joint spalling for low-trafficked JPCP.

Summary of GLMSELECT and ANOVA Results for Low- and High-Trafficked JPCP

A statistical ANOVA similar to that described for low-trafficked JPCP was done for all projects combined. All key factors for traffic, slab thickness, climate, and subgrade characteristics were considered. Two- and three-way interactions of variables were also evaluated. The results of the analyses are presented in figure 145.

PCC Transverse Joint Spalling—ALL TRAFFIC SPS-8, SPS-2, GPS-3

The GLM Procedure

Dependent Variable: PCTJTSPALLEd_NL

Source	DF	Sum of Squares	Mean Square	F Value	Pr > F
Model	2	2043.519518	1021.759759	6.02	0.0056
Error	36	6113.239757	169.812215		
Corrected Total	38	8156.759275			

R-Square	Coeff Var	Root MSE	PCTJTSPALLEd_NL Mean
0.250531	163.0829	13.03120	7.990537

Source	DF	Type III SS	Mean Square	F Value	Pr > F
JTSP*(1/THKPC)*PCCTEMP	2	2043.519518	1021.759759	6.02	0.0056

Parameter	Estimate	Standard Error	t Value	Pr > |t|
Intercept	2.35385105	13.05651815	0.18	0.8579
JTSP*(1/THKPC)*PCCTEMP High	0.95913447	8.44286369	0.11	0.9102
JTSP*(1/THKPC)*PCCTEMP Low	11.10459347	8.38066320	1.33	0.1935

Source: FHWA.

Figure 145. Screenshot. Summary of GLMSELECT and ANOVA results for JPCP transverse joint spalling for low- and high-trafficked JPCP.

Figure 145 shows the following:

- Pavements with higher traffic levels did not experience significantly higher levels of joint spalling overall; however, traffic did show a difference in some of the comparisons.

- One three-way interaction was significant, involving joint spacing, slab thickness, and in situ JPCP slab temperature. Various combinations of longer joint spacing, thin slabs, and high in situ JPCP slab temperature could cause a high amount of joint spalling. Specific results from the three-way interaction are as follows:
  - Joint spacing had a significant effect on joint spalling, with longer joints showing higher amounts of spalling.

  - JPCP layer thickness had a significant impact on JPCP transverse joint spalling extent after 15 yr in service. The additional 3-inch JPCP thickness reduced JPCP transverse joint spalling significantly.

  - The in situ JPCP slab temperature had a significant impact on spalling. The colder the temperature, the higher the joint spalling. This also manifested itself through the general climate, with freeze climates having greater spalling and higher numbers of freeze–thaw cycles, all showing that the colder the pavement, the higher the joint spalling. In situ JPCP temperature is believed to be an initiator of joint spalling since it correlates strongly with spalling; there is mechanistic support for this conjecture as well.

- The longer the joint spacing, the higher the percentage of spalled joints. This may be due to increased joint opening and closing with longer spacing resulting in higher stresses from incompressibles (e.g., fine sand particles) and also higher infiltration of incompressibles in cold weather.

ANALYSIS OF JPCP TRANSVERSE JOINT SPALLING DAMAGE

Estimating the proportion of overall JPCP transverse joint spalling damage due to environmental factors required the following:

- The overall JPCP transverse joint spalling of a selection of JPCP subjected to normal heavy traffic loadings (GPS-3 and SPS-2 companion sections) and environmental factors.

- The transverse joint spalling damage of JPCPs with similar JPCP thickness and materials subjected to low traffic loadings and similar environmental factors (SPS-8 projects).

The impact of various design and environmental factors on JPCP transverse joint spalling was also assessed.

Proportion of Overall JPCP Transverse Joint Spalling Damage Caused by Environmental Factors

Table 51 presents a summary of overall mean JPCP transverse joint spalling damage (GPS-3 and SPS-2 companion projects) and JPCP transverse joint spalling damage due to environmental

factors alone (SPS-8 projects) for thin and thick JPCPs. The proportion of overall JPCP transverse joint spalling damage attributable to environmental factors for thin JPCPs was approximately 88 percent. For thick JPCPs, the proportion of damage due to environmental factors was 0 percent. On average, the overall joint spalling damage after 15 yr in service of the heavily trafficked projects was 18.5 percent of lane area, and for the low-trafficked projects, JPCP transverse joint spalling damage on average was 11.9 percent. Thus, on average, proportion of JPCP transverse joint spalling ascribed to environmental conditions was 11.9/18.5 = 64.3 percent.

Table 51. Impact of JPCP thickness on JPCP transverse joint spalling damage.

JPCP Thickness	Overall Spalling Damage (SPS-2 and GPS-3) (%)	Spalling Damage due to Environmental Factors (SPS-8) (%)	Overall Damage due to Environmental Factors (%)
Thin	21.7	19	87.6
Thick	16.3	0	0.0
Mean	18.5	11.9	64.3

Generally, the proportion of JPCP transverse joint spalling damage associated with environmental factors to that associated with all causes, including loading and the same environmental factors, was approximately 64.3 percent. This distress was predominantly an environmental-related distress with traffic aggravating the problem.

Impact of Design and Environmental Factors on Overall JPCP Transverse Joint Spalling Damage

Table 52 and table 53 present the impact of environmental factors on JPCP transverse joint spalling damage.

Table 52. Impact of climate (wet/dry) on JPCP transverse joint spalling damage.

Climate	Overall Spalling Damage (SPS-2 and GPS-3) (%)	Spalling Damage due to Environmental Factors (SPS-8) (%)	Overall Damage due to Environmental Factors (%)
Dry	13.2	0.7	5.3
Wet	24.5	13.5	55.1

Table 53. Impact of climate (freeze/nonfreeze) on JPCP transverse joint spalling damage.

Climate	Overall Spalling Damage (SPS-2 and GPS-3) (%)	Spalling Damage due to Environmental Factors (SPS-8) (%)	Overall Damage due to Environmental Factors (%)
Freeze	23	15.8	68.7
Nonfreeze	6	0	0.0

The results presented in the tables indicate the following:

- The proportion of environmental damage was highest for wet–freeze climates (23 to 25 percent) and lowest for dry–nonfreeze climates (6 to 13 percent).

- The proportion of damage due to environmental factors was highest for freeze climates (68.7 percent) followed by wet climates (55.1 percent). Dry–nonfreeze climates experienced the lowest amounts of environmental damage at 5.3 and 0 percent, respectively.

CHAPTER 14. ANALYSIS OF SMOOTHNESS FOR SPS-8 AND COMPANION JPCP PROJECTS

This chapter describes the results of the preliminary and detailed analysis for JPCP smoothness. For LTPP, a longitudinal profile of the entire 500-ft project was measured and converted into IRI. Smoothness was measured in both the left and right wheel paths. For this analysis, the representative IRI for the entire 500-ft sample area was computed as an average of the left and right wheel path IRI measures. As the pavement projects evaluated were constructed with different initial IRI values, comparison of absolute IRI values after 15 yr in service would be misleading. Therefore, the smoothness performance measure used for analysis was ΔIRI, which is defined as the change in IRI within the 15-yr analysis period.

PRELIMINARY ANALYSIS OF AC PAVEMENT IRI PERFORMANCE

The following sections describe a statistical analysis to determine the significance of various environmental factors on JPCP smoothness (e.g., IRI).

Impact of Freeze and Nonfreeze Climates

Figure 146 shows the impact of freeze and nonfreeze climates on JPCP change in IRI for low- and high-trafficked projects.

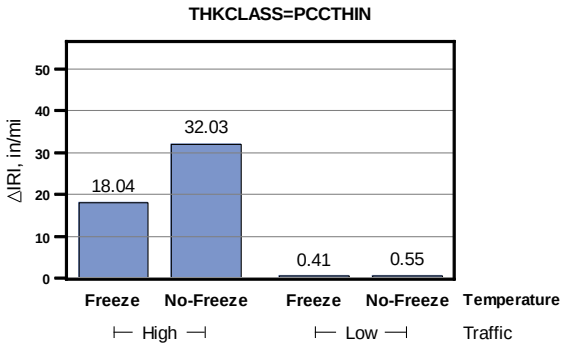

Source: FHWA.

A. Thin JPCPs.

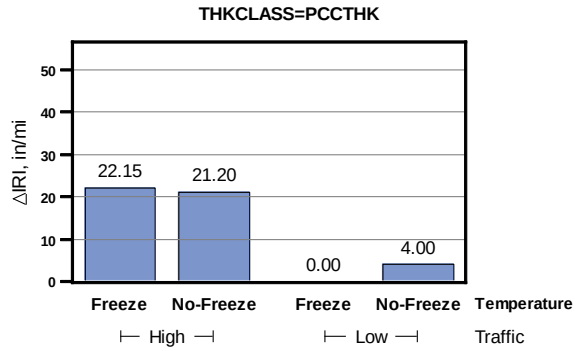

Source: FHWA.

B. Thick JPCPs.

Figure 146. Graphs. Impact of freeze and nonfreeze climates on JPCP change in IRI for low- and high-trafficked projects.

Figure 146 shows the following:

- In the absence of heavy traffic loads, IRI increased on average less than 1 inch/mi after 15 yr for either freeze or nonfreeze climates.
- JPCP subjected to higher traffic levels exhibited much higher levels of IRI increase (18 to 32 inches/mi) for thin JPCP. For thick JPCP, there was no increase in IRI. This was due to increased cracking and faulting development on the thinner JPCP.

- Freeze or nonfreeze climates showed a major impact on change in IRI only on thin JPCP. JPCP in nonfreeze climates showed nearly double change in IRI than JPCP in freeze climates.

Impact of Freeze–Thaw Cycles

Figure 147 shows the impact of low and high freeze–thaw cycles on JPCP change in IRI for low- and high-trafficked projects.

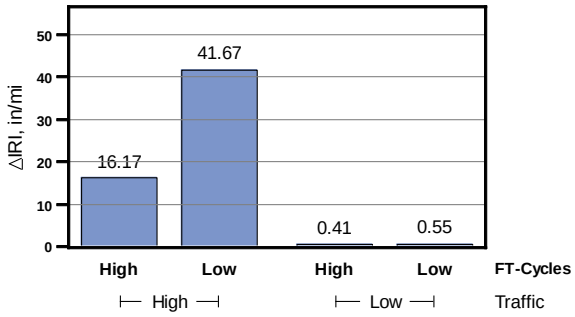

Source: FHWA.

A. Thin JPCPs.

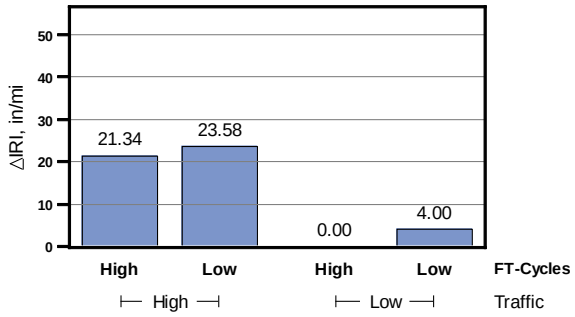

Source: FHWA.

B. Thick JPCPs.

Figure 147. Graphs. Impact of low and high freeze–thaw cycles on JPCP change in IRI for low- and high-trafficked projects.

Figure 147 shows the following:

- In the absence of heavy traffic loads, IRI increased less than 1 inch/mi after 15 yr. Thus, freeze–thaw cycles had no effect.
- Pavements subjected to higher traffic levels in general exhibited higher levels of IRI (16 to 41 inches/mi) when compared to low-trafficked pavements (0 to 4 inches/mi).
- Pavements subjected to lower levels of freeze–thaw cycles averaged across JPCP thickness exhibited higher levels of IRI increase.

Impact of Frost Depth

Figure 148 shows the impact of low and high frost depth on JPCP change in IRI for low- and high-trafficked projects.

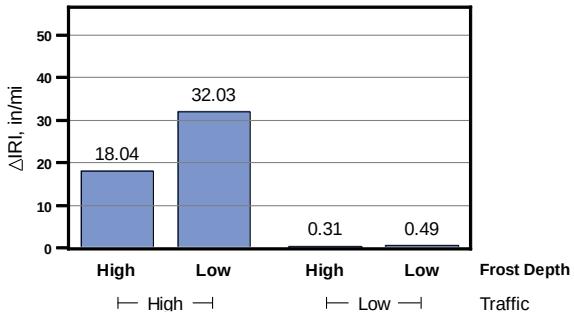

Source: FHWA

A. Thin JPCPs.

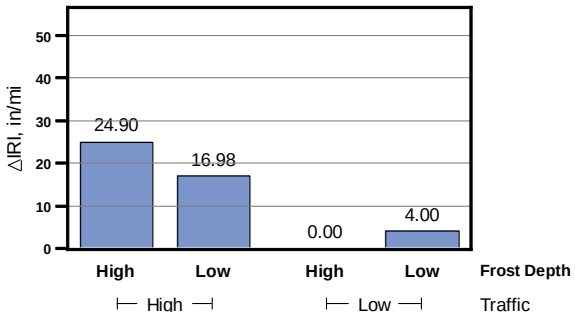

Source: FHWA

B. Thick JPCPs.

Figure 148. Graphs. Impact of low and high frost depth on JPCP change in IRI for low- and high-trafficked projects.

Figure 148 shows the following:

- In the absence of heavy traffic loads, IRI increased less than 1 inch/mi after 15 yr. Thus, frost depth had no effect by itself.
- For the high-trafficked projects, the change in IRI after 15 yr in service was high (17 to 32 inches/mi). Thin JPCP showed higher IRI increase in low frost depth areas, and thicker JPCP showed just the opposite.

Impact of PCC Temperature

Figure 149 shows the impact of low and high in situ JPCP temperature on JPCP change in IRI for low- and high-trafficked projects.

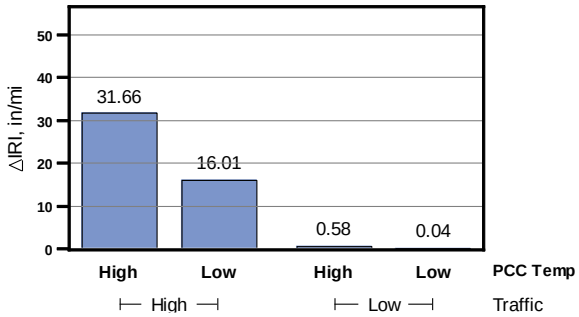

Source: FHWA.

A. Thin JPCPs.

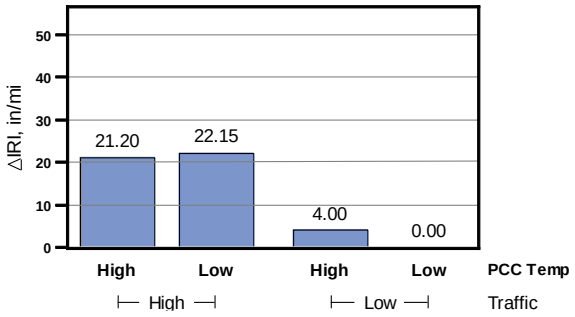

Source: FHWA.

B. Thick JPCPs.

Figure 149. Graphs. Impact of low and high PCC temperatures on JPCP change in IRI for low- and high-trafficked projects.

Figure 149 shows the following:

- In the absence of heavy traffic loads, IRI increased less than 1 inch/mi after 15 yr. Thus, neither freeze nor nonfreeze climates had an effect.

- For the high-trafficked projects with thin JPCP after 15 yr, IRI increased more in warmer climates (32 inches/mi) than in colder climates (approximately 16 inches/mi).

- For thicker JPCP, the PCC temperature did not appear to have an impact on IRI changes after 15 yr subjected to high traffic.

- Traffic level had a large effect on IRI change, with high-trafficked projects showing a greater IRI increase than low-traffic projects.

Impact of Rainfall

Figure 150 shows the impact of rainfall in dry and wet environments on JPCP change in IRI for low- and high-trafficked projects.

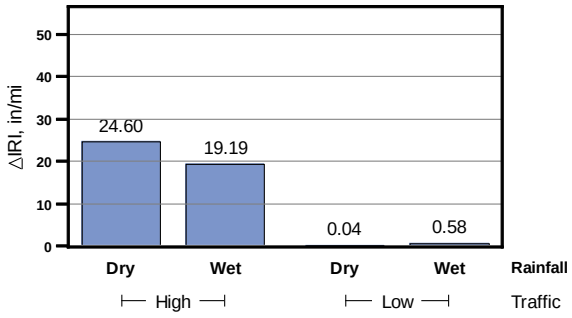

Source: FHWA.

A. Thin JPCPs.

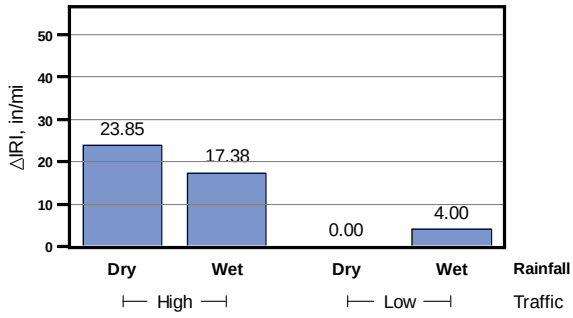

Source: FHWA.

B. Thick JPCPs.

Figure 150. Graphs. Impact of rainfall in dry and wet environments on pavement JPCP change in IRI for low- and high-trafficked projects.

Figure 150 shows the following:

- In the absence of heavy traffic loads, IRI increased less than 1 inch/mi after 15 yr. Thus, rainfall did not have any effect.

- The high-trafficked projects with both thick and thin JPCP showed greater IRI increases in dry climates than in wet climates.

- Traffic level had a significant effect on change in IRI, with high traffic experiencing an increase of 17 to 25 inches/mi and low traffic experiencing an increase of about 0 to 4 inches/mi regardless of thickness.

Impact of Base and Subgrade In Situ Moisture Content

Figure 151 shows the impact of low and high in situ moisture content on JPCP change in IRI for low- and high-trafficked projects.

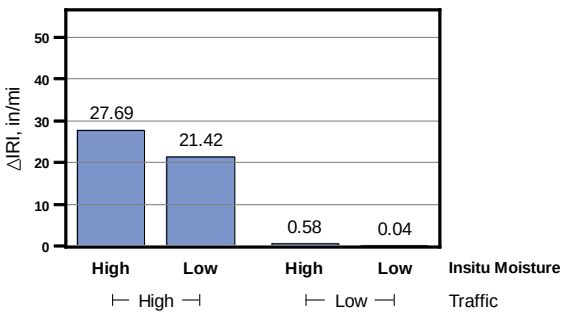

Source: FHWA.

A. Thin JPCPs.

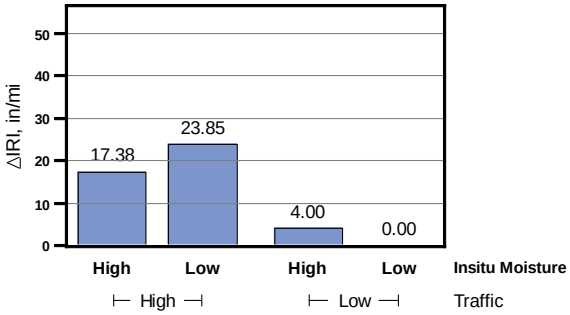

Source: FHWA.

B. Thick JPCPs.

Figure 151. Graphs. Impact of low and high base and subgrade in situ moisture content on JPCP change in IRI for low- and high-trafficked projects.

Figure 151 shows the following:

- In the absence of heavy traffic loads, IRI increased by 1 inch/mi after 15 yr for both thick and thin JPCP slab. Thus, moisture content had no effect.
- For the high-trafficked projects, the change in IRI after 15 yr was high (i.e., increased less than 17 inches/mi). The impact of base and subgrade moisture on change in IRI varied depending on JPCP thickness. For thin JPCP sections, higher base and subgrade moisture led to an increase in IRI from 21 to 27 inches/mi. For thick PCC sections, lower moisture led to an increase in IRI from 17 to 23 inches/mi.
- Traffic level had a large effect IRI, with high traffic showing a greater increase in IRI than low traffic.

Impact of Subgrade Type

Figure 152 shows the impact of subgrade type (i.e., fine or coarse) on JPCP change in IRI for low- and high-trafficked projects.

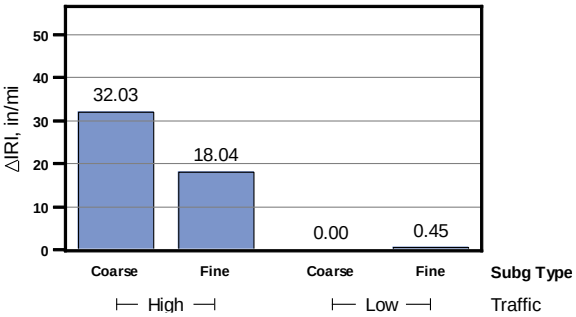

Source: FHWA.

A. Thin JPCPs.

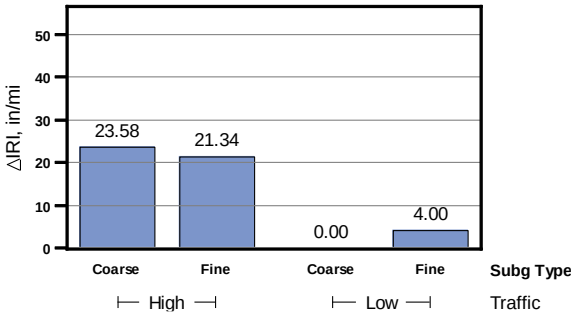

Source: FHWA.

B. Thick JPCPs.

Figure 152. Graph. Impact of subgrade type on JPCP change in IRI for low- and high-trafficked projects.

Figure 152 shows the following:

- In the absence of heavy traffic loads, IRI increased by 1 inch/mi after 15 yr. Thus, subgrade types had no effect.
- For the high-trafficked projects, the IRI increase exhibited after 15 yr in service was high (less than 18 inches/mi). The trend for both thin and thick JPCP was that coarse subgrades showed a higher loss of smoothness than a fine-grained subgrade.
- Traffic level had a large effect on IRI increase, with high traffic showing far more IRI increase than low traffic.

Impact of Subgrade Clay Content

Figure 153 shows the impact of low and high subgrade clay content on JPCP change in IRI for low- and high-trafficked projects.

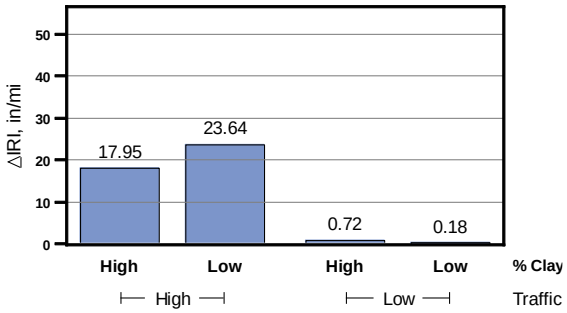

Source: FHWA.

A. Thin JPCPs.

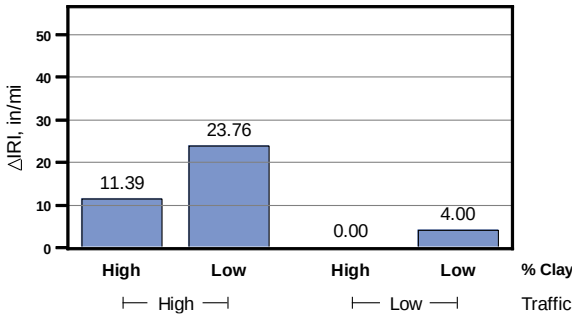

Source: FHWA.

B. Thick JPCPs.

Figure 153. Graphs. Impact of low and high subgrade clay content on JPCP change in IRI for low- and high-trafficked projects.

Figure 153 shows the following:

- In the absence of heavy traffic loads, IRI increased by less than 1 inch/mi after 15 yr. Thus, subgrade clay content had no effect on IRI.
- For the high-trafficked projects, IRI increased by more than 11 inches/mi after 15 yr, which is considered high. The difference in IRI increase due to subgrade clay content ranged from 5.5 to 12 inches/mi, with subgrade with low clay content always exhibiting higher levels of IRI increase.
- Traffic level had a large effect on IRI increase, with high traffic showing far more IRI increase than low traffic.

Impact of Subgrade Silt Content

Figure 154 shows the impact of low and high subgrade silt content on JPCP change in IRI for low- and high-trafficked projects.

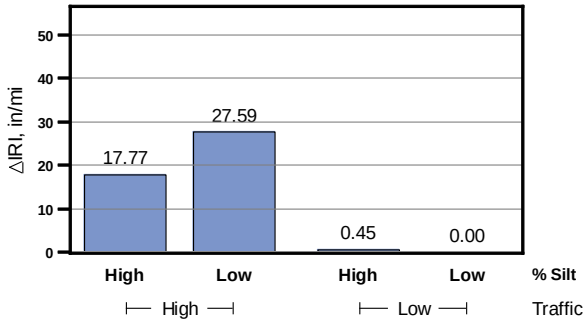

Source: FHWA.

A. Thin JPCPs.

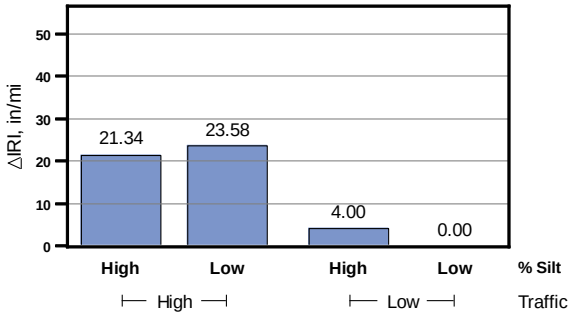

Source: FHWA.

B. Thick JPCPs.

Figure 154. Graphs. Impact of low and high subgrade silt content on JPCP change in IRI for low- and high-trafficked projects.

Figure 154 shows the following:

- In the absence of heavy traffic loads, IRI increased by less than 1 inch/mi after 15 yr. Thus, subgrade silt content had no effect on IRI.
- For the high-trafficked projects, the change in IRI after 15 yr in service was high (increase greater than 12 inches/mi) regardless of subgrade silt content. The trends show that JPCP constructed over lower silt content subgrades exhibited higher IRI increases.
- Traffic level had a large effect on IRI increase, with high traffic showing a greater increase in IRI than low traffic.

Impact of Subgrade Fine-Sand Content

Figure 155 presents graphs showing the impact of low and high subgrade fine-sand content on JPCP change in IRI for low- and high-trafficked projects.

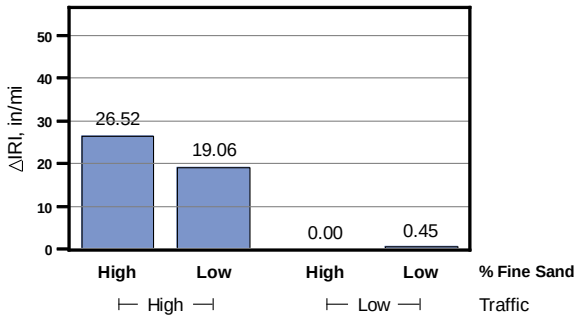

Source: FHWA.

A. Thin JPCPs.

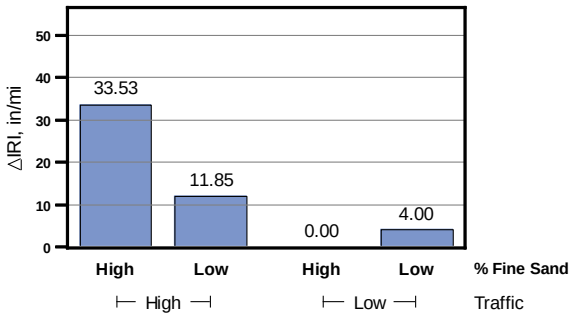

Source: FHWA.

B. Thick JPCPs.

Figure 155. Graphs. Impact of low and high subgrade fine-sand content on JPCP change in IRI for low- and high-trafficked projects.

Figure 155 shows the following:

- In the absence of heavy traffic loads, IRI increased by less than 1 inch/mi after 15 yr. Thus, subgrade sand content had no effect on IRI.
- For the high-trafficked projects, the change in IRI after 15 yr in service was high (i.e., increase greater than 12 inches/mi) regardless of subgrade fine-sand content. The difference in IRI increase for pavement constructed over subgrades with low or high fine-sand content ranged from 7 to 22 inches/mi. Pavement constructed over subgrades with high fine-sand content exhibited greater change in IRI.
- Traffic level had a large effect on IRI, with high traffic showing greater IRI increase than low traffic.

Impact of Subgrade PI

Figure 156 shows the impact of low and high subgrade PI on JPCP change in IRI.

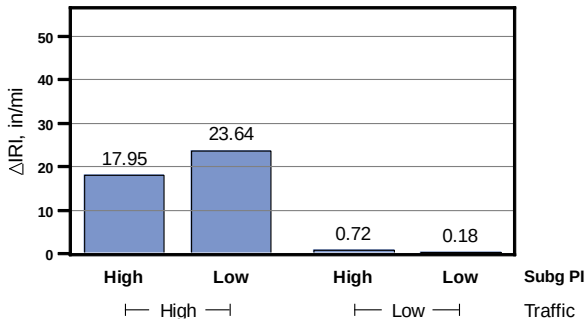

Source: FHWA.

A. Thin JPCPs.

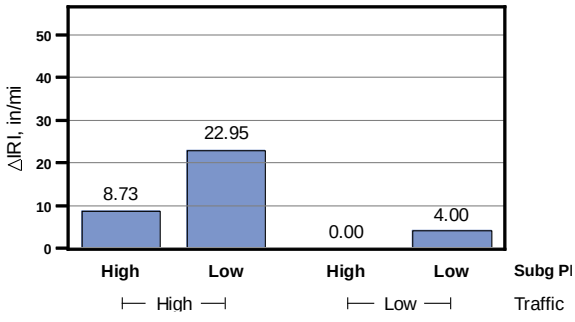

Source: FHWA.

B. Thick JPCPs.

Figure 156. Graphs. Impact of low and high subgrade PI on JPCP change in IRI for low- and high-trafficked projects.

Figure 156 shows the following:

- In the absence of heavy traffic loads, IRI increased by less than 1 inch/mi after 15 yr. Thus, subgrade PI had no effect on IRI increase.

- For the high-trafficked projects, the change in IRI after 15 yr was high (increased by 8 to 24 inches/mi) regardless of subgrade PI level. The difference in IRI for pavement constructed over subgrades with low/high PI was higher for thicker JPCP (difference of approximately 14 inches/mi). In general, pavements constructed over subgrades with low PI exhibited greater increases in IRI.

- Traffic level had a large effect on IRI increase, with high traffic showing a greater increase in IRI than low traffic.

DETAILED STATISTICAL ANALYSIS OF JPCP IRI PERFORMANCE

Statistical analysis like the one described in chapter 11 was performed with IRI as the dependent variable.

Summary of ANOVA Results for Low-Trafficked JPCP

The results of the statistical model selection and ANOVA procedures for low-trafficked JPCP are presented in figure 157. The results showed that subgrade (represented by fine-sand content) and in situ JPCP temperature were the only environmental variables that had a significant impact on IRI increase. The higher the sand content, the greater the IRI increase; the higher the in situ JPCP temperature, the greater the IRI increase. This implies that the warmer the climate, the greater the IRI increase. Thus, subgrade type (sandy fine grained versus coarse grained) and in situ JPCP temperature could be identified as possible initiators of IRI increase.

PCC Smoothness—LOW TRAFFIC SPS-8 ONLY

The GLM Procedure

Dependent Variable: DELTAIRI

Source	DF	Sum of Squares	Mean Square	F Value	Pr > F
Model	2	9.94035669	4.97017834	18.37	0.0516
Error	2	0.54122517	0.27061258		
Corrected Total	4	10.48158185			

R-Square	Coeff Var	Root MSE	DELTAIRI Mean
0.948364	44.95411	0.520204	1.157190

Source	DF	Type III SS	Mean Square	F Value	Pr > F
PCCTEMP	1	2.80236432	2.80236432	10.36	0.0845
SANDFINE	1	8.38578666	8.38578666	30.99	0.0308

Parameter		Estimate	Standard Error	t Value	Pr > |t|
Intercept		-2.169193670	0.65451830	-3.31	0.0802
PCCTEMP	High	1.893787843	0.58849533	3.22	0.0845
PCCTEMP	Low	0.000000000	. . .		
SANDFINE		0.368531714	0.06620289	5.57	0.0308

Source: FHWA.

Figure 157. Screenshot. Summary of GLMSELECT and ANOVA results for JPCP smoothness for low-trafficked JPCP.

Summary of GLMSELECT and ANOVA Results for Low- and High-Trafficked JPCP

A statistical analysis similar to that described for low-trafficked JPCP was done for all projects combined. The goal was to determine the cause of the increase in IRI between two possibilities: nonenvironmental variables or the previously identified environmental variables in conjunction with other variables. Because it was found that high-trafficked JPCP projects experienced significantly more IRI increase, the analysis sought to determine if increased JPCP thickness mitigated the development and progression of the distress. The results of the analyses are presented in figure 158.

PCC SMOOTHNESS—ALL TRAFFIC SPS-8, SPS-2, GPS-3

The GLM Procedure

Dependent Variable: DELTAIRI

Source	DF	Sum of Squares	Mean Square	F Value	Pr > F
Model	3	4473.91066	1491.30355	2.79	0.0635
Error	23	12307.28749	535.09946		
Corrected Total	26	16781.19815			

R-Square	Coeff Var	Root MSE	DELTAIRI Mean
0.266603	117.8536	23.13222	19.62793

Source	DF	Type III SS	Mean Square	F Value	Pr > F
AADTT*(1/THKPC)*PCCTEMP	2	3745.676306	1872.838153	3.50	0.0471
FOUNDATION	1	1270.571902	1270.571902	2.37	0.1370

Parameter		Estimate	Standard Error	t Value	Pr > |t|
Intercept		13.56583743	6.42136772	2.11	0.0457
AADTT*(1/THKPC)*PCCTEMP High		13.53911931	5.19450133	2.61	0.0158
AADTT*(1/THKPC)*PCCTEMP Low		4.17355890	7.30702358	0.57	0.5734
FOUNDATION	Coarse	-31.38682545	20.36878028	-1.54	0.1370
FOUNDATION	Fine	0.00000000	. . .		

Source: FHWA.

Figure 158. Screenshot. Summary of GLMSELECT and ANOVA results for JPCP IRI increase.

In summary, the results indicate the following:

- A three-way interaction was significant that included traffic, JPCP thickness, and in situ JPCP temperature. The most critical IRI increase conditions would be higher traffic, thinner JPCP, and warmer in situ temperature.
- Traffic application had a significant impact on IRI. This was visible on all of the bar graphs presented, and the difference with low traffic was large.
- JPCP thickness had a significant impact on IRI. The thinner the JPCP, the higher the IRI increase.
- In situ JPCP temperature was significant for all combined traffic and low traffic alone. The higher the in situ JPCP temperature (e.g., warm climates), the higher the IRI increase.

- For low-traffic SPS-8 projects alone, the amount of fine sand in the subgrade was significant. In other words, the coarser the soil, the greater the IRI increase. This result is reflected in the bar graph trends for higher traffic, in which every subgrade indicator showed that a more granular subgrade resulted in increased IRI over a fine-grained subgrade.

ANALYSIS OF DAMAGE RELATED TO CHANGES IN IRI

Estimating the proportion of overall JPCP IRI damage due to environmental factors required the following:

- The overall JPCP IRI damage of a selection of JPCP subjected to normal heavy traffic loadings (GPS-3 and SPS-2 companion sections) and environmental factors.

- The JPCP IRI damage of similar thickness and materials for JPCP subjected to low traffic loadings and similar environmental factors (SPS-8 sections).

The impact of various design and environmental factors on JPCP IRI damage was also assessed.

Proportion of Overall Change in IRI Damage due to Environmental Factors

Table 54 presents a summary of overall IRI increase damage and IRI increase damage due to only environmental factors. On average, overall IRI increased damage was 15 percent. For low-trafficked projects, IRI increased damage, on average, was 0.8 percent. Thus, the proportion of overall IRI increase damage due to environmental factors of typical heavily trafficked JPCP projects was 5.3 percent. Thus, the majority of damage was caused by traffic loadings.

Table 54. Impact of JPCP thickness on IRI increase.

JPCP Thickness	Overall JPCP Damage (%)	JPCP Damage due to Environmental Factors (%)	Overall Damage due to Environmental Factors (%)
Thin	15.4	0.3	1.9
Thick	14.6	2.7	18.5
Mean	15	0.8	5.3

Table 55 through table 57 present the impact of design and environmental factors on JPCP IRI increase damage.

Table 55. Impact of subgrade type on IRI increase.

Soil Type	Overall JPCP Damage (%)	JPCP Damage due to Environmental Factors (%)	Overall Damage due to Environmental Factors (%)
High PI, fine	8.9	0.5	5.6
Low PI, coarse or fine	15.5	1.0	6.5

Table 56. Impact of freeze and nonfreeze climates on JPCP IRI increase.

Climate	Overall JPCP Damage (%)	JPCP Damage due to Environmental Factors (%)	Overall Damage due to Environmental Factors (%)
Freeze	13.6	0.3	2.2
Nonfreeze	17.7	1.5	8.5

Table 57. Impact of wet and dry climates on JPCP IRI increase.

Climate	Overall JPCP Damage (%)	JPCP Damage due to Environmental Factors (%)	Overall Damage due to Environmental Factors (%)
Dry	16.1	0	0.0
Wet	12.1	1	8.3

The results presented in table 55 through table 57 indicate the following:

- The proportion of overall IRI increase damage attributable to environmental factors for thin JPCPs was approximately 2 percent. For thicker JPCPs, the proportion of damage due to environmental factors was 18.5 percent. Slab thickness did not have a significant impact on IRI increased damage.

- Although there was some significant difference in the proportion of environmental damage for JPCP constructed over fine subgrades with high PI when compared to those constructed over coarse subgrades, the difference was marginal.

- Wet and nonfreeze climates reported the highest proportions of environmental damage (8.3 to 8.5 percent) as compared to regions with deep freeze (2.2 percent) and dry climates (0 percent). This implies pavements constructed in wetter and warmer regions are more likely to exhibit significant IRI increase.

CHAPTER 15. PROPORTION OF OVERALL PAVEMENT DAMAGE DUE TO ENVIRONMENTAL FACTORS

This chapter shows the overall impact of AC pavement and JPCP damage attributable to environmental factors. A key objective of this research was to determine the proportion of overall pavement damage that can be attributed to environmental factors. Table 58 summarizes the distress-specific damage estimates for low- and high-trafficked AC pavements and JPCP.

Table 58. Summary of distress-specific overall pavement damage and proportion of overall damage attributed to environmental factors for AC pavements and JPCP.

Pavement Type	Performance Measure	Total Damage (GPS-3 and SPS-2 Projects Only) (%)	Pavement Damage due to Environmental Factors (SPS-8) Only (%)	Percentage of Total Damage due to Environmental Factors (%)
AC pavement	AC fatigue cracking[1]	46	6.7	14.6
AC pavement	Total rutting[2]	63.2	27.03	42.7
AC pavement	AC transverse cracking	54.8	24.7	45.1
AC pavement	Materials-related distresses[3]	43.8	25.6	58.4
AC pavement	IRI increase[4]	29.2	6.2	21.2
JPCP	PCC fatigue cracking[5]	33.9	2.8	8.3
JPCP	Transverse joint faulting	10.9	5.1	46.8
JPCP	Transverse joint spalling	18.5	11.9	64.3
JPCP	IRI increase[4]	15	0.8	5.3

[1]Alligator and longitudinal cracking in the wheel path.
[2]Rutting in the AC, base, and subgrade layers.
[3]Raveling, bleeding, block cracking, and potholes.
[4]Distress/damage from wheel path profile changes over time.
[5]Transverse slab cracking, longitudinal cracking in the wheel path, and slab corner breaks.

The following approach was used to determine the proportion of overall pavement damage that can be attributed to environmental factors:

- Develop a logical mathematical procedure to estimate overall pavement damage due to all the various causes of damage (e.g., repeated load fatigue, materials durability, climate) for the low- and high-trafficked AC and JPCP projects.

- Determine the proportion of total damage that is due to environmental factors only.

If all types of pavement deterioration were considered equal in damage, then the percentages shown in table 58 could be averaged.

AC pavement distress percentages due to environmental factors are as follows:

- Fatigue cracking = 14.6 percent.
- Total rutting = 42.7 percent.
- Transverse cracking = 45.1 percent.
- Materials-related distress = 58.4 percent.
- IRI increase = 21.2 percent.
- Mean = 36.4 percent.

JPCP distress percentages due to environmental factors are as follows:

- Fatigue cracking = 8.3 percent.
- Joint faulting = 46.8 percent.
- Joint spalling = 4.3 percent.
- IRI increase = 5.3 percent.
- Mean = 16.2 percent.

Weighting all distress categories equally, the average for all damage caused by the environment was 36 percent for AC pavements and 16 percent for JPCPs. An argument could be made that these categories are all critical distresses that could each lead to the need for major rehabilitation.

An argument could also be made that these categories are not all equally important for major rehabilitation. An analysis was conducted whereby the various components of overall pavement damage were weighted (using an established pavement rating procedure) and averaged to provide a perhaps more meaningful statistical measure of overall pavement damage.[51] The weights were assigned to each damage class in table 58 in a manner that mimics the levels of significance of each damage class (e.g., fatigue cracking has more significance than transverse cracking). The assigned weights were computed using the *DV* computational procedure outlined in ASTM D6433.[51] By using the *DV* procedure, the assigned weights were similar to those used to determine overall pavement condition reflected by the PCI. *DV* assigned to individual distress as part of the PCI estimation procedure was developed based on the consensus of experienced pavement engineers and reflects the contribution of each distress measure to overall pavement condition. A similar method for assigning weights to various components of pavement damage was used by Lytton et al.[56] The PCI-based weights developed for AC pavements were adopted for the JPCPs.

PROPORTION OF OVERALL PAVEMENT DAMAGE DUE TO ENVIRONMENTAL FACTORS FOR AC PAVEMENTS

This section describes the methodology and results of estimating the overall pavement damage due to environmental factors for AC pavements.

Methodology for Assigning Weights to the Different Damage Classes for AC Pavements

The PCI method uses a series of simple mathematical algorithms and curves to assign a weight/severity factor that reflects the effects of distresses on overall pavement condition. The methodology rationally converts the objective and subjective measures of distress types, extent, severity, and smoothness to deduct points for each type of observable pavement distress, sums the deduct points for all distress types, and deducts total *DV* from the perfect score of 100 as shown in figure 159.

$$\mathrm{PCI} = 100 - \sum_{i=1}^{n} DV_i$$

Figure 159. Equation. Estimation of *PCI*.

Where:

n = number of distress types present.
DV = deduct value, which is calculated by (weight for distress) × (weight for severity) × (weight for extent).

For this study, the PCI method was used to compute total *DV* as follows:

1. Determine typical amounts (extent and severity) of distresses for AC pavements after approximately 15 yr in service. A time period of 15 yr was selected because it is the life of the distresses of the AC pavements being analyzed.

2. Using the typical distress amounts in step 1, determine *DV* weighting factors for each distress type and IRI based on the PCI curves and relationships.

3. Compute total *DV* weighting factors for the distress groupings.

4. Estimate overall pavement damage for low- (SPS-8) and high-trafficked (GPS-3/SPS-2) pavements using the equation in figure 160.

$$g_{OVERALL} = \frac{\sum_{i=1}^{k} (DV_i * g_i)}{\sum_{i=1}^{k} (DV_i)}$$

Figure 160. Equation. Estimation of damage for individual distress/smoothness performance measure.

Where:

$g_{OVERALL}$ = individual damage for distress/IRI, *i*.
DV_i = weight assigned to a given distress/IRI damage, *i*.
g_i = individual damage for distress/IRI, *i*.

5. Determine the proportion of overall pavement damage due to environmental factors alone using the equation in figure 161.

$$\text{PCT\_DAM}_{\text{ENV}} = 100 * \frac{g_{OVERALL-ENV}}{g_{OVERALL-TOTAL}}$$

Figure 161. Equation. Estimation of percentage of overall damage due to environmental factors.

Where:

PCT_DAM_{ENV} = percentage of overall damage due to environmental factors.
$g_{OVERALL-ENV}$ = damage from environment only.
$g_{OVERAL-TOTAL}$ = total damage from load and environment.

By comparing the overall damage estimated from the low- and high-trafficked projects, the portion of overall pavement damage that can be attributed to environmental factors was determined.

Determination of Typical Amounts of Distresses for AC Pavements after 15 Yr in Service

The typical amount of distress present on all GPS-1 and SPS-1 AC pavements between the ages of 15 and 25 yr was determined as follows:

1. Identify all GPS-1 and SPS-1 AC projects in the LTPP database constructed before 1998.
2. Of the projects identified in step 1, determine the ones that were still in service after 15 yr.
3. For the projects identified in step 2, select distress reported between 15 and 25 yr and compute average values.
4. Compute percentage of distress as specified in ASTM D6433.[51]

The distribution of distresses presented (all severities) is presented in figure 162 through figure 171.

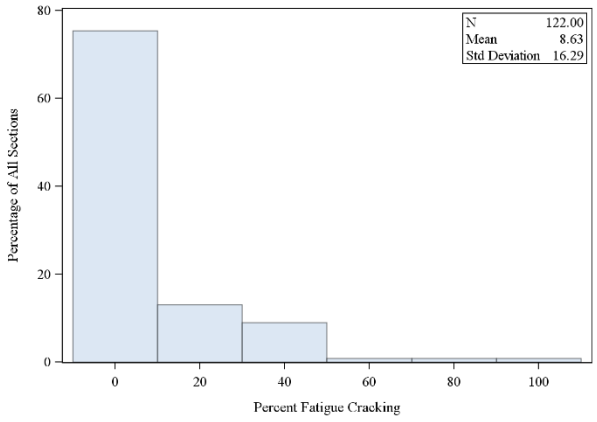

Source: FHWA.

Figure 162. Graph. Distribution of fatigue cracking for AC pavements after 15 yr in service.

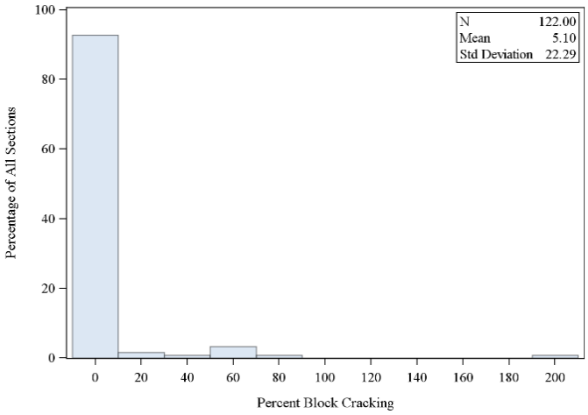

Source: FHWA.

Figure 163. Graph. Distribution of block cracking for AC pavements after 15 yr in service.

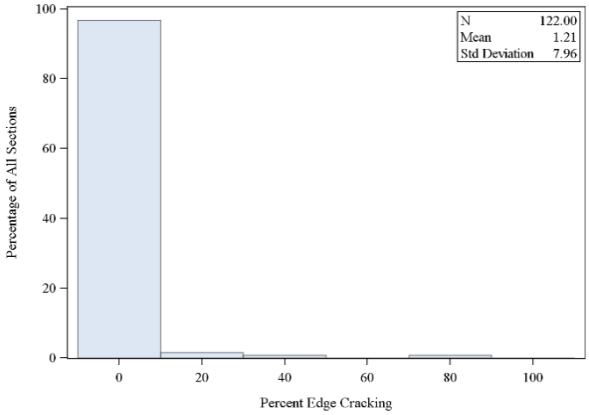

Source: FHWA.

Figure 164. Graph. Distribution of edge cracking for AC pavements after 15 yr in service.

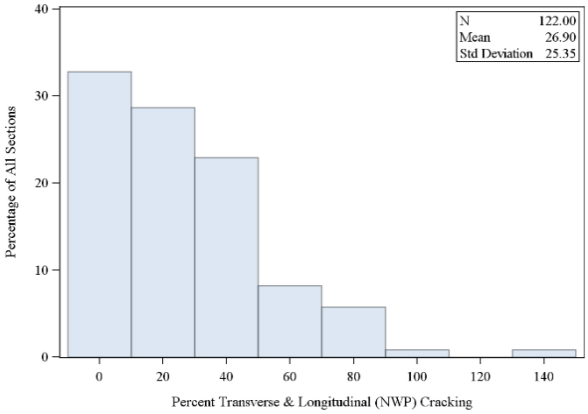

Source: FHWA.

Figure 165. Graph. Distribution of transverse and longitudinal (non-wheel path) cracking for AC pavements after 15 yr in service.

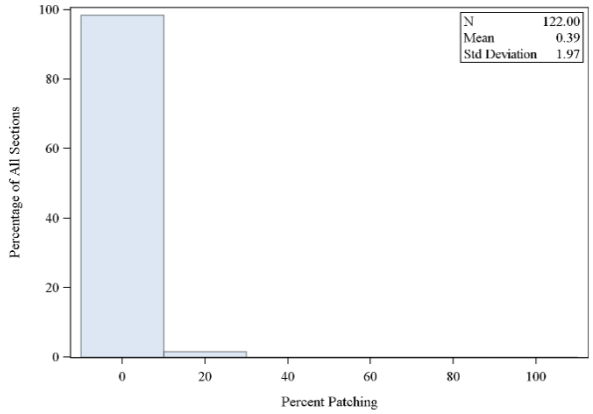

Source: FHWA.

Figure 166. Graph. Distribution of patching for AC pavements after 15 yr in service.

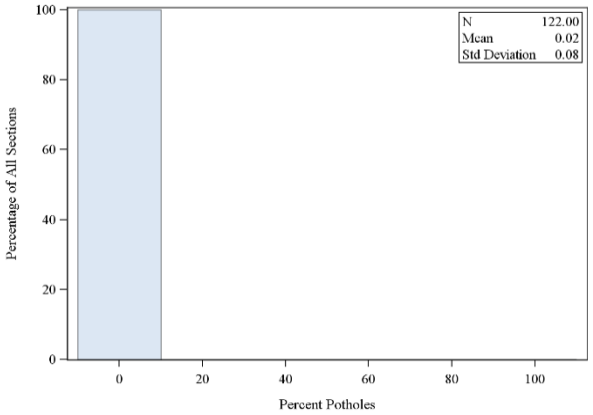

Source: FHWA.

Figure 167. Graph. Distribution of potholes for AC pavements after 15 yr in service.

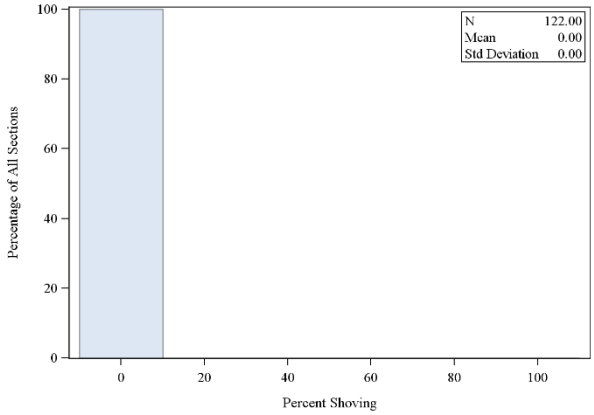

Source: FHWA.

Figure 168. Graph. Distributing of shoving for AC pavements after 15 yr in service.

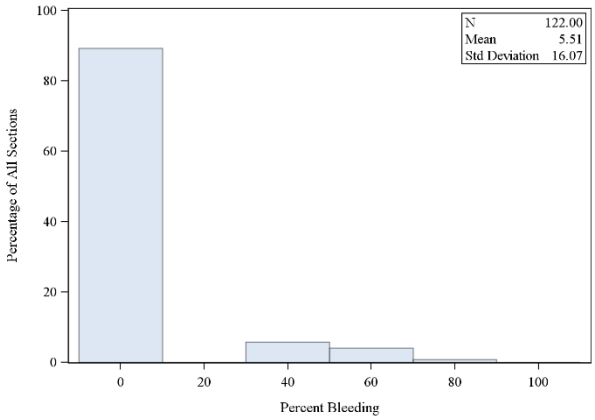

Source: FHWA.

Figure 169. Graph. Distributing of bleeding for AC pavements after 15 yr in service.

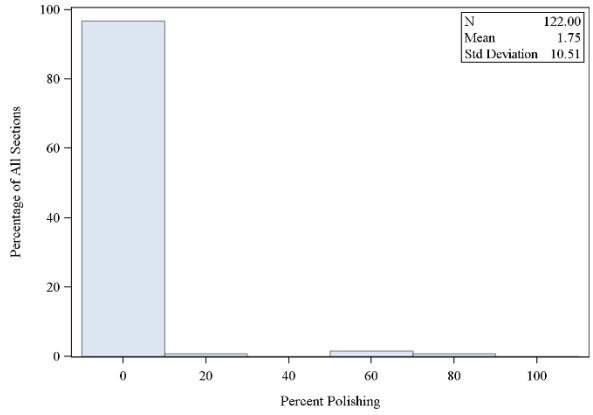

Source: FHWA.

Figure 170. Graph. Distribution of polishing for AC pavements after 15 yr in service.

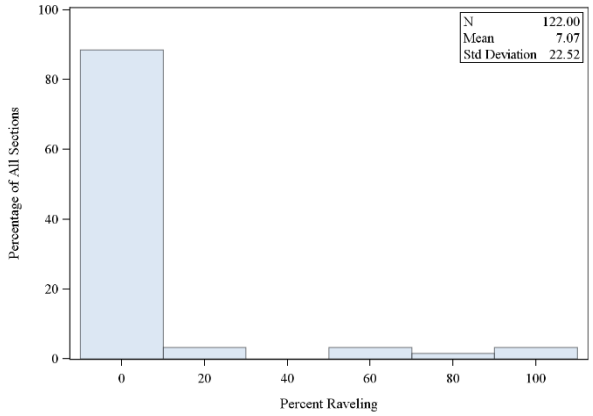

Source: FHWA.

Figure 171. Graph. Distribution of raveling for AC pavements after 15 yr in service.

Determination of *DV* Weighting Factors for Each Distress/IRI and Cumulative *DV* for Distress Groupings

Using the mean distress values of all the distress types in LTPP for AC pavements after 15 yr in service, *DVs* were computed using the ASTM D6433 procedure as follows:[51]

1. Determine mean *DV* of all distress types.
2. Determine *DV* for each distress type.
3. Compute cumulative *DV* for the groupings of distress types presented in table 59.

Table 59. PCI total and corrected PCI point deduct *DV* weighting factors computed for typical AC pavement after 15 yr in service.

Distress Category	Total *DV* PCI Points	Corrected *DV* PCI Points
Fatigue cracking	92.55	53.9
Total rutting	6.97	7.0
Transverse cracking	42.47	42.6
AC materials–related distresses	60.00	39.0
Edge cracking, patching, IRI increase, etc.	26.00	19.4

Estimating Overall Pavement Damage for Low- and High-Trafficked Pavements and Estimate Proportion of Total Damage Due to Environmental Factors

The overall pavement damage (i.e., the weighted average of the individual distress type/group damage) for low- and high-trafficked pavements was estimated using the equation presented in figure 160. The results are presented in table 60. The overall estimate of weighted damage due to environmental (climate and subgrade) factors was 36 percent to the total damage of a typical AC pavement in the database after 15 yr of service.

Table 60. Individual performance measure estimates of damage, *DV* weighting factors, and computed overall damage and proportion of damage due to heavy loads for AC pavements.

Performance Measure	PCI *DV* Weighting Factor	Heavily Trafficked Pavement Overall Damage (SPS-1, GPS-1, GPS-2)	Nontrafficked Overall Damage (SPS-8 Only)	Heavily Trafficked Pavement Overall Damage x Weighting Factor (BxC)	Nontrafficked Pavement Overall Damage x Weighting Factor (BxD)	Heavily Trafficked Pavement Damage Weighted Average (E Total / B Total)	Nontrafficked Pavement Damage Weighted Average (F Total / B Total)	Percentage of Heavily Trafficked Pavements Damage Due to Environmental Factors (100 H Total / G Total)
AC fatigue cracking	53.9	46.0	6.7	2479.2	361.1	NA	NA	NA
Rutting	7.0	63.2	27.0	442.4	189.2	NA	NA	NA
Transverse cracking	42.6	54.8	24.7	2334.5	1052.2	NA	NA	NA
AC materials–related distresses	39.0	43.8	25.6	1708.2	998.4	NA	NA	NA
Others (reflected by smoothness loss)	19.4	29.2	6.2	566.5	120.3	NA	NA	NA
Total	161.9	NA*	NA*	7531.0	2721.2	46.5	16.8	36.1

NA = not applicable

PROPORTION OF OVERALL PAVEMENT DAMAGE DUE TO ENVIRONMENTAL FACTORS FOR JPCP

For estimating overall pavement damage due to environmental factors for JPCP, the weighting factors developed for AC pavements were assumed. The overall pavement damage for low- and high-trafficked pavements were calculated using the equation presented in figure 160. The results are presented in table 61. The overall estimate of weighted damage due to environmental (climate and subgrade) factors was 24 percent to the total damage of typical JPCPs in the database. Note that this is after 15 yr of service life where not a lot of distress had developed.

Table 61. Individual performance measure estimates of damage, *DV* weighting factors, and computed overall damage and proportion of damage due to heavy loads for JPCP.

Performance Measure	PCI *DV* Weighting Factor	Heavily Trafficked Pavement Overall Damage (SPS-2, GPS-3)	Nontrafficked Overall Damage (SPS-8 Only)	Heavily Trafficked Pavement Overall Damage x Weighting Factor (BxC)	Nontrafficked Pavement Overall Damage x Weighting Factor (BxD)	Heavily Trafficked Pavement Damage Weighted Average (E Total / B Total)	Nontrafficked Pavement Damage Weighted Average (F Total / B Total)	Percentage of Heavily Trafficked Pavements Damage Due to Environmental Factors (100 H Total / G Total)
JPCP fatigue cracking	53.9	33.9	2.8	1827.2	150.9	NA	NA	NA
Joint faulting	7.0	10.9	5.1	76.3	35.7	NA	NA	NA
Joint spalling	42.6	18.5	11.9	788.1	506.9	NA	NA	NA
Others (reflected by smoothness loss)	19.4	15.0	0.8	291	15.5	NA	NA	NA
Total	122.9	NA*	NA*	2982.6	709.0	24.3	5.8	23.8

NA = not applicable.

SUMMARY

The proportion of damage for the different distress categories (e.g., load, materials) for AC pavements ranged from 14 to 58 percent. For AC pavements, environmental factors had the least impact on fatigue cracking, while AC materials–related distresses had the largest impact.

For JPCP, the proportion of damage for the different distress categories ranged from 5 to 64 percent. Environmental factors had a high impact on faulting and spalling damage/distress but very little impact on PCC materials-related distresses (there was no D-cracking or other materials distresses in any of the SPS-8 sections at 15 yr).

On average, 36 percent of AC pavement overall damage was due to the environment, while 24 percent of JPCP overall damage was due to the environment after 15 yr of service life.

CHAPTER 16. SUMMARY OF FINDINGS—AC PAVEMENT AND JPCP DESIGN AND MATERIALS SELECTION TO MITIGATE IMPACT OF ENVIRONMENTAL FACTORS

The main objective of this research study was to determine the impact of environmental factors on AC pavement and JPCP performance. A comprehensive evaluation was performed using data from LTPP low-trafficked SPS-8 and companion (high-trafficked) SPS- and -2 and GPS-1 and -3 projects. The comparisons (statistical and nonstatistical) are documented throughout this report. Also presented are estimates of pavement damage characterized per individual performance indicator type and overall composite average for all performance measures.

An outcome of all of these analyses was the compilation of the impact of various environmental factors on pavement performance and how these factors help to initiate or aggravate pavement damage, characterized using individual pavement performance measure or distress. By knowing the possible initiators and aggravators of individual pavement distresses, engineers should be able to better select the appropriate design features and materials properties to mitigate the impact of the given environmental factor and climatic region.

This chapter presents suggested improvements to pavement design and materials based on results from this study to mitigate pavement damage due to environmental factors. The information presented is based on the projects and performance data used for analyses. The high- and low-annual traffic ESAL are summarized as follows for reference purposes:

- Mean annual ESAL for the design lane of the high-trafficked AC pavements was 280,124.
- Mean annual ESAL for the design lane of the high-trafficked JPCP was 693,123.
- Mean annual SPS-8 project design lane ESALA for AC pavements and JPCP was 7,586.

AC PAVEMENTS

Table 62 summarizes the findings of environmental and site variables included in this study that initiate and aggravate AC pavement distress.

Table 62. Environmental and site factors that initiate and aggravate AC pavement distress.

Distress Type	Initiators (Mechanistic Basis)	Aggravators (Increasing Distress)	Impact of AC Thickness in Mitigating Distress
Fatigue cracking	Higher AADTT and higher fatigue cracking	• Warmer climates (which lead to higher AC temperatures) and increased cracking • Higher base/subgrade moisture content and higher cracking • Lower subgrade fine-sand content and higher cracking	Thinner AC layer and increased fatigue cracking
Rutting (permanent deformation)	Higher AADTT and higher rutting	High number of wet days (which affects base/subgrade moisture content) and higher rutting	Thinner AC layer and increased rutting
Transverse cracking	• Lower AC in situ temperature and higher transverse cracking • Higher air freeze–thaw cycles and higher transverse cracking • Subgrade type (fine grained soil types, reduced fine-sand content, and increased transverse cracking)	• Higher AADTT and far higher transverse cracking • Higher PI and higher transverse cracking • High amount transverse cracking in nonfreeze climates	Not significant
Materials durability distress	Higher AC temperature and higher materials durability distress	• Fewer freeze–thaw cycles and higher materials distress • Higher wet days and higher materials distress	Not significant
Smoothness, IRI	• Higher subgrade clay content and higher IRI increase • Higher AADTT and higher IRI increase	Higher freeze–thaw cycles and higher IRI increase	Reduced AC thickness and higher IRI increase

The findings regarding the impact of AC thickness to mitigate distress are also provided. The suggested improvements to pavement design and materials selection are presented as follows for the key distresses and smoothness:

- **AC fatigue cracking**—Traffic loadings were shown to be very significant in initiating fatigue cracking. AC thickness was a significant factor in mitigating fatigue cracking. Fatigue cracking was aggravated or increased in warmer climates (much less in colder climates), higher in situ AC temperatures, higher base and subgrade moisture content, and lower subgrade fine-sand content. Some of these are interrelated (e.g., climate, frost depth, and temperature). The mean AC wheel path fatigue (alligator) cracking for heavily trafficked pavements at 15 yr was 17 percent lane area for all sections, but this was much higher in the warmer climates. Traffic loadings (AADTT) were shown to be very significant in initiating fatigue cracking. Improving on future AADTT estimates, both future traffic volumes and in weights, for individual project design would result in more adequate pavement designs that would have lower fatigue cracking over the design life. Recommendations include improved consideration of AC design thickness, particularly in warmer climates, in wetter climates, and with subgrades with low sand content (e.g., fine-grained soils). Field results show that these environmental conditions are more conducive to fatigue cracking. On the other hand, the results showed that AC thickness was not as significant in colder climates.

- **Rutting (permanent deformation)**—Traffic loading was shown to be very significant in initiating total rutting (all layers). AC thickness was also a significant factor in mitigating total rutting. Rutting was aggravated or increased in wet climates as the number of wet days increased. The moisture content in the base and subgrade was higher in these areas. It is important to repeat the statement made earlier in the report that the test sections with the higher rut depths were much greater than the median values reported by Von Quintus and Simpson for LTPP sections.[57] Recommendations include improved consideration of AC thickness in warmer climates, in particular, and especially in wetter climates with more wet days. Field results show that these environmental conditions are more conducive to total rutting.

- **Transverse cracking**—Lower AC in situ temperature, higher numbers of air freeze–thaw cycles, and subgrade type (active and fine-grained soil types and reduced fine-sand content) are believed to have initiated and probably aggravated transverse cracking. Higher PI of the soil also aggravated or increased transverse cracking. One surprising finding was that there was a lot of transverse cracking in nonfreeze climates. This finding has been observed by different agencies in trying to calibrate the AASHTO ME pavement design transfer functions. Both Arizona and Georgia have significant levels of transverse cracks that cannot be explained through cold temperature events.[16,31,58] Thus, one of the recommendations from this study is to try and explain the occurrence of these transverse cracks in warm climate areas (e.g., potential permanent shrinkage mechanism).[9] However, the most surprising finding was that the amount of transverse cracking was far higher when the level of truck traffic was higher. Significant levels of transverse cracking were exhibited along some of the test sections located at the National Center for Asphalt Technology test track. These transverse cracks were found to be load-related. It is possible that many of the transverse cracks used in this analysis may be load-related.

- **Materials durability distress (e.g., block cracking)**—Higher AC temperature was identified as the common initiator of the various mechanisms related to AC materials durability distress. Aggravation variables identified include lower numbers of freeze–thaw cycles and higher numbers of wet days. Recommendations include improved consideration of the individual distress types that make up the materials durability distress in AC materials selection, specifically for warm and wet climates. Mixture durability distress appears to be most prominent in warm and wet climates.

- **IRI increase**—Higher subgrade clay content and higher traffic applications both appear to be initiators of higher IRI increase over time. There is clearly both a traffic loading and a subgrade component involved in the increase in IRI over time. The main aggravator was a greater number of annual freeze–thaw cycles. Recommendations include addressing the subgrade component through improved treatments to stabilize clay type of subgrades. The impact of traffic on IRI increase can only be addressed through a reduction in fatigue cracking, rutting, transverse cracking, and materials durability distress.

Environmental factors, including climate and subgrade, are an important aspect in the initiation and progression of distress and damage. Environmental factors accounted for 36 percent of total damage for AC pavements after 15 yr. Key climate and subgrade factors that initiated and aggravated AC pavement distress are as follows:

- **Climate**—AC pavements located in warmer nonfreeze climates exhibited significantly higher fatigue cracking and AC materials–related distress. This was more pronounced for the thin AC sections than for the thicker AC sections. Thus, warm climates are especially critical for AC fatigue cracking and AC materials-related distress, and significant efforts (design and materials selection) are needed to reduce these distresses. Pavements in colder climates were more likely to exhibit higher levels of transverse cracking and IRI increase although, surprisingly, significant amounts of transverse cracking are present in warmer climates also. There is obviously more than one mechanism causing transverse cracking, which needs further research and a solution.

- **AC in situ temperature**—Thin AC projects located in warmer climates exhibited significantly higher fatigue cracking levels (70 percent higher) than those located in colder environments. Thick AC projects located in warmer climates exhibited a smaller increase (19 percent) than those located in colder environments. Transverse cracking and IRI increase occurred more often the colder climates. These results indicate clearly that mixture design and materials selection need to be specific to the temperature where the pavement will be constructed to minimize distress. Specific temperature results were as follows:

    - **Freeze–thaw cycles**—Higher freeze–thaw cycles resulted in significantly higher IRI increase over 15 yr. Higher freeze–thaw cycles also led to increased transverse cracking. Conversely, materials durability distress was much lower in areas of higher freeze–thaw cycles. Different distress types clearly respond to climatic effects in different ways.

- **Precipitation**—Both wet days per year and base and subgrade moisture content were significant variables. Thin AC sections had significantly higher fatigue cracking levels (27.5 percent higher) when subjected to high precipitation. Thick AC sections showed no increase in fatigue cracking when subjected to high precipitation. Rutting was also significantly affected by precipitation, with more rutting occurring in locations with higher numbers of annual wet days. Full consideration of unbound materials softening when near saturation is needed to minimize this distress. Materials durability distress was also higher with increased precipitation. Therefore, in areas of higher precipitation, the structural design (reduced unbound material modulus in wet seasons), subdrainage design of some type or stabilization to remove potential problems, and materials selection (moisture susceptibility) are critical.

- **Subgrade**—Subgrade-related factors showed significant impact on all but two distresses examined (AC materials durability and rutting). Changing specific subgrade characteristics was found to significantly change AC fatigue cracking and transverse differences in distress. Results include the following:

  - The higher percent fine-sand content, the lower the AC fatigue cracking.
  - The higher the percent clay content, the higher the AC pavement IRI increase.
  - The higher the PI, the higher the AC transverse cracking and fatigue cracking.

Many of these findings are textbook results that have been known for decades, yet many pavements are still designed and constructed that show early deterioration caused by one or more of these variables.

JPCPS

Table 63 summarizes the environmental and site variables included in this study that initiate and aggravate JPCP distress. The findings regarding the impact of PCC thickness to mitigate distress are also provided.

Table 63. Summary of findings of environmental and site variables that initiate and aggravate JPCP distress.

Distress Type	Initiators (Mechanistic Basis)	Aggravators	Impact of PCC Thickness in Mitigating Distress
Fatigue cracking	Higher AADTT	• Lower precipitation (drier climate) and higher fatigue cracking • Higher in situ PCC temperature and higher fatigue cracking • Coarser subgrades and higher fatigue cracking	Significant (thinner PCC and increased fatigue cracking)
Joint faulting (All joints were doweled)	Higher AADTT	• Longer joint spacing (larger joint openings) and higher joint faulting • Higher subgrade clay content and higher joint faulting • Higher frost penetration (colder climate) and higher faulting	• Significant (thicker slabs subjected to higher traffic causing increased faulting). • Dowel diameter often not sufficient as slab thickness increases
Joint spalling	Lower PCC temperature (higher freeze/thaw cycles) and increased spalling	• Longer joint spacing and higher joint spalling • Higher AADTT and increased joint spalling	• Significant (thicker slabs and lower joint spalling)
Smoothness loss	• Coarse-grained subgrade and increased IRI increase • Higher AADTT and higher IRI increase	• Higher in situ PCC temperature (warmer climate) and higher IRI increase	• Significant (thicker JPCP slabs exhibit lower joint spalling and lower the loss of smoothness over time)

The suggested improvements to pavement design and materials selection are presented as follows for the key distresses and smoothness, along with site variables:

- **JPCP fatigue transverse cracking**—Traffic loadings were shown to be very significant in initiating fatigue cracking in JPCP. PCC thickness was also a very significant factor in mitigating fatigue cracking. Strong mechanistic support exists for reduced JPCP fatigue cracking due to increased PCC thickness. Fatigue cracking was aggravated in warmer climates with higher in situ PCC temperatures, increased in drier climates with lower precipitation (greater upward curling), and increased on subgrades with higher coarse-gained soils (perhaps stiffer subgrades and increased curling stresses). Traffic loadings were shown to be very significant in initiating fatigue cracking. Improving on future

traffic loading estimates, both future traffic volumes and in weights, for individual project design would result in more adequate pavement designs that would have lower fatigue cracking over the design life. Recommendations include improved consideration of JPCP design thickness, particularly in warmer climates and drier climates. This may be due to higher built-in construction temperature gradients, higher moisture gradients (dryer on top of slab), and higher negative temperature gradients in warmer climates (dryer on top of slab). Until the AASHTO ME pavement design procedure, climate was not even considered in JPCP design.[16]

- **Transverse joint faulting**—Traffic loadings were shown to be significant in initiating joint faulting in JPCP. This finding is fully supported by mechanistic concepts. Joint faulting in SPS-8 and higher traffic SPS-2 and GPS-3 projects was generally very low, as all joints were doweled. The thicker slabs showed slightly higher faulting than thinner slabs. This may be explained by the fact that the thicker slabs (GPS-3) were subjected to much higher truck-traffic volumes than the thinner slabs. The higher loadings on some JPCP may have increased joint faulting to make thickness appear to be significant. There were some JPCP sections where the thicker slabs did not have larger diameter dowels, and dowel diameter is the single most important variable in controlling joint faulting. Previous research has shown that thicker nondoweled JPCP faulted less than thinner nondoweled JPCP due to lower corner deflections of the thicker slabs.[12,59] However, when dowels are utilized, dowel diameter is the controlling factor for joint faulting. If dowel diameter would have been larger in all of the thicker pavements, faulting may have been lower in the thick pavements.

  Longer joint spacing resulted in higher joint faulting. This is explained by the fact that longer joint spacing results in a joint that opens much wider than shorter joints spacings. Wider joints lose aggregate interlock, and even though there are dowels to carry the shear load, a larger amount of faulting occurs over time. Shorter joint spacing has significant benefits in reduction of transverse cracking as well as joint faulting. Higher subgrade clay content resulted in higher joint faulting. This finding may be related to the amount of erodible fines that over time may contaminate the unbound base courses and thus lead to higher erosion and pumping beneath the joint.

  One further finding was that higher frost penetration resulted in higher faulting. Again, colder climates will result in wider joint openings and reduced aggregate interlock throughout the year. This will lead directly to higher erosion and higher joint faulting even with doweled joints under heavy traffic loadings.

  Another aspect of the faulting analysis was that the SPS-8 sections have very small joint faulting; the SPS-2 and GPS-3 sections had higher faulting, but it was still very limited. These results reflect the pavement condition at 15 yr only. Recommendations include the necessity of matching the dowel diameter to the slab thickness to control faulting. The traditional rule of thumb is to require a dowel diameter (inches) that is equal to or larger than the slab thickness (inches) divided by 8. A 12-inch slab would thus require a minimum 1.5-inch dowel diameter. The AASHTO Pavement ME Design software conducts a comprehensive analysis for a given dowel diameter and slab thickness and predicts joint faulting that can be assessed and a thicker dowel diameter utilized if

necessary to meet the criteria. This procedure often requires a slightly larger diameter (by 0.25 inch or so). Most of the pavements included in this study followed this rule and exhibited very little faulting. This result supports previous findings regarding the importance of dowel diameter and slab thickness to control joint faulting. Recommendations for critical climatic areas (e.g., colder climates with higher clay content subgrade) include the following:

  - The use of a design procedure that considers these factors including dowel diameter and thickness in predicting joint faulting.

  - Reduction of joint spacing to keep joints tighter. This result was validated based on the fact that most of these sections had very low faulting after 15 yr. For very heavy traffic, a stabilized base course may be a good solution to minimize pumping and erosion beneath the JPCP.

- **Joint spalling**—Traffic was not a significant factor in joint spalling, but it did show an impact in some comparisons (higher traffic and higher spalling). The prime initiator was the in situ slab temperature, which correlated well with other environmental factors like freeze–thaw cycles, which can be mechanistically related to damage caused by many cycles of freezing and thawing of saturated concrete (as exists near joints). The lower the in situ slab temperature, the higher the amount of joint spalling. Thus, cold temperatures and corresponding freezing and thawing of the slab appeared to correlate well with joint spalling. Thicker slabs also showed a reduced level of joint spalling. This may be explained by the fact that the frost line does not include the mid or lower portion of the slab as often (i.e., fewer freeze–thaw cycles lower into the pavement). Recommendations include using a more comprehensive evaluation of slsab mixture design to handle saturated freeze–thaw cycles over many years. Proper entrained air content and curing are essential. Internal curing may produce a concrete that is less permeable and less susceptible to freeze–thaw under saturated conditions.

- **IRI increase**—Traffic loadings and subgrade type were the potential initiators for IRI increase of JPCP. There is clearly both a traffic loading and a subgrade component involved in JPCP IRI increase over time, similar to AC pavement. One amazing statistic was that, for the low-traffic SPS-8 sections, the mean increase in IRI over 15 yr was only about 1 inch/mi. There is no obvious reason that a coarser grained subgrade would exhibit higher IRI increase for JPCP, but that is the result. The AC pavement analysis showed that increased clay content resulted in increased IRI increase (for rigid pavements, increased clay content resulted in lower IRI increase—just the opposite). The main aggravator of IRI increase was higher in situ slab temperature (warmer climate). The warmer the climate, the higher the IRI increase. This is perhaps due in part to increased slab upward curling in warmer climates and and increased fatigue cracking in this climate. The impact of traffic on IRI increase can only be addressed through following recommendations for a reduction in fatigue cracking, joint faulting, and joint spalling. Recommendations include additional study into the reasons why granular subgrades would have higher IRI increase than fine-grained subgrades.

- **JPCP thickness—**Thickness is a critical design feature that initiates JPCP distress. For this study, JPCP thickness was found to be significant for fatigue cracking, faulting, spalling, and IRI increase (note that faulting is highly correlated to IRI increase). For transverse fatigue cracking, joint faulting, spalling, and IRI increase, increasing JPCP thickness leads to lower levels of the distress. Increases in slab thickness also require direct consideration of increased dowel diameter to provide adequate steel to concrete bearing stress for higher traffic volumes. Trends developed as part of the preliminary data analysis showed thickness clearly having a mitigating effect on distress and damage development for regularly traffic loaded JPCP. Thus, the use of a thicker JPCP slab along with sufficient dowel size is essential to decreasing JPCP distress and damage for regularly loaded JPCP.

Environmental factors accounted for 24 percent (at 15-yr life) of total damage for JPCPs. Key climate and subgrade factors that initiate and aggravate JPCP distress are as follows:

- **Climate**—JPCP located in warmer nonfreeze climates exhibited significantly higher fatigue cracking and IRI increase. JPCP located in colder freeze climates exhibited significantly higher joint faulting and higher joint spalling.

- **JPCP in situ temperature (in the slab)**—The in situ JPCP temperature (averaged over the year for a number of years) had quite a significant impact on fatigue cracking, joint spalling, and IRI increase. Of course, increased JPCP temperature correlated well with temperature variables such as climate, freeze–thaw cycles, and frost depth. Additionally, increased JPCP temperature resulted in increased fatigue cracking, increased JPCP temperature resulted in lower joint spalling, and increased JPCP temperature resulted in higher IRI increase.

- **Freeze–thaw cycles**—Higher freeze–thaw cycles resulted in significantly higher joint faulting and joint spalling over 15 yr.

- **Precipitation**—Lower annual precipitation resulted in increased fatigue cracking of JPCP. Drier climates resulted in higher thermal gradients and higher moisture gradients in concrete slabs. This contributed to higher upward curling and top of slab tensile stresses that, combined with load-associated stresses, caused additional fatigue damage at the top of the slab with corresponding top–down transverse cracking.

- **Subgrade**—Subgrade-related variables had a significant impact on fatigue cracking, joint faulting, and IRI increase. The only distress not affected was understandably joint spalling. Results include the following:

    - The higher the coarser-grained subgrade, the higher the fatigue cracking. This result is difficult to explain. Coarse-grained soil typically has a higher modulus that leads to higher curling stresses at the top of the slab. This could lead to higher top–down fatigue cracking. This can be directly considered in AASHTOWare ME design.

- The higher the percent clay content, the higher the joint faulting. This may be related to pumping and erosion of the subgrade through the unbound aggregate base course layers beneath the JPCP slab.

- The higher the coarser grained subgrade, the higher the loss of smoothness.

As noted for the AC pavement findings, many of these findings are textbook results that have been known for many decades, yet many pavements are still designed and constructed that show early deterioration caused by one or more of these variables.

SUMMARY

An internal database was established of pavement design features, materials properties, and performance data for the SPS-8 flexible and rigid pavements as well as companion sections from the SPS and GPS sections. Site-by-site analyses of the LTPP SPS-8 projects were first conducted. Analyses of companion sections of SPS and GPS flexible and rigid pavements were then conducted to show the difference in performance and the causes involved under low traffic and under normal (much higher) traffic loadings. Recommendations were then developed for mitigating these effects through effective designs, materials selection, and construction and additional research suggested.

Finally, an estimate was made of the proportion of pavement damage caused by environmental factors through comparisons of pavement damage of low traffic SPS-8 performance with higher traffic "companion" SPS and GPS. Results for flexible pavement showed that 36 percent of total damage caused when loaded under normal traffic levels is related to environment (subgrade and climate variables) after 15 yr of service. Results for rigid pavement showed that 24 percent of total damage caused when loaded under normal traffic levels is related to environment (subgrade and climate variables) after 15 yr of service.

In addition, many results of interest to pavement and materials engineers were obtained through analysis of the performance of the SPS-8 and SPS and GPS companion sections. One of many interesting findings was that the occurrence of transverse cracking of AC pavement was significantly higher for companion pavements subjected to higher traffic loadings (SPS-1 and GPS-1) than under low traffic loadings (SPS-8) and also that it occurred in nonfreeze climates as well. Based on the results from this study, some suggested findings for improvement of pavement design and materials to minimize distress and to maximize performance in various critical climatic regions are presented. Results from this project may be useful in identifying and developing future research work in the LTPP program.

RECOMMENDATIONS FOR FUTURE EFFORTS

This section provides recommendations for AC pavement and JPCP for reducing pavement distress types and IRI in design and materials.

AC Pavement

No significant load deterioration of the low traffic SPS-8 AC pavements had taken place after 15 yr. However, significant environmental deterioration (e.g., subgrade and climate) had

occurred. Heavier trafficked SPS and GPS companion sections did show significant load and environmental deterioration. The analyses of the SPS-8 and the SPS and GPS companion section performance data showed many significant results. A few recommendations for future research efforts are as follows.

- Additional research on transverse cracking in warm climates is needed to answer specific questions on the cause or mechanism. Transverse cracks do have an impact on future pavement performance and roughness or IRI, so they are important and must be understood. Some specific questions include the following:

    - Why is there so much transverse cracking in climates that rarely experience freezing temperatures? This is not just a low temperature event or mechanism; other factors are contributing to their occurrence. This has been clearly demonstrated within this project, as well as in many other projects and local calibration studies with the AASHTO Pavement ME. (See references 5, 9, 31, 29, and 58.)

    - What other mechanisms are causing this distress in warm climates and how can it be reduced or mitigated during the mixture design process? More importantly, the performance grade binder specification does not take this condition into account.

- Additional research is needed on why there was much more transverse cracking on higher truck-traffic highways (SPS/GPS companion sections versus SPS-8). This is a very surprising result. It is common knowledge that fatigue cracks start as short longitudinal cracks in or adjacent to the wheel path. Some fatigue cracks, however, can also start as transverse cracks in the wheel path. Some of the test sections along the NCAT test track exhibited this characteristic. The question to be asked is: are these transverse cracks characteristics of surface initiated cracking? No forensic investigations have been completed on these sites to determine where these cracks have initiated. It is possible that these cracks are related to insufficient bond between hot mix asphalt lifts. So forensic investigations should be considered by the LTPP program to at least understand where these cracks initiate. Thus, are traffic loadings contributing to transverse cracking in AC pavements? If so, this represents a new area for modeling and prediction so that it may be controlled.

- Additional research on critical climate and subgrade conditions that resulted in unusual amounts of distress and loss of smoothness is needed. For example, fatigue cracking and rutting in warm and wet climates is far more than cold climates. The finding of significant transverse cracking in warm climates is another example, as noted previously. Results from this study can be used to better identify these conditions, and then specific recommendations to help State transportation departments to overcome these problems and improve performance can be developed, specifically related to the treatment of active soils. The data or soil properties included in the LTPP database are insufficient to identify the conditions resulting in additional pavement distress and loss of smoothness from these active soils. This has been a finding from multiple researchers, including the National Cooperative Highway Research Program 1-37A project.[12]

- Additional research is needed on the individual distress types that make up the materials durability distress in AC materials (e.g., bleeding, block cracking, potholes, and raveling), specifically for warm and wet climates. Mixture durability distress appears to be most prominent in warm and wet climates. To investigate the durability issue requires the use of forensic investigation. Thus, forensic investigations are suggested to understand if moisture damage is occurring in more of these sites with low traffic volumes, in comparison to the high traffic volume sites.

JPCP

A small amount of load or environmental deterioration of the low traffic SPS-8 JPCP had taken place at 15 yr. High-trafficked SPS and GPS companion sections did show more load and environmental (aggravation) deterioration. This analysis for JPCP should be repeated in 5 to 10 yr when it is expected that additional environmental deterioration will exist. Some recommendations for future research efforts are as follows:

- Additional research is needed on joint spalling in cold climates. There is sufficient joint deterioration that it will reduce the service life of JPCP located in cold freezing climates. Improvements would result in increased life of JPCP in cold climates.

- Additional research on critical climate and subgrade conditions that resulted in unusual amounts of distress and loss of smoothness for JPCP. For example, transverse fatigue cracking and IRI increase was significantly higher in warm nonfreeze climates. JPCP located in colder freeze climates exhibited significantly higher joint faulting and higher joint spalling. Results from such studies can be used to better identify these conditions, and then specific recommendations can be developed to help State transportation departments to overcome these problems and improve performance.

APPENDIX. DEFINITIONS OF CATEGORIES FOR ENVIRONMENTAL VARIABLES INCLUDED IN PRELIMINARY STATISTICAL ANALYSIS

This appendix includes a table of definitions of environmental variables that are used in the preliminary statistical analysis.

Table 64. Definitions of categories for environmental variables used in the preliminary statistical analysis.

Data Variable	Low	High
Temperature (°F-days)	Nonfreeze, average freezing index <150	Freeze, average freezing index >150
Rainfall/precipitation (inches/year)	Dry, average annual rainfall <20	Wet, average annual rainfall >20
In situ frost depth (computed using the ICM) (inch-days)	<4,000	>4,000
In situ base/subgrade moisture content (computed using ICM) (percent-days)	<900	>900
In situ AC/PCC layer temperature (sum of daily mean temperature computed using ICM) (°F)	<22,000	>22,000
Annual number of freeze–thaw cycles (days)	<55	>55
Subgrade type (dimensionless)	Coarse (less than 35 percent passing the No. 200 sieve)	Fine (greater than 35 percent passing the No. 200 sieve)
Subgrade fine-sand content (percent)	<20	>20
Subgrade silt content (percent)	<20	>20
Subgrade clay content (percent)	<30	>30
Subgrade PI (percent)	<20	>20
Mean depth to GWT depth (ft)	<30	>30

REFERENCES

1. Association of State Highway and Transportation Officials. (1972). *AASHTO Interim Guide for Design of Pavement Structures*, American Association of State Highway and Transportation Officials, Washington, DC.

2. Association of State Highway and Transportation Officials. (1986). *AASHTO Guide for Design of Pavement Structures*, American Association of State Highway and Transportation Officials, Washington, DC.

3. Association of State Highway and Transportation Officials. (1993). *AASHTO Guide for Design of Pavement Structures*, American Association of State Highway and Transportation Officials, Washington, DC.

4. Highway Research Board. (1962). *The AASHO Road Test, Report 7: Summary Report*, Special Report 61G, National Research Council, Washington, DC.

5. Association of State Highway and Transportation Officials. (2008). *Mechanistic-Empirical Pavement Design Guide Interim Edition: A Manual of Practice*, American Association of State Highway and Transportation Officials, Washington, DC.

6. Carpenter, S.H., Lytton, R.L., and Epps, J.A. (1972). *Environmental Factors Relevant to Pavement Cracking in West Texas*, Research Report No. 18-1, Texas Highway Department, Austin, TX.

7. Doré, G., Konrad, J.M., and Roy, M. (1999). "A Deterioration Model for Pavements in Frost Conditions," *Transportation Research Record 1655*, pp. 110–117, Transportation Research Board, Washington, DC.

8. Jackson N. and Puccinelli, J. (2006). *Effects of Multiple Freeze Cycles and Deep Frost Penetration on Pavement Performance and Cost*, Report No. FHWA-HRT-06-121, Federal Highway Administration, Washington, DC.

9. Jones, G.M., Darter, M.I., and Littlefield, G. (1968). "Thermal Expansion and Contraction of Asphaltic Concrete," *Proceedings of the Association of Asphalt Paving Technologists, 37*, pp. 56–100. DEStech Publications, Inc., Lancaster, PA.

10. Ovik, J.M., Birgisson, B., and Newcomb, D.E. (2000). *Characterizing Seasonal Variations in Pavement Material Properties for Use in a Mechanistic-Empirical Design Procedure*, Report No. MN/RC-2000-35, Minnesota Department of Transportation, St. Paul, MN.

11. Vinson, T., Hicks, G., and Janoo, V. (1996). "Low Temperature Cracking and Rutting in Asphalt Concrete Pavements. Roads and Airfields in Cold Regions," *ASCE Technical Council on Cold Region Engineering*, pp. 203–248, ASCE, New York, NY.

12. Applied Research Associates, Inc. (2004). *Guide for Mechanistic-Empirical Design of New and Rehabilitated Pavement Structures*, NCHRP Project 1-37A, Transportation Research Board, Washington, DC.

13. National Oceanic and Atmospheric Administration. "Climate Data Online," (website) National Oceanic and Atmospheric Administration, Washington, DC. Available online: http://www.ncdc.noaa.gov/cdo-web/, last accessed June, 8, 2016.

14. Larson, G. and Dempsey, B. (1997). *Integrated Climatic Model, Version 2.0*, Report No. DTFA MN/DOT 72114, Newmark Civil Engineering Laboratory, University of Illinois at Urbana–Champaign, Champaign, IL.

15. Zapata, C. and Houston, W. (2008). *Calibration and Validation of the Enhanced Integrated Climatic Model for Pavement Design*, NCHRP Report 602, Transportation Research Board, Washington, DC.

16. American Association of State Highway and Transportation Officials (2018). "*AASHTOWare Pavement ME Design*," American Association of State Highway and Transportation Officials, Washington, DC. (Website: http://me-design.com/MEDesign/?AspxAutoDetectCookieSupport=1, created 2008).

17. Federal Highway Administration. (2015). *The Long-Term Pavement Performance Program.* Federal Highway Administration, Washington, DC.

18. Strategic Highway Research Program. (1992a). *Specific Pavement Studies: Construction Guidelines for SPS-8, Study of Environmental Effects in the Absence of Heavy Loads*, Operational Memorandum No. SHRP-LTPP-OM-029, National Research Council, Washington, DC.

19. Strategic Highway Research Program. (1992b). *Specific Pavement Studies: Data Collection Guidelines for Experiment SPS-8, Study of Environmental Effects in the Absence of Heavy Loads*, Operational Memorandum No. SHRP-LTPP-OM-031, National Research Council, Washington, DC.

20. Strategic Highway Research Program. (1991a). *Specific Pavement Studies: Experimental Design and Research Plans for Experiment SPS-8, Study of Environmental Effects in the Absence of Heavy Loads*, Operational Memorandum No. (SHRP-LTPP-OM-031), National Research Council, Washington, DC.

21. Strategic Highway Research Program. (1992c). *Specific Pavement Studies: Material Sampling and Testing Requirements for Experiment SPS-8, Study of Environmental Effects in the Absence of Heavy Loads*, Operational Memorandum No. SHRP-LTPP-OM-030, National Research Council, Washington, DC.

22. Strategic Highway Research Program. (1991b). *Specific Pavement Studies: Guidelines for Nomination and Evaluation of Candidate Projects for Experiment SPS-8, Study of Environmental Effects in the Absence of Heavy Loads*, Operational Memorandum No. SHRP-LTPP-OM-025, National Research Council, Washington, DC.

23. American Association of State Highway and Transportation Officials. (1962). *AASHO Interim Guide for the Design of Flexible and Rigid Pavement Structures,* American Association of State Highway Officials, Washington, DC.

24. Pavement Interactive. (2008). "Rigid Pavement Response." (website). Pavement Interactive, Washington, DC. Available online: http://www.pavementinteractive.org/rigid-pavement-response/, last accessed October 12, 2008.

25. Roberts, F., Kandhal, P., Brown, E., Lee, D., and Kennedy, T. (1996). *Hot Mix Asphalt Materials, Mixture Design, and Construction,* Second Edition, National Asphalt Pavement Association Education Foundation, Lanham, MD.

26. Yilmaz, A. and Sargin, S. (2012). "Water Effect on Deteriorations of Asphalt Pavements," *The Online Journal of Science and Technology, 2*(1), pp. 84–89, Faculty of Technical Education, Düzce, Turkey.

27. Hicks, R.G., Santucci, L., and Ashchenbrener, T. (2003) "Introduction and Seminar Objectives on Moisture Sensitivity of Asphalt Pavements," *Transportation Research Board National Seminar,* pp. 3–19, San Diego, CA.

28. Herrington, P.R., Reilly, S., and Cook, S. (2005). *Porous Asphalt Durability Test,* Transfund New Zealand Research Report 265, Lower Hutt, New Zealand.

29. Tuckett, G.M., Jones, G. M. and G. Littlefield. (1970) "The Effects of Mixture Variables On Thermally Induced Stresses In Asphaltic Concrete And Discussion," *Association of Asphalt Pavement Technologists, 39*, pp. 703–744. DEStech Publications, Inc., Lancaster, PA.

30. Haas, R. (2003). "Good Technical Foundations are Essential for Successful Pavement Management," *Proceedings of Conference of Maintenance and Rehabilitation of Pavements MAIREPAV 2003,* Guimaraes, Portugal.

31. Darter, M., L. Titus-Glover, H. Von Quintus, B. B. Bhattacharya, and J. Mallela. (2016). "*Calibration and Implementation of the AASHTO Mechanistic-Empirical Pavement Design Guide in Arizona*," Report No. FHWA-AZ-14-606, Arizona Department of Transportation.

32. Yasarer, H. and Najjar, Y. (2012). "Development of Void Prediction Models for Kansas Concrete Mixes Used in PCC Pavement," *Procedia Computer Science, 8*, pp. 473–478, Elsevier, Amsterdam, Netherlands.

33. Armaghani, J.M., Larsen, T.J., and Smith L.L. (1987). "Temperature Response of Concrete Pavements," *Transportation Research Record, 1121*, pp. 23–33, Transportation Research Board, Washington, DC.

34. Joshi, A., Mehta, Y., Cleary, D., Henry, S., and Cunliffe, C. (2012). "Load Transfer Efficiency of Rigid Airfield Pavement Relationship to Design Thickness and Temperature Curling," *Transportation Research Record 2300,* pp. 75–82, Transportation Research Board, Washington, DC.

35. Thompson, M.R., Dempsey, B.J., Hill, H., and Vogel, J. (1987). "Characterizing Temperature Effects for Pavement Analysis and Design," *Transportation Research Record, 1121*, pp. 14–22, Transportation Research Board, Washington, DC.

36. McLeod, H. and Kirkvold, A. (2012). *D-Cracking Field Performance of Kansas Portland Cement Concrete Pavements Containing Limestone*, TRB Preprint 2012, Transportation Research Board, Washington, DC.

37. Monismith, C.L. (1989). *Interpretation of Laboratory Results for Design Purposes*, Workshop on Resilient Modulus Testing, Oregon State University, Corvallis, OR.

38. Low, P.F. and Margheim, J.F. (1979). "The Swelling of Clay, Basic Concepts and Empirical Equations," *Soil Science Society of America Journal, 43*, pp. 473–481, Alliance of Crop, Soil, and Environmental Science Societies, Madison, WI.

39. Schafer, W.M. and Singer, M.J. (1976). "Influence of Physical and Mineralogical Properties on Swelling of Soils in Yolo County, California," *Soil Science Society of America Proceedings, 40*, pp. 557–562, Alliance of Crop, Soil, and Environmental Science Societies, Madison, WI.

40. Parker J.C., Amos, D.F., and Zelazny, L.W. (1982). "Water Adsorption and Swelling of Clay Minerals in Soil Systems," *Soil Science Society of America Journal, 46*, pp. 450–456, Alliance of Crop, Soil, and Environmental Science Societies, Madison, WI.

41. Zhang, W. and Macdonald, R.A. (2002). *The Effects of Freeze-Thaw Periods on a Test Pavement in the Danish Road Testing Machine*, Ninth International Conference on Asphalt Pavements, International Society for Asphalt Pavements, St. Paul, MN.

42. Janoo, V., Barna, L., and Orchino, S. (1997). *Frost-Susceptibility Testing and Predictions for the Raymark Superfund Site*, Special Report 97-31, U.S. Army Cold Regions Research and Engineering Laboratory, Hanover, NH.

43. Casagrande, A. (1931). "Discussion of Frost Heaving," *Proceedings of the Highway Research Board*, pp. 168–172. Highway Research Board, Washington, D.C.

44. Ducker, A. (1940). *Frosteinwirkung auf bindige BOden (Action of Frost on Cohesive Soils)*, Strassenjahrbuch, Berlin, Germany.

45. Lambe, T.W. (1960). *The Character and Identification of Expansive Soils*, Technical Studies Report No. PHQ-701, Federal Housing Administration, Washington, DC.

46. Pavement Interactive. "Frost Action," (website) Pavement Interactive, Dover, DE. Available online: http://www.pavementinteractive.org/frost-action/, last accessed November 6, 2006.

47. Johnson, L.D. (1977). *Evaluation of Laboratory Suction Tests for Prediction of Heave in Foundation Soils*, Technical Rep. S-77-7, U.S. Army Engineers Waterways Experiment Station, Vicksburg, MS.

48. Olive W., Chleborad, A., Frahme, C., Shlocker, J., Schneider, R., and Schuster, R. (1989). *Swelling Clays Map of the Conterminous United States*, U.S. Geological Survey, Washington, DC. Available online: http://ngmdb.usgs.gov/Prodesc/proddesc_10014.htm, last accessed April 14, 2016.

49. Natural Resources Conservation Service. "Description of SSURGO Database," (website) U.S. Department of Agriculture, Washington, DC. Available online: http://www.nrcs.usda.gov/wps/portal/nrcs/detail/soils/survey/?cid=nrcs142p2_053627, last accessed June, 8, 2016.

50. National Water Information System: Web Interface. "USGS Water Data for the Nation," (website) U.S. Geological Survey, Washington, DC. Available online: http://waterdata.usgs.gov/nwis, last accessed June 8, 2016.

51. ASTM D6433. (2011). "Standard Practice for Roads and Parking Lots Pavement Condition Index Surveys," *Book of Standards Volume 04.03*, ASTM International, West Conshohocken, PA.

52. Rauhut, J.B., Lytton, R.L., and Darter, M.I. (1984). *Pavement Damage Functions for Cost Allocation, Vol. 1: Damage Functions and Load Equivalence Factors*, Report No. FHWA/RD-84/018, Federal Highway Administration, Washington, DC.

53. Holtz, R. and Kovacs, W. (1981). *An Introduction to Geotechnical Engineering*, Prentice-Hall Publishers. Upper Saddle River, NJ.

54. Federal Highway Administration. (2013). Long Term Pavement Performance Program, LTPP Database Standard Data Release (SDR) 27. Release January 2013. Available online: https://infopave.fhwa.dot.gov/Data/StandardDataRelease, last accessed January 1, 2015.

55. SAS® Institute, Inc. (2012). *SAS/STAT© Software Version 9.3*, SAS Institute Inc., Cary, NC.

56. Lytton, R.L., Scullion, T., Garrett, B.D., and Michalak, C.M. (1981). *Effects of Truck Weights on Pavement Deterioration*, Texas A&M Research Foundation, College Station, TX.

57. Von Quintus, H.L. and Simpson, A.L. (2000). *Structural Factors for Flexible Pavements—Initial Evaluation of the SPS-1 Experiment*, Report No. FHWA-RD-01-166, Federal Highway Administration, Washington, DC.

58. Von Quintus, H., Darter, M., Bhattacharya, B., and Titus-Glover, L. (2015). *Implementation and Calibration of the MEPDG in Georgia*, Report No. GADOT-TO-02-Task 7, Georgia Department of Transportation, Atlanta, GA.

59. Applied Research Associates, Inc. (2006). "Changes to the Mechanistic Empirical Pavement Design Guide Software through Version 0.900," *Research Results Digest 308*, NCHRP Project 1-40D, Transportation Research Board, Washington, DC.

HRDI-30/03-19(500)E